Cortical morphology in 22q11.2 deletion syndrome : a MRI study

Schaer, Marie

UNIVERSITÉ DE GENÈVE

FACULTÉ DE MÉDECINE

UNIVERSITÉ DE GENÈVE

DOCTORAT EN NEUROSCIENCES
des Universités de Genève et de Lausanne

UNIL | Université de Lausanne

UNIVERSITE DE GENEVE FACULTE DE MEDECINE

Professeur Stephan Eliez, directeur de thèse
Professeur Jean-Philippe Thiran, co-directeur de thèse (EPFL)

CORTICAL MORPHOLOGY IN 22Q11.2 DELETION SYNDROME : A MRI STUDY

THESE
présentée à la
Faculté de Médecine

de l'Université de Genève

pour obtenir le grade de
Docteur en Neurosciences

par

Marie SCHAER

de Genève

Thèse N° 20

Genève

Editeur ou imprimeur : Université de Genève

2008

UNIVERSITÉ
DE GENÈVE
FACULTÉ DE MÉDECINE

DOCTORAT EN NEUROSCIENCES
des Universités de Genève et de Lausanne

Thèse de

Marie SCHAER
originaire de Genève (GE)

Intitulée

CORTICAL MORPHOLOGY IN 22Q11.2 DELETION SYNDROME : A MRI STUDY

Soutenue le : 10 septembre 2008

* La Faculté de médecine, sur préavis du jury de thèse formé par :

Professeur Stephan Eliez, Faculté de médecine, Université de Genève, directeur
Professeur Jean-Philippe Thiran, Laboratoire de traitement du signal, EPFL, co-directeur
Professeur Christoph Michel, Faculté de médecine, Université de Genève
Docteur Jean-François Mangin, Commissariat à l'Energie atomique, Paris

Autorise l'impression de la présente thèse, sans prétendre par là émettre d'opinion sur les propositions qui y sont énoncées.

Genève, le 10 septembre 2008

Thèse n° 20

Professeur Jean-Louis Carpentier
Doyen

*N.B. La thèse imprimée doit porter la déclaration précédente * et remplir les conditions énumérées dans les « Informations aux étudiants relatives aux thèses de doctorat à l'Université de Genève ».*

This work was supported by a grant from the Swiss National Science Foundation
(323500-111165)

Remerciements – Acknowledgments

Tout d'abord, je tiens à remercier tout particulièrement Stephan à qui je dois beaucoup. Il m'a donnée une vision de carrière que peu de directeurs de thèse savent transmettre, me conseillant toujours sur les priorités à garder en tête en tant que chercheur-médecin; je tâcherai de suivre de mon mieux cette ligne sur laquelle il m'a lancée. Il a su me pousser à donner un maximum sans jamais être dirigiste, en me laissant la liberté de gérer les projets de neuroimagerie du labo. J'ai eu beaucoup de chance de t'avoir comme directeur de thèse, merci Stephan!

Je remercie sincèrement Jean-Philippe pour son enthousiasme à encadrer des MD-PhD à l'EPFL. Jean-Philippe a cette grande qualité de rendre les problèmes toujours si simples, j'espère réussir à garder un peu de cet esprit. Jean-Philippe, j'ai énormément apprécié ta gentillesse, et je me réjouis de pouvoir continuer à collaborer avec toi.

Je remercie aussi les membres du jury qui ont accepté cette charge. Premièrement, Christoph Michel, toujours si disponible pour les étudiants de l'école doctorale. Ensuite, Jean-François Mangin dont les travaux sur le plissement cortical m'ont beaucoup inspirée au cours de ces trois années, et qui a accepté de juger ce travail et de libérer une journée pour venir à Genève. Finalement, Dimitri Van De Ville qui a gentiment participé au comité d'examen au pied levé en juin passé.

Ce travail n'aurait certainement pas eu la même rigueur scientifique sans l'efficace supervision de Meritxell Bach Cuadra à l'EPFL. Merci pour ta disponibilité et pour tout ce que tu m'as appris! Merci aussi tous les autres membres du LTS pour leur accueil, et en particulier à Leila Cammoun qui a passé plusieurs heures à me transmettre ses connaissances en imagerie de diffusion, connaissances que je ne doute pas de finir par exploiter plus productivement un jour!

Un grand merci à tous les membres du labo de Genève pour les bons moments passés ensemble. Mes remerciements vont en particulier à Bronwyn et à Martin, avec qui j'ai eu beaucoup de plaisir à travailler, nous avons formé pendant ces trois années une belle équipe. Bron, tu as longtemps été la seule à comprendre mes élucubrations littéraires dans un anglais approximatif, je te remercie de m'avoir appris à formuler mes idées de manière plus compréhensible pour les autres! Martin, merci pour tes nombreux conseils et encouragements que j'ai particulièrement appréciés lors des congrès à Strasbourg, Montreux, ou Utrecht, et surtout jusqu'à la présentation finale de soutenance de ma thèse. Mes remerciements vont aussi à Marie-Christine qui a toujours été là pour faire face aux délais impossibles, ainsi qu'à tous les autres stagiaires qui sont passés par le labo de neuroimagerie: Daniela, Jérôme, Sandra B., Manolo, Léa, Ayse, Maude, Federico, Catherine A., Lucia, et Astrid. Je tiens aussi à remercier tout particulièrement Lucas Tamarit pour son aide précieuse lors de mes débuts dans la programmation Matlab.

I would like to thank sincerely people at the MGH who gave me the opportunity to integrate my *l*GI method into their awesome software. Specifically, Bruce Fischl who invited me to come in Boston, Nick Schmansky and Doug Greve for their incredible efficiency, and Rudolph Pienaar for his help and his hospitality when I was in Boston.

Je tiens à remercier le Fonds National Suisse de m'avoir permis de me consacrer à plein temps ce travail de recherche grâce à une bourse pendant ces trois années (SNF 323500-111165). Je remercie aussi Dominique Muller qui m'a transmis de précieux conseils qui furent efficaces lors de la préparation de cette demande de bourse. L'acquisition des IRM qui sont à la base de ce travail a été permise par le soutien du Centre d'Imagerie Biomédicale (CIBM) des Universités de Genève et Lausanne, ainsi que les Fondations Leenards et Louis-Jeantet.

Je remercie aussi mes amis pour leur soutien pendant ces trois années de thèse où je n'ai pas toujours été très disponible, en particulier Yaël, Vérane et Anne.

Je suis particulièrement reconnaissante envers mes parents qui m'ont toujours poussée à faire ce qui me plaisait, mais surtout à le faire jusqu'au bout; ils m'ont très largement soutenus tout au long de ce parcours et je les en remercie sincèrement. Une pensée particulière va aussi à mon frère, Guillaume, qui est depuis toujours l'exemple incarné qu'un problème technique n'a pas lieu de résister à la volonté qu'on a de le résoudre.

Finalement, ce travail de thèse n'aurait pas eu le même sens sans le soutien de Thomas au quotidien, son intérêt pour mon travail et son aide si fréquente. Je suis heureuse de pouvoir partager cette passion de la recherche avec toi, merci Thomas!

Contents

Version abrégée

La maturation du cerveau au cours de l'enfance fait partie des questions les plus fascinantes soulevées par le développement des neurosciences au cours des dernières dizaines d'années. Quels sont les mécanismes qui permettent à quelques centaines de grammes de neurones et à leurs connections de produire des fonctions complexes, telles que la réflexion, la mémoire, ou l'intelligence? La construction progressive des capacités cognitives au cours de l'enfance m'a toujours fascinée, d'une part, car elle semble suivre une cascade d'évènements bien ordonnés, remarquablement plastique, qui culmine par d'impressionnantes facultés à l'âge adulte. Et d'autre part, parce que cette cascade, la même qui vise à optimiser les capacités intellectuelles, semble parfois extrêmement fragile, tel qu'en témoignent les troubles envahissants du développement ou autres pathologies psychiatriques résultant de perturbations du développement cérébral. Si cette question du dévelopement cérébral peut être abordée sous des angles divers, l'imagerie structurelle cérébrale représente un moyen très prometteur de suivre le développement du cerveau *in vivo*.

La partie introductive de ce travail de thèse résume les progrès effectués dans le domaine de la neuroimagerie, qui permettent un accès relativement direct aux corrélats structurels de la maturation cérébrale normale ou pathologique. Ainsi, les trajectoires curvilinéaires d'épaisseur corticale observées au cours de l'adolescence pourraient être à même de refléter les remaniements de l'arborisation dendritique qui accompagnent l'optimisation de la fonction cérébrale. Aussi, les progrès des techniques de quantification de la morphologie tridimensionnelle du cortex, avec la possibilité de mesurer le plissement du cortex, semblent permettre une fenêtre sur le développement cérébral précoce.

Au cours de ce travail de thèse, nous nous proposons d'explorer le développement cérébral dans une maladie génétique fréquente: la microdélétion 22q11. Les enfants atteints de la microdélétion 22 présentent souvent un retard des acquisitions, qui affecte surtout la mémoire, l'intégration visuo-spatiale, et l'arithmétique. Au cours de leur adolescence, ces personnes font fréquemment l'expérience de symptômes psychotiques, tels qu'hallucinations ou délires. En particulier, l'incidence accrue de schizophrénie liée à la microdélétion 22 a même amené l'idée que cette condition génétique puisse représenter un modèle d'étude des mécanismes qui prédisposent à cette psychose. Au cours des dernières années, l'étude des corrélats cérébraux potentiellement responsables des déficits cognitifs ou des symptômes psychotiques a donc recu un vif intérêt.

Si la question des répercussions fonctionnelles des altérations cérébrales intéresse beaucoup, celle des mécanismes qui pourraient causer ces altérations reste plus largement inexplorée. Dans ce travail de thèse, nous nous efforçons de réunir une vue relativement exhaustive des altérations de la structure du cortex liées à la microdélétion, et de comprendre la relation de ces modifications entre elles dans une perspective développementale.

En préambule, trois études de régions d'intérêt m'ont permis de me familiariser avec les techniques de neuroimagerie classiques, avant de s'intéresser de plus près à la structure du cortex. Le plissement cortical a tout d'abord été mesuré à l'aide de l'Index de Gyrification, une méthode particulièrement attrayante par son élégante simplicité et sa facilité d'interprétation. Cependant, la manière dont l'Index de Gyrification avait été calculé jusqu'alors ne nous paraissait pas rendre compte de la complexité de la structure corticale avec suffisamment de précision. Ainsi, nous avons développé un nouvel outil de mesure du plissement cortical, inspiré de l'Index de Gyrification.

Les résultats obtenus dans la microdélétion avec cette nouvelle méthode nous ont permis de suggérer qu'un défaut d'expansion précoce du cortex pourrait être responsable des réductions de volume cortical observées. Dans un deuxième temps, nous avons aussi identifié que les malformations cardiaques, fréquentes dans le syndrome, exacerbent cette anomalie précoce, particulièrement à la jonction des lobes pariéto-occipitaux-temporaux.

Nous nous sommes ensuite intéressé à la maturation du cerveau au cours de l'enfance et de l'adolescence dans la microdélétion, et avons observé des trajectoires différentes de l'épaisseur du cortex avec l'âge, hautement suggestives d'une anomalie de l'optimisation de l'arborisation dendritique. Dans le chapitre consacré, nous discutons comment cette maturation anormale pourrait favoriser l'apparition de la symptomatologie psychotique chez les individus affectés par la microdélétion.

Ce travail de thèse représente plusieurs contributions dans le domaine du développement cérébral lié à la microdélétion 22, et illustre comment les techniques de neuromagerie structurelle peuvent être employées pour répondre à des questions de pathogenèse. A terme, une meilleure compréhension des mécanismes responsables des altérations cérébrales pourra certainement aider à développer des stratégies thérapeutiques dans le but d'aider les patients atteints de la microdélétion, ou ceux souffrant d'une schizophrénie.

Part I

Introduction

Context

I Behavioral neurogenetic

The recent development of neurosciences is on the way to revolutionize psychiatry. In particular, among recent developments in biological psychiatry, advances in the field of behavioral neurogenetic carry a strong potential for furthering our understanding of the etiopathogenesis of psychiatric disorders.

As recently reviewed by Martin (Martin, 2002), psychiatry and neurology, which were for long completely distinct medical disciplines, with separate departments, practices and research interests, are increasingly tied. Eric Kandel, a psychiatrist who received the Nobel Prize in 2000, describes academic psychiatry in the 1950s as a "psychoanalytically based and socially oriented discipline that was surprisingly unconcerned with the brain as an organ of mental activity" (Kandel, 1998). However, as he further depicts, progresses in neuropharmacology in the 1960-70s dramatically changed this view, given that "psychiatry was forced to confront neural science, if only to understand how specific pharmacological treatments were working". Following these neuropharmacological advances, increasing progresses were also made in other disciplines of neuroscience, such as neurophysiology, neuroimaging, cognitive neuroscience, or computational neuroscience. As a result of the increasing delineation of the biological correlates of mental processes, dialogues between psychiatry and neurosciences are now possible. More than a simple dialogue, we can even consider that the field of psychiatry is on the way to be revolutionized by an increasing definition of the neural pathways leading to the onset of mental diseases.

In the search for a better understanding of the pathogenesis of psychiatric disorders, the attention of geneticists, psychiatric or neurological clinicians or neuroscientists has been recently attracted by a few genetic conditions associated with specific behavioral or psychiatric impairments. **Behavioral neurogenetic** has emerged from the observation that neurodevelopmental and neuropsychiatric disturbances are various in their presentation and etiologies (Baumgardner et al., 1994; Reiss et al., 2000). Therefore, our opportunity to understand the pathogenesis of abnormal behavioral or cognitive manifestations relies on a narrow definition of homogenous subgroups. Being genetically homogenous, neurogenetic syndromes were thus elected as ideal candidates to "reveal insights into neurodevelopmental pathways that might otherwise be obscured or diluted when investigating more heterogeneous pathologies" (Reiss et al., 2000). Some of these neurogenetic conditions have even been designated as models for broader neurodevelopmental or neurodegenerative pathologies of unclear origin, such as Down syndrome and Alzheimer disease (Mann, 1988), or Fragile

X syndrome and autism (Hagerman et al., 2005). The syndrome that is studied in the present dissertation, 22q11 deletion syndrome has been proposed as a model for studying the pathways leading to schizophrenia (Murphy et al., 2001).

One of the more attractive feature of behavioral neurogenetic for research is that patients affected by the neurogenetic condition can be followed-up prior to, and until they develop the disease. Using such prospective design make it able to identify the physiological pathways over the course of disease development, and potentially define risk factors or biological markers. In a discipline like psychiatry, where symptoms are relatively non specific, it may be attractive to redefine a classification more grounded on biological basis. For instance, the identification of individuals at risk prior to the onset of symptoms may help to concentrate prevention resources (a strategy commonly used in all other medical disciplines, e.g. with the prescription of diet and drugs for lowering cholesterol in patients at risk for heart infarct). Alternatively, the definition of biological markers may serve to monitor the evolution of the disease, or the effect of treatment in affected patients. Ultimately, the integration of genetic, biology and neuroscience may completely transform the field of psychiatry, toward a "more scientifically rigorous medical discipline" (Kandel, 1998). Nowadays, behavioral neurogenetic is certainly the field that carries one of the strongest potential to lead such a transformation of the psychiatric discipline.

Overview of the manuscript

The present dissertation focuses on the anomalies of brain structure in 22q11 deletion syndrome, using neuroimaging techniques. This thesis uses the style *by articles*, meaning that the introductory part is primarily intended to provide basic knowledge for the reading of the articles (that replace the traditional *Method* and *Results* sections). The first part of the manuscript thus comprises four introductory chapters. First, a description 22q11 deletion syndrome is provided, with emphasis on the physical, cognitive, behavioral and psychiatric phenotype. The second chapter presents neuroimaging as a powerful tool for studying *in vivo* brain development, with an overview of image processing analysis techniques. The third chapter of the introduction focuses on gyrification (cortical folding), as a window on early brain development in neurodevelopmental disorders. The last chapter describes the current knowledge about the cerebral alterations typically associated with 22q11 deletion syndrome, and outlines the objectives of the thesis. In the second part of the manuscript, journal articles published (or submitted for publication) are reproduced. Finally, the third part of the dissertation provides an integrative, critical discussion of the studies.

Chapter 1

22q11.2 deletion syndrome

22q11 deletion syndrome (or 22q11.2 deletion syndrome) is a common genetic syndrome manifested with a variety of physical anomalies. During the last decades, the syndrome has received a large interest due to the increased frequency of schizophrenia, and was even elected as a model for studying the pathogenesis of this disease.

1.1 History of the syndrome

The first mention of the syndrome appeared in the literature more than 50 years ago, when Eva Sedlàckovà, a Czech phoniatrician, described a group of 26 children with hypernasal speech, facial dysmorphism, and mental retardation (Sedlàckovà, 1955). However, apart from a few speech specialists, this first report in Czech remained largely unknown (Vrticka, 2007). Another mention of the syndrome is then found a few years later, in a discussion where DiGeorge evokes his clinical experience with children presenting with immune deficiency due to the absence of thymus (DiGeorge, 1965). Approximately at the same time, Strong (Strong, 1968), and Cayler (Cayler, 1969) also described an association of typical facial features and congenital heart disease, that the later one denoted craniofacial Cayler syndrome.

Unaware of these previous fractioned descriptions of the syndrome, Shprintzen and colleagues published in 1978 an article entitled "A new syndrome involving cleft palate, cardiac anomalies, typical facies, and learning disabilities: velo-cardio-facial syndrome" (Shprintzen et al., 1978). Thus, even if the syndrome had already received punctual interest from logopedists or immune specialists, the more comprehensive picture published by Sphrintzen et al is generally considered as the original description of the syndrome.

In 1992, collaborators from the same group identified that the syndrome was associated with a deletion at 22q11 locus (Driscoll et al., 1992). As a result of the deletion identification, syndromes that were previously thought to be separate (but overlapping) entities were recognized to all bear a common genetic etiology (Scambler et al., 1992; Burn et al., 1993; Wilson et al., 1993; Giannotti et al., 1994; Matsuoka et al., 1994; McDonald-McGinn et al., 1995; Fokstuen et al., 2001). Velo-cardio-facial, Sedlàckovà, DiGeorge,

and Shprintzen syndromes, thus all encompass the same disorder, which is also known under several other names such as conotruncal anomaly face syndrome, Cayler cardiofacial syndrome (asymmetric crying facies), or CATCH 22. The later acronym, standing for **C**ardiac defects, **A**bnormal Facies, **T**hymic hypoplasia, **C**left palate, and **H**ypocalcemia, was later on discarded because of its pejorative connotation for an inextricable situation. Throughout the present dissertation, the more coherent, etiologically-defined term of 22q11 deletion syndrome (22q11DS) will be used[1].

1.2 Prevalence & Genetic

Reported annual incidence of 22q11DS varies from 1/9700 (Tezenas Du Montcel et al., 1996) to 1/6395 (Devriendt et al., 1998) or 1/5950 (Botto et al., 2003) cases per live births. However, as the mildest forms of the syndrome were probably not included in the population-based estimation, these numbers are considered as minimum incidences. Rather, an estimated incidence between 1/2000 and 1/4000 is commonly cited, making 22q11 deletion the most frequent interstitial deletion[2] in humans and the second most important genetic cause of mental delay after Down syndrome (trisomy 21).

22q11DS occurs most of the time sporadically (*de novo* mutation). The few familial cases (5-17%, Swillen et al., 1998) are inherited with an autosomal dominant mode. The extent of the deletion usually spans 3 megabases (Mb) of DNA over the long arm of chromosome 22, encompassing a total 40 genes. In 8% of cases, a smaller deletion of 1.5 Mb (30 genes) is observed (Lindsay et al., 1995; Carlson et al., 1997). Of note, the clinical presentations between the 3Mb and 1.5Mb deletions are undistinguishable.

The mechanism by which the deletion occurs is commonly accepted to rely on misalignment during meiosis. Indeed, the presence of low copy repeats flanking and within the critical deletion interval favors aberrant recombination of 22q chromosome (McDermid et al., 2002; Saitta et al., 2004). Chromosomal misalignment can also lead to duplication at 22q11, which has been associated with mental and speech delay in combination with various dysmorphic facial features, but without major birth defect (e.g. no cardiac malformations) (Ou et al., 2008).

Diagnosis of 22q11 deletion syndrome requires the use of fluorescence in situ hybridization (FISH) with probes from the DiGeorge Chromosomal Region (DGCR). The less than 5% of individuals with negative FISH testing are diagnosed with DNA-based assays, such a polymerase chain reaction (Fernandez et al., 2005). Prenatal diagnosis is available, in case of an affected parent, or if 22q11DS is suspected at prenatal ultrasound examination (through the presence of conotruncal cardiac defect or cleft palate) (Driscoll, 2001).

[1] Note that 22q11DS will be used for 22q11.2 deletion syndrome in this dissertation. There is indeed another genetic syndrome related to deletion at 22q11.3, but it is not the topic of the present work

[2] Interstitial deletion stands for a deletion that does not involve the terminal part of a chromosome

1.3 Signs & Symptoms

The phenotype associated with 22q11DS is variable, and more than 180 anomalies have been reported (see Table 1.1). The cardinal features, from which Shprintzen et al named the syndrome in 1978, encompass velo-pharyngeal insufficiency, cardiac defect, and facial dysmorphism.

Characteristic facial features Affected individuals typically have long face, hypertelorism (increased distance between eyes), retrognathia and prominent nasal bridge. Small ears with overfolded helix are also frequent. Photographs from affected patients of different age and ethnic origins are depicted in Figure 1.2.

Palate anomalies Velo-pharyngeal findings are among the most frequent anomalies in the syndrome. Cleft palate, short palate, or hypotonia of palate musculature result in velopharyngeal incompetence and hypernasal voice (Vantrappen et al., 1998). Investigations and treatment are not specific for 22q11DS, including surgical correction when needed, and logopedic interventions.

Cardiac malformations Congenital heart diseases (CHD) are among the key features of the syndrome, being reported in 50% (McDonald-McGinn et al., 1999) to 75% (Ryan et al., 1997) of patients with 22q11DS. The type of CHD observed in 22q11DS encompass mostly conotruncal heart defect[3], such as truncus arteriosus, Fallot tetralogy, or right sided aortic arch. Associated atrial and ventricular septal defects are common. Prospective studies of CHD have shown that deletion at 22q11 accounted for a consequent number of CHD diagnosed in the general population. Namely up to 10% of patients with specified ventricular septal defects, 35% of patients with conotruncal defects (among which 12% of Fallot and 20% of truncus arteriosus diagnoses), and of 50% of patients diagnosed with interrupted aortic arch have positive FISH testing for 22q11.2 deletion (reviewed by Hay, 2007). As a result, many centers now screen for the deletion when conotruncal defects are diagnosed.
The morbidity and mortality associated with CHD in 22q11DS is important. Indeed, according to a European collaborative study, almost all patients with 22q11DS that died during the first 6 months did because of CHD (Ryan et al., 1997). Aside from cardiac malformations, other vascular anomalies frequently associated with the syndrome are described in Table 1.1.

Immune system Immune deficiency related to thymic hypoplasia is frequent in 22q11 deletion syndrome. As a result, recurrent infections are often reported in children with the syndrome, but improve into adulthood. Severe immune deficiency is rare and treatment is usually unnecessary.

Other physical anomalies Growth retardation during childhood is common (Ryan et al., 1997). Seizures are often related to hypocalcemia (Ryan et al., 1997), and, thus, usually respond well to calcium supplements. Gastro-intestinal, ocular and skeletal anomalies and other anomalies are also reported in the syndrome, as listed in Table 1.1.

[3]Conotruncal heart defects define anomalies on the outflow tract

Velo-cardio-facial syndrome: specialist fact sheet

Velo-cardio-facial syndrome (VCFS) is caused by a deletion of a small segment of the long arm of chromosome 22. It is one of the most common genetic disorders in humans. The following list shows the anomalies that have been found in VCFS. No features are found in 100% of cases, but all occur with sufficient frequency to warrant assessment. If you have any questions, or if you would like to know more about VCFS, you may reach The Velo-Cardio-Facial Syndrome Educational Foundation by telephone at 315-464-6590, by fax at 315-464-5321, or by e-mail at vcfsef@mail.upstate.edu. The Foundation maintains a web site at www.vcfsef.org

Craniofacial / Oral Findings
1. Overt, submucous or occult submucous cleft palate
2. Retrognathia (retruded lower jaw)
3. Platybasia (flat skull base)
4. Asymmetric crying facies in infancy
5. Structurally asymmetric face
6. Functionally asymmetric face
7. Vertical maxillary excess (long face)
8. Straight facial profile
9. Congenitally missing teeth (one or several)
10. Small teeth
11. Enamel hypoplasia (primary dentition)
12. Hypotonic, flaccid facies
13. Downturned oral commissures
14. Cleft lip (uncommon)
15. Microcephaly
16. Small posterior cranial fossa

Eye Findings
17. Tortuous retinal vessels
18. Suborbital congestion ("allergic shiners")
19. Strabismus
20. Narrow palpebral fissures
21. Posterior emryotoxon
22. Small optic disk
23. Prominent corneal nerves
24. Cataract
25. Iris nodules
26. Iris coloboma (uncommon)
27. Retinal coloboma (uncommon)
28. Small eyes
29. Mild orbital hypertelorism
30. Mild vertical orbital dystopia
31. Puffy upper eyelids

Ear / Hearing Findings
32. Overfolded helix
33. Attached lobules
34. Protuberant, cup-shaped ears
35. Small ears
36. Mildly asymmetric ears
37. Frequent otitis media
38. Mild conductive hearing loss
39. Sensori-neural hearing loss (often unilateral)
40. Ear tags or pits (uncommon)
41. Narrow external ear canals

Nasal Findings
42. Prominent nasal bridge
43. Bulbous nasal tip
44. Midly separated nasal domes (nasal tip appear bifid)
45. Pinched alar base, narrow nostrils
46. Narrow nasal passage

Cardiac and Thoracic Vascular Findings
47. VSD (Ventricular Septal Defect)
48. ASD (Atrial Septal Defect)
49. Pulmonary atresia or stenosis
50. Tetralogy of Fallot
51. Right sided aorta
52. Truncus arteriosus
53. PDA (Patent Ductus Arteriosus)
54. Interrupted aorta, type B
55. Coarctation of the aorta
56. Aortic valve anomalies
57. Aberrant subclavian arteries
58. Vascular rings
59. Anomalous origin of the carotid artery
60. Transposition of the great vessels
61. Tricuspid atresia

Vascular anomalies
62. Medially displaced internal carotid arteries
63. Tortuous or kinked internal carotids
64. Jugular vein anomalies
65. Absence of interal carotid artery (unilateral)
66. Absence of vertebral artery (unilateral)
67. Low bifurcation of common carotid
68. Tortuous or kinked vertebral arteries
69. Raynaud's phenomenon
70. Small veins
71. Circle of Willis anomalies

Neurologic, brain and MR Findings
72. Periventricular cysts (mostly at anterior horns)
73. Small cerebellar vermis
74. Cerebellar hypoplasia / dysgenesis
75. White matter UBOs (Unidentified Bright Objects)
76. Generalized hypotonia
77. Cerebellar ataxia
78. Seizures
79. Strokes
80. Spina bifida / meningomyelocele
81. Mild developmental delay
82. Enlarged sylvian fissure

Pharyngeal / Laryngeal / Airway Findings
83. Upper airways obstruction in infancy
84. Absent or small adenoids
85. Laryngeal web (anterior)
86. Large pharyingeal airway
87. Laryngomalacia
88. Arytenoid hyperplasia
89. Pharyingeal hypotonia
90. Asymetric pharyingeal movement
91. Thin pharyngeal muscle
92. Unilateral vocal cord paresis
93. Reactive airway disease
94. Asthma

Abdominal / Kidney / Gut
95. Hypoplastic / aplastic kidney
96. Cystic kidneys
97. Inguinal hernias
98. Umbilical hernias
99. Malrotation of bowel
100. Diastasis recti
101. Diaphragmatic hernia (uncommon)
102. Hirschsprung megacolon (rare)

Limb Findings
103. Small hands and feet
104. Tapered digits
105. Short nails
106. Rough, red, scaly skin on hands and feet
107. Morphea
108. Contractures
109. Triphalangeal thumbs
110. Polydactyly, both pre- and postaxial (uncommon)
111. Soft tissue syndactyly

Problems in Infancy
112. Feeding difficulty, Failure-to-thrive
113. Nasal vomiting
114. Gastrophageal reflux
115. Irritability
116. Chronic constipation (not Hirschsprung megacolon)

Genitourinary Findings
117. Hypospadias
118. Cryptorchidism
119. Vesico-uteral reflux

Speech / Language Findings
120. Severe hypernasality
121. Severe articulation impairment (glottal stops)
122. Language impairment (usually mild delay)
123. Velopharyngeal insufficiency (usually severe)
124. High pitched voice
125. Hoarseness

Cognitive / Learning Findings
126. Learning difficulties (math concept, reading comprehension)
127. Concrete thinking, difficulty with abstraction
128. Drop in IQ scores in school years (test artifact)
129. Borderline normal intellect
130. Occaional mild mental retardation
131. Attention deficit hyperactivity disorder

Miscellaneous Anomalies
132. Spontaneous oxygen desaturation without apnea
133. Thrombocytopenia, Bernard-Soulier disease
134. Juvenile rheumatoid arthritis
135. Poor body temperature regulation

Psychiatric / Psychological Findings
136. Bipolar affective disorder
137. Manic depressive illness and psychosis
138. Rapid or ultrarapid cycling of mood disorder
139. Mood disorder
140. Depression
141. Hypomania
142. Schizoaffective disorder
143. Schizophrenia
144. Impulsiveness
145. Flat affect
146. Dysthymia
147. Cyclothymia
148. Social immaturity
149. Obsessive compulsive disorder
150. Generalized anxiety disorder
151. Phobias
152. Severe startle response

Immunologic Findings
153. Frequent upper respiratory infections
154. Frequent lower airway disease (pneumonia, bronchitis)
155. Reduced T cell population
156. Reduced thymic hormone

Endocrine Findings
157. Hypocalcemia
158. Hypoparathyroidism
159. Hypothyrodism
160. Mild growth deficiency, relative small stature
161. Absent, hypoplastic thymus
162. Small pituitary gland

Skelettal / Muscle / Orthopedic Findings
163. Scoliosis
164. Spina bifida occulta
165. Hemiverterbrae
166. Butterfly verterbrae
167. Fused verterbrae (usually cervical)
168. Osteopenia
169. Sprengel's anomaly, scapular deformation
170. Taliped equinovarus
171. Small skeletal muscles
172. Joint dislocations
173. Chronic leg pains
174. Flat foor arches
175. Hyperextensible / lax joints
176. Rib fusion
177. Extra ribs
178. Tethered cord
179. Syrinx

Skin / Integument Findings
180. Abundant scalp hair
181. Thin appearing skin (venous patterns easily visible)

Secondary Sequences / Associations
182. Robin sequence
183. DiGeorge sequence
184. Potter sequence
185. CHARGE associations
186. Holoprosencephaly (single case)

Some other facts about the syndrome
- Population prevalence (estimated): 1:2,000 people
- Birth incidence (estimated): 1:1,800 births
  Prevalence in infants with conotruncal heart anomalies:
- 10-30%
  Prevalence in cleft palate (without cleft lip): 8%

Table 1.1: *List of anomalies associated with 22q11DS, reformatted from the one written by Shprintzen, available on www.vcfsef.org*

Figure 1.2: *Some striking features emerge from the comparison of facial appearance of patients with 22q11DS[a], like long face and prominent nasal bridge. But compared to more stigmatizing syndromes, such as Down syndrome, these characteristics remain subtle. Indeed, even experienced clinicians were shown to be unable to reliably identify individuals with 22q11DS based solely on facial photographs (Becker et al., 2004).*

[a]Photographs are taken from the following publications (from left to right): First row: Vantrappen et al., 1998; Fryer, 1996; Vantrappen et al., 1998; McDonald-McGinn et al., 2005; McDonald-McGinn et al., 2005 – Second row: McDonald-McGinn et al., 2005; Fokstuen et al., 2001; McDonald-McGinn et al., 2005; Bassett et al., 2005 – Third row: McDonald-McGinn et al., 2005; Shprintzen, 2000; Bird et al., 2000; Gripp et al., 1997; Vrticka, 2007 – Last row: Fokstuen et al., 2001; Koolen et al., 2004; Vrticka, 2007; Bird et al., 2000; Sedlàckovà, 1955.

1.4 Developmental profile: cognitive & psychiatric phenotype

1.4.1 Preschool children

In young children with the syndrome, global development is known to be delayed (Gerdes et al., 1999; Solot et al., 2001), with a mean age of walking of 18 months (Oskarsdottir et al., 2005). Gross motor milestones are also retarded, with coordination and balance problems (Swillen et al., 1999). Even if intelligence is hardly measured in children below 3.5 years old, there are evidences that intellectual capacities may already be affected, with one third of children having with mild mental retardation, one third functioning in the borderline range, and one third in the average range (Gerdes et al., 1999). Speech delay is common (Golding-Kushner et al., 1985; Gerdes et al., 1999). Expressive language deficits partly rely on palate abnormalities, but concomitant deficit in receptive language is also reported (Scherer et al., 1999).

1.4.2 School age children

School age children typically present impairments in domains that were already affected when they were younger. For instance, gross and fine motor alterations are reported (Van Aken et al., 2007), and deficits in receptive and expressive language abilities (Glaser et al., 2002). Further, borderline to mild mental retardation is frequently observed, with mean Full Scale IQ around 70. IQ verbal scores are typically better than performances scores (i.e. IQ dissociation) (Moss et al., 1999; Swillen et al., 1999). More specifically, children with 22q11DS encounter learning and mnesic difficulties, with working memory (Sobin et al., 2005), arithmetic (Moss et al., 1999; Swillen et al., 1999) and visuo-spatial skills (Wang et al., 2000; Bearden et al., 2001) being particularly affected.

On the behavioral level, 40% of children meet criterion for attention-deficit/hyperactivity disorder (ADHD) (Gothelf et al., 2004), which has been suggested to rely on an impaired efficiency of the executive functions in these children (Sobin et al., 2004). Further psychiatric entities frequently diagnosed in children with 22q11DS encompass oppositional defiant disorder (16%-43%), specific and social phobias (23%-61%), generalized anxiety disorder (17%-29%), separation anxiety disorder (16%-21%), obsessive-compulsive disorder (4%-33%) and autism spectrum disorders (14%-45%) (Feinstein et al., 2002; Arnold et al., 2001; Antshel et al., 2007). Adolescents with 22q11DS often experience hallucinations or delusions, prodromal of subsequent full-blown psychosis or schizophrenia. The detailed prevalence of symptomatic manifestations along the psychotic continuum in the sample of patients with 22q11DS collected in Geneva is provided in Annex 2.

1.4.3 Adults with 22q11DS & psychosis

Similar cognitive difficulties are reported in adults as in children and adolescents with the syndrome. Specifically, impaired visuo-spatial processing, difficulties in problem solving and planning, and poor abstract and social thinking have been reported (Henry et al., 2002). If the mild intellectual delay presented by adults is often compatible with an

adapted profession, the key feature that determines the outcome is psychiatric status. Psychosis is reported in 50% of adults (Baker et al., 2005), whereas 30% of adults with the syndrome meet DSM-IV criteria for schizophrenia (Pulver et al., 1994; Murphy et al., 1999). Diagnostic criteria for schizophrenia are presented in the blue box below. As shown in Figure 1.3, with a 30% risk, 22q11 deletion syndrome represents one of the highest risk known to date for developing schizophrenia.

The question as to whether the schizophrenia observed in patients with 22q11DS is clinically similar to the schizophrenia seen in non-syndromic patients from the population has been debated. For instance, Murphy et al (Murphy et al., 1999) reported that 10 patients with 22q11DS had a significantly later onset of disease, and fewer negative symptoms, than 12 non-syndromic patients with schizophrenia. However, a few years later, Basset et al (Bassett et al., 2003) did not find any major difference between 16 patients with 22q11DS and schizophrenia and 46 non-syndromic patients with schizophrenia. Specifically, they reported no differences in age at onset, lifetime core positive or negative schizophrenic symptoms, and anxiety / depression symptoms or global functioning.

Diagnostic criteria for schizophrenia

Schizophrenia is a disease of late adolescence and early adulthood, that belongs to the broader class of psychosis. Psychosis defines a loss of contact with reality, typically associated with hallucinations, delusional beliefs and disorganized thought (DSM-IV, 2000). Among the formal diagnosis of psychoses listed in the DSM-IV, schizophrenia is specifically associated with positive and negative symptoms, encompassing two or more of the following: delusions, hallucinations, disorganized speech, grossly disorganized or catatonic behavior, and negative symptoms (i.e affecting flattening, alogia or avolition). To be considered as DSM-IV schizophrenia, these characteristic symptoms must last for at least 1 month over a consecutive period of 6 months, and must impair social and occupational functioning of the individual.

The following subtypes of schizophrenia are distinguished:
The paranoid type, including preoccupation with delusion and frequent auditory hallucinations.
The catatonic type, dominated by motor immobility, extreme negativism or excessive motor activity and stereotyped movements.
The disorganized type, with prominent disorganized speech or behavior.
The undifferentiated type, in which the criteria for paranoid, catatonic, or disorganized are not met.
The residual type, in which the negative symptoms are most prominent, and the positive symptoms are present but attenuated (e.g. odd beliefs, unusual perceptual experiences).

1.5 Why is 22q11DS a model for schizophrenia ?

As a result of the typical clinical presentation and increased risk for schizophrenia, researchers were rapidly interested in studying 22q11 deletion syndrome. The formal definition of 22q11DS as a model for schizophrenia relies on the following evidences:

- **Increased frequency of schizophrenia in patients with 22q11DS**
  According to the definition by Dykens, a behavioral phenotype is defined as "the

probability that persons with a genetic syndrome will show certain behavioral or developmental sequelæ relative to those without the syndrome" (Dykens, 1995). The 30% risk presented by patients affected with 22q11DS (Murphy et al., 1999; Bassett et al., 2003) is largely greater than the 1% commonly observed in the population (see Figure 1.3). Further, it was recently confirmed that the 30% estimation was not biased by recruitment considerations, as 32% of children prospectively followed-up during a 5 years period developed a psychotic disorder (Gothelf et al., 2007).

- **Increased frequency of 22q11DS in population of patients with schizophrenia**
  To be elected as a behavioral phenotype of a syndrome, not only increased frequency of the phenotype must be reported in the syndrome, but also higher rate of the syndrome must be found in patients with the behavior/psychiatric disorder. For example, autistic disorder is considered a behavioral phenotype of Fragile X syndrome because subjects with Fragile X syndrome have a high rate of autistic disorder and subjects with autistic disorder have an increased rate of the Fragile X mutation (Fombonne et al., 1997; Flint, 1998). Regarding 22q11DS and schizophrenia, the reported rate of the deletion in adults with schizophrenia ranges from 0.3% to 2% (Karayiorgou et al., 1995; Arinami et al., 2001), which is far higher than the 1/5950 annual incidence of 22q11DS in the general population (Botto et al., 2003). The rate of syndrome is even higher in patients with childhood-onset schizophrenia (5.7%) (Sporn et al., 2004), or in patients with schizophrenia presenting manifestations typical of 22q11DS. Indeed, 20% of schizophrenic patients with one manifestation (among cardiac or palate anomalies, typical facies, hypocalcemia, or learning disabilities) have been shown to have 22q11 deletion, whereas this number increase to 53% in schizophrenic patients with two of them (Gothelf et al., 1997; Bassett et al., 1998).

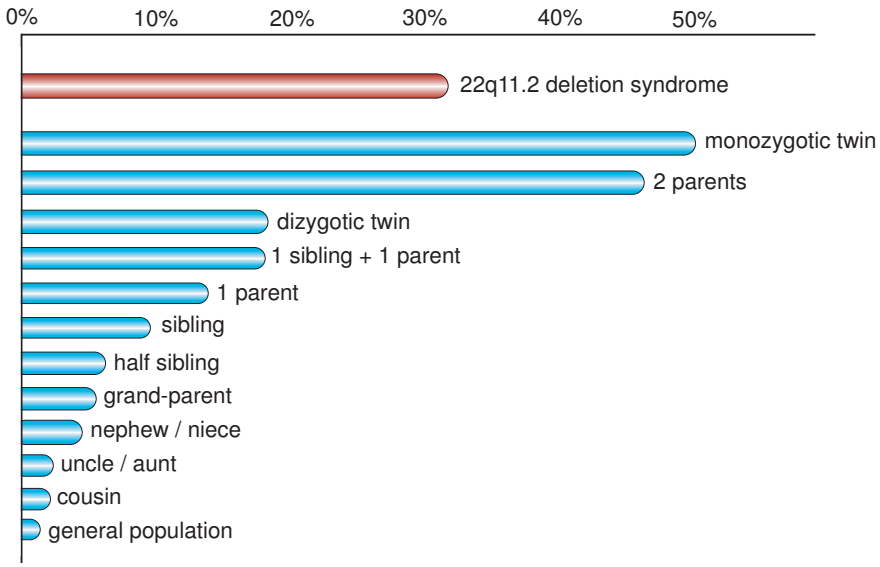

Figure 1.3: *Risk for developing schizophrenia (adapted from McGuffin et al., 1995). After having a monozygotic twin with schizophrenia (50% risk), and after being the child of two schizophrenic parents (46% risk), 22q11DS represents the third more elevated risk for developing schizophrenia.*

- **Linkage studies suggest that chromosome 22q might be a susceptibility locus for schizophrenia**
  In 22q11DS, linkage genetic studies provide a third criterion supporting the association between 22q11DS and schizophrenia. Indeed, there is evidence for 22q as a susceptibility locus with marker telomeric to or close to the 22q11 region (Pulver et al., 1994; Gill et al., 1996; Blouin et al., 1998; Shaw et al., 1998). However, like for all chromosomal regions suggested by linkage studies, replication of the results has been relatively inconsistent.

The combination of the three criteria above has elected 22q11DS as a model for schizophrenia (Murphy et al., 2001). Such a model is highly attractive in research for several reasons. First, 22q11DS is certainly a more convenient model than other high risks for developing schizophrenia. Indeed, the at-risk monozygotic co-twin is obviously not identified before the disease occurs in the co-twin, thus not allowing prospective studies of childhood and adolescence development. Conversely, 22q11 deletion syndrome is often diagnosed during the first years of life, so that affected patients can easily be followed-up until the firsts symptoms appear. Further, compared to the second most important risk for developing schizophrenia, namely having two schizophrenic parents, 22q11DS is certainly a more frequent situation. Finally, the risk for schizophrenia presented by patients with 22q11DS is genetically homogenous, becoming an ideal framework in which genes implicated in the onset of schizophrenia can be explored. Indeed, today, 22q11 deletion syndrome is the only known homogenous genetic model for schizophrenia.

1.5.1 Why are other manifestations in 22q11DS not considered as behavioral phenotypes ?

As recently reviewed by Gothelf et al (Gothelf et al., 2008), other phenotypes frequently observed in 22q11DS do not fulfill the association criteria to be eligible as models. For instance, attention-deficit/hyperactivity disorder (ADHD) is present in almost half the children with 22q11DS (Gothelf et al., 2004). However, ADHD is not a behavioral phenotype of 22q11DS because similarly high rates of ADHD (25% to 60%) were reported in association with other neurogenetic syndromes, including Fragile X (Sullivan et al., 2006), Williams (Leyfer et al., 2006), Prader-Willi (Wigren et al., 2005) or Turner syndromes (Russell et al., 2006). In addition, no cases of 22q11 deletion have been identified in children with ADHD from the general population (Bastain et al., 2002). Thus, we may assume that ADHD is a common, non-specific pathway for a variety of risk factors affecting brain development and function. Similarly, autistic spectrum disorders are not considered a behavioral phenotype of 22q11DS. Despite reported at high rates (14-45%) in children and adolescents with 22q11DS (Fine et al., 2005; Vorstman et al., 2006; Antshel et al., 2007), the rates of autistic spectrum disorders in 22q11DS are not higher than for other neurogenetic disorders (25-65%), such as Fragile X, tuberose sclerosis, or Angelman syndromes (Zafeiriou et al., 2007). Furthermore, there are yet no reports of high rates of 22q11.2 deletion in individuals with autistic disorder from the general population. Gothelf (Gothelf et al., 2008) suggested that the reported rates of autistic disorder and ADHD in neurogenetic syndromes reflect a pitfall of the DSM criteria, which were not designed for children with developmental disabilities. Indeed,

many children with developmental disabilities and mental retardation manifest deficits in attention and in social skills that are in line within the context of their developmental level. Therefore, neither ADHD nor autistic behaviors are considered to be specific behavioral phenotypes of 22q11DS.

1.6 Deleted genes & possible pathogenesis

The 22q11 deleted region encompasses 30 to 40 genes, among which almost all may be implicated in some specific aspects of the phenotype (reviewed in Maynard et al., 2002). However, among the 30 candidate genes, three genes have received more emphasis. For instance, TBX1 gene is thought be responsible for a large part of the physical anomalies, through disruption of neural crest development in embryo. Two other genes, COMT and PRODH, have also received a large interest regarding their role in neurotransmitters regulation, thus being possibly involved in the cognitive and psychiatric symptomatology. symptomatology.

1.6.1 TBX1

TBX1 belongs to a family of transcription factor that contain a DNA binding domain called *T-Box*. As the genes encompassed in the 22q11 deleted region have been identified, mice models have been proposed (Paylor et al., 2006). Specifically, a knock-out mouse for 24 genes corresponds to the 1.5Mb minimal deletion found in humans. Based on progressive reduction of the number of deleted genes in mice, it was identified that TBX1 plays a preponderant role in anomalies of neural crest cells migration. Indeed, TBX1 mutation in mice is responsible for similar physical phenotypes than reported in humans with 22q11DS, with cardiovascular and thymic malformations (Jerome et al., 2001; Lindsay et al., 2001; Merscher et al., 2001).

In humans, point mutation inactivating TBX1 (Yagi et al., 2003; Zweier et al., 2007) were identified in patients without the deletion, but who presented the typical physical phenotype

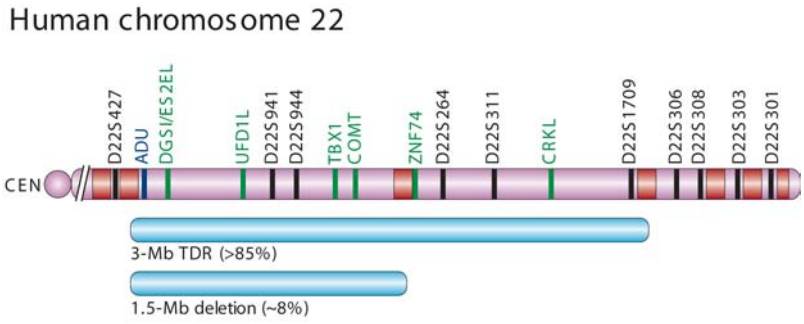

Figure 1.4: *Human 22q11 deletion region from (Lindsay, 2001). The genes more frequently implicated are delineated in green, and markers for the deletion in black. Red blocks represent low copy repeats, favoring aberrant recombination and leading to the 1.5 or 3Mb characteristic deletion.*

seen in 22q11DS. Thus, TBX1 may play a major role in the malformations associated with the syndrome. However, the implication of TBX1 in the behavioral and psychiatric phenotype remains controversial. Some authors claim that TBX1, which is not normally expressed in the brain, is thus unlikely to account for the cognitive and psychiatric aspects of the syndrome (Maynard et al., 2002). Others have reported behavioral and psychiatric symptoms in mice and humans with single TBX1 mutation (Paylor et al., 2006), thus arguing that 22q11DS may not be so different from a monogenic disease.

1.6.2 COMT & PRODH

Related to the behavioral and psychiatric phenotypes associated with the syndrome, two genes have received a wide interest: COMT and PRODH. COMT codes for catecholamine-O-methyltransferase, an enzyme involved in dopaminergic metabolism, mostly expressed in the prefrontal lobe. A common polymorphism is the substitution of one amino-acid in the COMT DNA (Val *vs* Met), which modifies the enzymatic activity (Chen et al., 2004). COMT polymorphism has been associated with regulation of cortical dopaminergic neurotransmission and performance on cognitive tasks involving the prefrontal cortex in schizophrenic and healthy patients, with patients bearing the Val allele performing less well than patients with Met (Egan et al., 2001; Meyer-Lindenberg et al., 2005). However, in 22q11DS inconsistent results regarding the effect of COMT polymorphism in patients with 22q11DS have been published. Bearden et al have reported poorer outcome in Val compared to Met patients with 22q11DS (Bearden et al., 2004; Bearden et al., 2005). A few years later, in a longitudinal study, Gothelf and colleagues have found that patients with Met showed more important cognitive decline and more severe psychotic symptoms than patients with 22q11DS and the Val allele (Gothelf et al., 2005). In a recent review (Gothelf et al., 2008), Gothelf explained the divergent of COMT polymorphism in patients with 22q11DS and non-syndromic patients according to the Goldman-Rakic model of an inverted-U shape relationship between cortical dopamine signaling and cognitive functioning (Goldman-Rakic et al., 2000) (See Figure 1.5). Of note, no difference in cognitive or executive functioning according to COMT polymorphism was observed in our sample of subjects collected in Geneva (Glaser et al., 2006).

PRODH (standing for proline dehydrogenase) gene encodes proline oxydase (POX). POX is a mitochondrial enzyme that catalyzes the conversion of proline into different metabolites including glutamate and GABA, two neurotransmitters that have been implicated in schizophrenia pathogenesis. Indeed, mice deficient in PRODH show schizophrenia related phenotypes, with abnormalities of sensorimotor gating (Gogos et al., 1999), and deficits in associative learning (Paterlini et al., 2005). In patients with schizophrenia, genetic variation in the PRODH gene has been associated with structural differences in the prefrontal region and have thus been suggested to modulate the schizophrenia phenotype in patients with 22q11DS (Zinkstok et al., 2008). However, as for COMT, studies encompassing very large samples of patients often reported no association between PRODH and schizophrenia (Williams et al., 2003; Glaser et al., 2006)

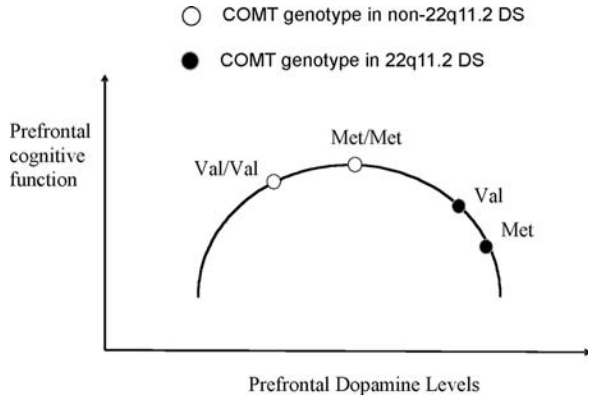

Figure 1.5: *Relationship between the dopaminergic level and cognitive function follows an inverted-U shape (figure from Gothelf et al. (2008) according to the model from Goldman-Rakic et al. (2000)). In the general population (white circles), the Val high-activity allele is associated with low dopamine level, which may be too less for optimal prefrontal function. By contrast, the low-activity Met allele is associated with higher dopamine level, appropriate for cognitive function. As individuals affected by 22q11DS have only one copy of the COMT gene, they have higher concentration of dopamine that places them on the right of the inverted-U shape. Even with the Val (high-activity) allele they still have too much dopamine for an optimal prefrontal function, whereas the dopamine concentrations are even higher with a single copy of the low-functioning Met allele.*

Chapter 2

Neuroimaging as a tool for studying brain development

The extraordinary burst of acquisition and cognition processes development during childhood are underlined by major microscopic and macroscopic changes in the brain. First delineated by postmortem studies, MRI has become a powerful tool for studying in vivo the structural correlates of brain maturation.

2.1 Magnetic Resonance Imaging for the study of brain development

Magnetic Resonance Imaging (MRI) takes advantage of the magnetic properties of atoms nuclei, i.e. their ability to align along a magnetic field. On the contrary to Computer Tomography (CT), MRI scanners do not use ionizing radiations, being therefore safe for the patient. Different contrasts in the images (T1-weighted, T2-weighted and Diffusion Tensor Imaging) are obtained from modifications to the acquisition parameters. As a result, the excellent contrast for visualizing soft tissues elects MRI as an ideal modality to study the brain development *in vivo*.

Less than thirty years ago, the entirety of our knowledge about the structural modifications occurring during brain development was derived from postmortem studies. The low rate of mortality during childhood and adolescence restrained large scale quantitative studies. Further, postmortem modifications of the intra- and extra-cellular liquid repartition rendered the measurements imprecise. Thus, the study of brain development, which was the exclusiveness of neuropathology, was completely revolutionized by the generalization of MRI exams. Nowadays, methodological developments that were permitted by the evolution of computer power allow the delineation of maturational morphological trends with increasing precision (see also the red box on the next page).

The study of cortical folding before the era of MRI and computers

To illustrate the practice of cortical anatomy at the middle of the XIXth century, a text written by Baillarger (Baillarger, 1853) is transcribed below. In order to preserve the sense and spirit of the text, it was kept in its original language; the symbol "–" denotes parts that were removed:

"Je me propose dans ce travail de déterminer l'étendue de la surface des hémisphères cérébraux –. La pie-mère – s'enfonce dans toutes les infractuosités, et sa surface est égale en étendue à la surface du cerveau. Si cette dernière membrane pouvait être déplissée, elle fournirait un moyen très simple et très exact de mesurer les surfaces cérébrales; mais il n'en est pas ainsi, et il faut chercher un autre procédé. La première idée qui se présente, c'est le déplissement du cerveau lui-même. – Malheureusement le déplissement du cerveau – soulève une objection très grave. La substance cérébrale est extensible, et les tiraillements exercés avec les doigts peuvent devenir une cause d'erreur. – Le procédé que j'emploie consiste à déplisser le cerveau, en substituant à l'action des doigts une dissection longue et minutieuse, ayant pout but d'éviter toute espèce de tiraillement. J'enlève peu à peu la plus grande quantité possible de substance blanche, et je réduis ainsi graduellement l'hémisphère à une très faible épaisseur. Quand la substance médullaire a été presque complètement enlevée, la membrane hémisphérique se déplisse, pour ainsi dire, d'elle-même, sinon en totalité, au moins suffisamment pour qu'on puisse l'étaler et la mouler très exactement avec du plâtre. Cette membrane cérébrale étant retirée du moule, on peut obtenir l'étendue de sa surface par le procédé suivant. On remplit peu à peu ce moule avec de la terre glaise en interposant un tissu mince dont la surface plane est ensuite très facile à mesurer mathématiquement. – Voici les résultats auxquels je suis arrivé par ce procédé. Sur cinq cerveaux, j'ai trouvé pour l'étendue des surfaces une moyenne de 1,700 centimètres carrés. – La différence d'un hémisphère à l'autre n'est guère que de 1/50 à 1/45, ce qui est une preuve de l'exactitude de la mesure."

The present chapter overviews methological aspects of image processing, and summarizes the most important contributions in the field of structural brain changes. Of note, given that cortical complexity is a central topic in this dissertation, the rationale for measuring cortical folding and related methodological aspects will be presented separately in the next chapter.

2.2 Neuroimaging techniques: an overview

The first quantitative studies providing morphometric measurements of the brain in samples of healthy individuals were published in the nineties. Until 1995-2000, these studies mainly measured gray or white matter volumes, by lobe or in specific regions of interests. The second generation of image processing techniques emerged around 2000, with voxel-based approaches. Soon thereafter, more reliable and anatomically correct three-dimensional reconstructions of the cortex were developed. Nowadays, these three techniques complement each other in everyday practice.

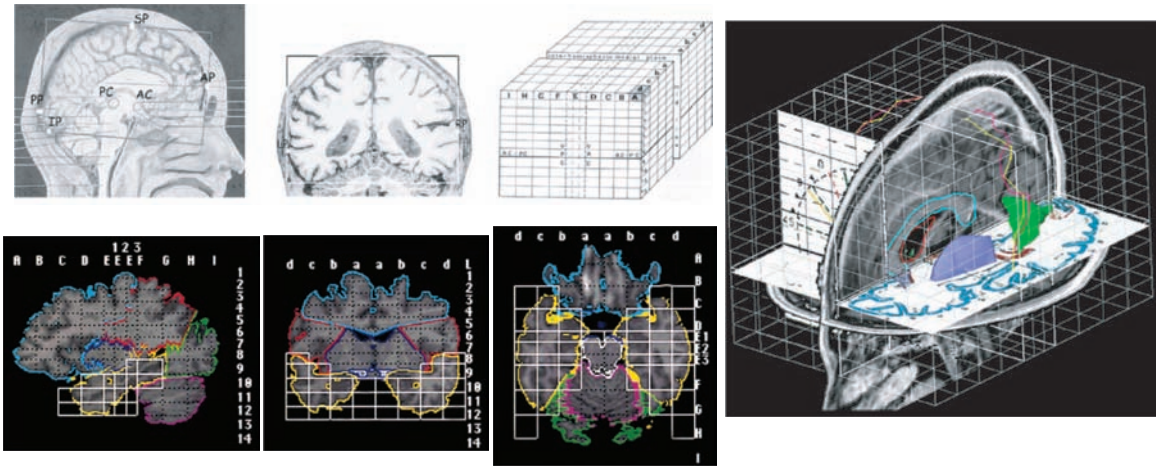

Figure 2.1: *The Talairach & Tournoux grid (1988) developed by two neurosurgeons uses the anterior commissure (AC) and the posterior commissure (PC) as landmarks for scaling boxes. In turn, the Talairach coordinates are easily used to define any structure, including entire lobes (as shown with the colors on the lower row). Images are taken from Han et al. (2004), Kates et al. (1999) and Ganser et al. (2004).*

2.2.1 Volumetric studies: lobes and Regions-Of-Interest (ROI)

Cerebral MRI datasets typically consist on a three-dimensional volume, where each voxel is attributed an intensity, which closely reflects the biological properties of the tissue. The intensity distribution of the image (histogram) is exploited to distinguish between gray, white matter and cephalo-spinal fluid (CSF), a process known as segmentation. In addition to voxel intensity, segmentation algorithms frequently use atlas-based information, or geometric information such as Markov chains to create probabilistic maps reflecting the distribution of the different tissue classes. The probabilistic maps are an elegant manner to cope with the possibility that a single voxel contains more than one tissue type (partial volume effect). Overall volumes of the different tissue compartments (gray and white matter) are computed as the sum of voxels multiplied by their tissular probability. Semi-automated atlas-based subdivisions or manual landmarks are then typically used to obtain a finer localization in cerebral lobes, and cerebellar volumes. For instance, Figure 2.1 depicts the use of the Talairach grid (Talairach et al., 1988) to subdivide automatically the brain into the four main lobes.

Smaller regions, such as the amygdala or the hippocampus, are outlined by hand on coronal or sagittal slices. Standardized, validated, protocols define precisely the boundaries of the structures (e.g. Kates et al., 1997). Applying the rules defined in the protocol, two independent raters should obtain similar volume estimation for the same subject. Although manual techniques may seem poorly reliable at a first sight, regions-of-interest analyses still represent the gold standard to measure the volume of specific structures. For example, despite automated methods for delineating the hippocampus exist, manual delineation still provide more accurate results, as compared to recent fully automated techniques (Tae et al., 2008). However, the ROI technique presents the disadvantage to be highly time-consuming. Further, the number of structures that could reliably be delineated is limited, because the anatomical boundaries circumscribing a structure are not always evident. Subcortical

structures are often accurately delineated, but the large inter-individual variability in sulci position (Ono et al., 1990) is a major issue impairing the delineation of cortical regions.

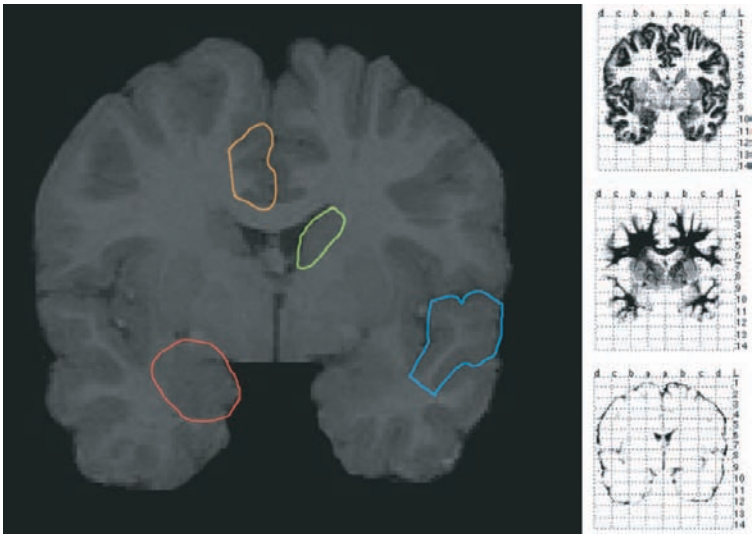

Figure 2.2: *On the left, a coronal slice on which region-of-interests are manually outlined (image from Schaer et al., 2007). Amygdala is drawn in red, cingulate gyrus in orange, caudate nucleus in green and superior temporal gyrus in blue. Prior to delineation, cerebral images are classically reoriented, and strictly validated protocols ensure a maximized reliability between different raters and across the sample of individuals. Measurements are then conducted on segmented images (right).*

2.2.2 Voxel-Based Morphometry (VBM)

Because regions-of-interest were particularly labor-intensive and required a hypothesis to select the structure to be examined, voxel-wise statistical approaches have been designed to identify regional differences in gray matter concentration quickly, and without regional a priori (Ashburner et al., 2000). Preprocessing in Voxel-Based Morphometry is intended to allow for statistical analyses of local gray or white matter density. Spatial normalization warps cerebral images to match a common template, and smoothing is implemented to cope with inter-individual differences in sulcal patterns. Then, statistical differences in

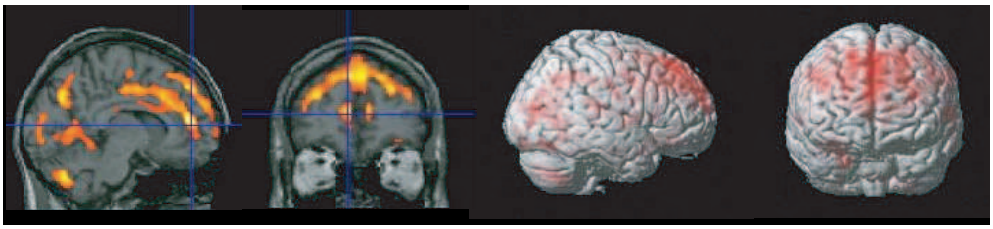

Figure 2.3: *Example of result using Voxel-Based Morphometry in images from our cohort. As illustrated with regions of smaller gray matter density (in yellow-red), focal differences can be identified independently of anatomically defined boundaries like it is the case for ROI techniques.*

gray or white matter concentration are computed at each voxel, using a general linear model (Statistic Parametric Mapping).

Voxel-based morphometry carries the main advantage of assessing quickly focal differences over the whole brain, using a completely automated process (see Figure 2.3 for an example of result) and has thus been extensively applied in a variety of neurodevelopmental and neurodegenerative conditions. Beside its apparent simplicity, one should be particularly careful when setting the parameters used in the spatial normalization, especially in conditions associated with a different brain shape. Indeed, Eckert and colleagues (2006) demonstrated completely different results depending on the choice of the registration parameters in children with Williams syndrome (who are known to have uniquely shaped brain with consistent posterior reductions). The major effect of parameters' choice on the results is also related to the fact that classical VBM does not allow a direct inference about volume, but informs on the deformation. To provide a more direct and accurate interpretation of the results, optimized VBM (Good et al., 2001) has been proposed, and uses the jacobian determinant to infer volumetric differences from the transformation process.

2.2.3 Three-dimensional cortical reconstructions

If VBM techniques allow for a rapid and completely automated estimation of focal differences, the volumic processing of VBM does not take into account the two-dimensional organization of the cortical sheet. Specifically, cortical regions that are near in terms of Euclidian distance may indeed be far away in terms of cortical arrangement (i.e. the banks of one sulcus). More recently, three-dimensional representations of the folded cortical sheet that better deal with this issue were proposed (Dale et al., 1999; Fischl et al., 1999; Magnotta et al., 1999), allowing precise estimations of cortical area, thickness or volume. Among the challenges encountered to create a good cortical reconstruction, are buried sulci, exclusion

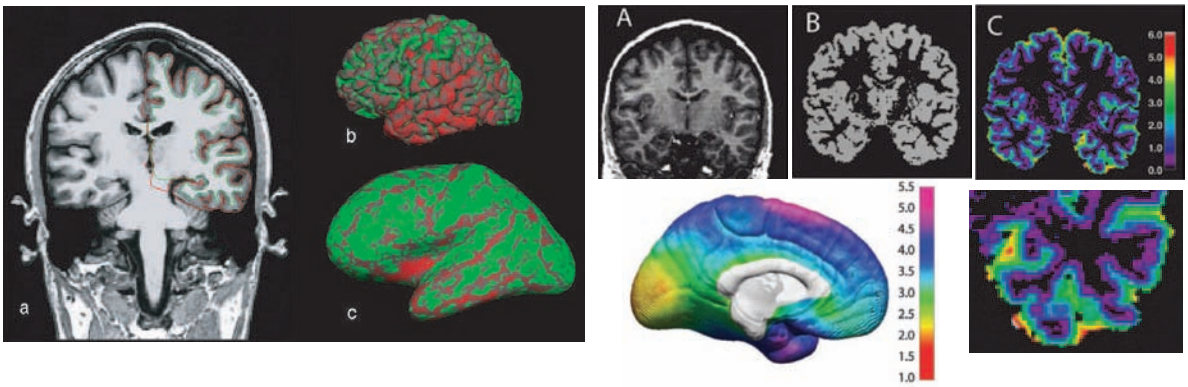

Figure 2.4: *The left side of the figure (Schaer et al., 2007) depicts measurements of cortical thickness based on 3D reconstruction of the cortical surfaces. Thickness is overlaid with a colorcoded scale on the pial and inflated representation of the brain. On the right, a non-mesh-based method is shown (Sowell et al., 2004), in which thickness is progressively coded from inner to outer layers of cortex using the 3D Eikonal Fire equation.*

of basal ganglia, and the need for a precise intersubject correspondence. Buried sulci are typically included by using constraints on the planar structure of the cortical sheet, and basal ganglia are often excluded using atlas-based masking. The resulting 3D cortical representations (meshes) typically comprise a fixed number of 100'000 (Magnotta et al., 1999) or a variable number of 80'000 to 150'000 vertices (Dale et al., 1999). Measurements of cortical thickness are computed at each vertex (Fischl et al., 2000; Lerch et al., 2005), and point-by-point registration is achieved through optimal alignment of sulcal patterns (Fischl et al., 1999; Thompson et al., 2003). As a result, cortical thickness measurements provide an exquisite precision in the localization of the alterations. Of note, methods for estimating thickness that are not based on reconstructions of the inner and outer cortical surfaces (see Figure 2.4) are also less precise.

Cortical thickness values are compared using vertex-wise statistics. Similarly to VBM, these statistics do not allow to control for Type-I error. For that reason, it has been of interest to develop methods allowing for the control of false positive errors, while retaining sufficient spatial resolution. Several groups have simultaneously proposed algorithms for sulcal recognition and classification (Fischl et al., 1999; Riviere et al., 2002), an information which is subsequently used to subdivide between the different cortical regions (Cachia et al., 2003; Desikan et al., 2006). Figure 2.5 details the processes used by one of these methods (Desikan et al., 2006), resulting in measurements of regional cortical volumes. For cortical regions, gyral parcellation may rapidly replace manually delimited ROI, as a powerful tool to obtain automatically accurate regional volumes without regional a priori.

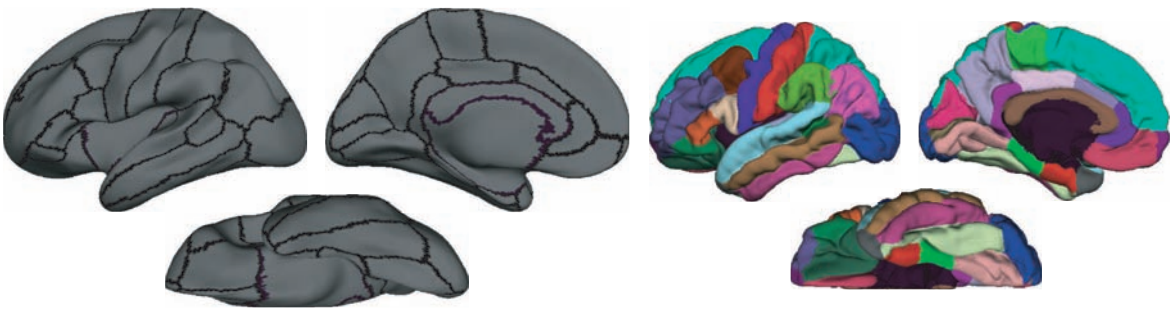

Figure 2.5: *Gyral parcellation method (Desikan et al., 2006), applied on an average template from our cohort. The left side of the figure shows the limits of the parcels on the inflated brain representation. The right side depicts the 34 cortical regions on the pial surface of the average subject.*

2.2.4 Diffusion Tensor Imaging (DTI)

Parallel to morphometric studies based on T1-weighted images, another modality gained the interest of researchers for quantifying brain structure: Diffusion Tensor Imaging (DTI). DTI is particularly adapted for analyzing the white matter structure (Pierpaoli et al., 1996), and changes in water content associated with maturation (Mukherjee et al., 2002).

Diffusion Tensor Imaging is based on the Brownian movement of water molecules, which is restrained by axons in the white matter. As a result, DTI images are considered to reflect

the microstructural properties of white matter. A minimum of six gradients (directions) is required to construct a tensor containing the information encoding the direction of water molecules movement at this point (see Figure 2.6). DTI sequences can typically contain up to 60 directions, whereas Diffusion Spectrum Imaging (DSI) most often comprise up to 200 directions. The tensor information is exploited using diverse manners. Colormap may be created to visualize the direction of fibers tracts. Alternatively, Fractional Anisotropy (FA) measures the orientation of the fiber tracts, which is commonly implemented to infer the degree of connectivity in neurodevelopmental conditions (Barnea-Goraly et al., 2003; Barnea-Goraly et al., 2003). Maps of FA are typically compared on a voxel-wise basis. More recently, tract based FA statistics, unbiased by differences in brain shape, have been proposed (Berman et al., 2005; Smith et al., 2006).

One step farther, fiber tracking offers a promising tool to reconstruct axonal trajectories in the brain from DTI images (Mori et al., 2002). Beyond the esthetics of "virtual axonal dissections" (Hagmann et al., 2003), methods are now being developed for quantitative comparisons of the pattern of axonal connections (Hagmann et al., 2007).

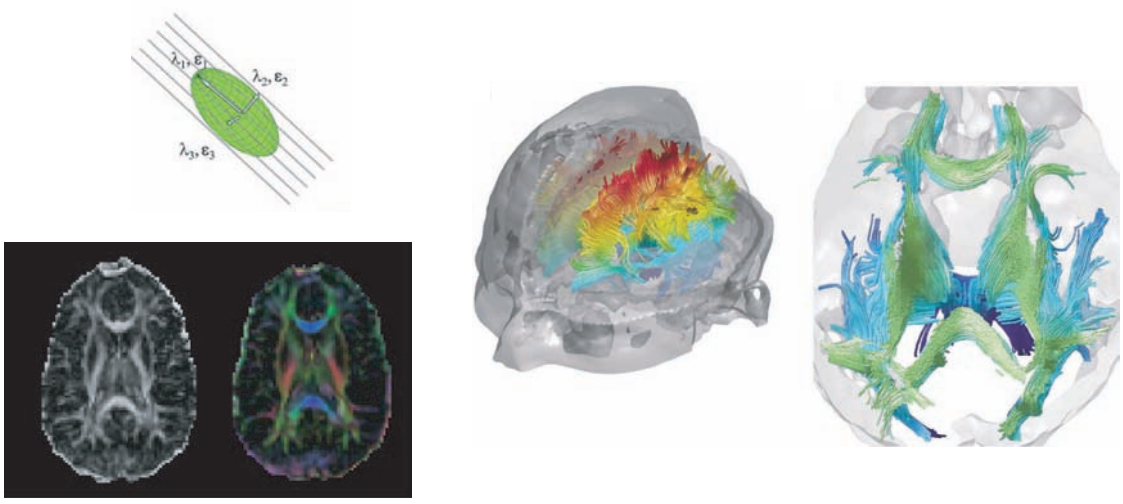

Figure 2.6: *On the left, upper image, the tensor reconstructed from DTI images is depicted (image from Kubicki et al., 2007). Below the tensor are examples of Fractional Anistropy map (left) and colormap (right) in one subject from our cohort. On the right, axonal reconstruction is depicted (image from Taylor et al., 2004).*

2.3 Normal brain maturation

A large part of what we know about human brain development is derived from postmortem studies, and studies in other mammals. The main events leading to the creation of brain structures involve differentiation, proliferation, and migration of neurons from the subventricular zone to their final position: the cortex. Then, axonal elongation is guided by the growth cone until their final destination. After axonal growth, all cerebral structures are considered to be created, but the brain tissue will be extensively remodeled *in utero*, and to a lower extent throughout the entire life. Indeed, the nervous system development occurs

with suproduction and subsequent eliminations of connections, which subserve increased efficiency and specificity of the neural networks (Changeux et al., 1976). Synapse formation (synaptogenesis), begins well before birth and continues during the first 2 years of life, leading to an excess of synapses. The onset of functionality in the cortex may correspond to the end of rapid synaptogenesis (Huttenlocher, 1979). For instance, visual cortex functions, such as the ability to perceive differences in the depth of field, emerge when synaptic density in the visual cortex reaches its maximal value (Wilson, 1988). Then, the subsequent dendritic reorganization during childhood encompasses the normal elimination of up to 40% of the synapses (Huttenlocher, 1979). Synaptic elimination, known as pruning, allows for an optimization of the neural circuitry through the elimination of surnumerous connections. During the pruning period, an increased sensitivity to environmental influences has led to the proposal of critical periods during brain development (see also the green box on next page).

We have seen that gray matter development and maturation encompass the refinement of the connections. Similarly, white matter undergoes consequent changes during brain maturation. Myelination of axons, which defines the development of oligodendrocytes surrounding axonal tracts, allows for an increase in conduction velocity of the electric signal. Myelination process begins from the mesencephalon, and progress from posterior to anterior regions (Yakovlev et al., 1967). Most of the myelination's process occurs *in utero* and during the first 2 years of life, but the process still progresses well into childhood and adulthood.

These maturational processes first delineated by microscopic studies are translated in observable volume changes during childhood and adolescence. It is known that 25% of the adult cerebral volume is approximately reached at birth (Dekaban, 1977). Prominent progressive events, such as glial proliferation, dendritic arborisation and myelination, lead to a fast growth, so that 80% of the adult volume is reached at age of 2, and 95% at the age of 5 (Dekaban, 1977). After that age, important modifications in the proportions of brain tissue still occurs (i.e altering the ratio of gray, white matter, and cephalo-spinal fluid (CSF)). For instance, regressive events in the gray matter, such as cell death and synapse elimination, reduce its volume (Cowan et al., 1984). Concomittantly, the progression of myelination increases white matter volume, so the the overall cerebral volume remains stable. As stated in the first part of the chapter, MRI stands as an ideal tool to study *in vivo* the remodeling of cerebral tissue that takes place during childhood, adolescence and adulthood.

Critical periods in development

As defined by Hensch (Hensch, 2005), a critical period is "a strict time windows during which experience provides information that is essential for normal development and permanently alter performance". The best known example of critical period has won the Nobel prize in 1981. Hubel and Wiesel discovered that monocular deprivation related to sutured eyelid during the critical period was causing functional blindness to the deprived eye (Hubel et al., 1964). Despite that the eye and optic nerve are completely functional after eye reopening, no more inputs from that eye were received by the visual cortex. Critical periods for more complex functions seem also to exist, as for example language. Huttenlocher points that the windows during which learning a second language is relatively effortless and accent-free terminates approximately at the age of 12 (Huttenlocher, 1999).

The synaptic correlates of critical periods have received a wide interest. It appears that the end of the critical period, changes in Nogo receptors configuration and rigidification of the extracellular matrix make it harder for further extensive plasticity to occur (Sengpiel, 2007). If prolongating the critical period may open unestimable opportunities for reeducation or for enhanced learning, the period of increased environmental sensitivity also rends the brain more vulnerable. Indeed, disorders of synaptic plasticity and pruning may be relevant for the study of specific psychopathologies. For instance, dysregulated pruning during the critical period have been suggested to participate to the onset of both addiction disorders (Arnsten et al., 2004; Crews et al., 2007) and schizophrenia (Hoffman et al., 1989; Keshavan et al., 1994).

2.3.1 Macroscopic brain maturation as studied with MRI

Volumetric studies

Among the extensive literature on normal brain maturation, the most referenced volumetric study is probably the one by Giedd and colleagues, based on 145 healthy subjects from 4 to 22 years old (Giedd et al., 1999). Thanks to repeated neuroimaging, they could observe the regional specificities of quadratic trajectory of gray matter changes with age (i.e. the increase during childhood, followed by peak and decrease in adolescence, see Figure 2.7). Parietal and frontal gray matter volumes were shown to peak around 12 years old for boys, and 11 years old for girls. Temporal gray matter showed a late maturation, peaking after the age of 16. Finally, occipital gray matter followed a different profile, with slight volumetric increase during the entire adolescence. A few interpretations can be made from these regional specificities. First, the earlier frontal and parietal peak in girls compared to boys may reflect an influence of sexual hormones on brain development (Giedd et al., 1997). Second, the regional maturational profile may be related to the development of the different cognitive processes. For instance, the late maturation of the temporal lobe may reflect language development, a competence that still consequently improves during late adolescence.

Evidences of the progressive and regressive events in the gray matter have also been delineated through functional studies. Indeed, PET studies have suggested that maturation of the local metabolic rate parallels the initial surproduction and subsequent pruning of synapses in the different cortical regions (Chugani et al., 1987). The reduced cerebral metabolism associated with cerebral maturation seems closely related to an improvement in cognitive capacities. For example, fMRI studies have established an inverse association between cerebral activation and arithmetic performances (Menon, 2000). Indeed, individuals solving correctly a calculation task were shown to activate less largely and less intensively

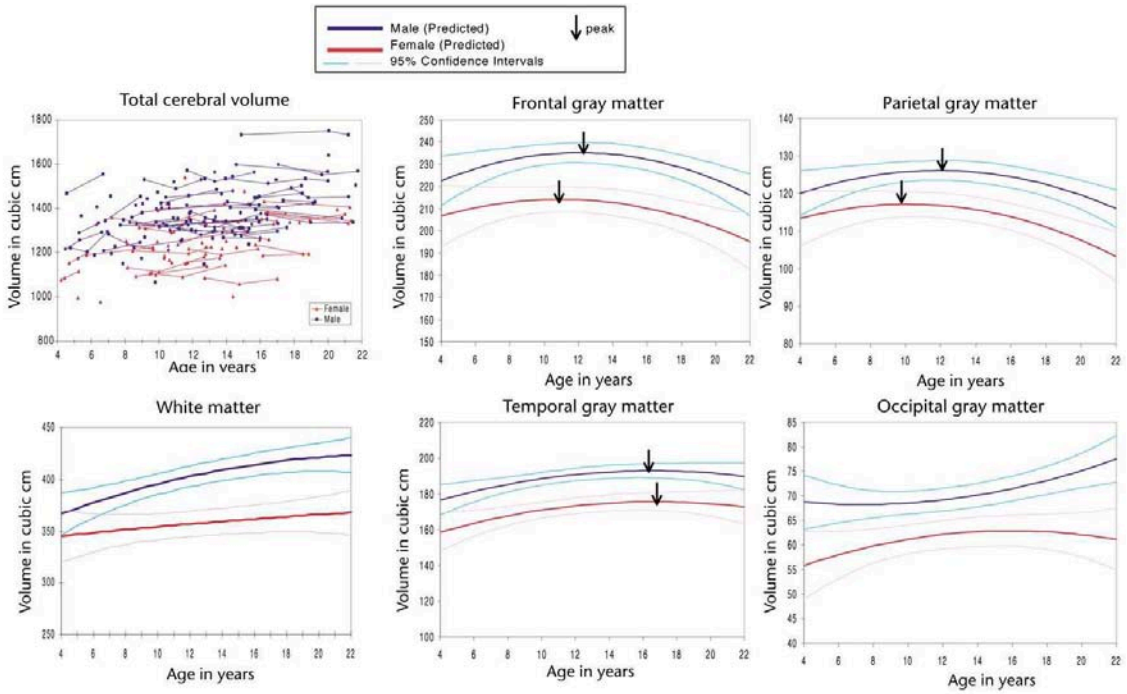

Figure 2.7: *Developmental course of lobar volume in children and adolescents (reformatted from Giedd et al., 1999). White matter is shown to follow a continuous, linear, increase, whereas arrows indicate peaks in the gray matter profile.*

the parietal cortex than individuals with poorer performances.

In summary, gray matter maturation is associated with different processes devoted to increase the efficiency of the neural system:

1. A decrease in synaptic density allowing the selection of the most appropriate connections
2. A reduction in the use of metabolic resources, as evidenced by PET and fMRI studies
3. On the macroscopic level, these transformations appear with gray matter volume reduction.

As a result of the striking regional and temporal similarities of these three processes, both cortical activation and gray matter volume have been suggested to be reliable marker of synaptic pruning, and hence, of critical periods during brain development.

Thickness studies

More recently, techniques of image analysis have evolved, and cortical thickness measurements have been proposed to delineate maturational changes with increasing precision. With their exquisite spatial resolution, thickness studies seem more able to reflect the cortical remodeling than were volume changes. A wide amount of studies have been conducted with healthy participants (Sowell et al., 2003; Gogtay et al., 2004; Thompson et al., 2004; Shaw et al., 2006; Shaw et al., 2008), confirming the potential of cortical thickness to reliably identify critical periods in brain development. Further, a growing

amount of studies have applied thickness measurements in patients with neurodevelopmental conditions, such as attention-deficit/hyperactivity disorder (ADHD) (Shaw et al., 2006; Shaw et al., 2008), autism (Chung et al., 2005; Hadjikhani et al., 2006; Hardan et al., 2006), or schizophrenia (Kuperberg et al., 2003; Thompson et al., 2004; Greenstein et al., 2006). Here, we briefly describe three studies that are, on our opinion, of particular interest in the field (Shaw et al., 2006; Shaw et al., 2007; Shaw et al., 2008).

1. **Cortical thickness trajectories in normal brain development (Shaw et al., 2008)**
In this study encompassing a total of 764 normative scans, Shaw et al explored the trajectories of thickness growth across the cerebral cortex. Using mixed model regression analysis at each cortical point, they were able to classify the trajectory at each point in cubic, quadratic, or linear (see figure). With such an impressive number of data, they identified that most cortical regions were following a thickening during childhood, followed by thinning during adolescence and stabilization into adulthood (in red). They further confirmed the heterochronous sequence of cortical development, with a precise description of regional variations in age of attaining the peak. Finally, they demonstrated that the pattern of cortical development mirrors previously histologically-defined cytoarchitectonic maps. For example, in the orbitofrontal cortex (lower part of the figure), the isocortex was shown to follow a cubic trajectory, whereas the allocortex showed a predominantly linear growth.

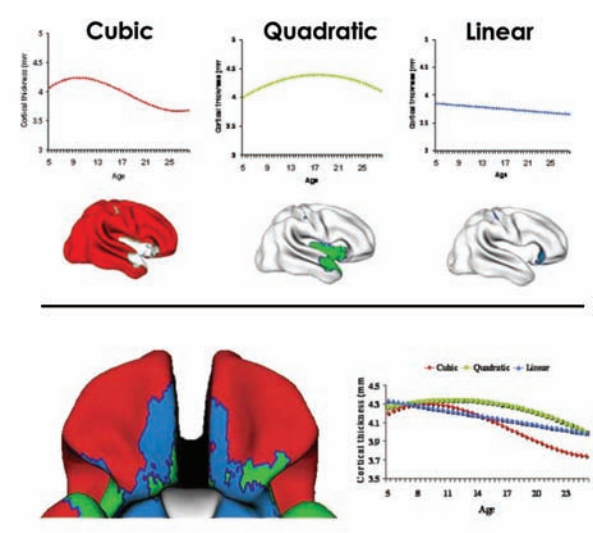

2. **Cortical thickness and intelligence in healthy children (Shaw et al., 2006)**
In this article published in *Nature*, Shaw et al sought to examine whether academic aptitudes impact cortical development. They subdivided a sample of 375 children into three IQ groups: superior (range 121-149), high (range 109-120) and average intelligence (range 83-108). Vertex-wise comparisons revealed that children with superior intelligence had a thicker cortex at youngest age (blue overlay aside), but a thinner cortex at the end of adolescence (red). This unique pattern, which was most prominent in the prefrontal cortex, corresponded to a faster rate of change of cortical thickness in the superior intelligence group. The rate of changes (reproduced aside) also demonstrated that the age of peaking (intersection with the x axis) was significantly older (11.2*yr*) in the superior intelligence group compared to the average group (5.6*yr*), possibly allowing for a prolonged period of circuitry refining.

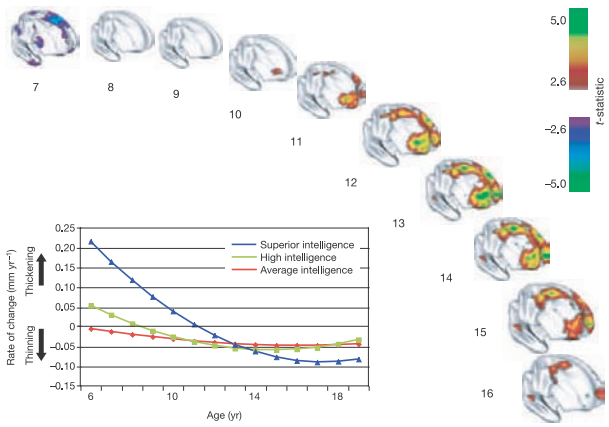

3. **Cortical thickness in children with ADHD (Shaw et al., 2007)**
   Using a total of 824 scans (223 children with ADHD and 223 typically developing children), Shaw et al delineated the quadratic growth trajectories of cortical thickness with age, and derived the age of attaining the peak. Their most compelling finding is that maturation proceeded in a similar manner, with primary sensory areas peaking before polymodal areas, but with a marked delay in children with ADHD. In the figure aside, the blue overlay depicts the delay in the group of children with ADHD compared to controls. Further, Kaplan-Meyer curves demonstrate that the median age of attaining peak was significantly retarded in children with ADHD ($10.5yr$) as compared to the group of typically developing controls ($7.5yr$).

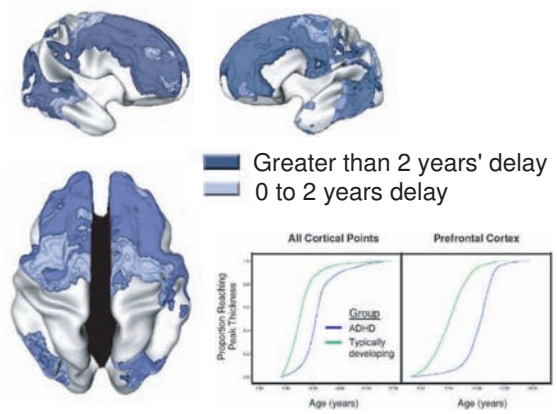

Each of the three thickness studies presented above has major implications to promote cortical thickness as one of the most important tool for following normal and abnormal brain maturation in children and adolescents. First, cortical thickness was shown to be able to reflect microscopic cortical architecture, with its dynamic being dependent upon the number of cortical layers. Second, intelligence was found to be related to a dynamic property of the brain, rather than relying on more gray matter volume at any one age. Third, thickness was found to be a powerful marker of cerebral maturation in neurodevelopmental conditions.

Chapter

3

Cortical folding (Gyrification)

Understanding why and how does the mammalian cerebral cortex fold has fascinated neuroscientists since more than a century. Experimental studies in animals have brought the commonly accepted view that sulci are shaped by axonal traction during gestation. In humans, the study of cortical morphology has also received a large interest, as a window on early brain development.

3.1 Phylogeny of cortical folding

The first studies aiming at understanding how the cerebral cortex folds mainly focused on the degree of convolution and its comparison across species (see Figure 3.1). Indeed, previous studies have suggested that a universal scaling rule may govern interspecies brain architecture (Prothero et al., 1984; Hofman, 1985; Zhang et al., 2000), with surface area increasing faster as a function of brain volume than cortical thickness. The drastic cortical expansion without major thickening may be genetically determined through the control of horizontal cell proliferation. Accordingly, the radial unit hypothesis (Rakic, 1988) postulates that the regulation of tangential (asymmetric) *vs* radial (symmetric) cell division during neuronal proliferation controls the final number of cortical column units, and hence cortical area. Evidence for such a mechanism was recently supported by knock-out mice studies, in which mutation of a gene controlling asymmetric neuronal division resulted in cortical folding (whereas the cortex of mice is normally smooth) (Chenn et al., 2002).

Figure 3.1: *From the observation of different mammalian species (image from www.brainmuseum.org), it becomes evident that the bigger brains are more convoluted. For instance, the dolphin brain at the center of the image shows the more complex pattern of sulci.*

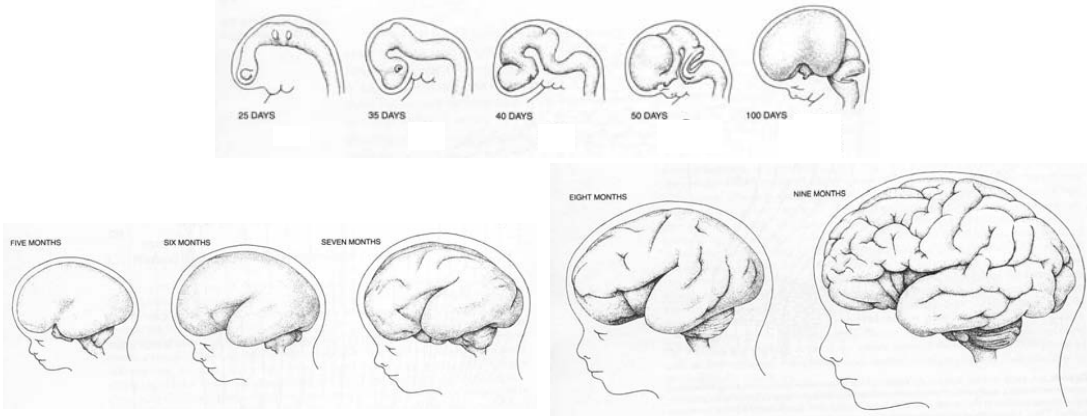

Figure 3.2: *In humans, cortical folding (gyrification) begins at the 4^{th} month of gestation, when neuronal migration is completed. The sylvian fissure is the first sulcus to appear, followed by the central sulcus and the parieto-occipital sulcus. By week 30^{th}, all primary sulci (largely similar between individuals) are formed (Armstrong et al., 1995). Secondary sulci, moderately variable, are then constituted. Finally, at week 36^{th}, tertiary sulcus, highly variable between individuals begin to appear (Chi et al., 1977).*

3.2 Ontogeny of cortical folding in humans

In humans, the study of cortical folding development in fetuses and newborns has relied for long solely on postmortem data and ultrasound examinations, which allowed the definition of a few qualitative markers of brain development. For instance, the appearance of sulci in the developing brain is now well defined (Worthen et al., 1986; Huang, 1991). Nowadays, a more precise establishment of quantitative norms of gyrification, such as the relationship between volume, surface area and / or degree of folding, may be more precise than solely the presence or absence of sulci. In turn, such quantitative markers may have large clinical applications as indicator of neurodevelopment. Ultrasound examinations, with their poor spatial resolution and high dependence on the radiologist experience, are unlikely to be able to provide accurate enough 3D cortical representations. Thus, the development of fetal MRI may open new perspectives for research on convolutional development. MRI has been proposed to study the fetal anatomy as early as 1983 (Smith et al., 1983), but concerns related to the safety restrained its use. If MRI exams remain counter-indicated during the first trimester of pregnancy (due to its possible impact on embryogenesis (Yip et al., 1994)), no sequelæ have been reported in pregnant women that were exposed to the magnetic field every day during the second and third trimester of pregnancy (Kanal et al., 1993). As a result, MRI is currently used as a supplementary diagnosis tool if abnormal fetal development is suspected on ultrasound examination. However, the use of fetal MRI for research purposes would require far better image quality than the one used in clinical setting, which is challenged by fetal motion. Current methodological developments focus on the possibility to obtain high resolution images from a set of low resolution images (thus less subjected to motion) (Rousseau et al., 2006).

Because of the challenges related to fetal neuroimaging, MRI of premature newborns have been used to delineate cortical folding development from 26 weeks of gestation onward (Rodriguez-Carranza et al., 2006; Dubois et al., 2008). The head of newborns being easily fixed, nice resolution images can be obtained while they sleep. In turn, accurate cortical representations are reconstructed and used to quantify cortical folding. However, prematurity is often associated with other deleterious medical conditions, so that the developmental picture obtained with these children may not truly reflect normal neurodevelopment. Of note, among 35 newborns that participated in the study of Dubois and colleagues (Dubois et al., 2008), 10 babies were having qualitative lesions sufficiently important to be observed on eye examination. Further, studies of gyrification in children and adolescents who were born prematurely have reported anomalies of cortical folding that persist in grown-up children (Gimenez et al., 2006; Kesler et al., 2006). In sum, if future technical developments permit precise fetal brain reconstructions from prenatal MRI, studying healthy fetuses will certainly stand as a better option than premature newborns to delineate the normal course of cortical development.

3.3 Determinants of cortical folding

As depicted in the last section, cortical sulci are largely determined by infancy. As a result, studying cortical morphology in children, adolescents and adults possibly convey a lot of information on the early development of their brain.

Understanding pathological convolutional development requires a precise delineation of the determinants of cortical folding. Nowadays, the processes leading to the creation of the folds, as well as the functional significance of the number, length, depth and orientation of sulci, remain largely unexplained. The three following models provide attempts at explaining how adult cortical morphology is built.

1. **Tension-based model of convolutional development (Van Essen, 1997)**
   This theory postulates that many features of the mammalian cortical shape can be explained by mechanical tension along axons, dendrites and glial processes during development. The disproportionately large cortical surface area is thought to be shaped by pulling strongly interconnected regions towards one another (see figure). In turn, this connectivist model results in a compact wiring of the nervous system. Experimental studies with lesion of the thalamo-cortical connections corroborate Van Essen's theory (Goldman-Rakic, 1980; Dehay et al., 1996). Applied to humans, the tension-based model would suggest that disturbed gyrification results from abnormal pattern of connectivity. For instance, larger gyri and deeper sulci may result from weaker local interconnections, with unchanged traction exerted by the long connections.

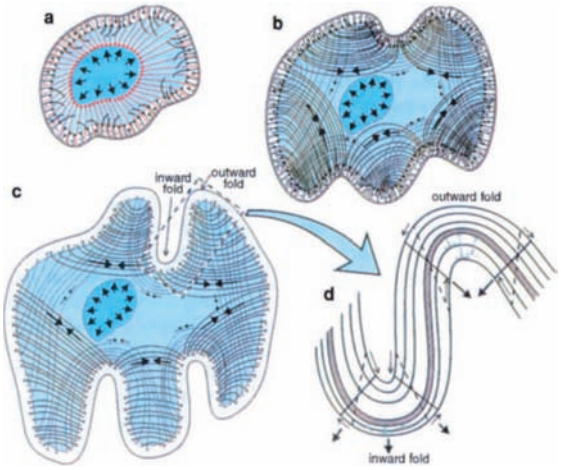

2. **Intrinsic cortical determinants of convolutions (Richman et al., 1975; Welker, 1990)**
   Welker (Welker, 1990) suggests that mechanical forces intrinsic to the cortex, rather than passive extra-cortical tension, can be primary determinants of convolutional development. This theory is grounded on evidences that many processes are differentially expressed in gyral crowns and in sulci, both in terms of intensity and timing. For instance, Welker points that neurons differentiate and grow earlier in gyri than in sulci, which is also accompanied by an earlier differentiation of the cortical sheets. Further, both synaptogenesis and glial proliferation appear more profuse and voluminous in gyral crowns than in fundi. Finally, rearrangement of cell adhesion molecules, affecting cortical rigidity, is likely to be also differentially regulated in gyri and sulci, thus actively shaping convolutions. The drawing aside, from (Welker, 1990), depicts developmental changes in radial and tangential orientation of cortical layers during convolutional development in the ferret brain. In the same direction, Richman et al (Richman et al., 1975) observed that differential growth of the layers results in buckling of an experimental cortical surface.

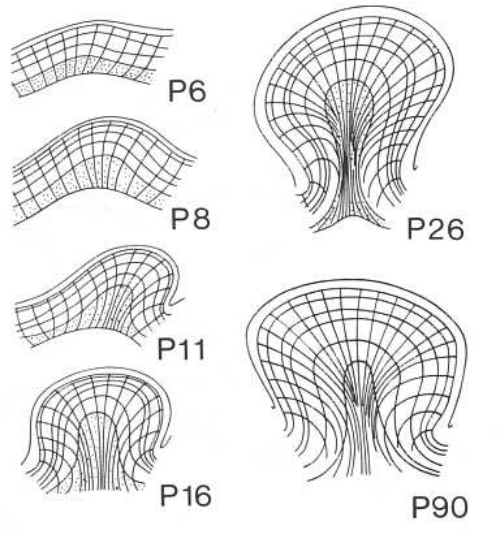

3. **The sulcal root hypothesis (Régis et al., 2005)**
   This theory proposed by a French neurosurgeon is more recent, and thus received less emphasis in the literature to date. The sulcal root model explains interindividual differences in sulcal patterns through different recombination of highly stable sulcal subunits. The elementary subunits (in green and red in the schematic drawing aside) may be interrupted by buried *plis de passage* or *annectant gyri*, in turn resulting in a different configuration of the sulcus. For instance, the lower row shows two different configuration of the superior temporal sulcus. The sulcal root model also questions the validity of the actual nomenclature of sulci and argues for the use of smaller sulcal entities to redefine the classification scheme. Ultimately, such a model identifying stable sulcal landmarks may largely facilitate the systematic study of the function – structure relationship.

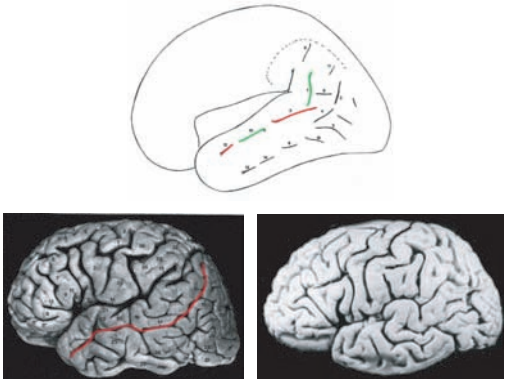

3.4 Abnormal cortical folding

The three models presented above illustrate how cortical folding is a tightly regulated process, dependent upon the normal completion of several other processes, such as normal neuronal proliferation and normal connectivity. As a result, abnormal gyrification often accompanies neurodevelopmental disorders, and the extent and intensity of abnormal folding may represent a window on the early brain development.

For instance, abnormal quantitative gyrification has been reported in different conditions, leading to various interpretations. Increased gyrification in children with Williams syndrome (Schmitt et al., 2002; Gaser et al., 2006) has been suggested to rely on a developmental arrest (Schmitt et al., 2002). In dyslexia, reduced cortical complexity may be associated with an increase in the number of long connections, and result in slowed down information processing (Casanova et al., 2004). Conversely, strong local interconnectivity may decrease gyri width. If this was the case, frontal over-connectivity in autism (Courchesne et al., 2005) would be responsible for the increased GI observed in the frontal lobes of autistic children (Hardan et al., 2004).

3.5 Studying cortical folding

Many different methods for studying cortical folding were proposed, grounded on different aspects. Some techniques focused on the quantity of cortical area allowed by the process of folding (surface-based method), while other focused on the elementary unit of cortical morphology: the sulcus (sulcal morphometry). Further, methods measuring geometry information were proposed, such as Fractal Dimension, or curvature-based methods.

3.5.1 Surface-based approaches: Gyrification Index

In the second half of the 20^{th} century, comparative neuroanatomists quantified folding using a simple zero-order surface ratio (Jerison, 1961; Haug, 1987). The Gyrification Index (GI) was defined as the ratio of the total folded cortical surface over the perimeter of the brain, delineated on two-dimensional coronal sections (see Figure 3.3). Many studies were conducted to quantify GI differences between species, and the first study of human postmortem data was published in 1988 (Zilles et al., 1988).

Zilles and colleagues reported that, despite a large variability in brain size, and in sulcal configuration, the degree of cortical folding was remarkably stable in adults (Zilles et al., 1988). Specifically, all individuals, independently of their age, gender, height or weight had an average Gyrification Index of 2.56, meaning that 60% of the cortical surface is hidden within the sulci. A few years later, Armstrong et al (Armstrong et al., 1995) also measured GI on postmortem formalin-fixed brain, including subjects from the first weeks of life until 95 years old. They observed a gradual increase in GI during the first months of life, peaking at 9 months old (120% of the adult GI value) and then a slight decrease to the stable value previously observed by Zilles et al. Thus, from childhood, GI has been proposed as a stable ontogenic feature, unaffected by age, sex, brain volume, body weight, and body length.

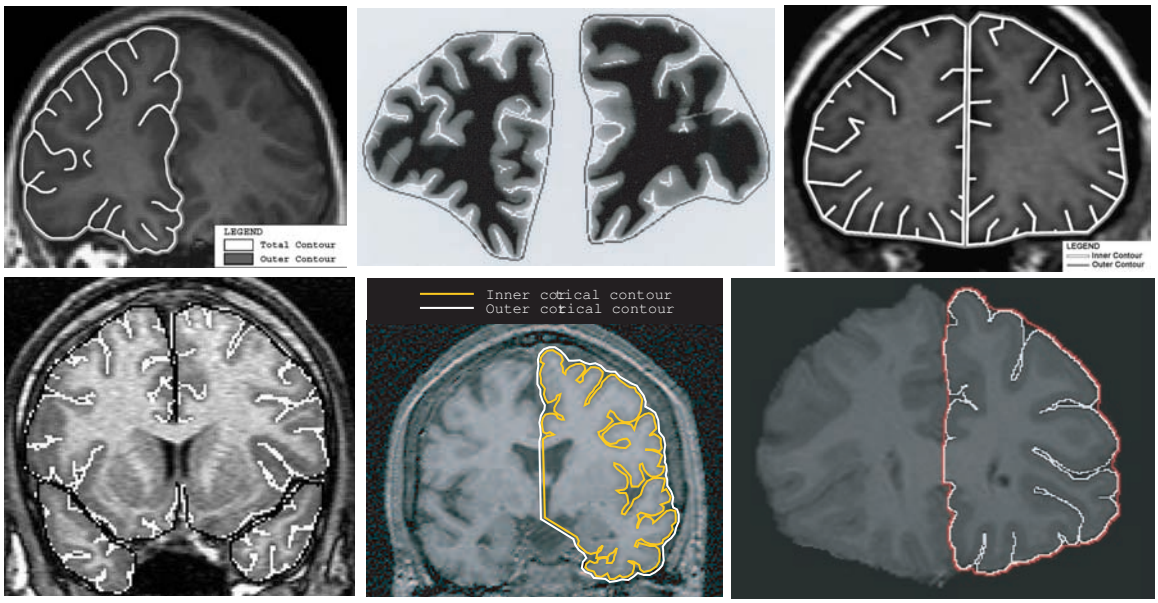

Figure 3.3: *Examples of Gyrification Index measured on coronal MRI sections, except on the first row - second column depicting a formalin-fixed postmortem brain. Images of the upper row are taken from Vogeley et al. (2000), Hardan et al. (2004), Jou et al. (2005); images of the lower row from Harris et al. (2004), Sallet et al. (2003), Schaer et al. (2006).*

Because of its easy interpretation and simplicity in implementation, many studies have been conducted using the Gyrification Index to identify abnormal cortical complexity in neurodevelopmental and psychiatric disorders (Kulynych et al., 1997; Vogeley et al., 2000; Schmitt et al., 2002; Sallet et al., 2003; Hardan et al., 2004; Harris et al., 2004; Schaer et al., 2006). Figure 3.3 shows how Gyrification Index was implemented on MRI coronal section in some of these studies. Among the numerous results obtained by these studies are a reduced GI in dyslexia (Casanova et al., 2004), and increased GI in autism (Hardan et al., 2004), Williams syndrome (Schmitt et al., 2002) and in children who were born prematurely (Kesler et al., 2006). Schizophrenia is probably the disease that has received the larger GI literature, with evidences for a decreased global GI (Kulynych et al., 1997; Sallet et al., 2003), along with increased prefrontal GI (Vogeley et al., 2000; Vogeley et al., 2001; Harris et al., 2004).

Despite the elegant simplicity of Gyrification Index, major issues are related to its methodological implementation. Firstly, most studies used manual delineation of the contours, which raises the question of reliability and reproducibility in the context of large-scale studies. There have been some attempts to adapt the Gyrification Index to automated 2D methods, either restricted to the prefrontal lobe (Moorhead et al., 2006), or separately measuring the four main lobes (Schmitt et al., 2002). But even automated methods are not ideal, given that they do not take into account the inherent three-dimensional nature of the cortical surface. As a result, GI measurements are sensitive to slice orientation, with variations up to 8% resulting from large rotation of the brain (Zilles et al., 1989). Also, because two-dimensional sections are independent one from another, buried sulci are not always included, underestimating cortical surface area. Finally, the precise localization of

gyral anomalies in sub-lobar regions is not possible with 2D slices.

3.5.2 Sulcal Morphometry

Sulcal morphometry is a method that relies on the identification of a set of sulci in order to compare some of their features. There are mainly two different approaches that were proposed to date. The first framework, described by Mangin and colleagues (Mangin et al., 2004), uses artifical neuroanatomists that are trained to identify sulci from a database. After achieving a reliable matching of the sulci, some sulcal features are compared, such as sulcal width or depth, position, or asymmetry indices. Another approach creates an outer surface enveloping the cortex (hull), and measures sulcal depth as the shortest distance between the pial and the hull surface (Van Essen, 2005). The later approach has the advantage of measuring the entire cortex at once, without focusing on a subset of sulci. However, only depth measurement can be provided by this method, which needs an accurate point-to-point surface registration.

A wide amount of results have been published using sulcal morphometry. For instance, asymmetries of the intraparietal fissure, inferior precentral and central sulcus have been identified as correlates of handedness (Mangin et al., 2004). In healthy individuals from 20 to 82 years old, Kochunov et al reported that sulcal width increases and depth decreasess with age for all sulci, except for the inferior frontal and orbitofrontal sulci (Kochunov et al., 2005). Aside from studies in typically developing individuals, other authors conducted studies in patients with neurodevelopmental conditions. For instance, reduced depth in the right intraparietal fissure of patients with Turner syndrome was found to be correlated with abnormal cortical function during an arithmetic task (Molko et al., 2004). In patients with Williams syndrome, reduction of the intraparietal sulcal depth were also reported (Kippenhan et al., 2005; Van Essen et al., 2006). Children with low-functioning autism were shown to have reduced sulcal depth in the frontal operculum and in the insula (Nordahl et al., 2007). Finally, a different morphology of the left paracingulate sulcus has been observed in patients with schizophrenia (Fujiwara et al., 2007), along with anomalies in the temporal sulcus, middle frontal sulcus and Broca's area specifically associated with resistant hallucinations (Cachia et al., 2008).

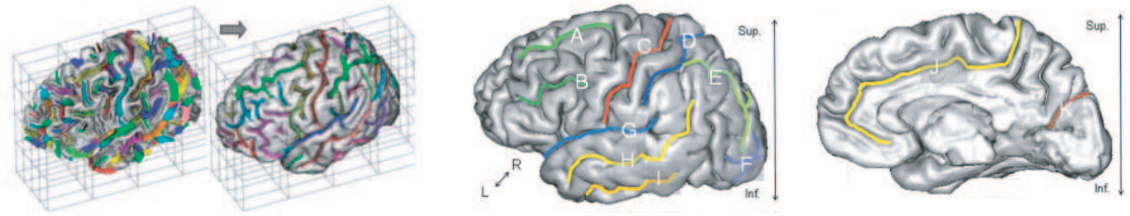

Figure 3.4: *Schematic overview of the processes involved in sulcal morphometry (reproduced from Kochunov et al., 2005). On the left, sulcal identification is completed using neural networks. On the right, lateral and medial views show primary and secondary sulci, on which measurements such as depth, length or asymmetry indices are computed.*

Among the advantages of sulcal morphometry, is its intuitive interpretation. Depth and width are geometrical notions that are easily understood, and that inform on biologically relevant substrates. For instance, depth alterations have been shown to correlate with gray matter volume (Kippenhan et al., 2005). However, the focus on the sulcus as an elementary unit may miss more regional changes. In some aspects, despite far more sophisticated, sulcal morphometry resembles ROI approaches, in that they focus in a subset of sulci, which have to be reliably delineated (e.g. highly variable sulci are less straightforwardly measured).

3.5.3 Fractal Dimension

Fractal dimension (FD) is a measure of cortical complexity that was frequently applied to the quantification of cortical folding (Thompson et al., 1996). FD is based on 3D cortical reconstructions, and informs about the irregularity in the cortical shape, which can be measured either over the whole hemisphere (Lee et al., 2004; Ha et al., 2005) or in lobes (Blanton et al., 2001; Luders et al., 2004; Narr et al., 2004).

One advantage of Fractal dimension is that it represents a compact measurement, condensing information about the frequency and depth of sulci. But the counter-side of this advantage is that information may be too condensed to evidence regional differences at the sub-lobar level. Moreover, Fractal Dimension remains challenging to interpret, in that this geometrical notion is less easily apprehended that for instance length, surface or volume. Finally, there are issues related to FD methodological implementation: most of the time, the images were scaled with an affine transformation prior to cortical mesh model reconstruction, which may affect measurements of cortical folding.

3.5.4 Curvature-based methods: Smoothed Mean Absolute Curvature

More recently, a curvature-based approach has been proposed for estimating local gyrification at thousands of points over the entire cortical surface (Luders et al., 2006). Smoothed absolute mean curvature quantifies the amount of local curvature on spherically-parameterized cortical mesh models (see Figure 3.5). To date, only three studies have applied this method to quantify differences in gyrification. The validation publication included a statistical analysis revealing normal changes in cortical folding associated with gender (Luders et al., 2006). The same authors also reported a moderate relationship between their smoothed absolute mean curvature and measurements of intelligence (Luders et al., 2007). Finally, increased curvature was reported in patients with Williams syndrome (Gaser et al., 2006).

The main advantage of the method proposed by Luders et al is that it represents the only method that measures gyrification with an exquisite spatial resolution. As for volumetric and thickness studies, evolution of neuroimaging techniques aim at an increasing precision in the delineation of the alterations, so that smoothed absolute mean curvature represents the most sophisticated technique for measuring cortical folding to date. However, we have two major concerns related to this method. The most important concern relate to the fact that there is no evidence that more curved surfaces contain more neurons, or any other direct neuroanatomical correlate of interest. Thus, we would question the use of curvature as a variable that may give valuable, biologically relevant, information. The second concern

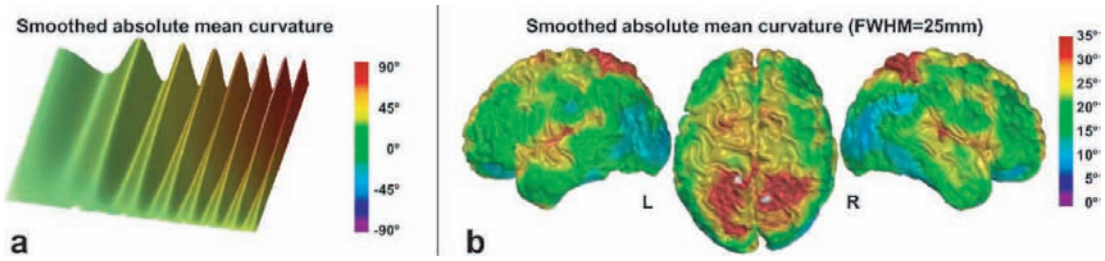

Figure 3.5: *Smoothed absolute mean curvature overlaid at each point over the cortical surface (from Luders et al., 2006). On the left of the image, a simulated folded surface is provided for interpretation.*

relates to the implementation of the method, which similarly to Fractal Dimension uses scaled images, and thus may bias gyrification measurements.

3.5.5 Toward other methods ?

This chapter depicted how the study of cortical folding may inform on the early brain development. Diverse methods for measuring gyrification have been presented, exploiting different geometrical notions, from depth, surface, and spatial frequency to curvature. We argue that, in order to contribute to the field, a new method overcoming the issues raised by the existing methods should combine their individual advantages. For instance, Gyrification Index demarks as a simple and elegant method with direct interpretations. However, the use of three-dimensional reconstruction now emerges as an essential requirement, as used by sulcal morphometry, fractal dimension and smoothed absolute mean curvature. Finally, increased spatial resolution, such as proposed by the curvature-based method, is a very attractive feature.

Chapter 4

Defining the cerebral phenotype in 22q11 deletion syndrome

Previous neuroimaging studies in 22q11DS have delineated a pattern of brain alterations, which may be tightly related to the cognitive and behavioral difficulties encountered by affected individuals. Future contributions in the field will largely rely on studies with consequent sample size or using recently developed methods, to build more precise hypotheses on the pathogenesis of brain alterations in the syndrome.

4.1 Qualitative findings in individuals with the syndrome

The first neuroimaging studies in subjects with 22q11DS were mostly qualitative, reporting a high rate of nonspecific brain alterations (Mitnick et al., 1994; Chow et al., 1999; van Amelsvoort et al., 2001; Shashi et al., 2004) or cases of severe cerebral malformations (Kraynack et al., 1999; Bolland et al., 2000). Others noted cerebral and cerebellar atrophy (Mitnick et al., 1994; Chow et al., 1999), in addition to an enlarged cavum septum pellucidum or cavum vergae (Mitnick et al., 1994; Chow et al., 1999; van Amelsvoort et al., 2001; Shashi et al., 2004). A high incidence of bright foci in the white matter on T2-weighted MRI has been observed (Chow et al., 1999), with frequent cysts around the frontal horn of the ventricle (Mitnick et al., 1994). Finally, numerous case reports of severe cortical malformations, manifesting with polymicrogyria[1] (Robin et al., 2006), were also published.

4.2 Quantitative findings in children and adolescents with the syndrome

Following the first qualitative delineations of cerebral anomalies associated with 22q11DS, numerous quantitative studies were conducted on larger sample of patients. Cerebral atrophy was confirmed, with a 8.5 to 11% volumetric decrease, affecting both gray and white matter (Eliez et al., 2000; Eliez et al., 2001; Kates et al., 2001). Further analyses then revealed a specific pattern of lobar alterations in children with 22q11DS. After adjusting for

[1] polymicrogyria is a cortical malformation caused by abnormal neuronal migration and characterized by a thick cortex with shallow sulci

the global reduction, relative frontal enlargement / preservation was observed along with disproportionate parietal lobe reduction (Eliez et al., 2000; Kates et al., 2001; Kates et al., 2004; Simon et al., 2005). This picture is consistent with a rostro-caudal gradient in cerebral alterations (Eliez et al., 2002), that is, an alteration in global brain shape along the antero-posterior axis. Region-of-interest (ROI) studies have mostly strengthened this rostro-caudal hypothesis, showing a more important reduction of the volume of posterior structures in children and adolescents with 22q11DS. For instance, the thalamus (Bish et al., 2004) and the corpus callosum (Antshel et al., 2005; Machado et al., 2007) are more reduced posteriorly. The head of the caudate nucleus was also found to be larger than its posterior part (Eliez et al., 2002; Kates et al., 2004; Campbell et al., 2006). Finally, the cerebellar reduction suggested by qualitative studies was confirmed by quantitative studies (Eliez et al., 2001; Bish et al., 2006), further substantiating the rostro-caudal gradient hypothesis.

Observations from DTI studies support disturbed white matter organization, with decreased Fractional Anisotropy predominantly found in the middle and superior frontal gyri (Barnea-Goraly et al., 2003) and diffusely in the parietal lobe (Barnea-Goraly et al., 2003; Barnea-Goraly et al., 2005; Simon et al., 2005). Although methodological problems related to the posterior displacement of the corpus callosum have been suspected of biasing voxel-based analyses and causing at least part of the anisotropy differences in the parietal lobes of affected patients (Simon et al., 2005), newer registration techniques have made it possible to confirm parietal tract alterations in 22q11DS (Sun et al., 2007).

4.2.1 Structure - Function Relationship in children and adolescents with 22q11DS

Table 4.1 summarizes the brain alterations typically observed in 22q11DS; for comparisons purpose, neuroanatomical findings in three other neurogenetic syndromes are also depicted. This large list of brain alterations is likely to be responsible for the cognitive and behavioral difficulties encountered by affected patients.

Frontal preservation: relationship with IQ and executive functions

In 22q11DS, the relative frontal lobe preservation has been suggested (Eliez et al., 2000) to allow the maintenance of a borderline IQ during childhood (Swillen et al., 1997), whereas other disorders with substantial frontal lobe reduction show more severe mental retardation (e.g. Rett (Reiss et al., 1993) or Williams (Reiss et al., 2000) syndromes). The frontal preservation is however surprising regarding the deficit in executive functioning (a typically frontally located function) presented by children with 22q11DS. Yet, a recent fMRI study using a verbal working memory task has shown that both children and adolescents with 22q11DS and children with learning difficulties recruited the frontal networks less efficiently than their typically developing siblings, but activated the operculum more readily (Kates et al., 2007). These findings suggest that both children with 22q11DS and children with learning difficulties may compensate for a disruption in the normal frontal neural networks by relying primarily on phonological rehearsal, which may explain their poorer performances.

Among other structures that may be related to executive dysfunction in the syndrome,

Structures	Down Syndrome (DS)	Williams Syndrome (WS)	Fragile X Syndrome (FraX)	22q11 DS
Total Brain Volume	↓[1-5]	↓[6]	Enlarged / preserved[7,8]	↓[9-11]
Cerebellum	Children: ↓[2,3,6] Adults: ↓[5,12-16]	↑as compared to DS[3,6,17] and controls[18,19,20]	↓vermis[8,21-25]	↓mostly vermis[26,27]
Frontal lobe	Children: ↓[2,6] Adults: ↓[4,5,12]	↑[19,28,29]	→[30]	Children: ↑[9,11,31,32] Adults: ↓[33,34]
Parietal lobe	↑Gray matter[2,3]	↓[3,19,28,35,36] ↓superior parietal lobule[37]	→[30]	Children: ↑[9,11,32]
Temporal lobe	→[2]	Thicker perisylvian cortex[38]	Young children ↓[30] Children/Adolescents: →[39]	→[40] Adults: ↓[33,34]
STG	↓[2,4,12]	↑[28,41]	→[30]	→[40]
Planum temporale	↓[42]	↑[43]		
Hippocampus	↓[4,5,12,44,45] ↑Parahippocampus[4,5,12]	→[28]	Children: ↑[39,46]	Children: ↓[40,48,49] Adults: →[50]
Occipital lobe	→[2]	↓[3,19,28,35,36]	→[30]	Children: ↓[9] or ↑[11] Schizophrenic: ↓[33]
Basal ganglia	Children: ↑[2,6] Adults: ↑[5,51]	↓Thalamus[28]	↑Caudate & thalamus[7,52]	↑Caudate (head)[31,53,54] Thalamus: ↓[55]
Corpus callosum	↓[45,46] (rostral)	↓[56-58]		↑[59-61]
DTI findings			↓FA[62]	↓FA[32,62,63]
Gyrification	↓Sulcal depth[4,64]	Short central sulcus[65] ↑Complexity[38,68,67] Shallower IPS[68,69]		↓Gyrification[70]
Neuropathology	Calcified basal ganglia[71,72] Amyloid plaques & neurofibrillary tangles[73]		Overabundant synapses & dendritic abnormalities[74-77]	

Abbreviations: STG: Superior Temporal Gyrus; IPS: IntraParietal Sulcus; DTI: Diffusion Tensor Imaging; FA: Fractional Anisotropy

Table 4.1: *Summary of the main findings in four neurogenetic syndromes (from Schaer et al., 2007). In order to keep the table more readable, the references were separately included in Annex 2.*

the cingulate gyrus may also be a relevant candidate. As the cingulate play a major role in executive functions (Carter et al., 1999), structural or functional cingulate alterations may be related to frequently cited attentional deficits reported in children with 22q11DS (Gothelf et al., 2004). However, given the extent of the cingulate gyrus across both frontal and parietal lobes, a specific cingulate reduction would not be evidenced using classical lobar measurements. To our knowledge, only one study to date has analyzed cortical changes on the medial aspect of the brain using a method capable of detecting regional differences with sub-lobar precision (Simon et al., 2005). Using voxel-based morphometry, Simon and colleagues observed decreased gray matter density in the cingulate gyrus. Aside from the relevance of cingulate reduction in attention deficits, Simon et al also suggested that the cingulate role in the "sense of self" may be particularly pertinent to psychotic manifestations frequently experienced by individuals with 22q11DS.

Parietal reduction: arithmetic and visuo-spatial difficulties

The significant volumetric decrease of the parietal lobe observed in children with 22q11DS is likely to account for part of the cognitive deficits. Specifically, parietal lobe dysfunction may be responsible for visuo-spatial deficits and lower performance in abstract reasoning tasks such as arithmetic (Eliez et al., 2001; Simon et al., 2005). Indeed, the first fMRI study of brain function in 22q11DS sought to explore the neural substrate underlying deficiencies in arithmetic reasoning (Eliez et al., 2001). Eight children with 22q11DS and 8 controls where asked to complete increasingly difficult mathematical tasks. The authors found that the children with the syndrome showed more intensive and diffuse activity in the inferior parietal regions only during performance of difficult 3-operand equations, whereas the controls showed a similar pattern of parietal activation during both the easy and the difficult tasks. In typically developing children, performance improves as the size and intensity of activation decrease, indicating that maturation proceeds with an optimization of brain circuitry. This pattern is consistent for various cognitive tasks, among them arithmetical reasoning (Menon et al., 2002), response inhibition (Tamm et al., 2002), and motor learning (Imamizu et al., 2000). Thus, the increase in activation in the parietal lobe of children with 22q11DS on fMRI scans supports the hypothesis of delayed maturation. Further, abnormal functioning of the parietal lobe may also cause learning difficulties in children with 22q11DS, as fMRI or PET studies have attributed a crucial role for the parietal cortex in normal mnesic processes (Shallice et al., 1994). Aside from relying on a parietal dysfunction, the key role of the hippocampus in memory also suggests a potential hippocampal contribution to mnesic impairments in 22q11DS. Indeed, previous neuroimaging studies have reported reduction of the medial temporal lobe (Eliez et al., 2001), but it remained unclear whether hippocampal reduction was related to the global cerebral reduction or not.

Social difficulties: a role for cerebellum and for structures involved in facial processing

Apart from its involvement in time perception impairment (Debbane et al., 2005) and motor difficulties (Sobin et al., 2006), cerebellar reduction may also play a role in social difficulties presented by children with 22q11DS (Golding-Kushner et al., 1985; Swillen et al., 1997; Swillen et al., 1999). Indeed, cerebellar vermis decrease was also reported in other neurogenetic and neurodevelopmental disorders such as Fragile X syndrome (Reiss et

al., 1991; Mazzocco et al., 1997), and autism (Courchesne et al., 1994). Given the typical social difficulties presented in these neurodevelopmental disorders (Cohen et al., 1988) and in 22q11DS, reduction of the cerebellar vermis may represent an important biological substrate for avoidant behaviors and communication problems. Furthermore, the enlarged posterior vermis (Reiss et al., 2000; Schmitt et al., 2001) found in the over-empathic subjects with Williams syndrome strengthen a hypothetical positive correlation between vermis size and social skills.

Other candidates that received interest for social difficulties in the syndrome are structures related with face perception. Indeed, deficient face-processing capabilities can ultimately lead to social difficulties and even psychotic symptoms, such as reference ideas (Baker et al., 2005; Debbane et al., 2006) or autistic traits (Vorstman et al., 2006; Antshel et al., 2007). In a recent fMRI study focusing on facial processing (Andersson et al., 2007), Andersson and colleagues observed a suppression of the normal face-selectivity activation of the fusiform gyrus in affected patients, electing the fusiform gyrus as an interesting marker for social impairements. If hyperactivation in parietal lobe possibly reflected delayed maturation, hypoactivation of the fusiform gyrus should rely on a different mechanism. Studies of normal gray matter have provided structural evidence that frontal and parietal lobe maturation precedes changes to the temporal lobes (Giedd et al., 1999). This suggests that frontal and parietal input is required for temporal lobe structural maturation. Indeed, the functional specificity of the fusiform face area (FFA) may rely on an acquired expertise (Gauthier et al., 2001) that requires efficient connections. In 22q11DS, disorganized input connections to the FFA may impair the development of this expertise and, thereby, activation of the FFA. The above considerations lend support for a more detailed investigation of the fusiform structure in 22q11DS.

4.3 Quantitative findings in adults with the syndrome

The pattern of cerebral alterations reported in adults with 22q11DS differs from the one observed in children and adolescents on several aspects. Studies in adults with 22q11DS reported widespread loss of brain tissue compared with normal controls (Chow et al., 2002) and with healthy individuals with developmental disabilities (van Amelsvoort et al., 2001). Specifically, the frontal and temporal lobes were reduced, eliminating the rostro-caudal gradient observed in children and adolescents with the syndrome. Accordingly, the caudate nucleus enlargement that was presumed to be part of the gradient was not observed in adults (van Amelsvoort et al., 2001). These children *vs* adults studies thus suggest an accelerated neurodegenerative process, affecting mostly the frontal and temporal lobes of individuals with the syndrome. Two interpretations can be derived from this hypothetic accelerated gray matter loss. First, given that frontal lobe enlargement may allow for the maintenance of the borderline IQ in children with 22q11DS (Eliez et al., 2000), an accelerated cortical frontal reduction may play a role in the drastic decrease in IQ observed with age (Swillen, 2006). Second, reduced frontal and temporal volumes are in line with the structural abnormalities observed in non-syndromic subjects with schizophrenia (Shenton et al., 2001), and may represent a first step toward the identification of markers and risk factors for schizophrenia in 22q11DS.

4.3.1 Specific anomalies associated with schizophrenia

If temporal and frontal reduction represent tempting candidates for further assessment of schizophrenia susceptibility, hypothesis based on the comparison of neuroimaging findings obtained by different research groups on children (Eliez et al., 2000; Kates et al., 2001; Simon et al., 2005; Campbell et al., 2006) and adults (van Amelsvoort et al., 2001; Chow et al., 2002) may be hazardous. For example, divergent findings may simply rely on differences in methodology or in sample selection (e.g. control subjects matched for IQ (van Amelsvoort et al., 2001) or typically developing individuals (Eliez et al., 2000; Chow et al., 2002; Simon et al., 2005)). Furthermore, such "children *vs* adults" comparison designs may not be able to identify specific changes associated with schizophrenia. Van Amelsvoort and colleagues (van Amelsvoort et al., 2004) thus compared adults with 22q11DS with schizophrenia (S-22q11DS) and without schizophrenia (NS-22q11DS). In addition to findings of a generalized decrease in the gray and white matter volume in the patients with schizophrenia, their results suggested that the more significant reduction in the frontal and temporal lobes may be associated with the presence of psychotic symptoms.

Aside from studies comparing patients with 22q11DS with and without schizophrenia, longitudinal studies offer an attractive possibility to assess intra-individual changes in brain anatomy over time. Thus, longitudinal design represents a powerful approach to isolate structural alterations distinctively associated with psychotic evolution. The first longitudinal study on 22q11DS patients corroborated the theory that the decrease in the prefrontal gray matter volume plays an important role in the susceptibility of adolescents with 22q11DS to psychosis (Gothelf et al., 2005). Following prospectively 24 children with 22q11DS and 23 subjects with idiopathic developmental disorder from childhood to early adulthood, Gothelf and colleagues identified that decline in prefrontal volume accompanies the emergence of psychosis. Further, they were able to designate the low activity allele of the catechol-O-methyltransferase (COMT) gene as a major risk factor for the development of psychotic symptoms. They proposed that the prediction of prefrontal reduction and subsequent psychiatric symptomatology according to COMT polymorphism rely on modified dopaminergic transmission (Mattay et al., 2003).

4.4 What remains to be measured in 22q11 deletion syndrome?

Facets of the typical brain phenotype are increasingly delineated in 22q11DS, with a well-documented pattern of structural alterations. We can thus reasonably wonder what remains to be measured. To our opinion, a contribution in the field nowadays requires to meet at least one of the following criteria:

- **First of all, include large sample size.** Normal inter-individual variations in brain structures are large, so that the delineating structural differences associated to any condition requires large sample size. Given the prevalence of 22q11DS, most previous studies published findings on relatively small number of subjects. Nowadays, contributions in the field of 22q11DS should no more constitute anecdotal findings, but should rather potentially hold true for all patients affected by the syndrome.

- **Include subjects with a large age range for cross-sectional studies, or longitudinal follow-up of the subjects over years, to provide a better delineation of the maturational pathways associated with the syndrome.** Former studies focused mostly on group of subjects with restrained age range (i.e. either children or adults). Also, there are very few studies focusing on adolescents with the syndrome, an age at which the brain changes substantially and associated with critical periods. As a result, only little known regarding how brain matures in the syndrome, and future studies focusing on this point are required.

- **Given the variability in the phenotype associated with 22q11DS, studies should not only delineate the alterations associated with the syndrome (i.e. compared to controls), but also identify the factors exacerbating alterations within 22q11DS.** Indeed, the increased delineation of the cerebral phenotype still fails to identify the factors responsible for the varying degree of alterations in the syndrome. For instance, as mentioned before, the identification of risk factors and markers for schizophrenia is one of the major challenges faced by researchers. Aside from psychosis, other factors may contribute to the varying intensity of the cerebral and cognitive phenotype in the syndrome. For instance, **genetic polymorphism inside and outside of the 22q11 deleted region** must be examined. Catecholamine-O-methyltransferase is one of this, but future work may delineate other genes outside of the 22q11 region that may interact with the deleted genes normal during brain development. Also, **congenital heart disease (CHD),** which affects more than half of individuals with 22q11DS (McDonald-McGinn et al., 1999), is known to alter brain structure and affect neurodevelopmental outcomes in non-syndromic children (Glauser et al., 1990 ; Miller et al., 2007). However, previous studies in 22q11DS have not demonstrated an impact of CHD on brain alterations (Bingham et al., 1997; Kates et al., 2001 ; Bearden et al., 2007). Absence of differences between 22q11DS patients with and without CHD may be due to methodological concerns in previous studies, such as small sample size and the inclusion of participants with widely varying CHD. Further, volumetric studies can miss regional cortical changes, so that an effect of cardiac anomalies cannot be ruled out. Ultimately, identifying the factors affecting the intensity of alterations may help to further delineate the etiology of these anomalies.

- **Use novel image processing techniques, to provide a more precise delineation of both the localization and the nature of structural alterations in 22q11DS.** Indeed, volumetric results by lobes have delineated the gross picture of the alterations, and regions-of-interest were manually delimited for a few set of structures. Time and reliability considerations limit the opportunity to manually subdivide the entire brain. Hopefully, recent methodological developments provide powerful tool for subdividing the entire cortex in regional volumes, providing a comprehensive view of the alterations.
  Aside from a better localization of the lesions, furthering our understanding also relies on a better delineation of the nature of the alterations. Indeed, cortical volume is the outcome of two differently regulated processes: thickness and area (which is in turn tightly related to cortical morphology). Thus, distinguishing the contributions of both factors may help to further understand the pathogenesis of volumetric reductions. For instance,

- **Thickness** is an attractive tool, with exquisite spatial resolution; being subject to developmental changes, cortical thickness has been suggested to be ideal for studying **brain maturation processes**. A first study assessed cortical thickness in a small group of children with 22q11DS (Bearden et al., 2007). They noted significant cortical thinning in the parieto-occipital and orbito-frontal regions in the study group compared to age- and gender-matched controls. However, their technique may have be biased by buried sulci or by scaling the images prior to measurements. Further, due to a restricted age range, they could not assess maturational effect on cortical thickness.
- **Morphology / Folding** of the cortex is **determined early in development** (see Chapter 3). Thus, alterations to gyral pattern are likely to inform on an early insult. In 22q11DS, the high frequency of polymicrogyria, a severe cortical malformation manifested with shallower sulci, put forward an association between 22q11DS and gyral abnormalities. If experienced radiologists can easily identify polymicrogyria, the diagnosis of more subtle gyral anomalies in 22q11DS may require the use of quantitative tools (see also Figure 4.2).

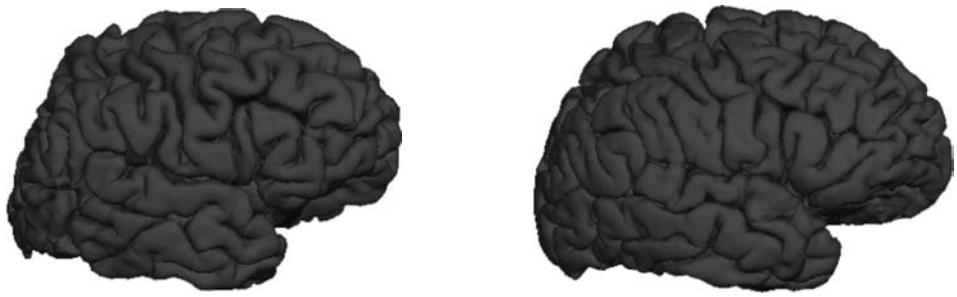

Figure 4.2: *Three-dimensional cortical reconstructions of the brain of two same-aged girls. In the patient, the global brain shape is typically altered with flattened parieto-occipital region, illustrating the rostro-caudal gradient of cerebral alterations associated with the syndrome. Furthermore, the pattern of cortical gyrification seems simplified, with enlargement of numerous sulci; the sylvian fissure is particularly affected.*

4.5 Objectives of the present thesis

Based on the above considerations, the present thesis aims at answering following objectives:

1. Further contribute to the delineation of the cerebral phenotype in 22q11DS through the use of classical neuroimaging methods in a large cohort of patient, i.e.
   (a) Provide specific volumetric measurements that were previously not reported in the syndrome. The following regions-of-interest were selected given their likelihood to participate to cognitive, behavioral or psychiatric alterations seen in 22q11DS: (1) the hippocampus, which may represent the neural substrate of memory impairments in 22q11DS; (2) the fusiform gyrus, which may be involved in facial processing deficits and impaired social skills; (3) the cingulate gyrus, which may participate to altered executive functions and psychiatric symptomatology in 22q11DS.
   (b) Apply a classical method for measuring gyrification. Two-dimensional Gyrification Index (Zilles et al., 1988) is probably the most popular method; its application in 22q11DS will hence allow direct comparisons with other neurodevelopmental conditions.
2. Develop a more satisfying method for the quantification of gyrification, and apply it to the study of 22q11 deletion syndrome. In addition to identify the gyral alteration associated with 22q11DS, we also aim at assessing whether cardiac anomalies would exacerbate gyral alterations within the syndrome.
3. Applied recently developed neuroimaging techniques for a more precise delineation of cerebral anomalies in 22q11DS:
   (a) Regional cortical volumes (Desikan et al., 2006), to confirm previous volumetric alterations and elaborate relationships between cortical folding, thickness and volume.
   (b) Cortical thickness, to provide a comprehensive picture of cortical maturation from childhood to adulthood in the syndrome.

Part II

Results

Results

To answer the objectives raised at the end of the *Introduction* section, the following journal articles are included in the *Results* section:

1. To further contribute to the delineation of the cerebral phenotype in 22q11DS through the use of classical neuroimaging methods:
   (a) Manually delimited Regions-Of-Interests:
      i. M. Debbané, M. Schaer, R. Farhoumand, B. Glaser, S. Eliez (2006) "Hippocampal volume reduction in 22q11 deletion syndrome", Neuropsychologia, 44(12): 2360-5 ***(Study 1a)***
      ii. B. Glaser, M. Schaer, S. Berney, M. Debbané, P. Vuilleumier, S. Eliez (2007) "Structural changes to the fusiform gyrus : a cerebral marker for social impairments in 22q11.2 deletion syndrome ?", Schizophrenia Research, 96(1-3): 82-86 ***(Study 1b)***
      iii. F. Dufour, M. Schaer, M. Debbané, R. Fahroumand, B. Glaser, S. Eliez (2008) "Cingulate gyral reductions are related to low executive functioning and psychotic symptoms in 22q11.2 deletion syndrome", Neuropsychologia, 46(12):2986-92 ***(Study 1c)***
   (b) Two-dimensional (classical) Gyrification Index:
      i. M. Schaer, J. E. Schmitt, B. Glaser, F. Lazeyras, J. Delavelle, S. Eliez (2006) "Abnormal pattern of cortical gyrification in velo-cardio-facial/DiGeorge syndrome (deletion 22q11.2): an MRI study", Psychiatry Research, 146(1): 1-11 ***(Study 2)***
2. To develop a more satisfying method for the quantification of gyrification, and apply it to the study of 22q11 deletion syndrome:
   (a) M. Schaer, M. Bach Cuadra, L. Tamarit, F. Lazeyras, S. Eliez, J.-P. Thiran (2008) "A surface-based approach to quantify local cortical gyrification", IEEE Transactions on Medical Imaging, 27(2):161-170 ***(Study 3)***
   (b) M. Schaer, B. Glaser, M. Bach Cuadra, M. Debbané, J.-P. Thiran, S. Eliez. "Congenital heart disease affects local gyrification in 22q11.2 deletion syndrome (22q11DS)", *in press* Developmental Medicine & Child Neurology ***(Study 4)***
3. To apply recently developed neuroimaging techniques for a more precise delineation of cerebral anomalies in 22q11DS :
   (a) M. Schaer, B. Glaser, M.-C. Ottet, M. Schneider, M. Bach Cuadra, M. Debbané, J.-P. Thiran, S. Eliez. "Regional cortical volumes and congenital heart disease: a MRI study in 22q11.2 deletion syndrome", *submitted* ***(Study 5)***
   (b) M. Schaer, M. Debbané, M. Bach Cuadra, M.-C. Ottet, B. Glaser, J.-P. Thiran, S. Eliez. "Trajectories of cortical thickness changes in 22q11 deletion syndrome (22q11DS): a cross-sectional and longitudinal study", *submitted* ***(Study 6)***

My contributions to the above articles is detailed here:

As a second author of *Studies 1a, 1b & 1c*, I was mainly involved in the image processing, using techniques that Stephan Eliez taught me.

In *Study 1a*, based on a previously validated protocol, I was in charge of designing the hippocampal subdivision according to anatomically relevant guidelines; I further conducted the subdivisions and measurements of the hippocampal heads, bodies and tails for all subjects enrolled in the study.

For *Study 1b*, as no satisfying protocol existed to delineate the fusiform gyrus, I designed and standardized a new protocol, I then conducted the inter-rater validation with Sandra Berney and further supervised her in drawing all subjects.

For *Study 1c*, I taught Federico Dufour the necessary neuroimaging skills to conduct measurements of the cingulate gyrus; I further supervised him in tracing and contributed critical inputs to the manuscript.

All other studies as a first author would not have been possible without the help and critical contributions of all authors, and in particular without supervision of both of my thesis directors, Stephan Eliez and Jean-Philippe Thiran. Nevertheless, I conducted the image processing, statistical analyses and wrote the manuscript of each one.

In addition, for *Study 3*, I entirely wrote the Matlab code of the algorithm, but the completion of the method and the publication in an engineer journal would not have been possible without the efficient supervision of Meritxell Bach Cuadra.

ELSEVIER

Neuropsychologia 44 (2006) 2360–2365

NEUROPSYCHOLOGIA

www.elsevier.com/locate/neuropsychologia

Hippocampal volume reduction in 22q11.2 deletion syndrome

Martin Debbané *, Marie Schaer, Riaz Farhoumand, Bronwyn Glaser, Stephan Eliez

Service Médico-Pédagogique, University of Geneva School of Medicine, 16-18 Boulevard St. Georges, Case Postale 50, CH-1211 Geneva 8, Switzerland

Received 1 October 2005; received in revised form 7 March 2006; accepted 3 May 2006
Available online 19 June 2006

Abstract

Hippocampal volume reduction and decreased memory skills form a characteristic neurofunctional alteration observed in schizophrenia. Individuals affected with 22q11.2 deletion syndrome (22q11DS), while exhibiting memory deficits throughout development, are also at high risk for developing schizophrenia. The present study sought to investigate hippocampal volume reduction as separate of global grey matter reduction in a large, independent sample of individuals with 22q11DS. Volumetric data from structural magnetic resonance imaging was obtained for 43 individuals affected with 22q11DS, aged 6–39 years of age, as well as for 40 healthy individuals matched for age and gender. Drawing of the amygdala was included to enhance the delineation of the hippocampus, and circumscription of both the amygdala and the hippocampus were executed using an increased resolution matrix. After controlling for total grey volume reductions observed in affected individuals, a significant decrease in hippocampus volume was observed in the 22q11DS group, driven by significant bilateral volumetric reduction of the body of the hippocampus. These results are discussed in reference to memory and cerebral alterations already reported in 22q11DS. Further, the specific implications of hippocampus body volume reduction are outlined in light of its anatomical relationships and its function in memory. Finally, reduction of hippocampal volume in 22q11DS is examined in the context of psychiatric risk status associated to the deletion.

Keywords: Hippocampus; Amygdala; VCFS; Memory; Schizophrenia

1. Introduction

The hippocampus receives input from all cortical association areas (Amaral & Witter, 1989) and serves as the final processing station of complex sensory information (Small, 2002). Moreover, it is recognized as a central structure for the functional neuroanatomy of different memory processes (Moscovitch et al., 2005). Recent evidence of hippocampal volume reduction (Heckers, 2001; McCarley et al., 1999) and functional alteration (Cirillo & Seidman, 2003; Weiss & Heckers, 2001) in individuals with schizophrenia suggests that the hippocampus also plays a central role in schizophrenic disorders.

To date, one study reports medial temporal lobe reduction in association with 22q11.2 Deletion Syndrome (22q11DS) (Eliez, Barnea-Goraly, Schmitt, Liu, & Reiss, 2001a); however, it remains unclear if this reduction is independent from grey matter density loss also characteristic of this population. This neurogenetic syndrome, also referred to as velo-cardio-facial syndrome (VCFS) (Shprintzen et al., 1978), is an autosomal dominant condition affecting approximately 1 out of 4300–7000 live births (Oskarsdottir, Vujic, & Fasth, 2001). It is usually caused by a 3 mb *de novo* deletion on the long arm of chromosome 22 (Shaikh et al., 2000). Important cerebral volumetric changes are associated with the deletion, such as reduced grey and white matter volumes (Eliez, Schmitt, White, & Reiss, 2000), reduced parietal and temporal lobes volumes (Eliez et al., 2001a; Eliez et al., 2000), reduced cerebellum and vermis volumes (Devriendt, Thienen, Swillen, & Fryns, 1996; Eliez, Schmitt, White, Wellis, & Reiss, 2001b), thalamic volume decrease (Bish, Nguyen, Ding, Ferrante, & Simon, 2004) and basal ganglia hypertrophy (Eliez, Barnea-Goraly, Schmitt, Liu, & Reiss, 2002; Kates et al., 2004). Cognitive development in affected individuals is characterized by learning difficulties (Swillen et al., 1999), speech and language difficulties (Glaser et al., 2002), attention deficits (Gothelf et al., 2004; Sobin et al., 2004) and below-average IQ (Golding-Kushner, Weller, & Shprintzen, 1985; Swillen et al., 1997).

Recent investigations into memory functions in 22q11DS reveal below-average performances in children and adolescents (Bearden et al., 2001), as well as adults (Henry et al., 2002).

* Corresponding author. Tel.: +41 22 327 43 03; fax: +41 22 327 43 20.
E-mail address: martin.debbane@medecine.unige.ch (M. Debbané).

0028-3932/$ – see front matter © 2006 Elsevier Ltd. All rights reserved.
doi:10.1016/j.neuropsychologia.2006.05.006

These performances occur in a risk-for psychosis context: transient psychotic experiences occur in up to 50% of adolescents and young adults with the deletion (Baker & Skuse, 2005; Debbané, Glaser, David, Feinstein, & Eliez, 2006), and 20–30% of affected individuals are reported to develop schizophrenia during adulthood (Murphy, Jones, & Owen, 1999). Given associations between decreased memory functions, reduced hippocampal volume and risk for psychosis (Lawrie et al., 2002; Wood et al., 2003), a precise delineation of hippocampal morphometry in 22q11DS can contribute valuable information to the underlying neural substrates of memory impairments and corollary psychiatric risk associated to the syndrome.

The objective of the present study is to examine hippocampal volume in a large and independent sample of individuals affected with 22q11DS. We argue that a robust finding of volumetric reduction of the hippocampus should be present after controlling for total grey matter volume. We perform sub-regional analyses of the hippocampus to screen for morphological specificities within the structure. The amygdala is employed as a control structure, and its volume is tabulated in order to provide greater specificity for hippocampus delineation (Nelson, Saykin, Flashman, & Riordan, 1998). On the basis of our previous report, we hypothesize that amygdala volume will not yield any group differences. We hypothesize that individuals with 22q11DS will exhibit reduced hippocampal volumes, independent of total grey matter reduction.

2. Materials and methods

2.1. Subjects

2.1.1. Individuals with 22q11.2 DS

Forty-three children and young adults (16 male, 27 female) with 22q11DS ages 6–37 (mean = 16.7 ± 8.7) participated in the study. All participants were right-handed, except for six affected individuals and three controls. The sample had a mean full-scale IQ score of 69.4 ± 11.5 as measured by the Wechsler Intelligence Scales for Children or Adults (WISC-III or WAIS-III). Participants were recruited through local patient associations. Thirty-six of the participants in the study had *de novo* deletions on chromosome 22q11.2 as confirmed by fluorescent in situ hybridization (FISH), and one had a familial deletion. Written informed consent was received from all parents and/or subjects under protocols approved by the Institutional Review Board of the Geneva University School of Medicine.

2.1.2. Comparison group

The comparison group was comprised of 40 typically developing individuals (17 males, 23 females) ages 6–39 (mean: 15.1 ± 7.9), with a mean IQ of 111.1 ± 13.4. Individuals were recruited through a newsletter distributed in public schools and the community. All participants were screened for the absence of neurological and psychiatric disorders through a medical intake interview and screening forms (Medical and Developmental History Form, the CBCL for individuals younger than 18, and the SCL-90 for individuals 18 and older). There were no significant differences between the two groups on age, gender, and handedness.

2.2. DNA analysis

Blood was collected from children with 22q11DS. The deletions were verified and their extent determined by two-color FISH, with cosmid probes cD0832 and c350, specific for the proximal and distal deletion regions respectively (Karayiorgou et al., 1995; Kurahashi et al., 1997).

2.3. MRI protocol

Magnetic resonance images were obtained using a Philips Intera 1.5 T scanner. Coronal images were acquired with a 3D volumetric pulse sequence using the following scan parameters: TR = 35 ms, TE = 6 ms, flip angle = 45°, NEX = 1, matrix size = 256 × 192, field of view = 24 cm^2. Resulting images were 124 contiguous slices with a thickness of 1.5 mm and in-plane resolution of 0.94 mm × 0.94 mm.

2.4. Image processing and measurement

SPGR image data were imported into the software program *BrainImage* v5.24 (http://www.spnl.stanford.edu/tools/brainimage.htm). This program permits semi-automated image analysis incorporating the following steps: (0) reslicing into ispotropic voxels (0.94 mm × 0.94 mm × 0.94 mm), (1) correction of voxel intensity non-uniformity, (2) realignment according to AC–PC plane, (3) removal of non-brain tissues, (4) segmentation of the brain into constituent tissue types using a constrained fuzzy algorithm based on voxel intensity and tissue boundaries. Details of these procedures have been published elsewhere (Reiss et al., 1998).

For all procedures, manual and automated, raters were blinded to subjects' identifying and diagnostic information. Circumscription of mesial temporal structures (amygdala and hippocampus) was performed based on a previously published protocol (Kates, Abrams, Kaufmann, Breiter, & Reiss, 1997). SPGR datasets were transformed from a 256 × 256 to a 512 × 512 resolution using bicubic interpolation in order to allow for more precision in the delineation of a region of interest (ROI).

Amygdala and hippocampus ROI delineations are represented in Fig. 1. Drawing of the amygdala was performed coronally, beginning on the slice where the anterior commisure first crosses the midline of the brain. Drawing began

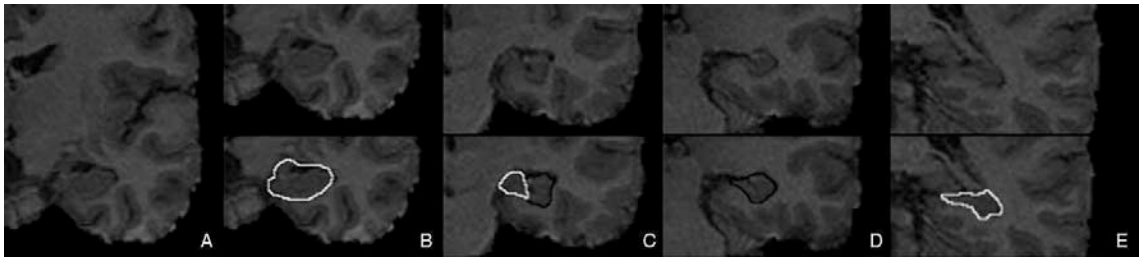

Fig. 1. Illustration of region of interest drawing of the hippocampus and subdivisions. Location of the left hippocampus is shown in (A). Hippocampus drawing is done in the rostro-caudal direction, beginning with the hippocampal head (B). The transition from head to body is defined when the fimbria is clearly distinguishable, dividing the hippocampus in two parts: the head medially (in white) and the body laterally (in black) (C). After this transition slice, hippocampal body is drawn (D), until the first slice on which the crus fornix becomes fully visible. The latter slice defines the most anterior slice of the hippocampal tail. Hippocampal tail (E; in white) is then delineated until it disappears.

infero-laterally, moving medially at the border between the amygdala and the white matter tract inferior to it. In the posterior regions of the amygdala, the superior border was partially defined by the presence of the entorhinal sulcus. The amygdala was drawn until it disappeared posteriorally. The anterior-most slice of the hippocampus was determined by the presence of landmarks: the alveus, the point where the superior horn of the lateral ventricle first points medially, the intensification of grey matter signal and an increased separation between grey and white matter, and the development of the laminar structure that distinguishes the hippocampus from the amygdala. Subsequent to the delineations, we divided the total hippocampus into head, body and tail segments. Duvernoy (1998) states that the hippocampal body has a highly characteristic shape on coronal sections, and is medially delimited by the fimbria (Duvernoy, 1998). Further, he illustrates how the junction between head and body is located when the uncus appears (in the caudo-rostral direction). According to these anatomical considerations, we used the following criterion: the coronal slice where the fimbria clearly divides the hippocampus in two parts (the body laterally and the head medially) was chosen as a transition slice to draw both structures (Fig. 1). In cases where the fimbria was not clearly illustrated, we selected the slice where the uncus disappears (from antero-posterior perspective). Hippocampal segments anterior to this section were defined as the head of the hippocampus, and hippocampal segments after this section constituted the body of the hippocampus. The following transition between hippocampal body and tail is commonly delimited on the first coronal slice on which the crus fornix becomes fully visible (Maller, Reglade-Meslin, Anstey, & Sachdev, 2006). We followed this transition using the crus fornix as the main transition landmark between body and tail of the hippocampus. Thereafter, volumes were measured and reliability analyses based on 10 datasets were conducted. Intraclass correlation coefficients were 0.93 and 0.94 for the amygdala and hippocampus, respectively.

2.5. Statistical analyses

Volumetric data met the necessary criteria (independence, normality, and homogeneity of variance) for employing parametric statistical analyses. ANOVA was used to compare the groups on mean total grey and white matter. Multiple analyses of covariance (MANCOVA) was utilized to determine whether the 22q11DS and comparison groups had a unique pattern of combined left and right volumes in the amygdala and hippocampus structures (total tissue values of the amygdala and the hippocampus) when covarying for total grey matter volume. For all sub-regional volumetric comparisons (right and left amygdala, right and left subdivisions of the hippocampus—head, body and tail), follow-up ANCOVA tested for specific group differences while adjusting for group differences in overall grey matter volume. Thereafter, significant parameters were first covaried for age to test for any potential effect. Then, the significant parameters were also covaried for IQ, as some authors have suggested that controlling for IQ yields a different analysis of brain morphology associated to 22q11DS (van Amelsvoort et al., 2001). An alpha of 0.05 (two-tailed) was used as the threshold for statistical significance in all analyses.

3. Results

Total brain tissue volumes (grey and white together) were approximately 12% smaller in the 22q11DS group relative to the comparison group (ANOVA; $F(1,81) = 28.9$; $p < 0.0001$). Reductions in total tissue were comparable for the left and right hemispheres when analyzed separately. Further segmentation of grey and white matter was conducted to describe group differences in total brain volumes (Table 1). Total grey matter volume in the brain was reduced (mean = 11.3%; ANOVA; $F(1,81) = 20.6$; $p < 0.0001$) to a similar degree as for white matter (12.1%; $F(1,73) = 11.6$; $p < 0.001$).

MANCOVA indicated a significant pattern of hippocampal morphological variation distinguishing persons with 22q11DS from comparison subjects (Wilks Lambda of 0.761; $F(8,73) = 2.86$; $p = 0.008$). Follow-up ANCOVA specifically indicated a significant bilateral reduction of the body of the hippocampus, and trend-like significance for the tail of the hippocampus (driven by right tail volumetric estimates) in the 22q11DS group compared to the control group (Table 1). When Age was introduced as a covariate, results remained unchanged. When IQ was included as a covariate, only the body of the hippocampus remained significantly reduced in the 22q11DS group ($F(3,78) = 4.14$, $p = 0.045$). Volumetric estimates of the amygdala did not yield any significant differences between groups.

Table 1
Segmented total tissue, grey and white volumetric comparisons, amygdala and hippocampus comparisons for 22q11DS vs. control subjects[a]

	22q11DS	Control	F	p value
Whole brain				
Total tissue	1105.9 ± 128.8	1251.1 ± 116.5	28.9	0.0001
Total grey	659.8 ± 81.4	743.8 ± 87.5	20.6	0.0001
Total white	446.1 ± 89.1	507.3 ± 73.3	11.6	0.001
Amygdala				
Total tissue	2.12 ± 0.42	2.21 ± 0.45	0.07	0.792
Left	1.09 ± 0.24	1.13 ± 0.23	0.03	0.958
Right	1.03 ± 0.21	1.08 ± 0.25	0.20	0.653
Hippocampus				
Total tissue	3.34 ± 0.46	3.85 ± 0.44	7.38	0.008
Head-total	1.72 ± 0.33	1.89 ± 0.31	1.48	0.227
Body-total	1.06 ± 0.20	1.30 ± 0.18	17.5	0.0001
Tail-total	0.48 ± 0.14	0.56 ± 0.12	3.83	0.054
Left-total	1.58 ± 0.27	1.81 ± 0.21	8.48	0.005
Right-total	1.69 ± 0.25	1.94 ± 0.23	10.01	0.002
Head-left	0.83 ± 0.20	0.90 ± 0.17	0.68	0.411
Head-Right	0.90 ± 0.16	0.99 ± 0.16	1.95	0.167
Body-left	0.51 ± 0.11	0.63 ± 0.09	17.81	0.0001
Body-right	0.55 ± 0.11	0.67 ± 0.11	11.93	0.001
Tail-left	0.24 ± 0.08	0.28 ± 0.06	2.56	0.114
Tail-right	0.24 ± 0.07	0.28 ± 0.08	4.14	0.045

[a] Volume estimates are expressed in cm^3.

In our sample, repeated-measures ANOVA revealed conventional right-left asymmetry in both subject groups, with right hippocampal volumes significantly larger than left hippocampal volumes ($F(1,81) = 41.37$, $p < 0.0001$) and no detectable difference between the groups by side ($F(1,81) = 0.227$, $p = 0.635$).

4. Discussion

The present study reports a bilateral hippocampal body reduction in 22q11DS, independent of overall volumetric grey matter reductions; this result does not differ when age or IQ are included in the analysis. Amygdala volumes were not found to differ between groups, confirming our preliminary finding (Eliez et al., 2001a). A right > left asymmetry of hippocampus volume was found in both groups, which is consistent with normal and clinical hemispheric morphology (Pegues, Rogers, Amend, Vinogradov, & Deicken, 2003; Weiss, Dewitt, Goff, Ditman, & Heckers, 2005). We discuss the implications that hippocampal body volume reduction can bear on memory function in 22q11DS, and how they relate to previously described morphological alterations. Further, we draw parallels

between 22q11DS and schizophrenia, and how these inform future research avenues in this genetically homogeneous population.

4.1. Implications for memory processes in 22q11DS

Research on neurogenetic disorders demonstrates how volumetric reduction in cerebral areas can alter related functionality (Karmiloff-Smith et al., 1998). Recent functional MRI studies illustrate how the body of the hippocampus acts as a spatiotemporal convergence segment of separate sensory input during associative learning (Small et al., 2001). The hippocampus not only associates the two spreading activations converging along the body segment, but also plays a determinant role in recalling the information minutes after encoding (Small, 2002). Thus alterations to the body of the hippocampus in 22q11DS could selectively impair binding operations that associate different sources of information (auditory and visual, for example), leaving other associations relatively intact (verbal–verbal, for example). While studies report memory impairments in 22q11DS using standardized assessment tools (Henry et al., 2002; Lajiness-O'Neill et al., 2005), more specific association and recall procedures are needed to better assess the consequences of regional hippocampal volume reduction found in the present report.

Concurringly, volume reduction of the hippocampal body could alter recollection-based memory performances, as they involve the integration of a target and related contextual information (Mandler, 1980). Several authors suggest that the hippocampus participates in recollection-based retrieval (Aggleton & Shaw, 1996; Yonelinas, 2001), but that familiarity-based recognition is not affected by hippocampal alterations (Mayes, Holdstock, Isaac, Hunkin, & Roberts, 2002; Vargha-Khadem et al., 1997). Further examination of memory for context in 22q11DS is necessary to determine the functional impact of decreased hippocampal volume observed in affected individuals. We have recently suggested that individuals with 22q11DS exhibit alteration of basic timing mechanisms (Debbané et al., 2005). Volume alteration of the hippocampus body could also impair memory for temporal context in affected individuals (Mayes et al., 2002).

4.2. Parallels between 22q11DS and schizophrenia

A decrease of hippocampal volume has been repeatedly observed in individuals with schizophrenia (Nelson et al., 1998). However, while some studies show greater posterior hippocampal volumetric reduction in patients with schizophrenia (Hirayasu, Shenton, Salisbury, & McCarley, 2000), others suggest anterior hippocampus volumetric reduction (Pegues et al., 2003; Szeszko et al., 2003), and still, others report diffuse hippocampal reduction in schizophrenia (Rajarethinam et al., 2001; Weiss et al., 2005). These discrepancies could be due to different factors, especially parcellation techniques, as most of these studies arbitrarily divide the hippocampus into anterior and posterior segments. The functional division along the longitudinal axis of the hippocampus stresses the importance of a tri-partite parcellation in structural imaging studies (Small, 2002).

Parallels between memory alterations in 22q11DS and in schizophrenia can also be observed. Recall procedures are known to yield greater memory impairments in individuals with schizophrenia (Aleman, Hijman, de Haan, & Kahn, 1999). Authors have suggested that the basis of recollection deficits in schizophrenia pertains to a difficulty in linking the separate aspects of an episode into a coherent and distinctive whole (Danion, Rizzo, & Bruant, 1999; Rizzo, Danion, van der Linden, & Grange, 1996), a task usually sustained by the hippocampus (Aggleton & Brown, 1999; Yonelinas & Levy, 2002). Furthermore, it has been observed that familiarity-based recognition is relatively unimpaired in individuals with schizophrenia, but that recollection-based recognition tasks yield substantial deficits (Achim & Lepage, 2003; Linscott & Knight, 2001; Pelletier, Achim, Montoya, Lal, & Lepage, 2005). Individuals with 22q11DS, who show increased prevalence of schizotypy (Baker and Skuse, 2005) and a 20–30% rate of schizophrenic morbidity (Murphy et al., 1999), do exhibit memory alterations in recall procedures (Henry et al., 2002). Further examination of familiarity and recollection processes are needed to better delineate the influence of hippocampal body alteration in this population.

The present study reports hippocampal body volume reduction in a group of individuals with 22q11DS. One major limitation to this study is the absence of specific memory tasks that could be associated to hippocampal volumes in order to assess the relationship between structure and function in this population. Research is under way to examine the specific memory processes that could be impaired by such structural alteration. Further research is also needed to clarify the relationship between hippocampal volume and risk for schizophrenia in this population. Finally, a detailed account of the mnemonic strengths and weaknesses in relation to morphological and functional cerebral alterations in 22q11DS are necessary to the formulation of adapted educative and therapeutic strategies.

Acknowledgements

We wish to thank all the participants who kindly volunteered for this study. We extend our special thanks to Sophie P. Dahoun, Michael A. Morris and Christine Hinard for genetic analyses, Frank Henry and François Lazeyras, as well as the Clinique des Grangettes, for MRI data acquisition. This research was supported by research grants to Stephan Eliez from the Swiss National Fund for Research (3200-063135.00/1, 3232-063134.00/1, and PP00B-102864), the NARSAD Foundation (2002 Lieber Investigator Award) and the Academic Society of Geneva.

References

Achim, A. M., & Lepage, M. (2003). Is associative recognition more impaired than item recognition memory in schizophrenia? A meta-analysis. *Brain and Cognition*, *53*(2), 121–124.

Aggleton, J. P., & Brown, M. W. (1999). Episodic memory, amnesia, and the hippocampal-anterior thalamic axis. *Behavioural Brain Science*, *22*(3), 425–444, discussion 444–489.

Aggleton, J. P., & Shaw, C. (1996). Amnesia and recognition memory: A re-analysis of psychometric data. *Neuropsychologia*, *34*(1), 51–62.

Aleman, A., Hijman, R., de Haan, E. H., & Kahn, R. S. (1999). Memory impairment in schizophrenia: A meta-analysis. *American Journal of Psychiatry*, *156*(9), 1358–1366.

Amaral, D. G., & Witter, M. P. (1989). The three-dimensional organization of the hippocampal formation: A review of anatomical data. *Neuroscience*, *31*(3), 571–591.

Baker, K. D., & Skuse, D. H. (2005). Adolescents and young adults with 22q11 deletion syndrome: Psychopathology in an at-risk group. *British Journal of Psychiatry*, *186*, 115–120.

Baxendale, S. A. (1997). The role of the hippocampus in recognition memory. *Neuropsychologia*, *35*(5), 591–598.

Bearden, C. E., Woodin, M. F., Wang, P. P., Moss, E., McDonald-McGinn, D., Zackai, E., et al. (2001). The neurocognitive phenotype of the 22q11 2 deletion syndrome: Selective deficit in visual-spatial memory. *Journal of Clinical and Experimental Neuropsychology*, *23*(4), 447–464.

Becker, T., Elmer, K., Schneider, F., Schneider, M., Grodd, W., Bartels, M., et al. (1996). Confirmation of reduced temporal limbic structure volume on magnetic resonance imaging in male patients with schizophrenia. *Psychiatry Research*, *67*(2), 135–143.

Bernasconi, N., Bernasconi, A., Caramanos, Z., Antel, S. B., Andermann, F., & Arnold, D. L. (2003). Mesial temporal damage in temporal lobe epilepsy: A volumetric MRI study of the hippocampus, amygdala and parahippocampal region. *Brain*, *126*(Pt 2), 462–469.

Bish, J. P., Nguyen, V., Ding, L., Ferrante, S., & Simon, T. J. (2004). Thalamic reductions in children with chromosome 22q11 2 deletion syndrome. *Neuroreport*, *15*(9), 1413–1415.

Cirillo, M. A., & Seidman, L. J. (2003). Verbal declarative memory dysfunction in schizophrenia: From clinical assessment to genetics and brain mechanisms. *Neuropsychology Review*, *13*(2), 43–77.

Danion, J. M., Rizzo, L., & Bruant, A. (1999). Functional mechanisms underlying impaired recognition memory and conscious awareness in patients with schizophrenia. *Archives of General Psychiatry*, *56*(7), 639–644.

Debbané, M., Glaser, B., Gex-Fabry, M., & Eliez, S. (2005). Temporal perception in velo-cardio-facial syndrome. *Neuropsychologia*, *43*(12), 1754–1762.

Debbané, M., Glaser, B., David M.K., Feinstein, C., & Eliez, S. (2006). Psychotic: symptoms in children and adolescents with 22q11.2 deletion syndrome; Neuropsychological and behavioral implications. Schizophrenia Research, 84 (2–3), 187–193.

Devriendt, K., Thienen, M. N., Swillen, A., & Fryns, J. P. (1996). Cerebellar hypoplasia in a patient with velo-cardio-facial syndrome. *Developmental Medicine and Child Neurology*, *38*(10), 949–953.

Duvernoy, H. M. (1998). *The human hippocampus* (Second completely revised and expanded edition). Springer.

Eliez, S., Barnea-Goraly, N., Schmitt, J. E., Liu, Y., & Reiss, A. L. (2002). Increased basal ganglia volumes in velo-cardio-facial syndrome (deletion 22q112). *Biological Psychiatry*, *52*(1), 68–70.

Eliez, S., Blasey, C. M., Schmitt, E. J., White, C. D., Hu, D., & Reiss, A. L. (2001). Velocardiofacial syndrome: Are structural changes in the temporal and mesial temporal regions related to schizophrenia? *American Journal of Psychiatry*, *158*(3), 447–453.

Eliez, S., Schmitt, J. E., White, C. D., & Reiss, A. L. (2000). Children and adolescents with velocardiofacial syndrome: A volumetric MRI study. *American Journal of Psychiatry*, *157*(3), 409–415.

Eliez, S., Schmitt, J. E., White, C. D., Wellis, V. G., & Reiss, A. L. (2001). A quantitative MRI study of posterior fossa development in velocardiofacial syndrome. *Biological Psychiatry*, *49*(6), 540–546.

Glaser, B., Mumme, D. L., Blasey, C., Morris, M. A., Dahoun, S. P., Antonarakis, S. E., et al. (2002). Language skills in children with velocardiofacial syndrome (deletion 22q112). *Journal of Pediatrics*, *140*(6), 753–758.

Golding-Kushner, K. J., Weller, G., & Shprintzen, R. J. (1985). Velo-cardio-facial syndrome: Language and psychological profiles. *Journal of Craniofacial Genetics and Developmental Biology*, *5*(3), 259–266.

Gothelf, D., Presburger, G., Levy, D., Nahmani, A., Burg, M., Berant, M., et al. (2004). Genetic, developmental, and physical factors associated with attention deficit hyperactivity disorder in patients with velocardiofacial syndrome. *American Journal of Medical Genetics B*, *126*(1), 116–121.

Heckers, S. (2001). Neuroimaging studies of the hippocampus in schizophrenia. *Hippocampus*, *11*(5), 520–528.

Henry, J. C., van Amelsvoort, T., Morris, R. G., Owen, M. J., Murphy, D. G., & Murphy, K. C. (2002). An investigation of the neuropsychological profile in adults with velo-cardio-facial syndrome (vcfs). *Neuropsychologia*, *40*(5), 471–478.

Hirayasu, Y., Shenton, M. E., Salisbury, D. F., & McCarley, R. W. (2000). Hippocampal and superior temporal gyrus volume in first-episode schizophrenia. *Archives of General Psychiatry*, *57*(6), 618–619.

Karayiorgou, M., Morris, M. A., Morrow, B., Shprintzen, R. J., Goldberg, R., Borrow, J., et al. (1995). Schizophrenia susceptibility associated with interstitial deletions of chromosome 22q11. *Proceedings of the National Academy of Science of the United States of America*, *92*(17), 7612–7616.

Karmiloff-Smith, A., Tyler, L. K., Voice, K., Sims, K., Udwin, O., Howlin, P., et al. (1998). Linguistic dissociations in williams syndrome: Evaluating receptive syntax in on-line and off-line tasks. *Neuropsychologia*, *36*(4), 343–351.

Kates, W. R., Abrams, M. T., Kaufmann, W. E., Breiter, S. N., & Reiss, A. L. (1997). Reliability and validity of MRI measurement of the amygdala and hippocampus in children with fragile x syndrome. *Psychiatry Research*, *75*(1), 31–48.

Kates, W. R., Burnette, C. P., Bessette, B. A., Folley, B. S., Strunge, L., Jabs, E. W., et al. (2004). Frontal and caudate alterations in velocardiofacial syndrome (deletion at chromosome 22q112). *Journal of Child Neurology*, *19*(5), 337–342.

Kurahashi, H., Tsuda, E., Kohama, R., Nakayama, T., Masuno, M., Imaizumi, K., et al. (1997). Another critical region for deletion of 22q11: A study of 100 patients. *American Journal of Medical Genetics*, *72*(2), 180–185.

Lajiness-O'Neill, R. R., Beaulieu, I., Titus, J. B., Asamoah, A., Bigler, E. D., Bawle, E. V., et al. (2005). Memory and learning in children with 22q112 deletion syndrome: Evidence for ventral and dorsal stream disruption? *Neuropsychology Developmental Cognition C Child Neuropsychology*, *11*(1), 55–71.

Lawrie, S. M., Whalley, H. C., Abukmeil, S. S., Kestelman, J. N., Miller, P., Best, J. J., et al. (2002). Temporal lobe volume changes in people at high risk of schizophrenia with psychotic symptoms. *British Journal of Psychiatry*, *181*, 138–143.

Linscott, R. J., & Knight, R. G. (2001). Automatic hypermnesia and impaired recollection in schizophrenia. *Neuropsychology*, *15*(4), 576–585.

Maller, J. J., Reglade-Meslin, C., Anstey, K. J., & Sachdev, P. (2006). Sex and symmetry differences in hippocampal volumetrics: Before and beyond the opening of the crus of the fornix. *Hippocampus*, *16*(1), 80–90.

Mandler, G. (1980). Recognizing: The judgment of previous occurence. *Psychological Review*, *87*, 252–271.

Mayes, A. R., Holdstock, J. S., Isaac, C. L., Hunkin, N. M., & Roberts, N. (2002). Relative sparing of item recognition memory in a patient with adult-onset damage limited to the hippocampus. *Hippocampus*, *12*(3), 325–340.

McCarley, R. W., Wible, C. G., Frumin, M., Hirayasu, Y., Levitt, J. J., Fischer, I. A., et al. (1999). MRI anatomy of schizophrenia. *Biological Psychiatry*, *45*(9), 1099–1119.

Moscovitch, M., Rosenbaum, R. S., Gilboa, A., Addis, D. R., Westmacott, R., Grady, C., et al. (2005). Functional neuroanatomy of remote episodic, semantic and spatial memory: A unified account based on multiple trace theory. *Journal of Anatomy*, *207*(1), 35–66.

Murphy, K. C., Jones, L. A., & Owen, M. J. (1999). High rates of schizophrenia in adults with velo-cardio-facial syndrome. *Archives of General Psychiatry*, *56*(10), 940–945.

Nelson, M. D., Saykin, A. J., Flashman, L. A., & Riordan, H. J. (1998). Hippocampal volume reduction in schizophrenia as assessed by magnetic resonance imaging: A meta-analytic study. *Archives of General Psychiatry*, *55*(5), 433–440.

Oskarsdottir, S., Vujic, M., & Fasth, A. (2004). Incidence and prevalence of the 22q11 deletion syndrome: A population-based study in western Sweden. *Archives of Disease in Childhood*, *89*(2), 148–151.

Pegues, M. P., Rogers, L. J., Amend, D., Vinogradov, S., & Deicken, R. F. (2003). Anterior hippocampal volume reduction in male patients with schizophrenia. *Schizophrinia Research*, *60*(2/3), 105–115.

Pelletier, M., Achim, A. M., Montoya, A., Lal, S., & Lepage, M. (2005). Cognitive and clinical moderators of recognition memory in schizophrenia: A meta-analysis. *Schizophrenia Research*, *74*(2/3), 233–252.

Rajarethinam, R., DeQuardo, J. R., Miedler, J., Arndt, S., Kirbat, R., Brunberg, J. A., et al. (2001). Hippocampus and amygdala in schizophrenia: Assessment of the relationship of neuroanatomy to psychopathology. *Psychiatry Research*, *108*(2), 79–87.

Reiss, A. L., Hennessey, J. G., Rubin, M., Beach, L., Abrams, M. T., Warsofsky, I. S., et al. (1998). Reliability and validity of an algorithm for fuzzy tissue segmentation of MRI. *Journal of Computer Assisted Tomography*, *22*(3), 471–479.

Rizzo, L., Danion, J. M., van der Linden, M., & Grange, D. (1996). Patients with schizophrenia remember that an event has occurred, but not when. *British Journal of Psychiatry*, *168*(4), 427–431.

Shaikh, T. H., Kurahashi, H., Saitta, S. C., O'Hare, A. M., Hu, P., Roe, B. A., et al. (2000). Chromosome 22-specific low copy repeats and the 22q112 deletion syndrome: Genomic organization and deletion endpoint analysis. *Human Molecular Genetics*, *9*(4), 489–501.

Shprintzen, R. J., Goldberg, R. B., Lewin, M. L., Sidoti, E. J., Berkman, M. D., Argamaso, R. V., et al. (1978). A new syndrome involving cleft palate, cardiac anomalies, typical facies, and learning disabilities: Velocardio-facial syndrome. *Cleft Palate Journal*, *15*(1), 56–62.

Small, S. A. (2002). The longitudinal axis of the hippocampal formation: Its anatomy, circuitry, and role in cognitive function. *Reviews in Neuroscience*, *13*(2), 183–194.

Small, S. A., Nava, A. S., Perera, G. M., DeLaPaz, R., Mayeux, R., & Stern, Y. (2001). Circuit mechanisms underlying memory encoding and retrieval in the long axis of the hippocampal formation. *Nature Neuroscience*, *4*(4), 442–449.

Sobin, C., Kiley-Brabeck, K., Daniels, S., Blundell, M., Anyane-Yeboa, K., & Karayiorgou, M. (2004). Networks of attention in children with the 22q11 deletion syndrome. *Developmental Neuropsychology*, *26*(2), 611–626.

Swillen, A., Devriendt, K., Legius, E., Eyskens, B., Dumoulin, M., Gewillig, M., et al. (1997). Intelligence and psychosocial adjustment in velocardiofacial syndrome: A study of 37 children and adolescents with vcfs. *Journal of Medical Genetics*, *34*(6), 453–458.

Swillen, A., Vandeputte, L., Cracco, J., Maes, B., Ghesquiere, P., Devriendt, K., et al. (1999). Neuropsychological, learning and psychosocial profile of primary school aged children with the velo-cardio-facial syndrome (22q11 deletion): Evidence for a nonverbal learning disability? *Neuropsychology Developmental Cognition Section C Child Neuropsychology*, *5*(4), 230–241.

Szeszko, P. R., Goldberg, E., Gunduz-Bruce, H., Ashtari, M., Robinson, D., Malhotra, A. K., et al. (2003). Smaller anterior hippocampal formation volume in antipsychotic-naive patients with first-episode schizophrenia. *American Journal of Psychiatry*, *160*(12), 2190–2197.

van Amelsvoort, T., Daly, E., Robertson, D., Suckling, J., Ng, V., Critchley, H., et al. (2001). Structural brain abnormalities associated with deletion at chromosome 22q11: Quantitative neuroimaging study of adults with velo-cardio-facial syndrome. *British Journal of Psychiatry*, *178*, 412–419.

Vargha-Khadem, F., Gadian, D. G., Watkins, K. E., Connelly, A., Van Paesschen, W., & Mishkin, M. (1997). Differential effects of early hippocampal pathology on episodic and semantic memory. *Science*, *277*(5324), 376–380.

Weiss, A. P., Dewitt, I., Goff, D., Ditman, T., & Heckers, S. (2005). Anterior and posterior hippocampal volumes in schizophrenia. *Schizophrenia Research*, *73*(1), 103–112.

Weiss, A. P., & Heckers, S. (2001). Neuroimaging of declarative memory in schizophrenia. *Scandivian Journal of Psychology*, *42*(3), 239–250.

Wood, S. J., Pantelis, C., Proffitt, T., Phillips, L. J., Stuart, G. W., Buchanan, J. A., et al. (2003). Spatial working memory ability is a marker of risk-for-psychosis. *Psychological Medicine*, *33*(7), 1239–1247.

Yonelinas, A. P. (2001). Components of episodic memory: The contribution of recollection and familiarity. *Philosophical Transactions of the Royal Society of London Series B—Biological Sciences*, *356*(1413), 1363–1374.

Yonelinas, A. P., & Levy, B. J. (2002). Dissociating familiarity from recollection in human recognition memory: Different rates of forgetting over short retention intervals. *Psychonomic Bulletin and Review*, *9*(3), 575–582.

Available online at www.sciencedirect.com
ScienceDirect
Schizophrenia Research 96 (2007) 82 - 86
SCHIZOPHRENIA RESEARCH
www.elsevier.com/locate/schres

Structural changes to the fusiform gyrus: A cerebral marker for social impairments in 22q11.2 deletion syndrome?

Bronwyn Glaser [a,*], Marie Schaer [a,e], Sandra Berney [a], Martin Debbane [a], Patrik Vuilleumier [c,d], Stephan Eliez [a,b]

[a] *Service Médico-Pédagogique, Department of Child Psychiatry, University of Geneva Medical School and University Hospitals, 16-18 bd St Georges, 1211 Geneva 8, Switzerland*
[b] *Department of Genetic Medicine and Development, University of Geneva Medical School and University Hospitals, Switzerland*
[c] *Behavioral Neurology and Imaging of Cognition, Clinic of Neurology, University Hospital and Department of Neurosciences, University Medical Center, Switzerland*
[d] *Swiss National Center of Affective Sciences, University of Geneva, Switzerland*
[e] *Signal Processing Institute, EPFL, LT55, Station 11, 1011 Lausanne, Switzerland*

Received 22 May 2007; received in revised form 9 August 2007; accepted 15 August 2007
Available online 10 September 2007

Abstract

Identifying the neural underpinnings of socio-emotional deficits in 22q11.2 deletion syndrome (22q11DS) may elucidate recurrent psychosis in affected individuals. In the current study, we investigate volumetric changes in 22q11DS to the fusiform gyrus (FG), a region associated with hypoactivity during fMRI, by manually tracing the FG in 42 individuals with 22q11DS and 54 healthy controls. Larger anterior FG volumes and smaller posterior volumes bilaterally are observed in 22q11DS after controlling for total brain volume. The results demonstrate structural changes to the FG in 22q11DS, providing evidence for neural vulnerability in regions related to social cognition.

Keywords: Velocardiofacial syndrome; 22q11 deletion syndrome; Fusiform gyrus; Structural MRI; Face processing; Psychosis

1. Introduction

The fusiform gyrus is consistently the location of maximal activation in fMRI studies of facial identity and expression (Haxby et al., 2000; Kanwisher et al., 1997), illustrating its centrality to the development of social cognition (Adolphs, 2003; Grossmann and Johnson, 2007). As a result FG dysfunction has become key to understanding socio-emotional deregulation in individuals with adult psychiatric conditions such as depression (Surguladze et al., 2005) and schizophrenia (Gur et al., 2002), as well as early developmental disorders such as autism (Waiter et al., 2004).

Individuals with 22q11.2 deletion syndrome (22q11DS), a rare genetic condition caused by a deletion on chromosome 22, demonstrate social withdrawal, mood problems and frequent psychotic manifestations (Baker and Skuse, 2005). Accordingly, 50% of children and

Abbreviations: 22q11DS, 22q11.2 deletion syndrome; FG, fusiform gyrus; MRI, magnetic resonance imaging.

* Corresponding author. Service médico-pédagogique, Bd St-Georges 16-18, Case postale 50, CH-1211 Geneva 8, Switzerland. Tel.: +41 22 327 43 02; fax: +41 22 327 43 20.
E-mail addresses: bronwyn.glaser@medecine.unige.ch (B. Glaser), marie.schaer@medecine.unige.ch (M. Schaer), candy@hispeed.ch (S. Berney), martin.debbane@medecine.unige.ch (M. Debbane), patrik.Vuilleumier@medecine.unige.ch (P. Vuilleumier), stephan.eliez@medecine.unige.ch (S. Eliez).

0920-9964/$ - see front matter © 2007 Elsevier B.V. All rights reserved.
doi:10.1016/j.schres.2007.08.016

adolescents deal with psychotic symptoms, mostly auditory hallucinations and ideas of reference, and 30% of adults are attributed a diagnosis of schizophrenia (Baker and Skuse, 2005; Debbane et al., 2006a). Weaker performances on measures of face recognition and processing (Glaser et al., 2006; Lajiness-O'Neill et al., 2005) and more severe emotional problems (Kates et al., 2006) are among a profile of cognitive deficits in 22q11DS, which are related to persistent reductions in grey and white matter (Zinkstok and van Amelsvoort, 2005). Recent fMRI studies have further related these deficits to functional impairments by demonstrating a reduced face-selective response in the fusiform gyrus when individuals with 22q11DS viewed faces (Andersson et al., in press) and impaired emotion processing in individuals with the syndrome (van Amelsvoort et al., 2006). This evidence for impaired functional face networks, especially pronounced in affected individuals with positive psychotic symptoms (Andersson et al., in press), suggests that structural brain alterations in 22q11DS may underlie social problems associated with the syndrome.

The goal of the current study was to further investigate a key region in face processing and social cognition in 22q11DS by measuring the fusiform gyrus (FG). A manual protocol for dividing the FG into anterior, medial, and posterior sub-divisions was thus created to identify alterations to subregions in 22q11DS.

2. Methods

2.1. Participants

Forty-two individuals affected by 22q11DS (24 females, 18 males, mean age: 13.98 years, SD = 5.08) and 54 matched healthy controls (31 females, 23 males, mean age: 13.44 years, SD = 5.46) were recruited consecutively through parent associations and nearby schools in the community, respectively. Eighteen of the individuals with 22q11DS and 29 of the controls also participated in a recent study of differences in cortical folding (Schaer et al., 2006). Written informed consent was received from all of the subjects' parents under protocols approved by the Institutional Review Board of the university hospital. FISH was used to confirm the 22q11.2 microdeletion in patients (Karayiorgou et al., 1995). Semi-structured interviews (DICA, SCID-I, K-SADS-PL) revealed psychotic symptoms, including hallucinations (31%) or delusions (38%), in 21 (50%) of the 22q11DS patients, a rate consistent with other 22q11DS samples (Baker and Skuse, 2005). Only one patient with a diagnosis of schizophrenia, who was medicated for psychotic symptoms at time of participation, could be scanned and included in the sample.

2.2. Collection of MRI data and creation of fusiform protocol

Cerebral magnetic resonance images were acquired using a Philips Intera 1.5 T scanner, details on the sequence parameters and pre-processing have been previously described (Debbane et al., 2006b; Eliez et al., 2001b; Schaer et al., 2006). AC-PC aligned coronal slices were subsequently used for delineating the FG.

A standardized protocol was created for manually tracing the FG based on previous parcellation of the temporal lobe (Kim et al., 2000) and atlas guidelines (Duvernoy, 1991). To create the protocol, the FG was first defined as the gyrus situated between the inferior temporal gyrus laterally, with the entorhinal cortex and the lingual gyrus, at the rostral and caudal ends respectively, on the medial side. In the past, structural imaging studies have calculated a more abbreviated measure of the FG, by excluding the antero-posterior extreme points (Lee et al., 2002). To measure the FG in its entirety, we extended previous boundaries by using the AC as the anterior limit of the FG. For the posterior limit, we used the transverse collateral sulcus (a point that is easily identifiable on all individuals) at 5 mm from the mid-sagittal slice to circumvent

Table 1
Fusiform volumes before and after adjustment for total cerebral volume

	22q11DS (N=42) Mean±SD	Controls (N=54) Mean±SD	ANCOVA F	df	p
Total brain volume	1000.539±117.331	1105.545±108.972	20.511	95	b.001
Fusiform gyrus					
Anterior section					
Right	4.508±1.125	4.563±0.757	4.809	94	0.031
Left	4.673±1.285	4.441±0.727	12.768	94	0.001
Medial section					
Right	4.619±1.049	5.303±1.066	0.601	94	0.440
Left	4.239±1.017	4.814±0.907	0.302	94	0.584
Posterior section					
Right	4.693±1.682	5.934±1.759	3.983	94	0.049
Left	4.888±1.380	5.982±1.691	5.071	94	0.027

Note: Raw measurements of the segmented parts of the fusiform are included in the table. Follow-up ANCOVA indicate that after correcting for differences in total brain tissue, the anterior sub-sections are significantly bigger in the 22q11DS group and the posterior sub-sections are significantly smaller bilaterally. All volumes are expressed in cm^3.

the frequent difficulty of finding a consistently identifiable posterior limit on coronal slices. The entire fusiform was then traced in the posterior to anterior direction. The anterior section corresponded to Talairach boxes E1–E3, the medial section to boxes F and G, and the rest was included as the posterior section.

2.3. Statistical analyses

Inter-rater reliability for manual tracing was established by two raters (MS and SB) on 10 randomly selected participants. The inter-rater alpha correlation coefficient was 0.9855 for the left hemisphere and 0.9847 for the right hemisphere.

Multivariate analysis of covariance was used to compare the two subject groups on the 6 sub-divisions of the FG (left and right). Given frequently reported differences in total volumes between-groups, all analyses were covaried by total tissue volume. Follow-up ANCOVA were then run to detect differences in the anterior, medial, and posterior parts bilaterally.

3. Results

Differences in total brain tissue volumes and FG sub-sections are reported in Table 1. After covarying for total brain tissue volume, significant differences in FG volumes were detected between 22q11DS and comparison subjects (Wilks Lambda of 0.812; $F(6,88) = 3.391$; $p = 0.005$). Specifically, follow-up ANCOVA indicated that individuals with 22q11DS had significantly larger anterior FG volumes and smaller posterior FG volumes bilaterally, as compared with controls (Table 1).

4. Discussion

The aim of this study was to test whether the FG is structurally altered in 22q11DS, given recent evidence for functional alterations to face and emotion processing (Andersson et al., in press; van Amelsvoort et al., 2006). After correcting for total intracranial volumes, we observed increased anterior and decreased posterior FG volumes in patients versus controls, thus varying the structure's characteristic "fusi-", or spindle-like, form in 22q11DS.

In 22q11DS, changes to the FG may affect individuals' abilities to accurately identify faces and process emotional stimuli (Andersson et al., in press), as well as inter-regional connectivity with amygdala, medial prefrontal lobe, and other limbic cortical regions. This idea is further supported by previous whole-brain volumetric imaging studies (Eliez et al., 2000; Simon et al., 2005), which echo observed FG changes. In 22q11DS, posterior cerebral structures are reduced in children and adults. By contrast, anterior brain structures appear preserved in children (Kates et al., 2001) and reduced in adulthood, suggesting abnormal pruning and maturational processes with age (van Amelsvoort et al., 2001). Quantitative alterations of cortical volumes are also accompanied by reductions in white matter (van Amelsvoort et al., 2001) and abnormal frontal-temporal and frontal-parietal tracts (Barnea-Goraly et al., 2003), as well as more diffuse patterns of activity in 22q11DS during fMRI studies (Andersson et al., in press; Eliez et al., 2001a; van Amelsvoort et al., 2006), consistent with changes to connectivity between structures.

A neurobiological hypothesis, implicating abnormal inter-regional connectivity, has been proposed in autism (Belmonte et al., 2004), another developmental disorder associated with face processing impairments (Behrmann et al., 2006) and increased anterior FG volumes (Waiter et al., 2004). Belmonte and colleagues hypothesize that in the case of autism, structural impairments may inhibit the formation of inter-regional connections and increase intra-regional connections (Belmonte et al., 2004). Posterior reduction and anterior preservation in the FG in children with 22q11DS may similarly contribute to face-specific impairments of the ventral temporal stream (Andersson et al., in press), a functionally defined region in which the specialization of discrete cortical areas appears to be highly dependent on the honing of inter-regional connections (Young, 1992).

The current study provides evidence for the reorganization of brain regions related to face and emotion recognition in the syndrome. Alterations to the FG have been previously noted in schizophrenia (Lee et al., 2002), with decreased posterior FG volumes especially linked to schizotypy (Takahashi et al., 2006). Accordingly, it is possible that structural changes to the FG and inter-regional tracts in 22q11DS may prime patients' psycho-social and neural vulnerability for the fusiform atrophy observed in adults with frequent psychotic manifestations (Lee et al., 2002).

Role of the funding source

Swiss National Research Funds to SE (PP00B-102864) and MS (323500-111165) supported the research in this manuscript, as well as a grant from the NARSAD Institute to SE. We hereby attest that these agencies had no further role in study design; in the collection, analysis and interpretation of data; in the writing of the report; and in the decision to submit the paper for publication.

Contributors

Bronwyn Glaser recruited and evaluated patients, designed the study, carried out all statistical analyses and wrote the report. Marie Schaer researched, designed, standardized and supervised manual measurement of the fusiform gyrus. After participating in the standardization of the protocol, Sandra Berney manually traced the fusiform in all subjects. Martin Debbané recruited and evaluated patients and gave feedback on the written report. Patrik Vuilleumier co-supervised Sandra Berney and Bronwyn Glaser, and contributed input to the written report. Stephan Eliez is the titled investigator of the funding grants. He taught Marie Schaer and Sandra Berney the necessary imaging measurement techniques and tools, carried out all clinical and MRI evaluations with participants, and helped revise the written report. All authors contributed to and have approved the final manuscript.

Conflict of interest

All authors declare that they have no conflicts of interest.

Acknowledgement

We thank J. Delavelle, F. Henry, and F. Lazeyras for their support and assistance with data collection, as well as the Center for Biomedical Imaging (CIBM) of the Geneva-Lausanne Universities and the EPFL, and the foundations Leenaards and Louis Jeantet. We would also like to acknowledge S. Dahoun, C. Hinard, M. Morris, and S. Antonarakis for their ongoing collaboration in the Department of Genetics. This work is made possible by the Swiss and French deletion 22q11 parent associations, Connect22 and Generation 22.

References

Adolphs, R., 2003. Cognitive neuroscience of human social behaviour. Nat. Rev., Neurosci. 4 (3), 165–178.

Andersson, F., Glaser, B., Spiridon, M., Debbane, M., Lazeyras, F., Delavelle, J., Vuilleumier, P., Eliez, S., in press. Impaired activation of face processing networks revealed by fMRI in 22q11.2 deletion syndrome. Biological Psychiatry (Jul 23 2007, Electronic publication ahead of print).

Baker, K.D., Skuse, D.H., 2005. Adolescents and young adults with 22q11 deletion syndrome: psychopathology in an at-risk group. Br. J. Psychiatry 186, 115-120.

Barnea-Goraly, N., Menon, V., Krasnow, B., Ko, A., Reiss, A., Eliez, S., 2003. Investigation of white matter structure in velocardiofacial syndrome: a diffusion tensor imaging study. Am. J. Psychiatry 160 (10), 1863 -1869.

Behrmann, M., Avidan, G., Leonard, G.L., Kimchi, R., Luna, B., Humphreys, K., Minshew, N., 2006. Configural processing in autism and its relationship to face processing. Neuropsychologia 44 (1), 110 -129.

Belmonte, M.K., Allen, G., Beckel-Mitchener, A., Boulanger, L.M., Carper, R.A., Webb, S.J., 2004. Autism and abnormal development of brain connectivity. J. Neurosci. 24 (42), 9228-9231.

Debbane, M., Glaser, B., David, M.K., Feinstein, C., Eliez, S., 2006a. Psychotic symptoms in children and adolescents with 22q11.2 deletion syndrome: neuropsychological and behavioral implications. Schizophr. Res. 84 (2-3), 187-193.

Debbane, M., Schaer, M., Farhoumand, R., Glaser, B., Eliez, S., 2006b. Hippocampal volume reduction in 22q11.2 deletion syndrome. Neuropsychologia 44 (12), 2360-2365.

Duvernoy, H.M., 1991. The Human Brain: Surface, Three-Dimensional Sectional Anatomy and MRI. Series. Springer-Verlag Wien, New York.

Eliez, S., Schmitt, J.E., White, C.D., Reiss, A.L., 2000. Children and adolescents with velocardiofacial syndrome: a volumetric MRI study. Am. J. Psychiatry 157 (3), 409-415.

Eliez, S., Blasey, C.M., Menon, V., White, C.D., Schmitt, J.E., Reiss, A.L., 2001a. Functional brain imaging study of mathematical reasoning abilities in velocardiofacial syndrome (del22q11.2). Genet. Med. 3 (1), 49-55.

Eliez, S., Blasey, C.M., Schmitt, E.J., White, C.D., Hu, D., Reiss, A.L., 2001b. Velocardiofacial syndrome: are structural changes in the temporal and mesial temporal regions related to schizophrenia? Am. J. Psychiatry 158 (3), 447-453.

Glaser, B., Debbane, M., Schaer, M., Martinez, S., Berney, S., Andersson, F., Spiridon, M., Vuilleumier, P., Eliez, S., 2006. What can face processing tell us about cognitive and social development in VCFS? 12th Annual International Scientific Meeting of the Velo-Cardio-Facial Syndrome Educational Foundation. Strasbourg, France.

Grossmann, T., Johnson, M.H., 2007. The development of the social brain in human infancy. Eur. J. Neurosci. 25 (4), 909-919.

Gur, R.E., McGrath, C., Chan, R.M., Schroeder, L., Turner, T., Turetsky, B.I., Kohler, C., Alsop, D., Maldjian, J., Ragland, J.D., Gur, R.C., 2002. An fMRI study of facial emotion processing in patients with schizophrenia. Am. J. Psychiatry 159 (12), 1992-1999.

Haxby, J.V., Hoffman, E.A., Gobbini, M.I., 2000. The distributed human neural system for face perception. Trends Cogn. Sci. 4 (6), 223Ð233.

Kanwisher, N., McDermott, J., Chun, M.M., 1997. The fusiform face area: a module in human extrastriate cortex specialized for face perception. J. Neurosci. 17 (11), 4302-4311.

Karayiorgou, M., Morris, M.A., Morrow, B., Shprintzen, R.J., Goldberg, R., Borrow, J., Gos, A., Nestadt, G., Wolyniec, P.S., Lasseter, V.K., et al., 1995. Schizophrenia susceptibility associated with interstitial deletions of chromosome 22q11. Proc. Natl. Acad. Sci. U S A 92 (17), 7612-7616.

Kates, W.R., Burnette, C.P., Jabs, E.W., Rutberg, J., Murphy, A.M., Grados, M., Geraghty, M., Kaufmann, W.E., Pearlson, G.D., 2001. Regional cortical white matter reductions in velocardiofacial syndrome: a volumetric MRI analysis. Biol. Psychiatry 49 (8), 677- 684.

Kates, W.R., Miller, A.M., Abdulsabur, N., Antshel, K.M., Conchelos, J., Fremont, W., Roizen, N., 2006. Temporal lobe anatomy and psychiatric symptoms in velocardiofacial syndrome (22q11.2 deletion syndrome). J. Am. Acad. Child Adolesc. Psych. 45 (5), 587- 595.

Kim, J.J., Crespo-Facorro, B., Andreasen, N.C., O'Leary, D.S., Zhang, B., Harris, G., Magnotta, V.A., 2000. An MRI-based parcellation method for the temporal lobe. NeuroImage 11 (4), 271-288.

Lajiness-O'Neill, R.R., Beaulieu, I., Titus, J.B., Asamoah, A., Bigler, E.D., Bawle, E.V., Pollack, R., 2005. Memory and learning in children with 22q11.2 deletion syndrome: evidence for ventral and dorsal stream disruption? Child Neuropsychol. 11 (1), 55-71.

Lee, C.U., Shenton, M.E., Salisbury, D.F., Kasai, K., Onitsuka, T., Dickey, C.C., Yurgelun-Todd, D., Kikinis, R., Jolesz, F.A., McCarley, R.W., 2002. Fusiform gyrus volume reduction in first-episode schizophrenia: a magnetic resonance imaging study. Arch. Gen. Psychiatry 59 (9), 775-781.

Schaer, M., Schmitt, J.E., Glaser, B., Lazeyras, F., Delavelle, J., Eliez, S., 2006. Abnormal patterns of cortical gyrification in velo-cardio-facial syndrome (deletion 22q11.2): an MRI study. Psychiatry Res. 146 (1), 1-11.

Simon, T.J., Ding, L., Bish, J.P., McDonald-McGinn, D.M., Zackai, E.H., Gee, J., 2005. Volumetric, connective, and morphologic changes in the

brains of children with chromosome 22q11.2 deletion syndrome: an integrative study. NeuroImage 25 (1), 169–180.

Surguladze, S., Brammer, M.J., Keedwell, P., Giampietro, V., Young, A.W., Travis, M.J., Williams, S.C., Phillips, M.L., 2005. A differential pattern of neural response toward sad versus happy facial expressions in major depressive disorder. Biol. Psychiatry 57 (3), 201 - 209.

Takahashi, T., Suzuki, M., Zhou, S.Y., Tanino, R., Hagino, H., Niu, L., Kawasaki, Y., Seto, H., Kurachi, M., 2006. Temporal lobe gray matter in schizophrenia spectrum: a volumetric MRI study of the fusiform gyrus, parahippocampal gyrus, and middle and inferior temporal gyri. Schizophr. Res. 87 (1-3), 116 - 126.

van Amelsvoort, T., Daly, E., Robertson, D., Suckling, J., Ng, V., Critchley, H., Owen, M.J., Henry, J., Murphy, K.C., Murphy, D.G., 2001. Structural brain abnormalities associated with deletion at chromosome 22q11: quantitative neuroimaging study of adults with velo-cardio-facial syndrome. Br. J. Psychiatry 178, 412 - 419.

van Amelsvoort, T., Schmitz, N., Daly, E., Deeley, Q., Critchley, H., Henry, J., Robertson, D., Owen, M., Murphy, K.C., Murphy, D.G., 2006. Processing facial emotion in adults with velo-cardio-facial syndrome: functional magnetic resonance imaging. Br. J. Psychiatry 189, 560 - 561.

Waiter, G.D., Williams, J.H., Murray, A.D., Gilchrist, A., Perrett, D.I., Whiten, A., 2004. A voxel-based investigation of brain structure in male adolescents with autistic spectrum disorder. NeuroImage 22 (2), 619 - 625.

Young, M.P., 1992. Objective analysis of the topological organization of the primate cortical visual system. Nature 358 (6382), 152 - 155.

Zinkstok, J., van Amelsvoort, T., 2005. Neuropsychological profile and neuroimaging in patients with 22Q11.2 Deletion Syndrome: a review. Neuropsychol. Dev. Cogn., Sect. C, Child Neuropsychol. 11 (1), 21 - 37.

Neuropsychologia 46 (2008) 2986–2992

Contents lists available at ScienceDirect

Neuropsychologia

journal homepage: www.elsevier.com/locate/neuropsychologia

Cingulate gyral reductions are related to low executive functioning and psychotic symptoms in 22q11.2 deletion syndrome

Federico Dufour[a,*], Marie Schaer[a,d], Martin Debbané[a,b], Riaz Farhoumand[a], Bronwyn Glaser[a,b], Stephan Eliez[a,c]

[a] *Service Médico-Pédagogique Research Unit, Department of Psychiatry, University of Geneva School of Medicine, 1 rue David-Dufour, Case Postale 50, 1211 Geneva 8, Switzerland*
[b] *Faculty of Psychology, University of Geneva, Switzerland*
[c] *Department of Genetic Medicine and Development, University of Geneva School of Medicine, Switzerland*
[d] *Signal Processing Institute, Swiss Federal Institute of Technology, Lausanne, Switzerland*

ARTICLE INFO

Article history:
Received 5 October 2007
Received in revised form 27 May 2008
Accepted 9 June 2008
Available online 21 June 2008

Keywords:
Cingulate gyrus
Neuroimaging
Psychosis
Velo-cardio-facial
Executive function
Schizophrenia

ABSTRACT

A similar pattern of deficits in executive function and neuroanatomical abnormalities is shared between 22q11.2 deletion syndrome (22q11DS) and schizophrenia, suggesting that common cerebral alterations may lead to cognitive dysfunction and promote the appearance of psychotic symptoms in 22q11DS individuals. Specifically, there is increasing evidence for involvement of the cingulate gyrus (CG) in executive dysfunction and the expression of positive symptoms in schizophrenia. The aim of our study is to examine CG morphology in a 22q11DS population and its potential role as a cerebral marker of executive dysfunction and the manifestation of psychotic symptoms. Using region of interest (ROI)-based analysis, we compared CG volumes from 58 children and adults affected by 22q11DS with 64 healthy age- and gender-matched controls. After covarying for total cranium grey matter and age, a bilateral reduced CG grey matter volume, driven by a decrease in anterior CG cortex, was observed among 22q11DS patients. Further post hoc analyses suggest correlations between right CG cortical reductions, low-executive functioning and the occurrence of psychotic symptoms. The CG structural abnormalities observed in 22q11DS are consistent with previous reports in schizophrenic patients and are associated with pre-morbid cognitive impairments. The mechanisms by which these changes may modulate executive functioning and the expression of psychosis are discussed.

1. Introduction

Recent studies suggest that individuals at high-risk for psychosis demonstrate structural abnormalities in the cingulate gyrus (CG) (Pantelis et al., 2003), especially reduced grey matter in the anterior cingulate (Borgwardt et al., 2007; Yamasue et al., 2004). As part of the limbic system, the CG is involved in executive function and shares numerous connections with prefrontal cortex and hippocampus (Bush, Luu, & Posner, 2000), two other regions significantly altered in schizophrenia (Gur, Keshavan, & Lawrie, 2007; Suzuki et al., 2005). Moreover, cognitive impairments linked with both of these structures, specifically executive function and working memory, are considered as putative endophenotypes and core features for schizophrenia (Bilder et al., 2000; Mohamed, Paulsen, O'Leary, Arndt, & Andreasen, 1999; Silver, Feldman, Bilker, & Gur, 2003; Snitz, Angus, MacDonald, & Carter, 2006). Increasing interest is given to identifying such potential endophenotypes, which represent important markers for the complex relationships between genes, brain and related cognitive functions.

It is now established that almost a third of individuals affected by 22q11.2 deletion syndrome (22q11DS), a neurogenetic autosomal dominant condition occurring in approximately 1 in 4000 live births (Oskarsdóttir, Vujic, & Fasth, 2004), eventually develop schizophrenia (Murphy, Jones, & Owen, 1999). Moreover, neuropsychological deficits associated with schizophrenia are already apparent in youngsters with 22q11DS. These deficits include impairments in executive function, sustained attention and verbal skills (Lewandowski, Shashi, Berry, & Kwapil, 2007). Studies on schizotypal manifestations in 22q11DS show that half of the adolescents with the syndrome experience transient positive psychotic symptoms, such as hallucinations and delusions (Baker & Skuse, 2005; Debbané, Glaser, David, Feinstein, & Eliez, 2006). Auditory hallucinations represent the earliest symptomatic manifestation of psychosis in children with 22q11DS, which can be observed as early as the age of 9 (Debbané et al., 2006a), and represent a powerful

* Corresponding author. Tel.: +41 22 388 96 72; fax: +41 22 388 96 83.
E-mail addresses: federico.dufour@etat.ge.ch, fede.dufour@bluewin.ch (F. Dufour).

0028-3932/$ – see front matter © 2008 Elsevier Ltd. All rights reserved.
doi:10.1016/j.neuropsychologia.2008.06.012

predictor for subsequent development of psychosis (Gothelf, Feinstein et al. 2007; Poulton et al., 2000). These observations lend support for the view of psychosis as a continuum (van Os & Tamminga, 2007), according to which cognitive and clinical manifestations of schizophrenia can be observed, at reduced levels of expression, in individuals prone to psychosis (Brewer et al., 2006).

As previously mentioned, subjects at high-risk for psychosis display brain morphological changes in addition to cognitive changes compared to healthy individuals. Neuroimaging studies of 22q11DS describe how cerebral alterations in the syndrome relate to schizophrenia (Chow, Zipursky, Mikulis, & Bassett, 2002; Zinkstok & van Amelsvoort, 2005). Individuals with 22q11DS display general structural brain abnormalities, including reduced total brain tissue, grey and white matter volumes (Eliez, Schmitt, White, & Reiss, 2000; Kates et al., 2001), increased ventricular and basal ganglia volumes (Eliez, Barnea-Goraly, Schmitt, Liu, & Reiss, 2002), decreased thalamic, hippocampal as well amygdala volumes (Bish, Nguyen, Ding, Ferrante, & Simon, 2004; Debbané, Schaer, Farhoumand, Glaser, & Eliez, 2006; Deboer, Wu, Lee, & Simon, 2007), and a reduction in cingulate grey matter density (Simon et al., 2005). In schizophrenic 22q11DS subjects compared to non-schizophrenic, further anatomical differences include decreased whole-brain total volume and total white matter and increased total and sulcal cerebrospinal fluid volume (van Amelsvoort et al., 2004). These results provide evidence for a specific pattern of schizophrenic-like cerebral alterations in 22q11DS. Additionally, the executive function deficits in 22q11DS (Lewandowski et al., 2007) have been closely related to structural abnormalities in the anterior CG in schizophrenia (Carter, MacDonald, Ross, & Stenger, 2001; Morey et al., 2005; Szeszko et al., 2000).

Research has demonstrated that structural cerebral alterations may disrupt related cognitive function (Bush et al., 2000; Karmiloff-Smith et al., 1998), potentially sustaining resulting psychopathological manifestations such as hallucinations (Aleman & Larøi, 2008). Frith, Friston, Liddle, & Frackowiak (1992) suggests that the anterior CG is key to positive symptom activity, and recent research supports this claim (Allen, Larøi, McGuire, & Aleman, 2008). In the verbal self-monitoring hypothesis proposed by Frith et al. (1992), positive symptoms involve misattributing the origin of self-generated mental events (thoughts, intentions, internal speech) to a source other than the self. These self-monitoring deficits, shown to involve the anterior CG (Allen et al., 2007), can promote the expression of hallucinations (Aleman & Larøi, 2008). Accordingly, both structural and functional alterations in the anterior CG are present among psychotic patients with positive symptoms (Choi et al., 2005; Shergill, Brammer, Williams, Murray, & McGuire, 2000; Wang et al., 2007). Therefore, given that 22q11DS patients are particularly prone to experience positive symptoms like hallucinations from a young age (Baker & Skuse, 2005; Debbané, Glaser et al., 2006), a careful analysis of CG structure and associated clinical symptoms seems worthwhile.

The aim of this study is to examine CG structure and its potential relationships with executive dysfunction and positive psychotic symptomatology in a sample of individuals with 22q11DS.

To accurately measure CG morphology, we employed a ROI-based analysis method for its high sensitivity and specificity, rather than voxel-based morphometry (VBM)-analysis, which can sometimes produce artifactual results (Eckert et al., 2006). We conducted this research on a large sample of affected children, adults and healthy controls. As suggested by previous VBM results (Simon et al., 2005), we expected CG volumes to be reduced in 22q11DS subjects. Following previous reports on executive dysfunction and CG alterations in schizophrenic patients (Carter et al., 2001; Morey et al., 2005; Szeszko et al., 2000), we explored whether altered CG morphology is associated with the deficits in executive function frequently observed in 22q11DS (Lewandowski et al., 2007). Finally, given evidence for an implication of CG integrity in the expression of positive psychotic symptoms, we expected to find structural differences in CG volume between psychotic and non-psychotic 22q11DS individuals.

2. Materials and methods

2.1. Subjects

2.1.1. 22q11DS group

Fifty-eight patients with 22q11DS aged 6–37 years (mean = 15.52 ± 8.75) participated in the study. Detailed demographic characteristics are presented in Table 1. The sample had a mean full-scale IQ score of 69.03 ± 11.79 as measured by the Wechsler Intelligence Scales for Children or Adults (WISC-III and WAIS-III) (Wechsler, 1991, 1997). The 22q11.2 deletion was confirmed in all patients using PCR direct sequencing. Written informed consent was received from all participating subjects, as well as the parents of subjects younger than 18 years of age, in accordance with protocols approved by the Institutional Review Board of Geneva University School of Medicine. At time of participation, a total of 10 patients were taking psychotropic medication, five of which had a diagnosis of schizophrenia.

The presence of positive psychotic symptoms was determined through semi-structured interviews with participants affected by 22q11DS and their parents. The parents of participants younger than 18 years responded to a computerized DICA-P (Reich, 2000), administered by a child and adolescent psychiatrist (S.E.). DICA-P software generated DSM-IV diagnoses as well as a listing by diagnostic criteria of all symptoms reported as present or absent. The DICA-P was supplemented with the K-SADS-PL (Kaufman et al., 1997) for evidence of psychosis and mood cycling. Participants older than 18 years were interviewed separately from their parents by the same psychiatrist (S.E.) using the SCID-I to generate DSM-IV diagnoses and criteria (First et al., 1993). This procedure was supplemented with the SADS-PL. The "degree of psychosis" scale (Table 1) represents a description of patients' psychotic symptoms and the severity. This scale has been used in a previous publication (Debbané, Glaser, & Eliez, 2008).

2.1.2. 22q11DS subgroups

Psychotic (n = 24, 11 males and 13 females) and non-psychotic (n = 18, 7 males and 11 females) subgroups were created from the 22q11DS group for post hoc analyses. This division corresponds to a degree of psychosis >0 (psychotic) or =0 (non-psychotic). Only patients older than age 9 were used (n = 42), given the age at which psychotic symptoms become relevant in the clinical picture of children with 22q11DS (Debbané, Glaser et al., 2006).

These patients also were divided into high-executive functioning (n = 20, 12 males and 8 females) and low-executive functioning (n = 20, 5 male and 15 female) subgroups. A composite score (WISC III-Digit span subtest + Stroop interference score) was used to assess level of executive function. Only for the executive function analyses, two of the 42 subjects were excluded due to an absence of data. Table 3 shows detailed group characteristics and Section 2.3 describes the executive function composite score.

2.1.3. Control group

The comparison group consisted of 64 healthy individuals aged 6–39 years (mean = 15.02 ± 8.09) with a mean IQ of 111.89 ± 13.02. An absence of past or present neurological and psychiatric disorders was established during a medical intake interview and by using scores from standardized screening forms (Medical and Developmental History Form, the CBCL for individuals younger than 18, and the SCL-90 for those older than 18).

2.2. Brain imaging

MRI was performed on a Philips Intera 1.5T scanner; 124 contiguous coronal slices with a thickness of 1.5 mm and in-plane resolution of 0.94 mm × 0.94 mm (TR = 35 ms, TE = 6 ms) were acquired. Image optimization was performed in BrainImage 5.2 following standard procedures whose details have been published elsewhere (Reiss et al., 1998; Schaer et al., 2006).

Manual circumscription of the cingulate gyrus ROI was performed based on a previously published protocol (Woodward et al., 2006) developed by the principal investigator (S.E.). Briefly, we first traced left and right CG on sagittal slices 5 mm lateral to the midline. Sagittal landmarks were used to draw CG boundaries on coronal slices. The CG was delimited medially by the inter-hemispheric cortical surface, and laterally by a line between the deepest extension of the CG sulcus and the deepest extension of CG grey matter adjacent to the corpus callosum (CC), and by the CG sulcus superiorly and the CC or the calcarine fissure inferiorly. A dynamic Talaraich grid (Talaraich & Tournoux, 1988) was then used to define four sub-regions of the CG: ventral anterior (VA; corresponding to A/B/C boxes of Talairach), dorsal anterior (DA; D/E1 boxes), cingulate body (CinB; E2/E3 boxes) and splenium cingulate (SCin; F/G boxes) (Fig. 1).

Table 1
Demographic and medical data

	22q11DS			Controls			ANOVA	
	n	Mean	S.D.	*n*	Mean	S.D.	*F*	*p*
Age	58	15.521	±8.751	64	15.024	±8.099	0.106	0.745
IQ	58	69.034	±11.799	64	111.89	±13.023	360.102	0.001
Gender 1/2		1.569	±0.499		1.609	±0.491	0.202	0.654
Male = 1	25			25				
Female = 2	33			39				
Degree of psychosis[a]	58	1.21	±1.67	NA	NA			
Psychotropic medication	10		0					
Schizophrenia	5		0					

[a] Degree of psychosis: 0 = no symptoms lifetime; 1 = hallucination or delusion (<3 lifetime); 2 = hallucination or delusion (>3 lifetime); 3 = hallucination or delusion (monthly basis); 4 = hallucination or delusion (weekly basis); 5 = DSM-IV schizophrenia diagnosis.

For all procedures, two independent raters, blind to the participants' diagnoses (FD, MS), traced the CG volumes of 10 randomly chosen subjects. Intra-class correlation coefficients for total left and right cingulate tissue volumes were 0.94, indicating good inter-rater reliability for measurements.

2.3. Statistics

An alpha of 0.05 (two-tailed) was used as the threshold for statistical significance. Specific covariates including total grey or white matter volumes, age, IQ or psychosis degree were used when necessary to exclude any non-significant free-standing results.

2.3.1. Volumetric comparisons between 22q11DS and control groups

First, ANOVA were used to compare total brain tissue, grey and white matter volumes between groups. Second, we used MANCOVA, with total cranium grey or white matter volumes respectively as covariates, to compare CG grey and white matter volumes bilaterally, and then to compare grey matter volumes from the four CG sub-regions for both hemispheres. Significant regional differences were then retested adding age as a covariate.

2.3.2. Post hoc volumetric analyses within 22q11DS and control subgroups

For the aforementioned reasons, only patients 9 years of age and older were included in post hoc analyses.

First, we defined high- and low-executive functioning subgroups by averaging the *z*-scores converted from standard scores obtained from the Digit Span and Stroop interference tasks. These tests were specifically chosen given that the anterior CG cognitive division is important for executive control (Bush et al., 2000). We then divided our sample of 22q11DS subjects by high (*z*-score > 0) and low (*z*-score < 0) executive-functioning individuals. An ANCOVA using age, IQ and degree of psychosis as covariates, and executive function as a group factor was then performed to compare high and low executive functioning subgroups on left/right CG grey matter volumes.

Second, we employed ANCOVA, with age as a covariate and presence of psychotic symptoms as a group factor to test the effect of psychosis on left and right CG grey matter volumes.

Finally, we repeated the same procedure for posterior CG regions (splenium cingulate sub-region), which were not expected to be related to executive function or psychotic symptoms.

We subsequently tested for any significant relationships between executive functioning and CG grey matter volumes within control subjects older than 9 (48 individuals split in 27 high- and 21 low-executive functioning control subjects).

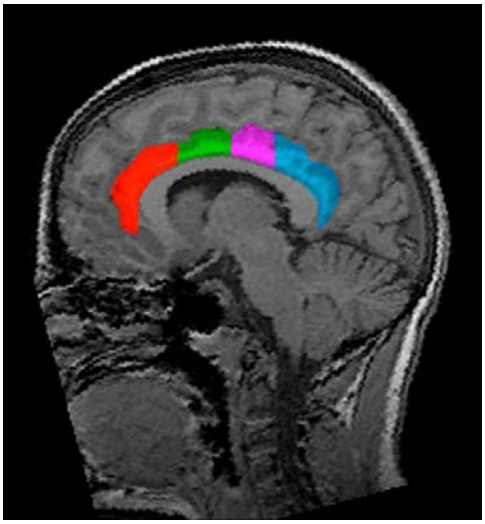

Fig. 1. Sub-regions of the cingulate gyrus are shown: ventral anterior (red), dorsal anterior (green), cingulate body (pink), splenium cingulate (blue). The ROI excluded sub-genual cingulate gyrus.

2.3.3. Relationship between executive function and psychotic symptoms in 22q11DS

ANOVA with psychotic symptoms as group factor and the executive function composite mean *z*-score as the dependent variable was used to test a potential relationship between level of executive-functioning and presence of psychotic symptoms.

3. Results

3.1. Volumetric comparisons between 22q11DS subjects and healthy controls

Subjects with 22q11DS showed a significant reduction in total brain tissue and grey and white matter volumes compared to the control group (total brain tissue: $p = 0.001$; total cranium grey matter: $p = 0.000$; total cranium white matter: $p = 0.001$) (Table 2). MANCOVA indicated smaller bilateral CG grey matter volumes in 22q11DS compared to controls (Wilks Lambda: $p = 0.002$, left: $p = 0.025$; right: $p = 0.003$). Further delineation of the CG sub-regions (Fig. 1) revealed that dorsal anterior and cingulate body grey matter volumes were also reduced bilaterally (Wilks Lambda: $p = 0.013$; $p = 0.004$ for left DA; $p = 0.002$ for right DA; $p = 0.027$ for left CinB; $p = 0.004$ for right CinB). Neither left nor right CG white matter volumes significantly differed between groups. Adding age as a covariate, we observed the same pattern of reduced CG volumes across 22q11DS subjects.

3.2. Post hoc volumetric analyses within 22q11DS and control subgroups

A significant reduction in right CG grey matter volume was observed in the low-executive functioning 22q11DS subgroup ($p = 0.02$) compared to the high-executive functioning 22q11DS subgroup. When comparing CG grey matter volumes and executive functioning within control subgroups, ANCOVA did not show any significant differences between groups ($p = 0.142$).

Further, a reduction in right CG grey matter in the 22q11DS psychotic group compared to the 22q11DS non-psychotic group, as well as a trend for reductions in the right DA ($p = 0.074$) and CinB ($p = 0.054$) anterior sub-regions were observed (Table 3).

Table 2
Volumetric comparisons between 22q11DS subjects and healthy controls

	22q11DS ($n = 58$)		Controls ($n = 64$)		ANCOVA	
	Mean	S.D.	Mean	S.D.	F	p
Total brain tissue[a]	1124.523	±138.71	1244.722	±102.87	29.915	0.001
Total cranium grey matter[a]	674.682	±85.813	743.839	±74.432	22.714	0.001
Total cranium white matter[a]	449.841	±90.035	500.883	±70.949	12.208	0.001
Cingulate gyrus						
Total left grey matter	11.238	±1.721	12.597	±1.847	5.18	0.025
Total right grey matter	12.167	±2.36	14.274	±2.16	9.31	0.003
Total left white matter	6.94	±1.352	7.288	±1.214	0.004	0.951
Total right white matter	6.677	±1.534	7.247	±1.129	0.864	0.355
Ventral anterior grey matter						
Left	2.484	±0.889	2.862	±1.29	2.059	0.154
Right	3.296	±1.181	3.736	±1.232	1.925	0.168
Dorsal anterior grey matter						
Left	1.904	±0.349	2.314	±0.619	8.46	0.004
Right	2.272	±0.536	2.784	±0.623	10.52	0.002
Cingulate body grey matter						
Left	1.692	±0.321	1.957	±0.346	4.995	0.027
Right	1.739	±0.374	2.091	±0.378	8.721	0.004
Splenium cingulate grey matter						
Left	5.156	±0.942	5.461	±0.945	0.003	0.957
Right	4.859	±1.025	5.661	±1.237	2.816	0.096

Note: Raw measurements of CG volumes are included in the table. Follow-up ANCOVA shows significant differences between groups after covarying for total cranium grey or white matter volume. All volumes are expressed in cm^3.

[a] ANOVA was used to statistically compare volumes.

To test whether these results were related to deficits in executive function and psychotic symptoms observed in 22q11DS, we performed the same analyses with the posterior segment of the CG (splenium cingulate sub-region), and did not observe a significant relationship with executive function or psychotic symptoms.

3.3. Relationship between executive function and psychotic symptoms in 22q11DS

ANOVA with psychotic symptoms as a group factor and the executive function mean z-score as a dependent variable indicated a trend ($p = 0.064$) toward a relationship between low executive functioning and the presence of psychotic symptoms. Indeed, the general distribution of psychotic symptoms among the low- and high-executive functioning 22q11DS individuals shows that 70% of the low-executive functioning subjects demonstrated psychotic symptoms versus 40% in the high-functioning subgroup (Table 3).

4. Discussion

To our knowledge, this is the first investigation of the cingulate gyrus structure using ROI-based analyses in 22q11DS individuals. The results demonstrate bilateral reductions in CG cortical volume compared to normal controls, driven by a decrease in anterior CG grey matter volumes, which remain significant after covarying for age and total grey matter volume. Further, post hoc analyses illustrated a reduction in the right CG grey matter volume in low-executive functioning patients, associating right CG alterations in 22q1DS with executive function deficits. We also observed an overall right CG grey matter reduction in the participants with 22q11DS reporting psychotic symptoms, and post hoc analyses revealed a trend toward right anterior CG grey matter reduction in relation to the presence of psychotic symptoms. Decreased statistical power in our post hoc analyses may have prevented the identification of specific CG sub-regional alterations linked to psychosis in 22q11DS. Finally, we observed a trend toward a correlation between low-executive functioning and the presence of psychotic symptoms.

Reductions in anterior cingulate grey matter volumes confirm CG alterations in 22q11DS compared to healthy controls, which were first reported by Simon and colleagues (2005) using voxel-based morphometry analyses. These findings are also compatible with anterior CG structural abnormalities found in individuals at high-risk for psychosis (Borgwardt et al., 2007), as well as in schizophrenia (Baiano et al., 2007). Using support from the literature on psychosis, in this discussion we will focus on the following points: (1) the implication of a relationship between executive function deficits and anterior CG changes; (2) the potential involvement of the anterior CG in the expression of psychotic symptoms in 22q11DS; and (3) suggestions for future explorations of brain structure and cognitive functions leading to positive symptom expression.

Cognitive studies have shown that executive function and working memory deficits related to the anterior CG (Carter et al., 2001; Morey et al., 2005; Szeszko et al., 2000) are present in most schizophrenic individuals (Bilder et al., 2000; Mohamed et al., 1999; Silver et al., 2003; Snitz et al., 2006). Neuroimaging studies have directly linked these deficits to the CG. Indeed, executive and working memory tasks normally activate the caudal part of the anterior CG (Bush et al., 2000), and a significant positive correlation between the volume of the right anterior CG and the ability to perform a go/no-go task has been previously reported (Bush et al., 2000). Thus, the relationship between right CG cortical reductions and low-executive functioning in 22q11DS patients may represent an endophenotypic marker signaling neurocognitive deficits associated with schizophrenia. A recent study of children and adolescents with 22q11DS reporting "schizophrenic-like" executive functioning deficits (Lewandowski et al., 2007) further supports this idea.

Pronounced CG structural alterations in individuals with psychosis and 22q11DS may provoke functional disruptions in a cerebral network responsible for the development of positive symptoms such hallucinations. The existing literature on high-risk and schizophrenic samples implicates the CG in the pathology of psychosis (Borgwardt et al., 2007; Pantelis et al., 2003; Yamasue et al., 2004). Suzuki and colleagues (2005) suggest that loss of

Table 3
Post hoc analyses among 22q11DS subjects aged above 9

	Psychotic 22q11DS subgroup ($n=24$)		Non-psychotic 22q11DS subgroup ($n=18$)		ANCOVA	
	Mean	S.D.	Mean	S.D.	F	p
Psychosis versus non-psychosis volumetric comparisons ($n=42$)						
Age[a]	20.482	±7.842	16.255	±8.561	2.763	0.104
IQ	64.208	±10.668	72.111	±10.867	5.555	0.066
Cingulate gyrus						
Total left grey matter	10.919	±1.729	11.661	±2.083	0.733	0.397
Total right grey matter	11.438	±2.53	13.485	±2.22	4.479	0.041
Dorsal anterior grey matter						
Left	1.852	±0.325	1.908	±0.345	0.13	0.72
Right	2.111	±0.552	2.519	±0.541	3.371	0.074
Cingulate body grey matter						
Left	1.58	±0.282	1.748	±0.348	1.417	0.241
Right	1.602	±0.292	1.919	±0.483	3.937	0.054
	High 22q11DS subgroup ($n=20$)		Low 22q11DS subgroup ($n=20$)		ANCOVA	
	Mean	S.D.	Mean	S.D.	F	p
High versus low executive functioning volumetric comparisons ($n=40$)						
Age[a]	15.817	±6.91	20.062	±8.229	3.12	0.085
IQ[a]	72.2	±9.299	64.85	±11.065	5.171	0.029
Cingulate gyrus						
Total left grey matter	11.75	±2.008	10.843	±1.735	1.293	0.324
Total right grey matter	13.615	±1.451	11.342	±2.859	6.142	0.020
Dorsal anterior grey matter						
Left	1.915	±0.331	1.838	±0.291	0.279	0.730
Right	2.506	±0.419	2.136	±0.631	2.45	0.105
Cingulate body grey matter						
Left	1.756	±0.314	1.556	±0.255	2.262	0.339
Right	1.918	±0.402	1.593	±0.362	3.576	0.117
Executive functioning-psychotic symptoms relationship						
Psychotic subjects	$n=8$		$n=14$			
Non-psychotic subjects	$n=12$		$n=6$			
	Psychotic subjects ($n=22$)		Non-psychotic subjects ($n=18$)		ANCOVA	
	Mean	S.D.	Mean	S.D.	F	p
Executive function composite mean z-score[a]	−0.217	±0.637	0.213	±0.789	3.641	0.064

Note: Raw measurements of CG volumes are included in table. Follow-up ANCOVA shows significant differences between groups. All volumes are expressed in cm^3.
[a] ANOVA was used to statistically compare groups.

inhibitory control, typically regulated in networks involving the prefrontal cortex and the anterior CG (Kerns et al., 2004), may be significant to the development of such symptoms, related to an anterior CG grey matter volume reduction in schizophrenia (Choi et al., 2005; Wang et al., 2007). Concordantly, Allen et al. (2008) review several reports illustrating anterior CG activity deficits during hallucinatory experiences. For example, the authors suggest that abnormal anterior CG and temporal cortex activation leads, in patients with auditory verbal hallucinations, to the misattribution of inner speech to an external source (Allen et al., 2007). Moreover, abnormal connections between the temporal and anterior CG cortex also contribute to verbal self-monitoring deficits, further sustaining auditory verbal hallucinations (Johns & McGuire, 1999; Mechelli et al., 2007). Finally, consistent with our structural findings of an altered right CG volume in 22q11DS patients with psychotic symptoms, Shergill et al. (2000) report the involvement of a large network of cortical areas prominently in the right hemisphere, including CG, in auditory hallucinations.

Although our data point to an association between right CG alteration, executive function and psychotic expression, it is difficult at this point to differentiate between the cause and effect of their putative contributions. Considering that CG grey matter reduction is a common finding among 22q11DS people compared to healthy individuals, two developmental hypotheses may be likely: (1) CG cortical alterations may disturb executive functioning in 22q11DS patients, thereby increasing the risk for psychotic symptom expression, or (2) CG cortical alterations may directly support hallucination-proneness thereby affecting executive function deficits in 22q11DS subjects. To date, longitudinal studies in 22q11DS find that cerebral alterations, most notably in dorsolateral prefrontal cortex, are related to cognitive alterations (verbal IQ decline) that accompany the rise of psychotic symptom expression (Debbané, Glaser et al., 2006; Gothelf et al., 2005). However, a direct relationship between developmental brain abnormalities and psychosis expression in 22q11DS has yet to be found (Gothelf, Penniman, Gu, Eliez, & Reiss, 2007).

One limitation of our study is that we cannot exclude an effect of IQ concerning the structural results between 22q11DS subjects and the control group. Indeed, the groups show significant differences in IQ, which are likely correlated with brain grey matter volume (Reiss, Abrams, Singer, Ross, & Denckla, 1996). Low IQ is probably a general result of the many specific developmental factors interacting in 22q11DS, like the ones specifically tested in this study. Covarying for IQ is an ongoing debate in research on neurodevelopmental syndromes because it often means covarying out the very effects in question. However, within-group analyses

clearly show the association between right CG alteration and psychotic symptoms in 22q11DS, independent of age or IQ. Another limitation is our inability to test for any effects of medication between the 10 individuals with 22q11DS following pharmacological treatment and healthy subjects because of the large variety of psychotropic drugs (neuroleptic, anti-epileptic, benzodiazepine, methylphenidate) prescribed to the participants. Finally, the assessment of psychotic symptoms will necessitate finer evaluation to better understand their developmental process in 22q11DS. Future studies employing dimensional measures characterizing frequency and intensity of hallucinations and delusions, and the distress and perturbation caused by these symptoms, may help to clarify the complex interactions between brain morphology, cognitive profile and the unfolding of positive symptoms psychosis.

Acknowledgments

This work was supported by Swiss National Research Funds to SE (PP00B-102864) and MS (323500-111165), in addition to a grant from the NARSAD Institute to SE. We thank our collaborators at the Center for Biomedical Imaging (CIBM), especially J. Delavelle, F. Henry and F. Lazeyras for their support and assistance with data collection, as well the EPFL, and the Leenaards and Louis Jeantet Foundations. We would also like to acknowledge S. Dahoun and S. Antonarakis for their ongoing collaboration in the Department of Genetics. This work is made possible by the Swiss and French deletion22q11 parent associations, Connect22 and Generation 22.

Financial disclosures: All authors of this manuscript have no biomedical financial support or conflict of interests.

References

Aleman, & Larøi. (2008). *Hallucinations: The science of idiosyncratic perception*. American Psychological Association.

Allen, P., Amaro, E., Fu, C. H., Williams, S. C., Brammer, M. J., Johns, L. C., & McGuire, P. K. (2007). Neural correlates of the misattribution of speech in schizophrenia. *British Journal of Psychiatry*, *190*, 162–169.

Allen, P., Larøi, F., McGuire, P. K., & Aleman, A. (2008). The hallucinating brain: A review of structural and functional neuroimaging studies of hallucinations. *Neuroscience and Biobehavioral Reviews*, *32*, 175–191.

Baiano, M., David, A., Versace, A., Churchill, R., Balestrieri, M., & Brambilla, P. (2007). Anterior cingulate volumes in schizophrenia: A systematic review and a meta-analysis of MRI studies. *Schizophrenia Research*, *93*, 1–12.

Baker, K. D., & Skuse, D. H. (2005). Adolescents and young adults with 22q11 deletion syndrome: Psychopathology in an at-risk group. *British Journal of Psychiatry*, *186*, 115–120.

Bilder, R. M., Goldman, R. S., Robinson, D., Reiter, G., Bell, L., & Bates, J. A. (2000). Neuropsychology of first-episode schizophrenia: Initial characterization and clinical correlates. *American Journal of Psychiatry*, *157*, 549–559.

Bish, J. P., Nguyen, V., Ding, L., Ferrante, S., & Simon, T. J. (2004). Thalamic reductions in children with chromosome 22q11.2 deletion syndrome. *Neuroreport*, *15*, 1413–1415.

Borgwardt, S. J., Riecher-Rössler, A., Dazzan, P., Chitnis, X., Aston, J., Drewe, M., et al. (2007). Regional grey matter volume abnormalities in the at risk mental state. *Biological Psychiatry*, *61*, 1148–1156.

Brewer, W. J., Wood, S. J., Phillips, L. J., Francey, S. M., Pantelis, C., Yung, A. R., et al. (2006). Generalized and specific cognitive performance in clinical high-risk cohorts: A review highlighting potential vulnerability markers for psychosis. *Schizophrenia Bulletin*, *32*, 538–555.

Bush, G., Luu, P., & Posner, M. I. (2000). Cognitive and emotional influences in anterior cingulate cortex. *Trends in Cognitive Sciences*, *4*, 215–222.

Campbell, L. E., Daly, E., Toal, F., Stevens, A., Azuma, R., Catani, M., et al. (2006). Brain and behaviour in children with 22q11.2 deletion syndrome: A volumetric and voxel-based morphometry MRI study. *Brain*, *129*, 1218–1228.

Carter, C. S., MacDonald, A. W., III, Ross, L. L., & Stenger, V. A. (2001). Anterior cingulate cortex activity and impaired self-monitoring of performance in patients with schizophrenia: An event-related fMRI study. *American Journal of Psychiatry*, *158*, 1423–1428.

Choi, J. S., Kang, D. H., Kim, J. J., Ha, T. H., Roh, K. S., Youn, T., & Kwon, J. S. (2005). Decreased caudal anterior cingulate gyrus volume and positive symptoms in schizophrenia. *Psychiatry Research*, *139*, 39–47.

Chow, E. W., Zipursky, R. B., Mikulis, D. J., & Bassett, A. S. (2002). Structural brain abnormalities in patients with schizophrenia and 22q11 deletion syndrome. *Biological Psychiatry*, *51*, 208–215.

Debbané, M., Glaser, B., David, M. K., Feinstein, C., & Eliez, S. (2006). Psychotic symptoms in children and adolescents with 22q11.2 deletion syndrome: Neuropsychological and behavioral implications. *Schizophrenia Research*, *84*, 187–193.

Debbané, M., Schaer, M., Farhoumand, R., Glaser, B., & Eliez, S. (2006). Hippocampal volume reduction in 22q11.2 deletion syndrome. *Neuropsychologia*, *44*, 2360–2365.

Debbané, M., Glaser, B., & Eliez, S. (2008). Encoding and retrieval processes in velo-cardio-facial syndrome (VCFS). *Neuropsychology*, *22*, 226–234.

Deboer, T., Wu, Z., Lee, A., & Simon, T. J. (2007). Hippocampal volume reduction in children with chromosome 22q11.2 deletion syndrome is associated with cognitive impairment. *Behavioral Brain Function*, *3*, 54.

Eckert, M. A., Tenforde, A., Galaburda, A. M., Bellugi, U., Korenberg, J. R., Mills, D., & Reiss, A. L. (2006). To modulate or not to modulate: Differing results in uniquely shaped Williams syndrome brains. *Neuroimage*, *32*, 1001–1007.

Eliez, S., Barnea-Goraly, N., Schmitt, J. E., Liu, Y., & Reiss, A. L. (2002). Increased basal ganglia volumes in velo-cardio-facial syndrome (deletion 22q11.2). *Biological Psychiatry*, *52*, 68–70.

Eliez, S., Schmitt, J. E., White, C. D., & Reiss, A. L. (2000). Children and adolescents with velocardiofacial syndrome: A volumetric MRI study. *American Journal of Psychiatry*, *157*, 409–415.

First, M. B., Opler, L. A., Hamilton, R. M., Linder, J., Linfield, L. S., Silver, J. M., et al. (1993). Evaluation in an inpatient setting of DTREE, a computer-assisted diagnostic assessment procedure. *Comprehensive Psychiatry*, *34*, 171–175.

Frith, C. D., Friston, K. J., Liddle, P. F., & Frackowiak, R. S. (1992). PET imaging and cognition in schizophrenia. *Journal of the Royal Society of Medicine*, *85*, 222–224.

Gothelf, D., Eliez, S., Thompson, T., Hinard, C., Penniman, L., Feinstein, C., et al. (2005). COMT genotype predicts longitudinal cognitive decline and psychosis in 22q11.2 deletion syndrome. *Nature Neuroscience*, *8*, 1500–1502.

Gothelf, D., Feinstein, C., Thompson, T., Gu, E., Penniman, L., Van Stone, E., et al. (2007). Risk factors for the emergence of psychotic disorders in adolescents with 22q11.2 deletion syndrome. *American Journal of Psychiatry*, *164*, 663–669.

Gothelf, D., Penniman, L., Gu, E., Eliez, S., & Reiss, A. L. (2007). Developmental trajectories of brain structure in adolescents with 22q11.2 deletion syndrome: A longitudinal study. *Schizophrenia Research*, *96*, 72–81.

Gur, R. E., Keshavan, M. S., & Lawrie, S. M. (2007). Deconstructing psychosis with human brain imaging. *Schizophrenia Bulletin*, *33*, 921–931.

Johns, L. C., & McGuire, P. K. (1999). Verbal self-monitoring and auditory hallucinations in schizophrenia. *Lancet*, *353*, 469–470.

Karmiloff-Smith, A., Tyler, L. K., Voice, K., Sims, K., Udwin, O., Howlin, P., et al. (1998). Linguistic dissociations in williams syndrome: Evaluating receptive syntax in on-line and off-line tasks. *Neuropsychologia*, *36*, 343–351.

Kates, W. R., Burnette, C. P., Jabs, E. W., Rutberg, J., Murphy, A. M., Grados, M., et al. (2001). Regional cortical white matter reductions in velocardiofacial syndrome: A volumetric MRI analysis. *Biological Psychiatry*, *49*, 677–684.

Kaufman, J., Birmaher, B., Brent, D., Rao, U., Flynn, C., Moreci, P., et al. (1997). Schedule for Affective Disorders and Schizophrenia for School-Age Children-Present and Lifetime Version (K-SADS-PL): Initial reliability and validity data. *Journal of the American Academy of Child and Adolescent Psychiatry*, *36*, 980–988.

Kerns, J. G., Cohen, J. D., MacDonald, A. W., Cho, R. Y., Stenger, V. A., & Carter, C. S. (2004). Anterior cingulate conflict monitoring and adjustments in control. *Science*, *303*, 1023–1026.

Lewandowski, K. E., Shashi, V., Berry, P. M., & Kwapil, T. R. (2007). Schizophrenic-like neurocognitive deficits in children and adolescents with 22q11 deletion syndrome. *American Journal of Medical Genetics. Part B, Neuropsychiatric Genetics*, *144*, 27–36.

Mechelli, A., Allen, P., Amaro, E., Fu, C. H., Williams, S. C., Brammer, M. J., et al. (2007). Misattribution of speech and impaired connectivity in patients with auditory verbal hallucinations. *Human Brain Mapping*, *28*, 1213–1222.

Mohamed, S., Paulsen, J. S., O'Leary, D., Arndt, S., & Andreasen, N. (1999). Generalized cognitive deficits in schizophrenia: A study of first-episode patients. *Archives of General Psychiatry*, *56*, 794–854.

Morey, R. A., Inan, S., Mitchell, T. V., Perkins, D. O., Lieberman, J. A., & Belger, A. (2005). Imaging frontostriatal function in ultra-high-risk, early, and chronic schizophrenia during executive processing. *Archives of General Psychiatry*, *62*, 254–262.

Murphy, K. C., Jones, L. A., & Owen, M. J. (1999). High rates of schizophrenia in adults with velo-cardio-facial syndrome. *Archives of General Psychiatry*, *56*, 940–945.

Oskarsdóttir, S., Vujic, M., & Fasth, A. (2004). Incidence and prevalence of the 22q11 deletion syndrome: A population-based study in Western Sweden. *Archives of Disease in Childhood*, *89*, 148–151.

Pantelis, C., Velakoulis, D., McGorry, P. D., Wood, S. J., Suckling, J., Phillips, L. J., et al. (2003). Neuroanatomical abnormalities before and after onset of psychosis: A cross-sectional and longitudinal MRI comparison. *Lancet*, *361*, 281–288.

Poulton, R., Caspi, A., Moffitt, T. E., Cannon, M., Murray, R., & Harrington, H. (2000). Children's self-reported psychotic symptoms and adult schizophreniform disorder: A 15-year longitudinal study. *Archives of General Psychiatry*, *57*, 1053–1058.

Reich, W. (2000). Diagnostic interview for children and adolescents. *Journal of American Academy of Child and Adolescent Psychiatry*, *39*, 59–66.

Reiss, A. L., Abrams, M. T., Singer, H. S., Ross, J. L., & Denckla, M. B. (1996). Brain development, gender and IQ in children: A volumetric imaging study. *Brain*, *119*, 1763–1774.

Reiss, A. L., Hennessey, J. G., Rubin, M., Beach, L., Abrams, M. T., Warsofsky, I. S., et al. (1998). Reliability and validity of an algorithm for fuzzy tissue segmentation of MRI. *Journal of Computer Assisted Tomography*, *22*, 471–479.

Schaer, M., Schmitt, J. E., Glaser, B., Lazeyras, F., Delavelle, J., & Eliez, S. (2006). Abnormal patterns of cortical gyrification in velo-cardio-facial syndrome (deletion 22q11.2): An MRI study. *Psychiatry Research*, *146*, 1–11.

Shergill, S. S., Brammer, M. J., Williams, S. C., Murray, R. M., & McGuire, P. K. (2000). Mapping auditory hallucinations in schizophrenia using functional magnetic resonance imaging. *Archives of General Psychiatry*, *57*, 1033–1038.

Silver, H., Feldman, P., Bilker, W., & Gur, R. C. (2003). Working memory deficit as a core neuropsychological dysfunction in schizophrenia. *American Journal of Psychiatry*, *160*, 1809–1816.

Simon, T. J., Ding, L., Bish, J. P., McDonald-McGinn, D. M., Zackai, E. H., & Gee, J. (2005). Volumetric, connective, and morphologic changes in the brains of children with chromosome 22q11.2 deletion syndrome: An integrative study. *Neuroimage*, *25*, 169–180.

Snitz, B. E., Angus, W., MacDonald, III, & Carter, C. S. (2006). Cognitive deficits in unaffected first-degree relatives of schizophrenia patients: A meta-analytic review of putative endophenotypes. *Schizophrenia Bulletin*, *32*, 179–194.

Suzuki, M., Zhou, S. Y., Takahashi, T., Hagino, H., Kawasaki, Y., Niu, L., et al. (2005). Differential contributions of prefrontal and temporolimbic pathology to mechanisms of psychosis. *Brain*, *128*, 2109–2122.

Szeszko, P. R., Bilder, R. M., Lencz, T., Ashtari, M., Goldman, R. S., Reiter, G., et al. (2000). Reduced anterior cingulate gyrus volume correlates with executive dysfunction in men with first-episode schizophrenia. *Schizophrenia Research*, *43*, 97–108.

Talaraich, J., & Tournoux, P. (1988). *Co-planar stereotaxic atlas of the human brain*. New York: Thieme.

van Amelsvoort, T., Daly, E., Henry, J., Robertson, D., Ng, V., Owen, M., et al. (2004). Brain anatomy in adults with velocardiofacial syndrome with and without schizophrenia: Preliminary results of a structural magnetic resonance imaging study. *Archives of General Psychiatry*, *61*, 1085–1096.

van Os, J., & Tamminga, C. (2007). Deconstructing psychosis. *Schizophrenia Bulletin*, *33*, 861–862.

Wang, L., Hosakere, M., Trein, J. C., Miller, A., Ratnanather, J. T., Barch, D. M., et al. (2007). Abnormalities of cingulate gyrus neuroanatomy in schizophrenia. *Schizophrenia Research*, *93*, 66–78.

Wechsler, D. (1991). *Wechsler intelligence scale for children* (3rd edn). The Psychological Corporation.

Wechsler, D. (1997). *Wechsler intelligence scale for adults* (3rd edn). The Psychological Corporation.

Woodward, S. H., Kaloupek, D. G., Streeter, C. C., Martinez, C., Schaer, M., & Eliez, S. (2006). Decreased anterior cingulate volume in combat-related PTSD. *Biological Psychiatry*, *59*, 582–587.

Yamasue, H., Iwanami, A., Hirayasu, Y., Yamada, H., Abe, O., Kuroki, N., et al. (2004). Localized volume reduction in prefrontal, temporolimbic, and paralimbic regions in schizophrenia: An MRI parcellation study. *Psychiatry Research*, *131*, 195–207.

Zinkstok, J., & van Amelsvoort, T. (2005). Neuropsychological profile and neuroimaging in patients with 22Q11 2 Deletion Syndrome: A review. *Child Neuropsychology*, *11*, 21–37.

Available online at www.sciencedirect.com
SCIENCE DIRECT®
Psychiatry Research: Neuroimaging 146 (2006) 1–11
PSYCHIATRY RESEARCH NEUROIMAGING
www.elsevier.com/locate/psychresns

Abnormal patterns of cortical gyrification in velo-cardio-facial syndrome (deletion 22q11.2): An MRI study

Marie Schaer [a], J. Eric Schmitt [c], Bronwyn Glaser [a], François Lazeyras [d], Jacqueline Delavelle [d], Stephan Eliez [a,b,*]

[a] Service Médico-Pédagogique, Department of Psychiatry, University of Geneva School of Medicine, Geneva, Switzerland
[b] Department of Genetic Medicine and Development, University of Geneva School of Medicine, Geneva, Switzerland
[c] Department of Psychiatry and Human Genetics, VCU Medical Center, Virginia Commonwealth University, Richmond, VA, USA
[d] Department of Radiology, University of Geneva Hospitals, Geneva, Switzerland

Received 8 February 2005; received in revised form 29 September 2005; accepted 1 October 2005

Abstract

Velo-cardio-facial syndrome (VCFS), also known as 22q11.2 deletion syndrome, is a common genetic condition associated with increased risk for developing schizophrenia. Given that cortical malformations play an integral role in the pattern of neuroanatomical alterations associated with VCFS, the aim of the present study was to quantify and localize gyral abnormalities. Magnetic resonance images were obtained on a 1.5 T scanner. The gyrification index (GI), a measure of the degree of cortical complexity, was differentially calculated for each lobe using a semi-automated protocol. The GI was calculated for 37 patients affected by VCFS as well as for 36 comparison individuals group-matched for age, handedness, and gender. The subjects affected by VCFS showed a significant decrease in the GI in the frontal and parietal lobes compared with the control group. The pattern of decreased gyrification in the frontal and parietal lobes further defines the structural changes associated with the syndrome and suggests underlying abnormalities in neural connectivity. Aberrant connectivity may be partially responsible for the cognitive and behavioral impairments in the syndrome, as well as the high incidence of schizophrenia among affected individuals.

Keywords: 22q11 deletion syndrome; VCFS; Gyrification index; Schizophrenia; Cortical complexity

1. Introduction

Due to its enlarged size and concurrent cortical folding, the human cerebral cortex has assumed a highly convoluted (gyrencephalic) shape. This expansion has allowed for an increase in surface area and neuronal number without a proportionate increase in head size. The degree of cortical folding, as measured by the gyrification index (GI), is a remarkably stable value among human beings. GI values reach their peak between 6 and 9 months of age, and then gradually decrease to a level that remains constant into adulthood (Armstrong et al., 1995). Most adults from the typically developing population have comparable GI values, and the GI is considered a stable ontogenic feature, unaffected by age, sex, brain volume, body weight, and body length (Zilles et al., 1988). Therefore, modifications to the normal developmental course of gyrification during

* Corresponding author. Service Médico-Pédagogique, University of Geneva School of Medicine, Boulevard Saint Georges 16-18, Case postale 50, CH-1211 Geneva 8, Switzerland. Tel.: +41 22 327 43 00; fax: +41 22 327 43 20.
E-mail address: stephan.eliez@medecine.unige.ch (S. Eliez).

0925-4927/$ - see front matter © 2005 Elsevier Ireland Ltd. All rights reserved.
doi:10.1016/j.pscychresns.2005.10.002

childhood (Armstrong et al., 1995) may be responsible for brain alterations in certain neurogenetic disorders and psychiatric conditions. Accordingly, an increase in GI has been explained by a delay in brain maturation in autism (Hardan et al., 2004) and by a developmental arrest in Williams syndrome (Schmitt et al., 2002).

The current study attempts to explore gyrification abnormalities and their relevance to the neuropsychiatric phenotype in a frequent genetic condition, velo-cardio-facial syndrome (VCFS), or 22q11 deletion syndrome (22q11DS). Velo-cardio-facial syndrome is a neurogenetic disorder most commonly caused by a 3 Mb de novo deletion on chromosome 22q11.2 (Shprintzen et al., 1978). VCFS affects 1 in 5000 live births (Scambler, 2000). It is typically characterized by specific physical anomalies (Goldberg et al., 1993; Ryan et al., 1997; Shprintzen et al., 1978) as well as cognitive and learning impairments (Gerdes et al., 1999; Moss et al., 1999; Swillen et al., 1997; Swillen et al., 1999b). Sobin et al. (2005) reported pronounced deficits in visuo-spatial memory, visual attention, and working memory. Individuals affected by VCFS are also at increased risk for psychopathology; higher rates of attentional problems have been reported in pediatric samples (Gothelf et al., 2004), as well as a high prevalence of withdrawn and avoidant behaviors (Papolos et al., 1996; Swillen et al., 1997, 1999a). Furthermore, the fact that one third of persons affected by VCFS are reported to develop schizophrenia in late adolescence or early adulthood (Baker and Skuse, 2005; Murphy et al., 1999) suggests the syndrome as a homogeneous genetic model for studying neuroanatomical changes associated with the onset of psychosis (Bassett and Chow, 1999; Murphy and Owen, 2001).

The VCFS phenotype has been related to a pattern of brain alterations occurring in the syndrome. Quantitative neuroimaging studies have revealed decreased gray and white matter volumes in children and adolescents with VCFS, with the parietal lobe being particularly affected (Chow et al., 2002; Eliez et al., 2000, 2001c; Kates et al., 2001; Simon et al., 2005). Conversely, frontal lobe volumes have been reported as increased or relatively preserved in childhood (Eliez et al., 2000; Kates et al., 2004, 2001; Simon et al., 2005), but substantially reduced by adulthood (Chow et al., 2002). Also, aberrant neurodevelopmental trajectories in volumes of the temporal lobe and hippocampal volumes have been suggested by cross-sectional studies, implying that these structures may be reduced in adulthood (Eliez et al., 2001b). Volumetric alterations to the frontal, parietal, and temporal lobes are accompanied by changes in the organization of regional white matter tracts, as observed with diffusion tensor imaging techniques (Barnea-Goraly et al., 2003; Simon et al., 2005). Moreover, aberrant functional activation in the left parietal region revealed during an arithmetic task suggests that abnormal connectivity underlies impairments in mathematical reasoning and parietal lobe function in VCFS (Eliez et al., 2001a). According to hypotheses put forth in studies of gyrification (Dehay et al., 1996; Rakic, 1988; Van Essen, 1997), early abnormal connectivity is likely to change initial cortical morphology. Further, numerous case reports of cortical dysgenesis in patients with VCFS (Bingham et al., 1998; Bird and Scambler, 2000; Cramer et al., 1996; Ehara et al., 2003; Ghariani et al., 2002; Kawame et al., 2000; Sztriha et al., 2004; Koolen et al., 2004; Worthington et al., 2000), most frequently in the frontal and parietal regions, may provide insight into the etiology of gyral alterations in VCFS.

To date, altered gyrification has been reported in a number of pathologies, from experimentally induced lesions in macaques to humans with specific psychiatric or neurogenetic conditions. Animal studies suggest that size and degree of folding of the cortical surface may be determined by degree of thalamic input during the first half of gestation, with a drastic decrease in gyrification being reported after prenatal lesions to the thalamocortical connections in macaque monkeys (Dehay et al., 1996; Rakic, 1988). A model of tension-based morphogenesis (Van Essen, 1997) also has been applied to studies of cortical folding in abnormal human brain development due to neurogenetic conditions. One neuro-mechanical hypothesis suggests that gyral complexity is driven by underlying neural circuitry; thus, the strength of the local cortical interconnections determines gyrification (Van Essen, 1997). In detail, Van Essen's theory postulates that weaker local interconnections may lead to larger gyri and deep sulci due to traction exerted by the long connections (i.e. thalamocortical or cortico-cortical between different cortical regions). Decreased gyrification in dyslexia is thought to be responsible for slowed down information processing due to an increase in the number of long connections (Casanova et al., 2004). Conversely, strong local interconnectivity may decrease gyri width. If this were the case, frontal over-connectivity in autism (Courchesne and Pierce, 2005) would be responsible for the increased GI in the frontal lobes of autistic children (Hardan et al., 2004).

Similar explanations (Jou et al., 2005; Sallet et al., 2003) have been applied to gyral abnormalities in psychiatric conditions such as in schizophrenia (Harris et al., 2004a,b; Kulynych et al., 1997; Sallet et al.,

2003; Vogeley et al., 2000, 2001). In studies of schizophrenia, the GI has been reported as increased in certain regions and decreased in others. The most frequently reported finding is a reduction of gyrification in the left hemispheres of schizophrenic patients compared with normal subjects (Kulynych et al., 1997; Sallet et al., 2003). The overall left hemispheric decrease may be related to a recurrent GI decrease in the left frontal region (Harris et al., 2004b; Kulynych et al., 1997; Sallet et al., 2003), which also has been reported in high-risk individuals before the onset of schizophrenia (Jou et al., 2005). Other GI abnormalities in schizophrenia include an increase in right temporal GI (Harris et al., 2004b) as compared with normal control subjects. Based on a slightly different calculation (slice-by-slice algorithm), right prefrontal hypergyria has been demonstrated in schizophrenic patients compared with normal controls (Vogeley et al., 2000) and unaffected siblings (i.e. high-risk individuals) (Harris et al., 2004a; Vogeley et al., 2001).

To investigate cortical surface changes associated with brain alterations in VCFS, a syndrome known to be associated with a high risk for developing schizophrenia (Baker and Skuse, 2005; Murphy et al., 1999), we used a lobar-specific automated protocol for measuring hemispheric gyrification (Kesler et al., in press; Schmitt et al., 2002) based on the Zilles method (Zilles et al., 1988). We hypothesized that gyrification abnormalities would be observed in regions with frequently reported morphological alterations or aberrant connectivity. Specifically, we expected to observe gyrification alterations in parietal, frontal, and temporal regions. We expected the least degree of change to occipital lobe gyrification, since it has not tended to be implicated in volumetric studies or cortical dysgenesis case reports.

2. Methods

2.1. Subjects

2.1.1. Individuals with velo-cardio-facial syndrome

Thirty-seven children and young adults (11 male, 26 female) with VCFS with an average age of 16.6 ± 9.1 years participated in the study. Patients had an average IQ of 69.5 ± 11.6. All participants were recruited through announcements in parent association newsletters. Only native French- or English-speaking individuals were included in the sample, and all individuals were assessed in their native language. Thirty-six of the participants in the study had de novo deletions on chromosome 22q11.2 as confirmed by a fluorescent in situ hybridization technique (FISH), and one had a familial deletion. To reduce diagnostic uncertainty, only children with a confirmed 22q11.2 deletion were included in the study.

The parents of the children and adolescents (younger than 18, $n=23$) were administered a semi-structured interview (computerized DICA-P), as well as the Psychosis Module of the Schedule for Affective Disorders and Schizophrenia for School-Age Children—Present and Lifetime (K-SADS-PL Parent Version; Kaufman et al., 1997) by a child and adolescent psychiatrist (SE). The parent interview was followed by a clinical examination of the subjects focusing on symptoms and problems revealed during the parent interviews.

For subjects older than 18 ($n=14$), a structured clinical interview was conducted separately with the subjects and the parents by a child and adolescent psychiatrist (SE), including the Structured Clinical Interview for DSM-IV Axis I Disorders (SCID-I) (First et al., 1997) and the Psychosis Module of the Schedule for Affective Disorders and Schizophrenia Present and Lifetime (SADS-PL). Seventeen patients presented psychotic symptoms (45.9%, 5 males, 12 females, age 20.5 ± 7.5), eight had a diagnosis of psychosis (21.6%, 5 males, 3 females, age 21.1 ± 8.9), and three were diagnosed as schizophrenic (8.1%, 1 male, 2 females, age 30.5 ± 1).

2.1.2. Comparison group

The comparison group comprised 36 typically developing individuals (15 males, 21 females) with an average age of 14.4 ± 8.2 years and average IQ of 110.5 ± 16.5. Individuals were recruited through a newsletter distributed at public schools in the Geneva community. Medical history and parent-report (Child Behavior Checklist in children and adolescents) (Achenbach, 1991) and self-report (Symptom Checklist-90-Revised in adolescents and adults) (Derogatis, 1983) questionnaires were used to screen out psychiatric problems in our control group. Subjects with a history of past or present neurological or psychiatric disorders were excluded. The control group was matched for handedness, age, and gender with the VCFS group.

Written informed consent was received from all subjects, as well as the parents of subjects younger than 18 years of age, in accordance with protocols approved by the Institutional Review Board of Geneva University School of Medicine.

2.2. Imaging

Cerebral magnetic resonance images were acquired using a Philips Intera 1.5 T scanner. Coronal images

were acquired with a 3D volumetric pulse sequence using the following scan parameters: TR=35 ms, TE=6 ms, flip angle=45°, NEX=1, matrix size=256×192, field of view=24 cm^2, slice thickness=1.5 mm, 124 slices.

Images were imported into the software *BrainImage* (Reiss, 2004) in order to perform a semi-automated image analysis consisting of the following steps: (1) correction of voxel intensity non-uniformity, (2) removal of non-brain tissues, (3) segmentation of the brain into constituent tissue types using a constrained fuzzy algorithm based on voxel intensity and tissue boundaries, and (4) positional normalization and division of the data into anatomic subregions using a stereotactically based parcellation method (Talairach and Tournoux, 1988). Details of these procedures are published elsewhere (Andreasen et al., 1996; Kaplan et al., 1997; Kates et al., 1999; Reiss et al., 1998).

A region of interest (ROI) circumscribing the lateral ventricles was manually delineated, and all encircled pixels were changed to white (intensity 255 in an 8-bit color table). This procedure was performed to prevent the ventricle–brain perimeter from being included as part of the cortical perimeter in subsequent measurements (see below). These procedures have been described elsewhere (Subramaniam et al., 1997). In addition, the posterior fossa was circumscribed and removed using methods based on a previously validated protocol (Aylward and Reiss, 1991).

The remaining cerebral tissue was parceled spatially based on Talairach sectors that divide the cerebrum into its four major lobes for each hemisphere (Subramaniam et al., 1997). To localize gyrification anomalies, each lobe was measured separately.

2.3. Calculation of the gyrification index

The gyrification index (GI) was defined as the ratio of the inner perimeter of the brain (following all contours into the sulcul crevices) over the perimeter of the outer surface. These contours were delineated using an automated software-based procedure (Schmitt et al., 2002). First, the image was classified into gray matter, white matter, and cerebro-spinal fluid (CSF) using a dual thresholding algorithm that establishes discrete tissue segmentation based on the histogram of voxel intensities throughout the image (Otsu, 1979). The inner contour of the brain was then defined as the perimeter including all voxels classified as brain tissue (i.e. voxels that were either gray or white matter). Since it excluded all CSF and null voxels, this ROI circumscribed all sulci of the brain.

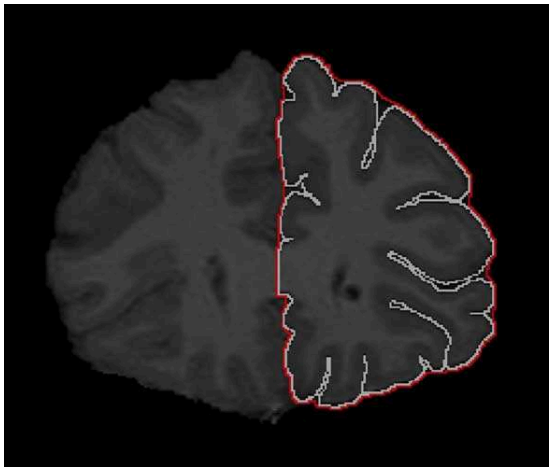

Fig. 1. Illustration of the GI on a coronal slice in the left frontal lobe. The inner perimeter is delineated in white and the outer perimeter in red.

To generate the ROI for the outer brain surface, a relaxed convex hull morphological operator was applied with the inner contour ROI as its argument (Lancaster et al., 1999). The algorithm determines the smallest convex polygon that includes all points of the original, inner contour ROI. This algorithm essentially retraces the inner contour ROI, using a virtual "ball" with a fixed diameter (in this case 6 voxels, approximately 6 mm). Because of the predefined size of the ball, the resultant ROI did not include the sulci and therefore represents a measure of the outer surface (i.e. convex hull of the inner surface ROI) (Fig. 1). The outer perimeter was then measured. The GI calculations were automatically repeated for each image slice (Schmitt et al., 2002) using the following equation, as initially described by Zilles et al. (1988):

$$GI = \frac{\sum_{j=1}^{n} P_i t}{\sum_{j=1}^{n} P_o t}$$

where P_i=the inner perimeter for slice j, P_o=the outer perimeter for slice j, t=slice thickness, and n=the number of slices in the image (Fig. 1). The result of each component of this equation is the surface area of the brain (or lobe), from either its inner or outer contour. The variable t and the units of the perimeter cancel each other out, producing the unit-less ratio GI.

2.4. Calculation of gyrification index for the right prefrontal region

After obtaining the results for GI in the four main lobes bilaterally, to further test our VCFS group for the

right prefrontal hypergyria observed in schizophrenic patients, we subsequently modified our GI algorithm to obtain a measure of gyrification in the right prefrontal lobe that would be commensurate with previous studies (Harris et al., 2004a,b; Sallet et al., 2003; Vogeley et al., 2000, 2001). Thus, we recalculated the GI for each slice in the right prefrontal region, with $GI = P_i / P_o$, and compared the rostrocaudal course of the GI values of VCFS subjects to control participants.

The prefrontal region was defined according to previous studies. Vogeley et al. (2000, 2001) traced the inner and outer contour for the slice anterior to the genu of the corpus callosum, as well as for two slices situated at 10 and 20 mm rostrally. Harris et al. (2004a,b) used slice-by-slice measurements of all the slices from the first slice where ribbons of white matter were distinguishable, up to the slice containing the genu of the corpus callosum (about 10 slices, 1.88 mm thick). Sallet et al. (2003) compared the rostrocaudal course of the first five slices of the brain (3.6 mm thick). Therefore, we individually recalculated GI for the first 20 slices of the spatially reoriented right hemisphere (0.9375 mm thick). Visual examination of 10 randomly selected subjects confirmed that the 20th slice always fell around the genu of the corpus callosum.

2.5. Data analysis

2.5.1. Data analysis for the left and right hemispheres and the four main lobes

Gyrification data met the necessary assumptions for parametric statistical analyses (independence, homogeneity of variance, and normality). One-way analyses of variance (ANOVAs) were used to compare the GI of VCFS patients and control participants for the right and left hemispheres. Multiple analyses of variance (MANOVAs) were performed to determine if the VCFS and comparison groups had unique patterns of combined GI in the four lobes (frontal, parietal, occipital, and temporal) in the left and right hemispheres. Follow-up ANOVA was then used to measure lobar GI differences between groups. For all comparisons, the significance threshold was set at $P < 0.05$.

2.5.2. Data analysis for the right prefrontal region

To avoid a potential confound, the three schizophrenic patients in our sample were excluded for analyses of the prefrontal region. Repeated measures ANOVAs, with group as the between-subjects variable and the first 20 slices of the spatially reoriented brains as the within-subjects variable, were used to analyze the GI in the right prefrontal region.

3. Results

No significant differences in the GI of the right and left hemispheres were detected between the VCFS and control groups (left: $F = 3.27$, $P = 0.075$; right: $F = 0.57$, $P = 0.453$). However, MANOVA for GI revealed a significant pattern of lobar differences between individuals affected by VCFS and control participants (Wilks λ of 0.611, $F(8,64) = 4.11$, $P < 0.001$). Results of the group comparisons of GI for each of the four main lobes, as well as for the right and left hemispheres, can be found in Table 1. In summary, measures of the GI in the VCFS group were significantly smaller for the frontal and parietal lobes than in the control group (Table 1). No differences in GI between groups were found in the temporal and occipital lobes.

For the right prefrontal region, between-group comparisons using repeated measures ANOVA did not reveal significant differences for the GI between groups. Greenhouse–Geisser corrected values for the repeated measures were as follows: $F(19,1292) = 1.671$, $P = 0.134$. In summary, despite a high incidence of psychotic symptoms in our sample, VCFS subjects unaffected by schizophrenia at the time of MRI acquisition did not show evidence for the right prefrontal hypergyria demonstrated in schizophrenic patients (Harris et al., 2004a; Vogeley et al., 2000, 2001) (Fig. 2).

Table 1
Mean GI values of individuals with and without velo-cardio-facial syndrome

		Mean	S.D.	*F*	*P*
Left hemisphere	Normal control	2.9864	0.4341	3.272	0.075
	VCFS	2.8247	0.3231		
Left frontal	Normal control	2.3964	0.3289	5.7	0.020
	VCFS	2.2257	0.2825		
Left parietal	Normal control	2.5543	0.3220	12.5	0.001
	VCFS	2.3285	0.2146		
Left temporal	Normal control	1.9378	0.2080	1.1	0.291
	VCFS	1.9879	0.1936		
Left occipital	Normal control	2.5432	0.3478	1.5	0.229
	VCFS	2.4610	0.2178		
Right hemisphere	Normal control	3.0421	0.4221	0.6	0.453
	VCFS	2.9625	0.4757		
Right frontal	Normal control	2.4621	0.3607	4.0	0.049
	VCFS	2.2991	0.3346		
Right parietal	Normal control	2.5420	0.3552	4.6	0.034
	VCFS	2.3889	0.2421		
Right temporal	Normal control	2.0242	0.2612	0	0.950
	VCFS	2.0286	0.3359		
Right occipital	Normal control	2.5320	0.2674	0.1	0.756
	VCFS	2.5119	0.2814		

F and *P* values are based on ANOVA comparisons between patients with VCFS and normal controls.

4. Discussion

The present study represents an initial attempt to quantify cortical gyrification in a group of individuals with VCFS using the gyrification index (GI), an automated measure of gyral complexity. Previous reports of abnormal cortical gyrification in the syndrome (Bingham et al., 1998; Bird and Scambler, 2000; Cramer et al., 1996; Ehara et al., 2003; Ghariani et al., 2002; Kawame et al., 2000; Koolen et al., 2004; Sztriha et al., 2004; Worthington et al., 2000), especially polymicrogyria or pachygyria, came from clinical case reports done by radiologists, which were easily influenced by individual differences and were dependent on the expertise of the clinician. In the current study, children, adolescents, and young adults with VCFS displayed aberrant patterns of cortical folding, compared with typically developing individuals of comparable age and gender. Decreased gyrification in the brains of affected subjects was observed in the frontal and parietal lobes, the regions most frequently associated with volumetric changes or altered connectivity. By contrast, there was no evidence for alterations to the temporal or occipital lobes.

There are several explanations for the pathogenesis of the decreased cortical complexity observed in the study. As proposed by several authors, the neuro-mechanical model of Van Essen (1997) provides a good framework for understanding how gyrification may indicate abnormal underlying connectivity. In VCFS, decreased gyrification in the frontal and parietal lobe manifests with large gyri and deep sulci (see Fig. 3). This pattern of decreased folding with large gyri could be due to weak local interconnections in the frontal and parietal lobes, according to the tension-based morphogenesis model (Van Essen, 1997). In the frontal lobe, decreased organization of white matter tracts has been observed using diffusion imaging tensor techniques in the middle frontal gyri bilaterally, as well as in the left superior frontal gyrus (Barnea-Goraly et al., 2003). In the parietal lobes, white matter tract disorganization has been reported in the postcentral gyri bilaterally and in the left superior parietal gyrus (Barnea-Goraly et al., 2003). Moreover, disrupted connectivity within the parietal and prefrontal network is thought to contribute to the frequently observed arithmetic and visuospatial impairments in the syndrome (Eliez et al., 2001a).

Multiple etiological explanations may be proposed for the observed gyrification abnormalities. In the parietal lobe, an abnormal early developmental process may explain decreased gyrification. Evidence for a reduction in parietal lobes has already been reported in children with VCFS (Chow et al., 2002; Eliez et al., 2000; Kates et al., 2001; Simon et al., 2005). According to Rakic's hypothesis, a decrease in the thalamic afferences to the cortex during the first part of gestation would explain both the reduction in parietal gray matter (Eliez et al., 2000; Simon et al., 2005) and the currently reported decreased GI through an impairment in cortical expansion (Dehay et al., 1996; Rakic, 1988). Further, reported decreases in white matter volumes in the parietal lobe (Eliez et al., 2000; Kates et al., 2001; Simon et al., 2005) would support reduced thalamocortical connections, thereby altering normal cortical development in the syndrome.

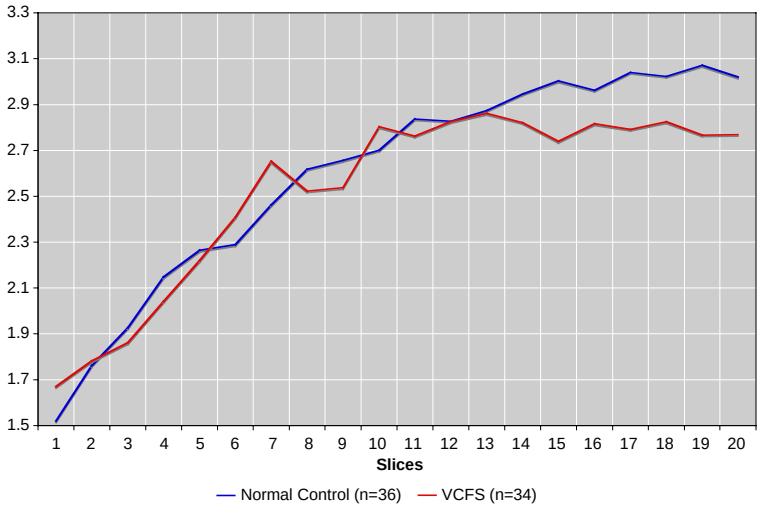

Fig. 2. Group comparison of the rostrocaudal course of the GI in the right prefrontal region (20 slices, 0.94 mm thick). The absence of right prefrontal hypergyria in our sample of VCFS subjects without schizophrenia compared with normal controls further strengthens the association between increased right prefrontal GI and schizophrenia.

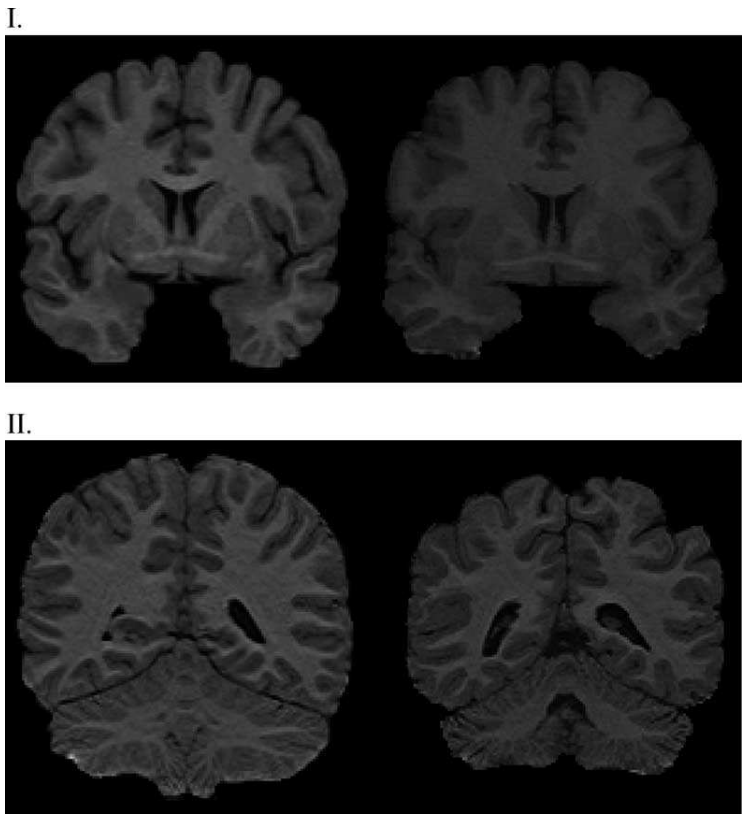

Fig. 3. An illustration of cortical folding in frontal coronal (I) and parietal (II) sections of a control participant (left) compared with a patient with VCFS (right). The patient shows larger gyri with shallower sulci than the control participant in the superior frontal region, as well as in the superior parietal region.

Conversely, volumetric findings indicate changes of a different nature in the frontal lobes of VCFS patients, with a relative preservation (i.e. enlargement relative to the overall reduction) reported in affected children (Eliez et al., 2000; Kates et al., 2001). Although it is less clear how abnormal development of the frontal lobe affects gyrification without modifying volume, the parietal and frontal cortices share a common vascular peculiarity during development. Namely, the most common locations of dysplastic cortex are in the posterior frontal and the parietal regions (Barkovich et al., 1995). Indeed, in 12 patients with VCFS for whom cortical dysgenesis, either polymicrogyria or pachygyria, was reported, the parietal lobe was affected in 11 cases (Bingham et al., 1998; Bird and Scambler, 2000; Cramer et al., 1996; Ghariani et al., 2002; Kawame et al., 2000; Koolen et al., 2004; Sztriha et al., 2004; Worthington et al., 2000) and the frontal lobe was involved in nine cases (Bingham et al., 1998; Bird and Scambler, 2000; Cramer et al., 1996; Ghariani et al., 2002; Kawame et al., 2000; Koolen et al., 2004; Sztriha et al., 2004; Worthington et al., 2000). Most authors suggest that many, if not most, cases of polymicrogyria are caused by ischemia occurring during a critical period of cortical development, resulting from either infection (cytomegalovirus), maternal shock, or twin–twin transfusion syndrome (Barkovich et al., 1995; Guerrini et al., 2000). The ischemic etiology of polymicrogyria may explain its characteristic localization restricted either to the territory of a main artery or to the watershed between major arterial territories (Guerrini et al., 2000). Posterior frontal and parietal regions are especially vulnerable because they represent an intravascular boundary zone at the mid-second trimester of gestation, when both the middle and posterior cerebral arteries are fully formed (Eecken, 1959). Given that vascular anomalies are one of the cardinal symptoms of VCFS (Shprintzen et al., 1978), genetically induced anomalies of cerebral vessels may result in abnormal neuronal migration and gyral alterations through circulatory disturbances in the developing brain (Bird and Scambler, 2000; Dambska and Laure-Kamionowska, 2001; Ehara et al., 2003; Kawame et al., 2000). TBX1, a gene involved in vascular development

(Chieffo et al., 1997; Merscher et al., 2001), may be a candidate gene responsible for the differences in gyrification observed in the frontal and parietal lobes in VCFS.

Finally, contrary to our hypothesis, we did not observe gyral alterations in the temporal lobe. In addition to abnormal developmental processes, gyrification may also be affected by secondary pathological processes when GI values are normally stabilized (i.e. during adolescence or adulthood). For example, different models of alterations to gyrification are proposed for age-related atrophy (Kulynych et al., 1997). If atrophic sulcal widening were accompanied by proportionate reductions in cortical surface area (e.g. total brain volume reduction), GI would remain stable (Kulynych et al., 1997). By contrast, differential atrophy with enlargement of the sulci without proportionate brain reduction would increase the inner contour of the brain, thereby increasing GI. Reported alterations in the temporal lobe in VCFS led us to erroneously expect increased gyrification in the left temporal region through a secondary pathological process. A report of enlarged left Sylvian fissure in children with VCFS (Bingham et al., 1997), taken together with a decrease in left temporal gray volumes with age (Eliez et al., 2001b), led us to believe that an atrophic process would open the sulci, thereby increasing GI in the temporal lobe. Even if this were the case, multiple reasons may exist why we do not observe differences in temporal lobe gyrification. First, given that overall GI tends to be decreased in subjects with VCFS, a regional GI increase rather than a decrease may not be discernible, either due to our method of measurement or because more subjects would be needed to detect a difference. Second, the nature of the atrophy previously observed in the temporal region (Eliez et al., 2001b) may be associated with stable GI measures. Specifically, if atrophic sulcal widening were accompanied by a concurrent proportionate reduction in cortical surface, temporal lobe atrophy would probably not lead to increased gyrification (Eliez et al., 2001b).

The observed pattern of gyral alterations may have potential applications for the development of schizophrenia in VCFS. Numerous gyral alterations have been associated with schizophrenia. Namely, a reduction in gyrification in the left (Kulynych et al., 1997; Sallet et al., 2003) and right hemispheres (Sallet et al., 2003) has been reported in schizophrenic patients compared with control participants. Lobar assessment of GI has revealed a decrease in gyrification in the frontal lobe bilaterally (Kulynych et al., 1997; Sallet et al., 2003), an increase of GI in the right prefrontal region (Harris et al., 2004b; Sallet et al., 2003; Vogeley et al., 2000), and an increase in the right temporal lobe (Harris et al., 2004b). Moreover, observed alterations to gyrification in the frontal lobe of VCFS patients appear to be primordial for the development of schizophrenia. Of interest, a recent study of young adolescents at high risk for developing schizophrenia (Jou et al., 2005) reported decreased GI in the left frontal lobes premorbid to the onset of psychotic symptomatology. Together with our observation of decreased frontal GI in VCFS, the study by Jou et al. suggests that decreased gyrification in the left frontal lobe may represent a neuroanatomical marker for susceptibility to schizophrenia. This may also explain why differences in left frontal GI were not appearant when affected individuals were compared with a high-risk group (Harris et al., 2004a). By contrast, right prefrontal hypergyria was demonstrated in schizophrenic patients compared with control participants (Sallet et al., 2003; Vogeley et al., 2000) as well as their unaffected siblings (Harris et al., 2004a; Vogeley et al., 2001). Thus, we could postulate that decreased GI in the left frontal lobe may be related to increased susceptibility to schizophrenia and right prefrontal hypergyria may be associated with the disease itself. The fact that we did not find a difference in gyrification in the right prefrontal lobe between patients with VCFS and comparison subjects (Fig. 2) further emphasizes a hypothesis of different cerebral changes between individuals at high risk or patients with the disease itself. According to Van Essen (1997), gyral similarities between schizophrenic patients and high-risk individuals would reinforce a neurodevelopmental model of schizophrenia (Weinberger, 1995), in which case alterations to frontal connectivity would precede the disease and disconnectivity in the prefrontal region would characterize it (Weinberger et al., 1992).

This first attempt at defining GI in VCFS suggests new avenues for inquiry. Given that neural circuitry is key to functional impairments, decreased gyrification in the frontal and parietal lobes likely plays a role in the cognitive, behavioral, and psychiatric impairments associated with VCFS. To continue to learn about the intersection between changes in brain structure, gyrification, and the resulting phenotype, alternate methodological approaches for quantifying brain alterations will be needed. Future longitudinal studies are required to evaluate the role of cortical folding malformations in the predisposition to or the onset of schizophrenia. Future studies including individuals homogeneous for the severity of their psychotic symptoms will help to clarify the relationship between gyrification and schizophrenic progression. Also, a more specific evaluation of

the pattern of connectivity underlying gyral alterations, for example, by using fiber tracking based on diffusion tensor images, may show how gyrification is influenced by neural connections. Finally, initial quantitative evidence for gyral abnormalities in VCFS encourages further investigation of changes in cortical morphology, such as cortical thickness. Complex frameworks for analyzing cortical data have recently been developed, using deformation maps on geometric models of the cortex (Thompson et al., 2004). In the future, three-dimensional analysis of cortical patterns will undoubtedly become a powerful tool for assessing gyral alterations in vivo in persons affected by psychiatric or neurogenetic conditions.

Acknowledgments

This research was supported by a grant from Swiss National Research Funds to Dr. Stephan Eliez (3200-063135.00/1, 3232-063134.00/1, and PP00B-102864). This work also was partially supported by a grant from NARSAD to Dr. Eliez. The authors would like to thank Franck Henry for his help in scanning the subjects.

References

Achenbach, T.M., 1991. Manual for the Child Behavior Checklist/4-18 and 1991 Profile. Department of Psychiatry, University of Vermont, Burlington, VT.

Andreasen, N.C., Rajarethinam, R., Cizadlo, T., Arndt, S., Swayze II, V.W., Flashman, L.A., O'Leary, D.S., Ehrhardt, J.C., Yuh, W.T., 1996. Automatic atlas-based volume estimation of human brain regions from MR images. Journal of Computer Assisted Tomography 20 (1), 98–106.

Armstrong, E., Schleicher, A., Omran, H., Curtis, M., Zilles, K., 1995. The ontogeny of human gyrification. Cerebral Cortex 5 (1), 56–63.

Aylward, E.H., Reiss, A., 1991. Area and volume measurement of posterior fossa structures in MRI. Journal of Psychiatric Research 25 (4), 159–168.

Baker, K.D., Skuse, D.H., 2005. Adolescents and young adults with 22q11 deletion syndrome: psychopathology in an at-risk group. British Journal of Psychiatry 186, 115–120.

Barkovich, A.J., Rowley, H., Bollen, A., 1995. Correlation of prenatal events with the development of polymicrogyria. American Journal of Neuroradiology 16 (4 Suppl), 822–827.

Barnea-Goraly, N., Menon, V., Krasnow, B., Ko, A., Reiss, A., Eliez, S., 2003. Investigation of white matter structure in velocardiofacial syndrome: a diffusion tensor imaging study. American Journal of Psychiatry 160 (10), 1863–1869.

Bassett, A.S., Chow, E.W., 1999. 22q11 deletion syndrome: a genetic subtype of schizophrenia. Biological Psychiatry 46 (7), 882–891.

Bingham, P.M., Zimmerman, R.A., McDonald-McGinn, D., Driscoll, D., Emanuel, B.S., Zackai, E., 1997. Enlarged Sylvian fissures in infants with interstitial deletion of chromosome 22q11. American Journal of Medical Genetics 74 (5), 538–543.

Bingham, P.M., Lynch, D., McDonald-McGinn, D., Zackai, E., 1998. Polymicrogyria in chromosome 22 detection syndrome. Neurology 51 (5), 1500–1502.

Bird, L.M., Scambler, P., 2000. Cortical dysgenesis in 2 patients with chromosome 22q11 deletion. Clinical Genetics 58 (1), 64–68.

Casanova, M.F., Araque, J., Giedd, J., Rumsey, J.M., 2004. Reduced brain size and gyrification in the brains of dyslexic patients. Journal of Child Neurology 19 (4), 275–281.

Chieffo, C., Garvey, N., Gong, W., Roe, B., Zhang, G., Silver, L., Emanuel, B.S., Budarf, M.L., 1997. Isolation and characterization of a gene from the DiGeorge chromosomal region homologous to the mouse Tbx1 gene. Genomics 43 (3), 267–277.

Chow, E.W., Zipursky, R.B., Mikulis, D.J., Bassett, A.S., 2002. Structural brain abnormalities in patients with schizophrenia and 22q11 deletion syndrome. Biological Psychiatry 51 (3), 208–215.

Courchesne, E., Pierce, K., 2005. Why the frontal cortex in autism might be talking only to itself: local over-connectivity but long-distance disconnection. Current Opinion in Neurobiology 15 (2), 225–230.

Cramer, S.C., Schaefer, P.W., Krishnamoorthy, K.S., 1996. Microgyria in the distribution of the middle cerebral artery in a patient with DiGeorge syndrome. Journal of Child Neurology 11 (6), 494–497.

Dambska, M., Laure-Kamionowska, M., 2001. The role of glial–pial barrier lesions and impaired vascularization in anomalous formation of cortical convolutions. Brain and Development 23 (4), 223–227.

Dehay, C., Giroud, P., Berland, M., Killackey, H., Kennedy, H., 1996. Contribution of thalamic input to the specification of cytoarchitectonic cortical fields in the primate: effects of bilateral enucleation in the fetal monkey on the boundaries, dimensions, and gyrification of striate and extrastriate cortex. Journal of Comparative Neurology 367 (1), 70–89.

Derogatis, L.R., 1983. SCL-90-R Administration, Scoring and Procedures Manual II. Clinical Psychometric Research, Towson, MD.

Eecken, H.M.V., 1959. The Anastomoses Between the Leptomeningeal Arteries of the Brain: Their Morphological, Pathological and Clinical Significance. Charles C Thomas, Publisher, Springfield, IL.

Ehara, H., Maegaki, Y., Takeshita, K., 2003. Pachygyria and polymicrogyria in 22q11 deletion syndrome. American Journal of Medical Genetics 117A (1), 80–82.

Eliez, S., Schmitt, J.E., White, C.D., Reiss, A.L., 2000. Children and adolescents with velocardiofacial syndrome: a volumetric MRI study. American Journal of Psychiatry 157 (3), 409–415.

Eliez, S., Blasey, C.M., Menon, V., White, C.D., Schmitt, J.E., Reiss, A.L., 2001. Functional brain imaging study of mathematical reasoning abilities in velocardiofacial syndrome (del22q11.2). Genetics in Medicine 3 (1), 49–55.

Eliez, S., Blasey, C.M., Schmitt, J.E., White, C.D., Hu, D., Reiss, A.L., 2001. Velocardiofacial syndrome: are structural changes in the temporal and mesial temporal regions related to schizophrenia? American Journal of Psychiatry 158 (3), 447–453.

Eliez, S., Schmitt, J.E., White, C.D., Willis, V.G., Reiss, A.L., 2001. A quantitative MRI study of posterior fossa development in velocardiofacial syndrome. Biological Psychiatry 49 (6), 540–546.

First, M.B., Spitzer, R.L., Gibbon, M., Williams, J.B.W., 1997. Structured Clinical Interview for DSM-IV. American Psychiatric Press, Washington, DC.

Gerdes, M., Solot, C., Wang, P.P., Moss, E., LaRossa, D., Randall, P., Goldmuntz, E., Clark III, B.J., Driscoll, D.A., Jawad, A., Emanuel, B.S., McDonald-McGinn, D.M., Batshaw, M.L., Zackai, E.H., 1999. Cognitive and behavior profile of preschool children

with chromosome 22q11.2 deletion. American Journal of Medical Genetics 85 (2), 127–133.

Ghariani, S., Dahan, K., Saint-Martin, C., Kadhim, H., Morsomme, F., Moniotte, S., Verellen-Dumoulin, C., Sebire, G., 2002. Polymicrogyria in chromosome 22q11 deletion syndrome. European Journal of Paediatric Neurology 6 (1), 73–77.

Goldberg, R., Motzkin, B., Marion, R., Scambler, P.J., Shprintzen, R.J., 1993. Velo-cardio-facial syndrome: a review of 120 patients. American Journal of Medical Genetics 45 (3), 313–319.

Gothelf, D., Presburger, G., Levy, D., Nahmani, A., Burg, M., Berant, M., Blieden, L.C., Finkelstein, Y., Frisch, A., Apter, A., Weizman, A., 2004. Genetic, developmental, and physical factors associated with attention deficit hyperactivity disorder in patients with velocardiofacial syndrome. American Journal of Medical Genetics 126B (1), 116–121.

Guerrini, R., Barkovich, A.J., Sztriha, L., Dobyns, W.B., 2000. Bilateral frontal polymicrogyria: a newly recognized brain malformation syndrome. Neurology 54 (4), 909–913.

Hardan, A.Y., Jou, R.J., Keshavan, M.S., Varma, R., Minshew, N.J., 2004. Increased frontal cortical folding in autism: a preliminary MRI study. Psychiatry Research: Neuroimaging 131 (3), 263–268.

Harris, J.M., Whalley, H., Yates, S., Miller, P., Johnstone, E.C., Lawrie, S.M., 2004. Abnormal cortical folding in high-risk individuals: a predictor of the development of schizophrenia? Biological Psychiatry 56 (3), 182–189.

Harris, J.M., Yates, S., Miller, P., Best, J.J., Johnstone, E.C., Lawrie, S.M., 2004. Gyrification in first-episode schizophrenia: a morphometric study. Biological Psychiatry 55 (2), 141–147.

Jou, R.J., Hardan, A.Y., Keshavan, M.S., 2005. Reduced cortical folding in individuals at high risk for schizophrenia: a pilot study. Schizophrenia Research 75 (2–3), 309–313.

Kaplan, D.M., Liu, A.M., Abrams, M.T., Warsofsky, I.S., Kates, W.R., White, C.D., Kaufmann, W.E., Reiss, A.L., 1997. Application of an automated parcellation method to the analysis of pediatric brain volumes. Psychiatry Research: Neuroimaging 76 (1), 15–27.

Kates, W.R., Warsofsky, I.S., Patwardhan, A., Abrams, M.T., Liu, A.M., Naidu, S., Kaufmann, W.E., Reiss, A.L., 1999. Automated Talairach atlas-based parcellation and measurement of cerebral lobes in children. Psychiatry Research: Neuroimaging 91 (1), 11–30.

Kates, W.R., Burnette, C.P., Jabs, E.W., Rutberg, J., Murphy, A.M., Grados, M., Geraghty, M., Kaufmann, W.E., Pearlson, G.D., 2001. Regional cortical white matter reductions in velocardiofacial syndrome: a volumetric MRI analysis. Biological Psychiatry 49 (8), 677–684.

Kates, W.R., Burnette, C.P., Bessette, B.A., Folley, B.S., Strunge, L., Jabs, E.W., Pearlson, G.D., 2004. Frontal and caudate alterations in velocardiofacial syndrome (deletion at chromosome 22q11.2). Journal of Child Neurology 19 (5), 337–342.

Kaufman, J., Birmaher, B., Brent, D., Rao, U., Flynn, C., Moreci, P., Williamson, D., Ryan, N., 1997. Schedule for Affective Disorders and Schizophrenia for School-age Children-Present and Lifetime Version (K-SADS-PL): initial reliability and validity data. Journal of the American Academy of Child and Adolescents Psychiatry 36 (7), 980–988.

Kawame, H., Kurosawa, K., Akatsuka, A., Ochiai, Y., Mizuno, K., 2000. Polymicrogyria is an uncommon manifestation in 22q11.2 deletion syndrome. American Journal of Medical Genetics 94 (1), 77–78.

Kesler, S.R., Vohr, B., Schneider, K.C., Katz, K.H., Makuch, R.W., Reiss, A.L., Ment, L.R., in press. Increased temporal lobe gyrification in preterm children. Neuropsychologia.

Koolen, D.A., Veltman, J.A., Renier, W.O., Droog, R.P., van Kessel, A.G., de Vries, B.B., 2004. Chromosome 22q11 deletion and pachygyria characterized by array-based comparative genomic hybridization. American Journal of Medical Genetics A 131 (3), 322–324.

Kulynych, J.J., Luevano, L.F., Jones, D.W., Weinberger, D.R., 1997. Cortical abnormality in schizophrenia: an in vivo application of the gyrification index. Biological Psychiatry 41 (10), 995–999.

Lancaster, J.L., Fox, P.T., Downs, H., Nickerson, D.S., Hander, T.A., El Mallah, M., Kochunov, P.V., Zamarripa, F., 1999. Global spatial normalization of human brain using convex hulls. Journal of Nuclear Medicine 40 (6), 942–955.

Merscher, S., Funke, B., Epstein, J.A., Heyer, J., Puech, A., Lu, M.M., Xavier, R.J., Demay, M.B., Russell, R.G., Factor, S., Tokooya, K., Jore, B.S., Lopez, M., Pandita, R.K., Lia, M., Carrion, D., Xu, H., Schorle, H., Kobler, J.B., Scambler, P., Wynshaw-Boris, A., Skoultchi, A.I., Morrow, B.E., Kucherlapati, R., 2001. Tbx1 is responsible for cardiovascular defects in velo-cardio-facial/DiGeorge syndrome. Cell 104 (4), 619–629.

Moss, E.M., Batshaw, M.L., Solot, C.B., Gerdes, M., McDonald-McGinn, D.M., Driscoll, D.A., Emanuel, B.S., Zackai, E.H., Wang, P.P., 1999. Psychoeducational profile of the 22q11.2 microdeletion: a complex pattern. Journal of Pediatrics 134 (2), 193–198.

Murphy, K.C., Owen, M.J., 2001. Velo-cardio-facial syndrome: a model for understanding the genetics and pathogenesis of schizophrenia. British Journal of Psychiatry 179, 397–402.

Murphy, K.C., Jones, L.A., Owen, M.J., 1999. High rates of schizophrenia in adults with velo-cardio-facial syndrome. Archives of General Psychiatry 56 (10), 940–945.

Otsu, 1979. A threshold selection method from gray-level histograms. IEEE Transactions on Systems, Man, and Cybernetics 9, 62–66.

Papolos, D.F., Faedda, G.L., Veit, S., Goldberg, R., Morrow, B., Kucherlapati, R., Shprintzen, R.J., 1996. Bipolar spectrum disorders in patients diagnosed with velo-cardio-facial syndrome: does a hemizygous deletion of chromosome 22q11 result in bipolar affective disorder? American Journal of Psychiatry 153 (12), 1541–1547.

Rakic, P., 1988. Specification of cerebral cortical areas. Science 241 (4862), 170–176.

Reiss, A.L., 2004. BrainImage. Stanford University, Stanford, CA.

Reiss, A.L., Hennessey, J.G., Rubin, M., Beach, L., Abrams, M.T., Warsofsky, I.S., Liu, A.M., Links, J.M., 1998. Reliability and validity of an algorithm for fuzzy tissue segmentation of MRI. Journal of Computer Assisted Tomography 22 (3), 471–479.

Ryan, A.K., Goodship, J.A., Wilson, D.I., Philip, N., Levy, A., Seidel, H., Schuffenhauer, S., Oechsler, H., Belohradsky, B., Prieur, M., Aurias, A., Raymond, F.L., Clayton-Smith, J., Hatchwell, E., McKeown, C., Beemer, F.A., Dallapiccola, B., Novelli, G., Hurst, J.A., Ignatius, J., Green, A.J., Winter, R.M., Brueton, L., Brondum-Nielsen, K., Scambler, P.J., et al., 1997. Spectrum of clinical features associated with interstitial chromosome 22q11 deletions: a European collaborative study. Journal of Medical Genetics 34 (10), 798–804.

Sallet, P.C., Elkis, H., Alves, T.M., Oliveira, J.R., Sassi, E., Campi de Castro, C., Busatto, G.F., Gattaz, W.F., 2003. Reduced cortical folding in schizophrenia: an MRI morphometric study. American Journal of Psychiatry 160 (9), 1606–1613.

Scambler, P.J., 2000. The 22q11 deletion syndromes. Human Molecular Genetics 9 (16), 2421–2426.

Schmitt, J.E., Watts, K., Eliez, S., Bellugi, U., Galaburda, A.M., Reiss, A.L., 2002. Increased gyrification in Williams syndrome:

evidence using 3D MRI methods. Developmental Medicine and Child Neurology 44 (5), 292–295.

Shprintzen, R.J., Goldberg, R.B., Lewin, M.L., Sidoti, E.J., Berkman, M.D., Argamaso, R.V., Young, D., 1978. A new syndrome involving cleft palate, cardiac anomalies, typical facies, and learning disabilities: velo-cardio-facial syndrome. Cleft Palate Journal 15 (1), 56–62.

Simon, T.J., Ding, L., Bish, J.P., McDonald-McGinn, D.M., Zackai, E.H., Gee, J., 2005. Volumetric, connective, and morphologic changes in the brains of children with chromosome 22q11.2 deletion syndrome: an integrative study. NeuroImage 25 (1), 169–180.

Sobin, C., Kiley-Brabeck, K., Daniels, S., Khuri, J., Taylor, L., Blundell, M., Anyane-Yeboa, K., Karayiorgou, M., 2005. Neuropsychological characteristics of children with the 22q11 deletion syndrome: a descriptive analysis. Neuropsychology, Development, and Cognition. Section C. Child Neuropsychology, A Journal on Normal and Abnormal Development in Childhood and Adolescence 11(1), 39–53.

Subramaniam, B., Hennessey, J.G., Rubin, M.A., Beach, L.S., Reiss, A.L., 1997. Software and methods for quantitative imaging in neuroscience: the Kennedy Krieger Institute Human Brain Project. In: Koslow, S.H., Huerta, M.F. (Eds.), Neuroinformatics: An Overview of the Human Brain Project. Lawrence Erlbaum, Mahwah, N.J.

Swillen, A., Devriendt, K., Legius, E., Eyskens, B., Dumoulin, M., Gewillig, M., Fryns, J.P., 1997. Intelligence and psychosocial adjustment in velocardiofacial syndrome: a study of 37 children and adolescents with VCFS. Journal of Medical Genetics 34 (6), 453–458.

Swillen, A., Devriendt, K., Legius, E., Prinzie, P., Vogels, A., Ghesquiere, P., Fryns, J.P., 1999. The behavioural phenotype in velo-cardio-facial syndrome (VCFS): from infancy to adolescence. Genetic Counseling 10 (1), 79–88.

Swillen, A., Vandeputte, L., Cracco, J., Maes, B., Ghesquiere, P., Devriendt, K., Fryns, J.P., 1999. Neuropsychological, learning and psychosocial profile of primary school aged children with the velo-cardio-facial syndrome (22q11 deletion): evidence for a non-verbal learning disability? Neuropsychology, Development and Cognition. Section C. Child Neuropsychology, A Journal on Normal and Abnormal Development in Childhood and Adolescence 5 (4), 230–241.

Sztriha, L., Guerrini, R., Harding, B., Stewart, F., Chelloug, N., Johansen, J.G., 2004. Clinical, MRI, and pathological features of polymicrogyria in chromosome 22q11 deletion syndrome. American Journal of Medical Genetics 127A (3), 313–317.

Talairach, J., Tournoux, P., 1988. Co-Planar Stereotaxic Atlas of the Human Brain. Georg Thieme Verlag, Stuttgart-New York.

Thompson, P.M., Hayashi, K.M., Sowell, E.R., Gogtay, N., Giedd, J.N., Rapoport, J.L., de Zubicaray, G.I., Janke, A.L., Rose, S.E., Semple, J., Doddrell, D.M., Wang, Y., van Erp, T.G., Cannon, T.D., Toga, A.W., 2004. Mapping cortical change in Alzheimer's disease, brain development, and schizophrenia. NeuroImage 23 (Suppl 1), S2–S18.

Van Essen, D.C., 1997. A tension-based theory of morphogenesis and compact wiring in the central nervous system. Nature 385 (6614), 313–318.

Vogeley, K., Schneider-Axmann, T., Pfeiffer, U., Tepest, R., Bayer, T.A., Bogerts, B., Honer, W.G., Falkai, P., 2000. Disturbed gyrification of the prefrontal region in male schizophrenic patients: a morphometric postmortem study. American Journal of Psychiatry 157 (1), 34–39.

Vogeley, K., Tepest, R., Pfeiffer, U., Schneider-Axmann, T., Maier, W., Honer, W.G., Falkai, P., 2001. Right frontal hypergyria differentiation in affected and unaffected siblings from families multiply affected with schizophrenia: a morphometric MRI study. American Journal of Psychiatry 158 (3), 494–496.

Weinberger, D.R., 1995. From neuropathology to neurodevelopment. Lancet 346 (8974), 552–557.

Weinberger, D.R., Berman, K.F., Suddath, R., Torrey, E.F., 1992. Evidence of dysfunction of a prefrontal-limbic network in schizophrenia: a magnetic resonance imaging and regional cerebral blood flow study of discordant monozygotic twins. American Journal of Psychiatry 149 (7), 890–897.

Worthington, S., Turner, A., Elber, J., Andrews, P.I., 2000. 22q11 deletion and polymicrogyria—cause or coincidence? Clinical Dysmorphology 9 (3), 193–197.

Zilles, K., Armstrong, E., Schleicher, A., Kretschmann, H.J., 1988. The human pattern of gyrification in the cerebral cortex. Anatomy and Embryology 179 (2), 173–179.

IEEE TRANSACTIONS ON MEDICAL IMAGING, VOL. 27, NO. 2, FEBRUARY 2008 161

A Surface-Based Approach to Quantify Local Cortical Gyrification

Marie Schaer*, Meritxell Bach Cuadra, Lucas Tamarit, François Lazeyras, Stephan Eliez, and Jean-Philippe Thiran, *Senior Member, IEEE*

***Abstract*—The high complexity of cortical convolutions in humans is very challenging both for engineers to measure and compare it, and for biologists and physicians to understand it. In this paper, we propose a surface-based method for the quantification of cortical gyrification. Our method uses accurate 3-D cortical reconstruction and computes local measurements of gyrification at thousands of points over the whole cortical surface. The potential of our method to identify and localize precisely gyral abnormalities is illustrated by a clinical study on a group of children affected by 22q11 Deletion Syndrome, compared to control individuals.**

***Index Terms*—Cortical complexity, gyrification, neuroimaging, statistical analysis, surface-based anatomical modeling.**

I. Introduction

APPREHENDING the complexity of cortical folding remains one of the most formidable challenges following recent advances in neuroimaging techniques [1], [2]. The increasing interest in the study of cortical complexity is driven by its potential to delineate and understand normal maturation [3]-[5], abnormal brain development [6]-[16], or neurodegenerative processes [2], [17], [18]. For example, an increase in the frontal cortical complexity during childhood suggests that normal ongoing maturational processes continuously remodel the cortical shape [4]. As the elastic properties and microstructure of neuronal sheets [19] and axonal connectivity [20] influence cortical folding, cortical complexity may reveal the underlying structural configuration of the brain. Also, cortical complexity may convey crucial information in the understanding of pathological processes associated with neurodevelopmental disorders. For example, it has been suggested that increased gyrification in Williams syndrome relies on a developmental arrest due to microvascular infarcts during early cortical development [15]. Altogether, these findings suggest that cortical complexity subtly reßects underlying biological processes associated with normal or abnormal cognitive functioning. Therefore, the development of reliable and precise algorithms to study gyrification is certainly key in our future understanding of normal and abnormal brain development.

Initial moves to assess cortical complexity were made in the second half of the twentieth century by comparative neuroanatomists, who had observed that an increase in the cortical area during mammalian evolution was accompanied by an increase in folding [21], [22]. They proposed the use of a simple zero-order surface ratio to quantify cortical folding. The Gyrification Index (GI) was defined as the ratio of the total folded cortical surface over the perimeter of the brain, delineated on 2-D coronal sections [23]. Because of its easy interpretation and its simplicity in implementation, many studies have been conducted using the Gyrification Index to identify abnormal cortical complexity in neurodevelopmental and psychiatric disorders [8]-[10], [12], [14]-[16], [24], [25]. However, dissent regarding traditional methodological usage of the Gyrification Index remains a major issue. First, surfaces are delineated on coronal sections, which do not take into account the inherent 3-D nature of the cortical surface. Perimeter measurements may be biased by slice orientation, and buried sulci cannot always be included. Also, the precise localization of gyral anomalies in sublobar regions is not possible in 2-D slices. Last but not least, most studies (except [14], [15], [26]) used manual delineation of the contours, which raises the question of reliability and reproducibility in the context of large-scale studies. Recently, there have been some attempts to adapt the Gyrification Index to a fully automated 2-D method [27]. Technological developments now provide high quality 3-D reconstructions of the cortex (e.g., FreeSurfer [28] or SureFit [29]). The use of 3-D reconstruction overcomes the problems caused by manual tracing, as well as the problem of buried sulci. To date, attempts to advance a 3-D extension of the Gyrification Index were either global [30] or based on sulcal regions of interest [31]. As the cortex is thought to grow by radial expansion [32], a 3-D approach of the Gyrification Index that is not restrained by the sulcal walls would be of great interest in specifying the regions of abnormal cortical expansion associated with specific pathological conditions.

In this paper, we present a new method to quantify and compare local cortical gyrification at thousands of points over the whole hemisphere. Our local 3-D Gyrification Index (lGI) measures the amount of cortical surface invaginated in the sulci,

Manuscript received March 8, 2007; revised June 19, 2007. This work was supported in part by the Swiss National Research Funds under Grant 323500-111165, Grant 3200-063135, Grant 3232-063134, and Grant PP00B-102864 and by a grant from the NARSAD Institute. This work was also supported by the Center for Biomedical Imaging (CIBM) of the Geneva - Lausanne Universities and the EPFL, as well as the foundations Leenaards and Louis-Jeantet. *Asterisk indicates corresponding author*.

*M. Schaer is with Service Médico-Pédagogique, Department of Psychiatry, University of Geneva School of Medicine, 1211 Geneva, Switzerland and with Signal Processing Institute, Ecole Polytechnique Fédérale de Lausanne, 1015 Lausanne, Switzerland (e-mail: marie.schaer@medecine.unige.ch).

M. Bach Cuadra and J.-P. Thiran are with Signal Processing Institute, Ecole Polytechnique Fédérale de Lausanne, 1015 Lausanne, Switzerland (e-mail: meritxell.bach@epfl.ch; jp.thiran@epfl.ch).

L. Tamarit is with Image and Signal Processing Laboratory, School of Engineering, 1211 Geneva, Switzerland (e-mail: lucas.tamarit@cisa.unige.ch).

F. Lazeyras is with Department of Radiology, Geneva University Hospitals, 1205 Geneva, Switzerland (e-mail: francois.lazeyras@hcuge.ch).

S. Eliez is with Service Médico-Pédagogique, Department of Psychiatry, University of Geneva School of Medicine, 1211 Geneva, Switzerland and with Department of Genetic Medicine and Development, University of Geneva School of Medicine, 1205 Geneva, Switzerland (e-mail: stephan.eliez@medecine.unige.ch).

Digital Object Identifier 10.1109/TMI.2007.903576

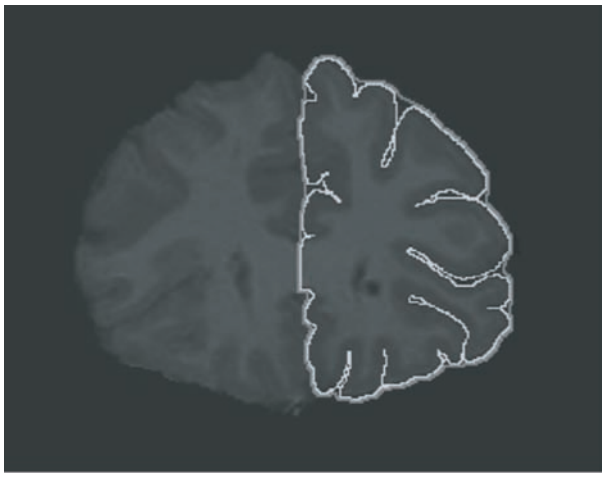

Fig. 1. Illustration of the 2-D Gyrification Index as originally described by Zilles [23] (figure from [14]). GI is classically computed on coronal sections, after volume realignment in the AC-PC plane, as the ratio of the pial perimeter (in white) over the outer perimeter (in gray).

in circular regions of interest. We tested the potential of our method to identify and localize subtle gyral anomalies, by conducting a group comparison between 12 girls affected by 22q11 Deletion Syndrome, a neurodevelopmental condition of genetic origin [33], and 12 typically developing children matched for age (girls only, mean age 9.75 ± 1.4).

The rest of this paper is organized as follows. In Section II, we introduce the new method for quantifying the local Gyrification Index (*l*GI). Section III presents a clinical implementation of the method based on 24 young girls. Finally, in Section IV, we briefly discuss the results of our statistical analysis, and develop the relationship between *l*GI and the other methods for measuring cortical shape.

II. A New Surface-Based Method for Quantifying Local Gyrification

The Gyrification Index is commonly computed on coronal sections using the following equation [23]:

$$\mathrm{GI}|_{2-D} = \frac{\sum_{j=1}^{N} P_P^j \cdot t}{\sum_{j=1}^{N} P_O^j \cdot t} \tag{1}$$

where j indexes the slice, P_P^j is the pial cortical perimeter of slice j, P_O^j is the outer perimeter of slice j, t is slice thickness, and N is the number of slices in the image (see Fig. 1).

A. Three-Dimensional Extension of GI

We first extend the Gyrification Index in a 3-D space, using the areas of cortical mesh models instead of perimeters. In our implementation using mesh models with triangular faces, the following equation replaces the classical 2-D GI:

$$\mathrm{GI}|_{3-D} = \frac{\sum_{j=1}^{M_P} A_P^j}{\sum_{j=1}^{M_O} A_O^j} \tag{2}$$

where A_P^j and A_O^j are the area of the face j in the 3-D mesh of the pial surface and of the outer surface, respectively, and M_P and M_O are the total number of faces in the pial and outer mesh, respectively. In order to compute the outer surface, Batchelor [30] proposed the use of the convex hull of the pial surface. However, as mentioned in [35] and [36], the convex hull is not really an accurate representation of the envelope of the brain, because it does not adhere to the hemisphere. That is why Batchelor called it a convexity ratio and not a 3-D-Gyrification Index [30]. The minimal value for the convexity ratio correspond a smooth and perfectly convex object (i.e., convexity ratio equal to 1). We want the 3-D-Gyrification Index to be minimal for a smooth object having the same general shape as the hemisphere (i.e., with no sulci). Therefore, the outer surface was specifically reconstructed for that purpose. The following section presents the surface reconstruction process. The whole process is summarized in Fig. 2.

1) Pial Surface: The pial cortical surface is first reconstructed in 3-D space, with a submillimeter accuracy. In our work, this is done using the FreeSurfer [28] software that subdivides the process into several subtasks.

First, the intensity of the original medical resonance imaging (MRI) is normalized and voxels not considered as brain tissue are removed using a "skull-stripping" procedure. Second, brain tissue segmentation is completed, based on intensity information, on the laminar structure of the gray- white matter interface [28] and on an automated atlas-based subcortical masking [37]. The segmentation process thus results in a single filled white matter volume for each hemisphere, which is covered with a triangular tessellation (white surface). Then, this initial tessellation is repositioned using a deformable surface algorithm that minimizes an energy term guided by local MRI intensity values [38], resulting in two smoothed tessellated cortical hemispheres. Finally, the same surface deformation algorithm is applied from the white surface toward the gray matter - CSF interface, resulting in the pial surface. Moreover, the self-intersection in the surfaces is prevented [38]. The white matter and pial surfaces are careful inspected, and topological defects resulting in inaccurate or nonspherical surfaces are removed manually. The resulting pial surface is derived from the white surface with a point-to-point correspondence [28], and is topologically correct with no self-intersection [39]. For these reasons, 3-D reconstructions of the cortical surface cope more successfully with the problem of buried sulci than 2-D perimeters, which are not continuous and have no correspondence between the inner and outer faces of the cortical mantle.

At this point, a 3-D mesh of the pial surface consisting of $\sim$120 000 vertices, with an average face area of 0.5 mm^2, becomes available and its envelope (outer surface) needs to be computed.

2) Outer Surface: As proposed in [35] and [36], an outer hull tightly warping the pial surface can be efficiently computed using a morphological closing operation. For this purpose, we first convert the pial mesh into a binary volume, and then close the sulci using a sphere of 15 mm diameter as the structural element. The diameter of 15 mm was experimentally chosen in that it closes the main sulci. Kao *et al.* [35] used 10 mm, but observed in their experiment that a 50% increase or decrease in

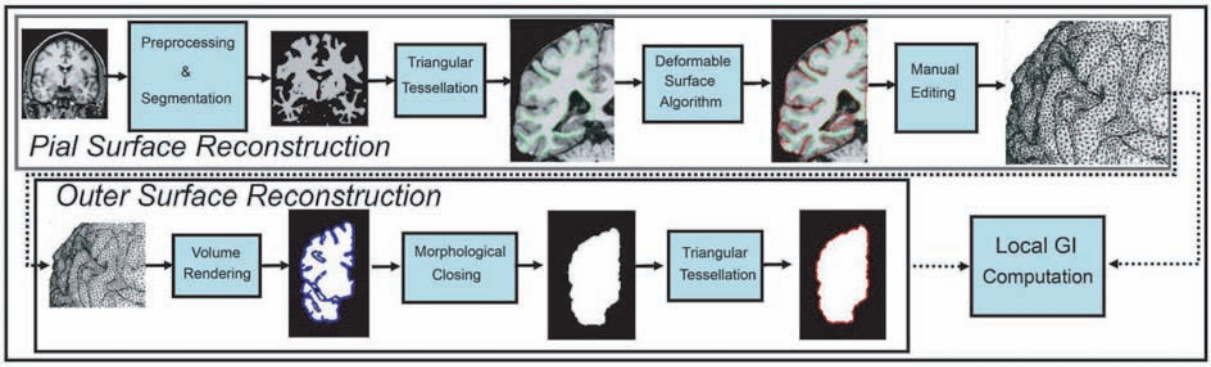

Fig. 2. Block diagram summarizing the main steps of our method for pial surface reconstruction (top row) and outer surface reconstruction (bottom row) before measuring the local Gyrification Index.

this parameter does not substantially affect the result. Finally, we create a 3-D triangulated mesh on the binary closed volume. The resulting outer mesh is typically made of an average vertices number of 55 000, with an average face area of 0.4 mm^2.

At this point, a global 3-D extension of the Gyrification Index can be computed using (2). The main purpose of this work is, however, to propose a local measurement of the Gyrification Index, which we set out in detail in the following section.

B. Local Gyrification Measurements for Each Vertex of the Outer Surface

In 2005 [31], Rettmann proposed a local Gyrification Index based on sulcal regions of interest, with the purpose of quantifying the local amount of cortex buried within the sulcal folds, in specific sulcal regions. This measurement is an interesting localized variation of the 3-D Gyrification Index, but remains constrained in areas defined by the sulcal walls. Thus, sulcal-based GI depends heavily on accurate and robust sulcal segmentation, and could be related to a sulcal depth measurement. We propose a local Gyrification Index measurement, that we here denote *l*GI, which is not constrained by the sulci. The *l*GI at a given point on the cortical surface is computed as the ratio between the surface of a circular region of interest on the outer surface, centered at this point, and the surface of the corresponding region of interest on the pial surface. At each point on the outer surface, it reflects the amount of cortex buried within the sulcal folds in the surrounding area. Formally

$$l\mathrm{GI}|_{3-D}^{\mathrm{Outer}}(v_i) = \frac{\mathrm{ROI}_P}{\mathrm{ROI}_O} = \frac{\sum_{\forall j \in S'(v_i,r)} A_P^j}{\sum_{\forall j \in S(v_i,r)} A_O^j} \quad \forall v_i \in S_O \quad (3)$$

where

- A_O^j is the area of the face j of the outer surface. The surface of the region of interest ROI_O on the outer surface is calculated as the sum of those areas for all faces j comprised in the intersection of the outer surface S_O with a sphere $S(v_i, r)$ centered on vertex v_i of the outer surface with a radius r.
- A_P^j is the area of the face j of the pial surface. The surface of the region of interest ROI_P on the pial surface is calculated as the sum of those areas for all faces j belonging to the corresponding pial region of interest $S'(v_i, r)$. The correspondence between the regions of interest on the outer (ROI_O) and pial (ROI_P) surfaces is described in the following section.

1) ROI on the Outer Surface, ROI_O: For each vertex v_i of the outer envelope, we define a circular region of interest through the intersection of the outer surface S_O with a sphere S centered on v_i with a radius r [Fig. 3(a)]. To set this radius, we specifically kept in mind that its diameter has to remain larger than the gyral width, so that it can take into account more than one sulcus at a time. Based on visual inspection, we first choose a radius of 25 mm for the *l*GI calculation, as it integrates an appropriate number of sulci but still allows for an accurate localization in sublobar regions [see Fig. 3(c)- (e)]. In a second time, we tested the effect of different radii on *l*GI measurements; the results of this analysis are presented in Section II-D.

2) Region of Interest on the Pial Surface, ROI_P: For each ROI_O, we define a corresponding area ROI_P on the pial surface. First, we isolate the vertices of the outer surface that are situated on the perimeter of the ROI_O [Fig. 3(b)]. To avoid redundancies, we retain only one fifth of the vertices situated on the perimeter of the ROI_O. Then, we find the vertices of the pial mesh that are closest to each of the outer perimeter's selected points [Fig. 3(c)]. The vertices defined on the pial mesh at that point are considered as the perimeter of the future ROI_P. In order to close the pial ROI, the vertices are linked via the geodesic path[1] between them [Fig. 3(d)]. The ROI_P comprises all the faces of the pial mesh contained within the resulting closed path [Fig. 3(e)]. Thus, the ROI_P considers the full depth and width of all the sulci opening at the brain surface in the perimeter defined by the ROI_O.

At this point, *l*GI value is computed for each of the vertex v_i of the outer surface according to the (3).

C. Cortical Maps of lGI

In order to obtain cortical maps of local gyrification for subsequent statistical comparisons, we propagate the *l*GI values from the outer mesh to the pial mesh. Accurate comparison of any

[1]Using the "dijk" function by Michael G. Kay, MATLOG toolbox, http://www.ise.ncsu.edu/kay/matlog/

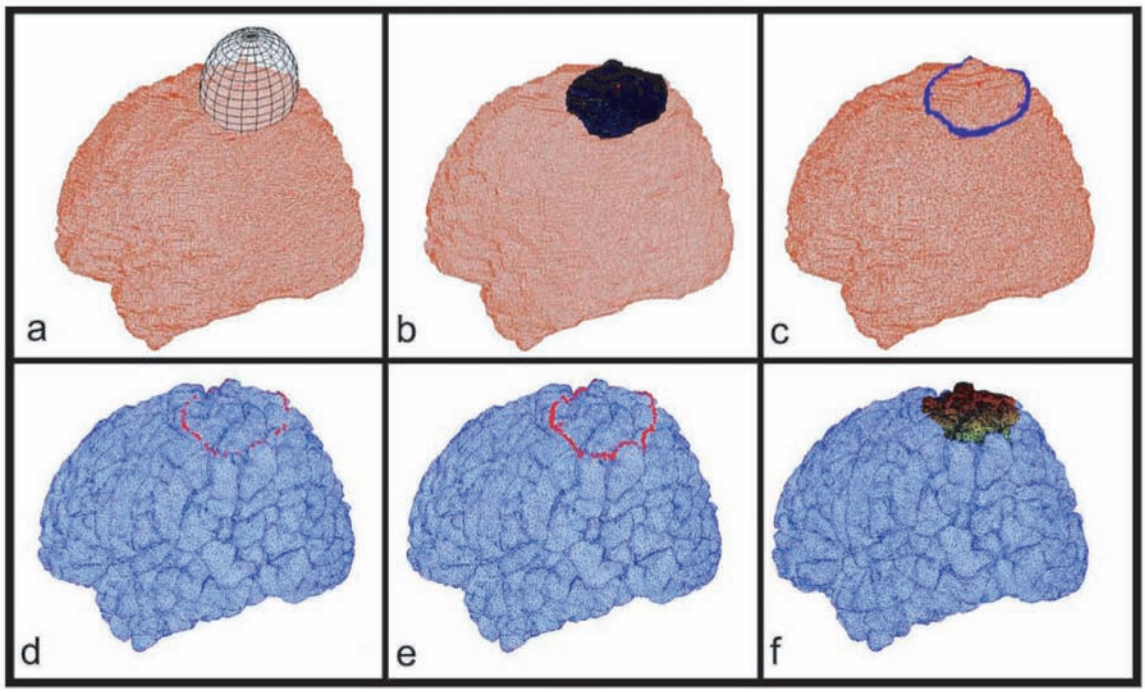

Fig. 3. Illustration of the different steps for GI computation. In the upper row, the creation of the outer region of interest ROI_O is shown on the outer surface (red); in the lower row, the creation of the pial region of interest ROI_P on the pial surface (blue) is illustrated. In (a), a sphere $S(v_i,r)$ centered on v_i of radius $r = 25$ mm is plotted on the outer surface (red). The intersection between the outer surface S_O and the sphere defines the outer region of interest ROI_O (b in blue). The perimeter of the ROI_O is delineated in blue in (c). In (d), the points of the pial surface (blue) corresponding to the ROI_O perimeter are highlighted in red. Linking of these points is achieved through the geodesic path between them, resulting in the ROI_P perimeter (in red, in e). The faces of the pial mesh enclosed by the ROI_P perimeter define the pial region of interest. Finally, the GI value attributed to the vertex v_i (b, red point) is computed as the ratio of the areas of both corresponding regions of interest.

cortical feature (i.e., cortical thickness, sulcal depth, gyrification, etc.) between two different subjects relies on a precise mapping between each cortical region in the brain of individual and a corresponding region in another. Surface-based registration using spherical coordinates system guided by sulcal aligment has proven its accuracy in localizing structural and functional features of the human cortex [40]. As the *l*GI quantifies the spatial frequency and the depth of sulci, a precise intersubject registration based on sulcal patterns is crucial, to avoid differences in gyrification caused by misalignment. For this reason, we need to put the data back to the subject's own coordinate system, in other words we need pial cortical maps in which each vertex is attributed an *l*GI value. The aim of the propagation is to redistribute *l*GI values to the pial surface, with respect to their prior involvement in the whole computational process. Each vertex v_j of the pial surface will receive a weighted part of the *l*GI value for which he contributed to, weighting being inversely proportionate to the distance between the v_j and the normal axis X to the outer surface at the vertex v_i at which *l*GI was measured (the center of the outer ROI). Mathematically

$$l\mathrm{GI}_{3-D}^{\mathrm{Pial}}(v_j) = \frac{\sum_{\forall v_i, v_j \in S'(v_i,r)} \mathrm{GI}_{3-D}^{\mathrm{Outer}}(v_i) \cdot \left[1 - \frac{1}{d(v_j, X(v_i))}\right]}{\sum_{\forall v_j \in S'(v_i,r)} \left[1 - \frac{1}{d(v_j, X(v_i))}\right]} \quad \forall v_j \in S_P \quad (4)$$

where the sum is taken over all *l*GI values associated with v_i in which the vertex v_j of the pial surface $R(S, v_i)$ was considered; $\mathrm{GI}_{3-\mathrm{D}}^{\mathrm{Outer}}(v_i)$ is the local GI as defined in (3) at the vertex v_i belonging to the outer surface S_O, and $d(v_j, X)$ is the distance from the vertex v_j to the normal axis X of the vertex v_i. Note that

$$0 < \left[1 - \frac{1}{d(v_j, X(v_i))}\right] \leq 1. \quad (5)$$

D. Effect of the Sphere Radius on the lGI Cortical Maps

As expected, the individual variance of the *l*GI values plotted in Fig. 4 indicates that maximal values are located around the sylvian fissure. This major maximum reflects the large amount of insular cortex hidden within the sylvian fissure during early gyrogenesis. Using a radius of 20 or 25 mm, other (more moderate) local maxima are observed along the intraparietal sulcus, the superior temporal sulcus, and near the intersection of the parieto-occipital sulcus and the calcarine sulcus. Similar to the sylvian fissure, the other moderate maxima are located in sulci that are among the first to appear in the fetal cortex during development [41], strengthening the hypothesis that *l*GI may be closely tied to neural development. With larger radii, *l*GI cortical maps are progressively smoothed; and the maxima on the lateral aspect of the hemisphere are diluted, resulting in a single large maximal convergence around the sylvian fissure. This convergence brings to mind images from Toro and Burnod's [42]

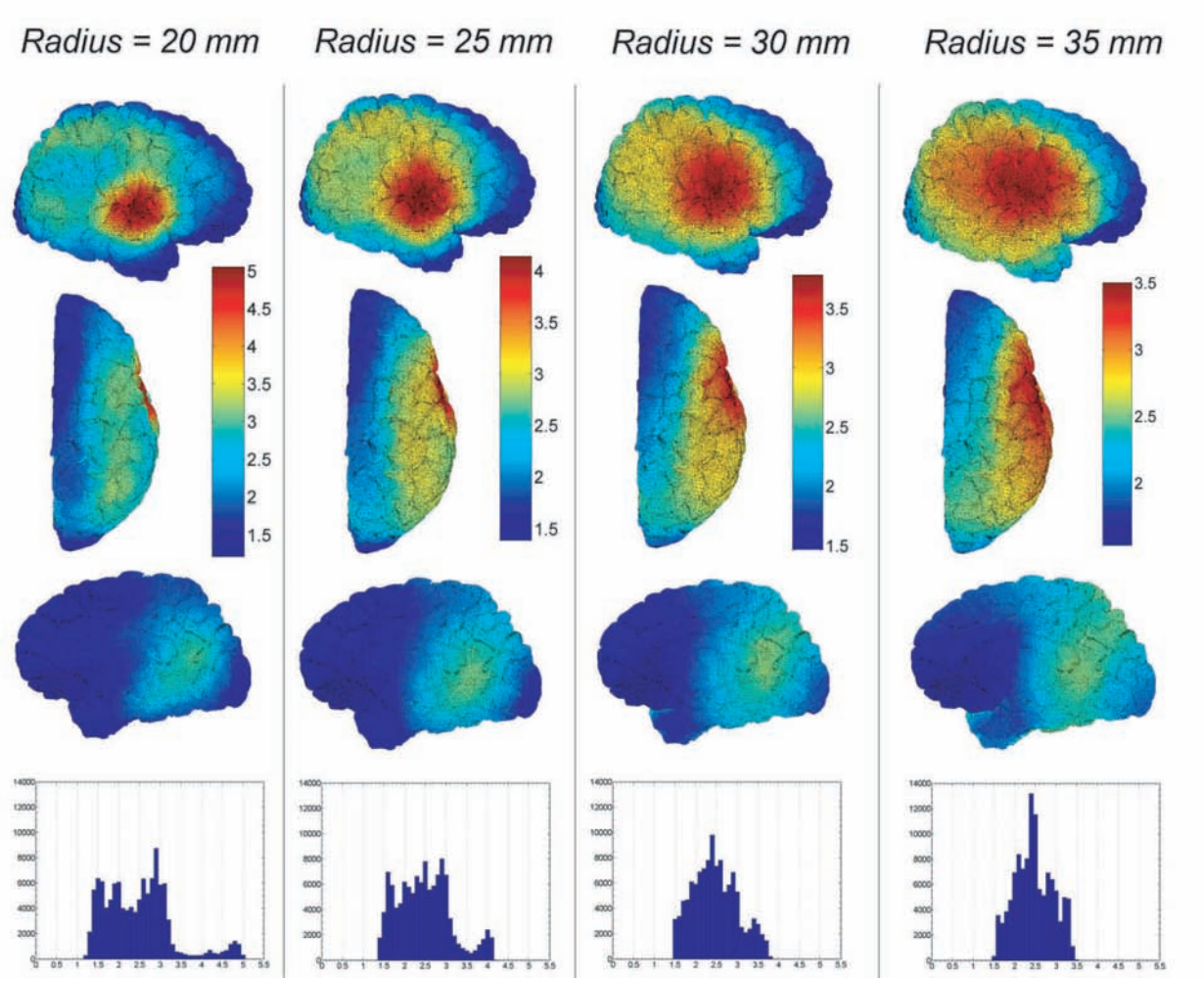

Fig. 4. Example of color overlays of *l*GI, using a radius of 20, 25, 30, and 35 mm. For each radius, lateral, dorsal, and medial views of the right hemisphere are presented, along with their corresponding scale. The histograms in the bottom row display the distribution of *l*GI measurements. Using a radius of 20 mm, *l*GI values range from 1.2 and 5.1, whereas increasing the radius narrows the range of *l*GI values (for 35 mm: 1.5- 3.5). On the 20-mm color-coded cortical map, maximal *l*GI measurements are observed around the sylvian fissure, the intraparietal sulcus, the superior temporal sulcus and, on the medial view, at the intersection of the parieto-occipital with calcarine sulci). Those maxima are progressively smoothed by larger radii, so that only two diffuse maxima are visible with a 35 mm radius. The histograms resulting from larger radii show a concomitant evolution toward a Gaussian distribution of *l*GI values.

and Clouchoux *et al.* [43] work on parameterization of the cortical surface. Both group's attempts at registering cortical surfaces with minimal distortion suggest an orthogonal organization schema of cortical folding patterns, with the main sulci oriented in longitudinal and latitudinal directions around the insular pole and the central sulcus. Therefore, it is of developmental interest that cortical *l*GI maps using a large radius also demonstrate convergence in the sylvian fissure. Given that our method aims to delineate local anomalies in gyrification, we use a more contrasted *l*GI distribution for subsequent clinical analysis (a radius of 20 or 25 mm).

III. Clinical Application

22q11 Deletion syndrome (22q11DS) is a neurogenetic condition affecting one per 5000 live births [44]. Typical symptoms include physical anomalies [44], [45], cognitive impairment [46], and psychiatric symptoms [46], [47]. Specifically, one-third of individuals affected will develop schizophrenia [47], [48], and 22q11DS is therefore considered as a genetic model for schizophrenia [49]. Cortical anomalies are thought to be key in the cognitive and psychiatric phenotype, as decreased cortical volume is classically observed [50], [51]. Clinical observations reported severe cases of polymicrogyria mainly restricted to the frontal, parietal, and perisylvian regions [52]- [57], providing evidence that cortical morphology is altered in the syndrome. To complement these qualitative observations, we previously conducted a quantitative analysis [14], using an automated algorithm for measuring the classical 2-D Gyrification Index [15]. In this earlier study, we identified decreased gyrification in the frontal and the parietal lobes of 37 patients with 22q11DS compared to 36 control subjects. We also observed that decreased Gyrification Index manifests with smaller gyri and shallower sulci in the patients' brain, so that reduced GI in 22q11DS may represent a mild cortical malfor-

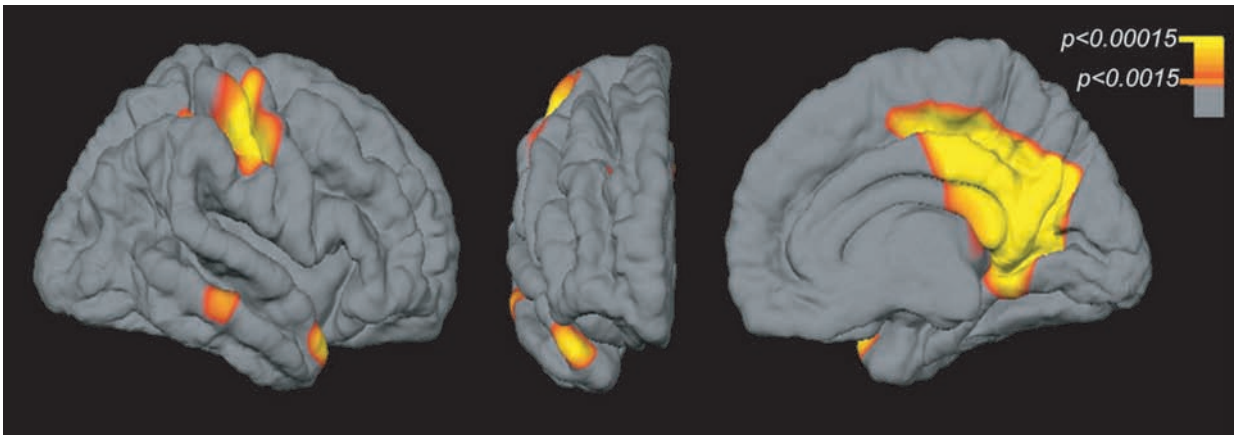

Fig. 5. Statistical differences in the *l*GI values between patients and control subjects (lateral, frontal, and medial views of the average cortical surface). The regions showing significantly decreased *l*GI in patients with 22q11DS compared with normal controls are highlighted (colorbar: *p* value). Increased *l*GI in patients compared with controls is not observed in any of the cortical regions.

mation in a continuum toward the polymicrogyric appearance of the cortex reported in the most severely affected patients.

In the present study, we aimed at conducting a clinical validation of our new method in a syndrome where abnormal gyrification has been qualitatively and quantitatively reported. Measuring gyrification at thousands of points over the whole hemisphere, we postulate that *l*GI will provide a more precise localization of the gyral anomalies in the brain of patients affected by 22q11 Deletion Syndrome.

A. Subjects and Imaging

As a preliminary study intended to test the *l*GI method, the analysis is restricted to the right hemisphere on a small sample of individuals only. Also, in order to avoid potential confounding effects, we selected stringently our groups with regards to age and gender. The control group consisted of 12 typically developing girls with no history of neurological or psychiatric disorders and with an average age of 10.0 ± 2.0 years old, and a mean IQ of 113. The patient group comprised 12 girls affected by 22q11 Deletion Syndrome, with an average age of 9.8 ± 2.0, and a mean IQ of 74. Written informed consent was received from all the parents of the subjects, in accordance with protocols approved by the Institutional Review Board of University of Geneva.

Cerebral T1-weighted MRIs were obtained using a Philips Intera 1.5 T scanner. Coronal images were acquired with a 3-D volumetric pulse sequence using the following scan parameters: $\mathrm{TR} = 35$ ms, $\mathrm{TE} = 6$ ms, $\mathrm{flip\ angle} = 458, \mathrm{NEX} = 1$, $\mathrm{matrix\ size} = 256 \times 192, \mathrm{field\ of\ view} = 24\ \mathrm{cm}^2$, $\mathrm{slice\ thickness} = 1.5$ mm, 124 slices. Cortical mesh models and local Gyrification Index at each vertex of the reconstructed surface were obtained according to the procedures described above. For *l*GI calculations, we used a sphere radius of 25 mm.

B. Statistical Analysis

In order to compare the local value of the Gyrification Index obtained for each individual, the cortical surface was registered to an average spherical surface representation that optimally align sulcal and gyral features across subjects [38], [40]. A study-specific template was created averaging the surfaces from the right hemisphere of the 24 subjects from our sample [40]. Data were then resampled for each participant into the common average spherical coordinate system aligning cortical folding patterns [38], [40]. Smoothing of the data on the mesh employed an iterative nearest-neighbor averaging procedure with full-width at half-maximum (FWHM) of 10 mm. Statistical *l*GI difference maps were created computing a general linear model to assess the effect of diagnosis on the local GI value at each vertex. Due to the severely restricted age range, age was not included as a variable in the general linear model. Correction for multiple comparison was done using a false discovery rate of 0.01 to set the significance threshold, corresponding to an uncorrected $p = 0.0015$ in our sample [58].

C. Results

Fig. 5 shows the statistical comparison of the *l*GI in the right hemisphere between 12 girls affected by 22q11 Deletion Syndrome and 12 typically developing girls. We observe a significant *l*GI decrease in the parietal region of the 22q11DS affected patients, with a large cluster extending from the posterior cingulate into the precuneus ($p < 0.00018$) on the medial aspect of the hemisphere, and a cluster around the postcentral sulcus ($p < 0.001$) on the lateral aspect. We also observe another cluster in the temporal lobe, around the medial and superior temporal sulci ($p < 0.001$). There is no region of increased *l*GI in 22q11DS individuals compared to control subjects.

Fig. 6 provides a comparison between the average value of *l*GI and the classical 2-D GI for all vertices over the right hemisphere. Mean 2-D-GI values for the right hemisphere are consistent with our previous study on a larger sample of individuals with 22q11DS [14], no significant differences observed between groups ($p = 0.380$). Perimeters measurements on coronal sections are sensitive to slice orientation [59] or may be biased by the difficulty to include buried sulci, resulting in a large variance in whole-hemisphere 2-D-GI measurements. Due to their

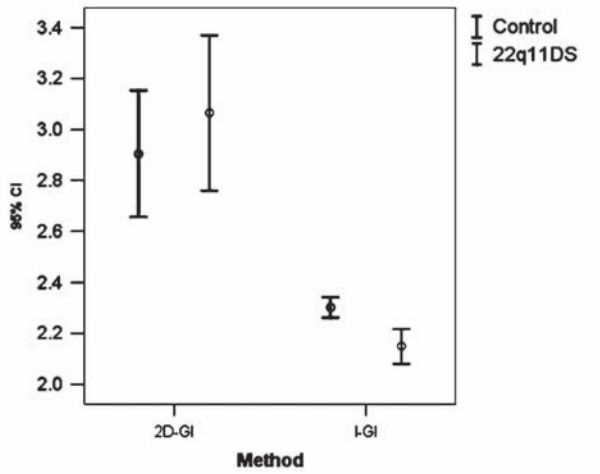

Fig. 6. Plots showing mean and standard deviation of right hemisphere lGI values and classical 2-D-GI measurements in each group. The 2-D-GI values resulting from the semi-automated method, as measured in [14], show a large standard deviation, with average 2-D-GI appearing even higher in patients with 22q11DS than controls. This difference is far from significant ($F_{1,23} = 0.803, p = 0.380$), as demonstrated by the overlapping confidence intervals. By contrast, despite the small sample size, 3-D GI detects a difference between the groups, showing reduced average lGI in patients compared to controls ($F_{1,23} = 11.776, p = 0.002$).

large standard deviations, classical 2-D approaches for measuring Gyrification Index may not be appropriate for delineating group differences. However, the use of accurate 3-D cortical reconstruction drastically reduces the variance in these measurements, and we observe a significantly smaller average lGI value in the right hemisphere of patients compared to controls ($p = 0.002$).

IV. Discussion

A. Clinical Results

The aim of the clinical study was to test the behavior of our local Gyrification Index on patients affected by 22q11 Deletion Syndrome. Radiologists reported several cases of polymicrogyria in the syndrome, affecting particularly the parietal, perisylvian, and frontal regions. The only quantitative study to date [14] uses automated delineations of contours on coronal sections [15]. In this study, we previously found a decreased Gyrification Index in the frontal and parietal lobes of patients as compared to those with normal development. Despite the small sample size of the current study, the present results using lGI are able to replicate previous qualitative and quantitative observations of decreased cortical complexity. Further, our method provides a finer topological localization of the anomalies, previously observed in the whole right frontal and parietal lobes. Specifically, we find decreased gyrification in the parietal lobe in two constricted regions: on the medial face of the parietal lobe, and around the postcentral gyrus on the lateral face (see Fig. 5). Also, we observe decreased lGI in the medial third of the temporal lobe, which was missed by 2-D algorithm. In the frontal lobe, we, however, do not replicate our previous finding of decreased cortical complexity in this small sample of young girls with 22q11 Deletion syndrome. The latter discrepancy may be related to differences in age, gender or sample size between the two studies.

Although the present study was intended as a proof-of-concept on a restricted sample of individuals, these preliminary results further define the pattern of cortical malformations associated with 22q11DS syndrome. Replication of the analyses on both hemispheres in a more diversified sample of patients will certainly help in the understanding of the biological basis associated with the cognitive and psychiatric phenotype of affected individuals.

B. Methods Measuring Cortical Complexity

Apart from the classical GI, many different approaches have been described to study the interindividual variability in sulcal patterns. We offer a brief overview of the most frequently used in clinical studies, from the most global to the more localized approaches, and consider elements of comparison between these methods and lGI.

Fractal dimension (FD) has been proposed to provide global measurements of the cortical complexity based on a 3-D parametric mesh [60] or on a skeletonized binary volume [61]. Fractal dimension condenses information about the irregularity in the cortical shape over the whole hemisphere [7], [61], or in lobar regions [4], [13], [62]. FD is a compact measure that has been widely used to assess normal and abnormal brain development [7], [61], [63]-[65]. However, as recently discussed in [66], concrete geometrical interpretation of fractal dimension remains challenging. Compared to FD, lGI is also able to condense information about the frequency and depth of sulci, but is easier to interprete. lGI quantifies the proportion of cortical area which is buried within the sulci in a given area, and therefore directly depends upon the amount and size of the sulci.

Other methods for assessing sulcal depth [17], [67], length [67], width [17], or asymmetry index [5] are grouped under the heading of sulcal morphometry. Sulci are classically identified with automated procedures using a congregation of neural networks [68]. Compared to sulcal morphometry, lGI also reflects the sulcal conformation, but in a circular approach. Sulcal morphometry is based on the interesting idea that sulcal configuration can convey information about the early development of cortex. Analyses of sulcal pattern reveal the existence of "plis de passage," which are reminiscent of the first folds [69]. As the cortex grows primarily by radial expansion [32], we postulate that lGI is also able to reflect early cortical development, but in a different manner. Indeed, lGI quantifies the excess or defect in cortical expansion in specific regions over the whole hemisphere.

More recently, a curvature-based approach has been proposed for estimating local gyrification at thousands of points over the entire cortical surface [6], [70]. Smoothed absolute mean curvature quantifies the amount of local curvature on spherically-parameterized cortical mesh models. Among all the measurements of cortical complexity, smoothed absolute mean curvature is the closest to our algorithm. However, the essence of both measures differs, as can be illustrated using notions of differential geometry. Differential geometry is defined with respect to surfaces with zero-thickness, and thus may not

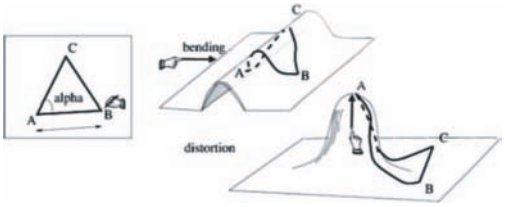

Fig. 7. Illustration of extrinsic and intrinsic properties of a surface using differential geometry. Extrinsic curvature refers to folding which is created with no distortion, as a sheet of paper that we can crumple. As illustrated by the triangle drawn on the left sheet, distances on the surface are not altered by bending; in other terms, extrinsic properties of a surface are not directly related to its area. Extrinsic curvature is measured mathematically using mean curvature, and directly characterizes the geometrical configuration of the surface in space. Intrinsic curvature denotes folding that has been created by distortion, or shearing, and is best understood using an example: folding a spherical surface without modifying its area is impossible. The figure on the right shows how the distortion of a sheet alters distances on its surface. Gaussian curvature measures the intrinsic curvature of a surface, in the sense that it captures the excess or deficit in the surface as compared to a plane at the point. (Adapted from [30]).

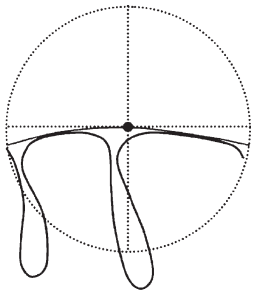

Fig. 8. Schematic 2-D illustration of the variation in the area of the outer region of interest ROI_O. As the outer surface is not perfectly planar, the area delineated through the intersection of the outer surface (in light gray) with a sphere centered at v_i (gray point) of radius r is larger than the area of a circle having the same radius r. This results in slight variations in the area of the outer region of interest. However, we assume that these variations are negligible as compared to the area of the pial region of interest (in dark gray).

always be appropriate to characterize the cortical shape. However, differential geometry has been widely used to understand more fully and characterize measures of cortical shape (see [30], [71]- [73]). Mathematically, differential geometry allows the distinction of two kinds of curvature: extrinsic or mean curvature, and intrinsic or Gaussian curvature (see Fig. 7). Smoothed absolute mean curvature [70] is characteristically an extrinsic measurement, highly dependent upon surface configuration. Gaussian curvature quantifies the excess of deficit in area as compared to a plane in the nearest neighborhood on each point of the surface. *l*GI resembles Gaussian curvature, but covers a wider area of 50 mm diameter. *l*GI would be an alternative surface-based measure of Gaussian curvature only if the ROI_P perimeter exactly superposes the ROI_O contour, but, nevertheless, the ratio *l*GI provides similar information. Thus, the mathematics of curvature illustrates that smoothed absolute mean curvature and *l*GI capture different properties of the cortical geometry smoothed absolute curvature typically measures the shape of the cortical surface, whereas *l*GI conveys information about the underlying cortical area. Therefore, we postulate that *l*GI reflects easily interpretable biological correlates, such as cortical volume, or neuronal number. It is however important to note that intrinsic and extrinsic properties of a surface may be hardly distinguishable for highly convoluted surfaces, so that smoothed absolute curvature and *l*GI may be geometrically related in some way which is difficult to *a priori* infer. Recently, inspired by smoothed absolute curvature method, other curvature-based descriptors were proposed to characterize more precisely local shape and size of cortical complexity [74]. Future work will certainly be needed to propose an integrative interpretation of the increasing variety of cortical complexity measures, toward a better understanding of normal gyral conformation and a clear etiopathogenic approach of cortical malformations.

A last divergence between curvature-based methods and *l*GI resides in the preprocessing of the images. To date, curvature-based approaches typically used affine transformation of the brain volume into the standard space of the International Consortium for Brain Mapping-305 (ICBM-305) average brain [75] prior to cortical mesh models reconstruction [6], [70], [74], which may affect curvature measurements. In the current study, all the *l*GI measurements were computed on cortical surfaces based on images in their native space. Independently of intersubject registration, the absence spatial normalization ensures that the observed differences are due to a real decrease in cortical area (related to diminished frequency and depth of sulci) rather than to an effect of scaling.

V. Limitations of the Present Study

In the present study, we have proposed a new method for quantifying local gyrification, and promising results were shown. There are, however, some limitations in our approach. One limitation in our implementation of the *l*GI is that the surface ratio is not measured on exactly the same outer area for each vertex. This means that we measure the amount of invaginated cortical surface in a slightly varying perimeter. In the present study, the ROI_O is obtained with the intersection of the outer surface with a sphere. As the outer surface is not planar, the resulting ROI_O area is not of exactly $\pi \cdot r^2$ (Fig. 8). Specifically, in regions of high curvature of the outer surface, such as those near to the superior sagittal sinus, the area of the ROI_O is larger. We tested the impact of such variations on two subjects in the study. We found a standard deviation of less than 7.5% of the mean ROI_O area value for all the vertices of the hemisphere. This corresponds to a circular region on the outer surface having a mean radius of 28.8 mm (instead of the 25 mm of our sphere), with the minimum found at 26.4 mm and the maximum at 32.2 mm. In comparison, the standard deviation for the pial region of interest is of 31.5% of the mean ROI_P area (corresponding to planar circular regions from 29 mm radius to 64.5 mm); we therefore assume that the slight variation in the ROI_O areas is negligible compared to the differences between the ROI_O and ROI_P areas.

The proposed approach requires a high amount of time to compute the *l*GI evaluation for all the vertices. To compute each ROI_P perimeter, we first use the "Dijkstra" algorithm[1] to find the shortest geodesic path between the selected vertices. Then, the whole ROI_P enclosed by the perimeter is found using neighborhood information. Both perimeter delineation and

ROI_P reconstruction are time consuming, but robust. Furthermore, our code is implemented in MATLAB, which is probably not the most suitable for computing so many loops. However, the present manuscript is intended to present a feasibility study, and future developments will include an optimization for the speeding-up of the computational process.

VI. Conclusion

In this paper, we presented a new method for quantifying the Gyrification Index with a fine topological resolution over the whole hemisphere. Using validated procedures for accurate cortical reconstructions, we first implemented an outer surface closely enveloping the hemisphere. Then, we proposed a new algorithm for measuring a local Gyrification Index at each vertex of the entire cortical surface. The outcome of our method suggests that the decreased cortical complexity reported in 22q11 Deletion Syndrome may be powered by restricted regions of abnormal cortical expansion mostly located in the parietal lobe and on the medial surface of the hemisphere.

Acknowledgment

The authors would like to thank J. van Oosterom for proofreading the manuscript and J.-F. Mangin for helpful comments on parameterization of the cortical surface.

References

[1] J. F. Mangin, D. Riviere, A. Cachia, D. Papadopoulos-Orfanos, D. L. Collins, A. C. Evans, and J. Regis, "Object-based strategy for morphometry of the cerebral cortex," *Inf. Process. Med. Imag.*, vol. 18, pp. 160-171, 2003.

[2] P. M. Thompson, J. Moussai, S. Zohoori, A. Goldkorn, A. A. Khan, M. S. Mega, G. W. Small, J. L. Cummings, and A. W. Toga, "Cortical variability and asymmetry in normal aging and alzheimer's disease," *Cereb. Cortex*, vol. 8, no. 6, pp. 492-509, 1998.

[3] E. Armstrong, A. Schleicher, H. Omran, M. Curtis, and K. Zilles, "The ontogeny of human gyrification," *Cereb. Cortex*, vol. 5, pp. 56-63, 1995.

[4] R. E. Blanton, J. G. Levitt, P. M. Thompson, K. L. Narr, L. Capetillo-Cunliffe, A. Nobel, J. D. Singerman, J. T. McCracken, and A. W. Toga, "Mapping cortical asymmetry and complexity patterns in normal children," *Psych. Res.: Neuroimag.*, vol. 107, pp. 29-43, 2001.

[5] J. F. Mangin, D. Riviere, A. Cachia, E. Duchesnay, Y. Cointepas, D. Papadopoulos-Orfanos, P. Scifo, T. Ochiai, F. Brunelle, and J. Regis, "A framework to study the cortical folding patterns," *Neuroimage*, vol. 23, pp. 129-138, 2004.

[6] C. Gaser, E. Luders, P. M. Thompson, A. D. Lee, R. A. Dutton, J. A. Geaga, K. M. Hayashi, U. Bellugi, A. M. Galaburda, J. R. Korenberg, D. L. Mills, A. W. Toga, and A. L. Reiss, "Increased local gyrification mapped in williams syndrome," *Neuroimage*, vol. 33, pp. 46-54, 2006.

[7] T. H. Ha, U. Yoon, K. J. Lee, Y. W. Shin, J. M. Lee, I. Y. Kim, K. S. Ha, S. I. Kim, and J. S. Kwon, "Fractal dimension of cerebral cortical surface in schizophrenia and obsessive-compulsive disorder," *Neurosci. Lett.*, vol. 384, pp. 172-176, 2005.

[8] A. Y. Hardan, R. J. Jou, M. S. Keshavan, R. Varma, and N. J. Minshew, "Increased frontal cortical folding in autism: A preliminary MRI study," *Psychiatry Res.*, vol. 131, pp. 263-268, 2004.

[9] J. M. Harris, H. Whalley, S. Yates, P. Miller, E. C. Johnstone, and S. M. Lawrie, "Abnormal cortical folding in high-risk individuals: A predictor of the development of schizophrenia?," *Biol. Psychiatry*, vol. 56, pp. 182-189, 2004.

[10] J. M. Harris, S. Yates, P. Miller, J. J. Best, E. C. Johnstone, and S. M. Lawrie, "Gyrification in first-episode schizophrenia: A morphometric study," *Biol. Psychiatry*, vol. 55, pp. 141-147, 2004.

[11] R. J. Jou, A. Y. Hardan, and M. S. Keshavan, "Reduced cortical folding in individuals at high risk for schizophrenia: A pilot study," *Schizophr. Res.*, vol. 75, pp. 309-313, 2005.

[12] J. J. Kulynych, L. F. Luevano, D. W. Jones, and D. R. Weinberger, "Cortical abnormality in schizophrenia: An in vivo application of the gyrification index," *Biol. Psychiatry*, vol. 41, no. 10, pp. 995-999, May. 15, 1997.

[13] K. L. Narr, R. M. Bilder, S. Kim, P. M. Thompson, P. Szeszko, D. Robinson, E. Luders, and A. W. Toga, "Abnormal gyral complexity in first-episode schizophrenia," *Biol. Psychiatry*, vol. 55, pp. 859-867, 2004.

[14] M. Schaer, J. E. Schmitt, B. Glaser, F. Lazeyras, J. Delavelle, and S. Eliez, "Abnormal patterns of cortical gyrification in velo-cardio-facial syndrome (deletion 22q11.2): An MRI study," *Psychiatry Res.*, vol. 146, pp. 1-11, 2006.

[15] J. E. Schmitt, K. Watts, S. Eliez, U. Bellugi, A. M. Galaburda, and A. L. Reiss, "Increased gyrification in williams syndrome: Evidence using 3-D MRI methods," *Dev. Med. Child. Neurol.*, vol. 44, pp. 292-295, 2002.

[16] K. Vogeley, T. Schneider-Axmann, U. Pfeiffer, R. Tepest, T. A. Bayer, B. Bogerts, W. G. Honer, and P. Falkai, "Disturbed gyrification of the prefrontal region in male schizophrenic patients: A morphometric postmortem study," *Am. J. Psychiatry*, vol. 157, pp. 34-39, 2000.

[17] P. Kochunov, J. F. Mangin, T. Coyle, J. Lancaster, P. Thompson, D. Riviere, Y. Cointepas, J. Regis, A. Schlosser, D. R. Royall, K. Zilles, J. Mazziotta, A. Toga, and P. T. Fox, "Age-related morphology trends of cortical sulci," *Human Brain Mapp.*, vol. 26, pp. 210-220, 2005.

[18] V. A. Magnotta, N. C. Andreasen, S. K. Schultz, G. Harris, T. Cizadlo, D. Heckel, P. Nopoulos, and M. Flaum, "Quantitative in vivo measurement of gyrification in the human brain: Changes associated with aging," *Cereb. Cortex*, vol. 9, no. 2, pp. 151-160, 1999.

[19] D. P. Richman, R. M. Stewart, J. W. Hutchinson, and V. S. Caviness, Jr., "Mechanical model of brain convolutional development," *Science*, vol. 189, pp. 18-21, 1975.

[20] D. C. Van Essen, "A tension-based theory of morphogenesis and compact wiring in the central nervous system," *Nature*, vol. 385, pp. 313-318, 1997.

[21] H. Haug, "Brain sizes, surfaces, and neuronal sizes of the cortex cerebri: A stereological investigation of man and his variability and a comparison with some mammals (primates, whales, marsupials, insectivores, and one elephant)," *Am. J. Anat.*, vol. 180, pp. 126-142, 1987.

[22] H. J. Jerison, "Quantitative analysis of evolution of the brain in mammals," *Science*, vol. 133, pp. 1012-1014, 1961.

[23] K. Zilles, E. Armstrong, A. Schleicher, and H. J. Kretschmann, "The human pattern of gyrification in the cerebral cortex," *Anat. Embryol.*, vol. 179, pp. 173-179, 1988.

[24] P. C. Sallet, H. Elkis, T. M. Alves, J. R. Oliveira, E. Sassi, C. C. de Castro, G. F. Busatto, and W. F. Gattaz, "Reduced cortical folding in schizophrenia: An MRI morphometric study," *Am. J. Psychiatry*, vol. 160, pp. 1606-1613, 2003.

[25] K. Vogeley, R. Tepest, U. Pfeiffer, T. Schneider-Axmann, W. Maier, W. G. Honer, and P. Falkai, "Right frontal hypergyria differentiation in affected and unaffected siblings from families multiply affected with schizophrenia: A morphometric MRI study," *Am. J. Psychiatry*, vol. 158, pp. 494-496, 2001.

[26] S. R. Kesler, B. Vohr, K. C. Schneider, K. H. Katz, R. W. Makuch, A. L. Reiss, and L. R. Ment, "Increased temporal lobe gyrification in preterm children," *Neuropsychologia*, vol. 44, pp. 445-453, 2006.

[27] T. W. Moorhead, J. M. Harris, A. C. Stanfield, D. E. Job, J. J. Best, E. C. Johnstone, and S. M. Lawrie, "Automated computation of the gyrification index in prefrontal lobes: Methods and comparison with manual implementation," *Neuroimage*, vol. 31, pp. 1560-1566, 2006.

[28] A. M. Dale, B. Fischl, and M. I. Sereno, "Cortical surface-based analysis I. segmentation and surface reconstruction," *Neuroimage*, vol. 9, pp.179-194, 1999.

[29] D. C. van Essen, J. Dickson, J. Harwell, D. Hanlon, C. H. Anderson, and H. A. Drury, "An integrated software system for surface-based analyses of cerebral cortex," *J. Amer. Med. Info. Assoc.*, vol. 8, pp. 443-459, 2001.

[30] P. G. Batchelor, A. D. C. Smith, D. L. Hill, D. J. Hawkes, T. C. Cox, and A. F. Dean, "Measures of folding applied to the development of the human fetal brain," *IEEE Trans. Med. Imag.*, vol. 21, no. 8, pp. 953-965, 2002.

[31] M. E. Rettmann, M. A. Kraut, J. L. Prince, and S. M. Resnick, "Cross-sectional and longitudinal analyses of anatomical sulcal changes associated with aging," *Cereb. Cortex*, vol. 16, pp. 1584-1594, 2006.
[32] P. Rakic, "Radial unit hypothesis of neocortical expansion," in *Novartis Found Symp.*, 2000, vol. 228, pp. 30-42.
[33] R. J. Shprintzen, "Velocardiofacial syndrome and digeorge sequence," *J. Med. Genet.*, vol. 31, pp. 423-424, 1994.
[34] A. J. Barkovich, H. Rowley, and A. Bollen, "Correlation of prenatal events with the development of polymicrogyria," *AJNR Am. J. Neuroradiol.*, vol. 16, pp. 822-827, 1995.
[35] C. Y. Kao, M. Hofer, G. Sapiro, K. Rehm, J. Stern, and D. Rottenberg, "A geometric method for automatic extraction of sulcal fundi," *IEEE Trans. Med. Imag.*, vol. 26, no. 4, pp. 530-540, 2007.
[36] C. Y. Kao, M. Hofer, G. Sapiro, J. Stern, and D. Rottenberg, "A geometric method for automatic extraction of sulcal fundi," in *3rd IEEE Int. Symp. Biomed. Imag.: Macro Nano*, Arlington, VA, 2006.
[37] B. Fischl, D. H. Salat, E. Busa, M. Albert, M. Dieterich, C. Haselgrove, A. van der Kouwe, R. Killiany, D. Kennedy, S. Klaveness, A. Montillo, N. Makris, B. Rosen, and A. M. Dale, "Whole brain segmentationautomated labeling of neuroanatomical structures in the human brain," *Neuron*, vol. 33, no. 3, pp. 341-355, 2002.
[38] B. Fischl, M. I. Sereno, and A. M. Dale, "Cortical surface-based analysis II: Inflation, flattening, and a surface-based coordinate system," *Neuroimage*, vol. 9, no. 2, pp. 195-207, 1999.
[39] B. Fischl, A. Liu, and A. M. Dale, "Automated manifold surgery: Constructing geometrically accurate and topologically correct models of the human cerebral cortex," *IEEE Trans. Med. Imag.*, vol. 20, no. 1, pp. 70-80, 2001.
[40] B. Fischl, M. I. Sereno, R. B. Tootell, and A. M. Dale, "High-resolution intersubject averaging and a coordinate system for the cortical surface," *Hum. Brain Mapp.*, vol. 8, no. 4, pp. 272-284, 1999.
[41] C. Garel, E. Chantrel, H. Brisse, M. Elmaleh, D. Luton, J. F. Oury, G. Sebag, and M. Hassan, "Fetal cerebral cortex: Normal gestational landmarks identified using prenatal MR imaging," *AJNR Am. J. Neuroradiol.*, vol. 22, pp. 184-189, 2001.
[42] R. Toro and Y. Burnod, "Geometric atlas: Modeling the cortex as an organized surface," *Neuroimage*, vol. 20, pp. 1468-1484, 2003.
[43] C. Clouchoux, O. Coulon, D. Riviere, A. Cachia, J. F. Mangin, and J. Regis, "Anatomically constrained surface parameterization for cortical localization," in *Med. Image Comput. Comput. Assist. Interv. Proc.*, 2005, pp. 344-351.
[44] R. J. Shprintzen, A. M. Higgins, K. Antshel, W. Fremont, N. Roizen, and W. Kates, "Velo-cardio-facial syndrome," *Curr. Opin. Pediatr.*, vol. 17, pp. 725-730, 2005.
[45] R. Goldberg, B. Motzkin, R. Marion, P. J. Scambler, and R. J. Shprintzen, "Velo-cardio-facial syndrome: A review of 120 patients," *Am. J. Med. Genet.*, vol. 45, pp. 313-319, 1993.
[46] A. Swillen, L. Vandeputte, J. Cracco, B. Maes, P. Ghesquiere, K. Devriendt, and J. P. Fryns, "Neuropsychological, learning and psychosocial profile of primary school aged children with the velo-cardio-facial syndrome (22q11 deletion): Evidence for a nonverbal learning disability?," *Child Neuropsychol.*, vol. 5, pp. 230-241, 1999.
[47] D. Gothelf, G. Presburger, A. H. Zohar, M. Burg, A. Nahmani, M. Frydman, M. Shohat, D. Inbar, A. Aviram-Goldring, J. Yeshaya, T. Steinberg, Y. Finkelstein, A. Frisch, A. Weizman, and A. Apter, "Obsessive-compulsive disorder in patients with velocardiofacial (22q11 deletion) syndrome," *Am. J. Med. Genet. B. Neuropsychiatr. Genet.*, vol. 126, pp. 99-105, 2004.
[48] A. S. Bassett, K. Hodgkinson, E. W. Chow, S. Correia, L. E. Scutt, and R. Weksberg, "22q11 deletion syndrome in adults with schizophrenia," *Am. J. Med. Genet.*, vol. 81, pp. 328-337, 1998.
[49] K. C. Murphy and M. J. Owen, "Velo-cardio-facial syndrome: A model for understanding the genetics and pathogenesis of schizophrenia," *Br. J. Psychiatry*, vol. 179, pp. 397-402, 2001.
[50] S. Eliez, S. E. Antonarakis, M. A. Morris, S. P. Dahoun, and A. L. Reiss, "Parental origin of the deletion 22q11.2 and brain development in velocardiofacial syndrome: A preliminary study," *Arch. Gen. Psychiatry*, vol. 58, pp. 64-68, 2001.
[51] T. J. Simon, L. Ding, J. P. Bish, D. M. McDonald-McGinn, E. H. Zackai, and J. Gee, "Volumetric, connective and morphologic changes in the brains of children with chromosome 22q11.2 deletion syndrome: An integrative study," *Neuroimage*, vol. 25, no. 1, pp. 169 180, Mar. 2005.
[52] P. M. Bingham, D. Lynch, D. McDonald-McGinn, and E. Zackai, "Polymicrogyria in chromosome 22 delection syndrome," *Neurology*, vol. 51, pp. 1500-1502, 1998.
[53] H. Ehara, Y. Maegaki, and K. Takeshita, "Pachygyria and polymicrogyria in 22q11 deletion syndrome," *Am. J. Med. Genet. A*, vol. 117, pp. 80-82, 2003.
[54] S. Ghariani, K. Dahan, C. Saint-Martin, H. Kadhim, F. Morsomme, S. Moniotte, C. Verellen-Dumoulin, and G. Sebire, "Polymicrogyria in chromosome 22q11 deletion syndrome," *Eur. J. Paediatr. Neurol.*, vol. 6, pp. 73-77, 2002.
[55] H. Kawame, K. Kurosawa, A. Akatsuka, Y. Ochiai, and K. Mizuno, "Polymicrogyria is an uncommon manifestation in 22q11.2 deletion syndrome," *Am. J. Med. Genet.*, vol. 94, pp. 77-78, 2000.
[56] L. Sztriha, R. Guerrini, B. Harding, F. Stewart, N. Chelloug, and J. G. Johansen, "Clinical, MRI, and pathological features of polymicrogyria in chromosome 22q11 deletion syndrome," *Am. J. Med. Genet. A*, vol. 127, pp. 313-317, 2004.
[57] S. Worthington, A. Turner, J. Elber, and P. I. Andrews, "22q11 deletion and polymicrogyria - cause or coincidence?," *Clin. Dysmorphol.*, vol. 9, pp. 193-197, 2000.
[58] C. R. Genovese, N. A. Lazar, and T. Nichols, "Thresholding of statistical maps in functional neuroimaging using the false discovery rate," *Neuroimage*, vol. 15, pp. 870-878, 2002.
[59] K. Zilles, A. Schleicher, C. Langemann, K. Amunts, P. Morosan, N. Palomero-Gallagher, T. Schormann, H. Mohlberg, U. Burgel, H. Steinmetz, G. Schlaug, and E. Roland, "Quantitative analysis of sulci in the human cerebral cortex: Development, regional heterogeneity, gender difference, asymmetry, intersubject variability and cortical architecture," *Human Brain Mapp.*, vol. 5, pp. 218-221, 1997.
[60] P. M. Thompson, C. Schwartz, R. T. Lin, A. A. Khan, and A. W. Toga, "Three-dimensional statistical analysis of sulcal variability in the human brain," *J. Neurosci.*, vol. 16, pp. 4261-4274, 1996.
[61] J. M. Lee, U. Yoon, J. J. Kim, I. Y. Kim, D. S. Lee, J. S. Kwon, and S. I. Kim, "Analysis of the hemispheric asymmetry using fractal dimension of a skeletonized cerebral surface," *IEEE Trans. Biomed. Eng.*, vol. 51, pp. 1494-1498, 2004.
[62] E. Luders, K. L. Narr, P. M. Thompson, D. E. Rex, L. Jancke, H. Steinmetz, and A. W. Toga, "Gender differences in cortical complexity," *Nat. Neurosci.*, vol. 7, pp. 799-800, 2004.
[63] M. J. Cook, S. L. Free, M. R. Manford, D. R. Fish, S. D. Shorvon, and J. M. Stevens, "Fractal description of cerebral cortical patterns in frontal lobe epilepsy," *Eur. Neurol.*, vol. 35, no. 6, pp. 327-335, 1995.
[64] L. Zhang, D. Dean, J. Z. Liu, V. Sahgal, X. Wang, and G. H. Yue, "Quantifying degeneration of white matter in normal aging using fractal dimension," *Neurobiol. Aging*, 2006.
[65] L. Zhang, J. Z. Liu, D. Dean, V. Sahgal, and G. H. Yue, "A three-dimensional fractal analysis method for quantifying white matter structure in human brain," *J. Neurosci. Methods*, vol. 150, pp. 242-253, 2006.
[66] K. Im, J. M. Lee, U. Yoon, Y. W. Shin, S. B. Hong, I. Y. Kim, J. S. Kwon, and S. I. Kim, "Fractal dimension in human cortical surface: Multiple regression analysis with cortical thickness, sulcal depth, and folding area," *Human Brain Mapp.*, vol. 27, no. 12, pp. 994-1003, 2006.
[67] N. Molko, A. Cachia, D. Riviere, J. F. Mangin, M. Bruandet, D. Le Bihan, L. Cohen, and S. Dehaene, "Functional and structural alterations of the intraparietal sulcus in a developmental dyscalculia of genetic origin," *Neuron*, vol. 40, pp. 847-858, 2003.
[68] D. Riviere, J. F. Mangin, D. Papadopoulos-Orfanos, J. M. Martinez, V. Frouin, and J. Regis, "Automatic recognition of cortical sulci of the human brain using a congregation of neural networks," *Med. Image Anal.*, vol. 6, no. 2, pp. 77-92, 2002.
[69] J. Regis, J. F. Mangin, T. Ochiai, V. Frouin, D. Riviere, A. Cachia, M. Tamura, and Y. Samson, ""Sulcal root" generic model: A hypothesis to overcome the variability of the human cortex folding patterns," *Neurol. Med. Chir. (Tokyo)*, vol. 45, pp. 1-17, 2005.
[70] E. Luders, P. M. Thompson, K. L. Narr, A. W. Toga, L. Jancke, and C. Gaser, "A curvature-based approach to estimate local gyrification on the cortical surface," *Neuroimage*, vol. 29, pp. 1224-1230, 2006.
[71] L. D. Griffin, "The intrinsic geometry of the cerebral cortex," *J. Theor. Biol.*, vol. 166, pp. 261-273, 1994.
[72] P. H. Todd, "Gaussian curvature as a parameter of biological surface growth," *J. Theor. Biol.*, vol. 113, pp. 63-68, 1985.
[73] D. C. Van Essen and J. H. Maunsell, "Two-dimensional maps of the cerebral cortex," *J. Comput. Neurol.*, vol. 191, pp. 255-281, 1980.
[74] D. Tosun, A. L. Reiss, A. D. Lee, R. A. Dutton, K. M. Hayashi, U. Bellugi, A. M. Galaburda, J. R. Korenberg, D. L. Mills, A. W. Toga, and P. M. Thompson, "Use of 3-D cortical morphometry for mapping increased cortical gyrification and complexity in williams syndrome," in *Proc. IEEE Int. Symp. Biomed. Imaging (ISBI): Nano Macro*, Arlington, VA, 2006, pp. 1172-1175.
[75] J. C. Mazziotta, A. W. Toga, A. Evans, P. Fox, and J. Lancaster, "A probabilistic atlas of the human brain: Theory and rationale for its development the international consortium for brain mapping (ICBM)," *Neuroimage*, vol. 2, no. 2, pp. 89-101, 1995.

Congenital heart disease affects local gyrification in 22q11.2 deletion syndrome (22q11.2DS)*

Marie Schaer†, Bronwyn Glaser, Meritxell Bach Cuadra, Martin Debbané, Jean-Philippe Thiran, Stephan Eliez

Abstract

22q11.2 deletion syndrome (22q11.2DS) is a common genetic condition associated with cognitive and learning impairments. In the current report, we apply a three-dimensional method for quantifying gyrification at thousands of points over the cortical surface to imaging data from 44 children, adolescents and young adults with 22q11.2DS (mean age 17.2 years [SD 9.1; range: 6-37]; 17 males, 27 females) and 53 healthy participants (mean age 15.3 years [SD 8.5; range: 6-40]; 21 males, 32 females). Several clusters of reduced gyrification were observed, further substantiating the pattern of cerebral alterations presented by children with the syndrome. Comparisons within 22q11.2DS demonstrated an effect of congenital heart disease (CHD) on cortical gyrification, with reduced gyrification at the parieto-temporo-occipital junction in patients with CHD, as compared to patients without. Reductions in gyrification can resemble mild polymicrogyria, suggesting early abnormal neuronal proliferation or migration, providing support for an effect of hemodynamic factors on brain development in 22q11.2DS. The results also shed light on the pathophysiology of acquired brain injury in other populations with CHD.

*This article is currently in press, *Developmental Medicine & Child Neurology* (Mac Keith Press)

†**Corresponding author:** Marie Schaer, Service Médico-Pédagogique, 1 rue David Dufour, Case Postale 50, 1211 Geneva 8, Switzerland. E-mail: marie.schaer@medecine.unige.ch. Phone: +41 22 388 67 31 - Fax: + 41 22 388 67 69.

Affiliations: Marie Schaer is with Service Médico-Pédagogique in Geneva and with Swiss Federal Institute of Technology in Lausanne.
Bronwyn Glaser and Martin Debbané are with Service Médico-Pédagogique in Geneva.
Meritxell Bach Cuadra and Jean-Philippe Thiran are with Swiss Federal Institute of Technology in Lausanne.
Stephan Eliez is with Service Médico-Pédagogique in Geneva and with Department of Genetic Medicine and Development in Geneva

Introduction

22q11.2 deletion syndrome (22q11.2DS) is a neurogenetic disorder affecting 1 in 5000 live births[1]. Children with 22q11.2DS typically present impairment in domains such as memory and attention, as well as fine motor skills, and visuospatial abilities[2]. Previous attempts at delineating the cortical correlates responsible for cognitive deficits in children and adolescents with the syndrome have consistently identified reductions in cortical gray matter[2-4], detecting some of the regions that are most altered in the syndrome (e.g. the parietal lobe). However, volumetric alterations are a product of changes to either cortical thickness or area, the latter of which is dependent on the degree of folding. Therefore, new three-dimensional methods measuring thickness and gyrification may contribute more detailed information about the etiopathogenesis of cortical alterations.

While cortical thickness is particularly informative about the dynamics of cortical maturation[5], changes in cortical morphology may help to elucidate early developmental processes. For example, enlarged sylvian fissures in children with 22q11.2DS can result from abnormal opercular development during embryogenesis[6]. In a previous study using a 2D method, we identified reduced Gyrification Index in the frontal and parietal lobes[7], suggesting a simplified gyral pattern and decreased surface area in these regions. However, 2D methods are not optimal for quantifying complex cortical convolutions. More recently, we tested a new three-dimensional technique for the quantification and localization of cortical surfaces changes[8], improving both accuracy and overall precision.

Understanding the etiopathogenesis of cortical anomalies in 22q11.2DS also relies on the identification of factors that determine phenotypic expression. Congenital heart disease (CHD), which affects more than half of individuals with 22q11.2DS[9], may be one such factor because it is known to alter brain structure and affect neurodevelopmental outcomes

in non-syndromic children[10,11]. Previous studies of 22q11.2DS have not demonstrated an impact of cardiac defects on cerebral phenotype[4,6,12]. However, our inability to differentiate between 22q11.2DS patients with and without CHD may be due to methodological problems, such as small sample sizes and the grouping of participants with widely varying CHD. Moreover, volumetric studies can easily miss cortical changes in certain regions. To address these issues, the present study includes: 1) One of the largest samples of children, adolescents and young adults with the syndrome collected to date; 2) 22q11.2DS patients with and without CHD based on strict cardiac surgery criteria; and 3) A newly developed method, independent of regional a priori hypotheses and boundaries, to determine the extent to which CHD affects the expression of gyral anomalies in 22q11.2DS.

Materials & Methods

Participants

Forty-four (17M, 27F) children, adolescents and young adults with 22q11.2 deletion syndrome aged 6 to 37 years (mean 17.2 [SD 9.1]) were recruited through announcements to regional parent associations in Switzerland and France. The 22q11.2 deletion was confirmed in all participants. Mean full-scale IQ (FSIQ) in the 22q11.2DS group was 68.5 [SD 12.1].

The comparison group, comprised of 53 (21M, 32F) typically developing individuals aged 6 to 40 years (mean: 15.3 [SD 8.5]), was recruited through a newsletter distributed at public schools and in the Geneva community. A medical intake interview, as well as parent-report (Child Behavior Checklist in children and adolescents) and self-report (Symptoms Checklists YSR and Auto-ABCL in adolescents and adults) behavioral questionnaires were used to screen control participants. Individuals with a history of past or present neurological or psychiatric disorders were excluded. Written informed consent was received from all participants, as well as from the parents of participants younger than 18 years of age, in accordance with protocols approved by the Institutional Review Board of Geneva University School of Medicine. Mean FSIQ in controls was 111.9 [SD 13.2].

CHD in 22q11.2DS

Parents of participants were asked if their child had signs of a cardiac problem or had undergone heart surgery. In addition, medical reports, including ultrasound examinations and surgical reports, were examined. Seventeen (7M, 10F; mean age: 14.5 [SD 8.1]) of the 44 patients with 22q11.2DS were identified as having a history of major CHD (6 persons with tetralogy of Fallot, 4 with interrupted aortic arch and 7 with various septal defects commonly associated with pulmonary hypertension). All patients in the CHD sub-group had undergone palliative or reparative surgery before the age of 4, except one 6 year-old girl who was to be operated on shortly after participation. Nine other patients were excluded from the CHD analyses (mean age: 17.0 [SD 6.0]), due to unclear cardiovascular status (including one patient with retro-oesophagal subclavian artery and five patients with a history of ventricular septal defect with spontaneous closure). The no-CHD sub-group was composed of 18 patients without CHD (7M, 11F; mean age: 20.0 [SD 10.7]), all with normal cardiac ultrasounds and without history of cardiorespiratory complications at birth. Although the age difference between the CHD and no-CHD sub-groups did not reach significance (p=0.134), we controlled for age in all statistical comparisons.

FSIQ was similar in the sub-group with (67.8 [SD 12.9]) and without CHD (67.4 [SD 12.1]), but there was a non-significant trend toward lower IQ in the 6 patients with tetralogy of Fallot (FSIQ: 62.8 [SD 12.4], Age: 14.1 [SD 8.4]) as compared to the 11 with acyanotic CHD (interrupted aortic arch and septal defects combined) (FSIQ: 70.5 [SD 12.8], Age: 14.7 [SD 8.3]). Given non-significant age differences between the CHD and no-CHD groups, we subsequently divided children and adolescents (younger than 16 years) and adults to check for age-related IQ differences in the CHD groups. Exploratory IQ comparisons in patients younger than 16 years of age did not demonstrate significant differences in Full-Scale IQ (FSIQ), Verbal IQ (VIQ), or Performance IQ (PIQ) between children with and without CHD. However, the VIQ >PIQ dissociation frequently observed in 22q11.2DS[13] was seen in children with CHD. The 11 children with CHD scored, on average, 10 points higher on VIQ than PIQ, whereas the 9 children without CHD scored 4 points lower on VIQ than PIQ (Two-sample Students t-test: p=0.021, t(18)=-2.879). In patients older than 16, this IQ dissociation was no longer apparent, but adults with CHD had significantly lower VIQ (n=6, VIQ=55 [SD 2.3]) than adults without (n=9, VIQ=69.8 [SD 13.7]; two-sample Students t-test: p=0.026, t(13)=2.506).

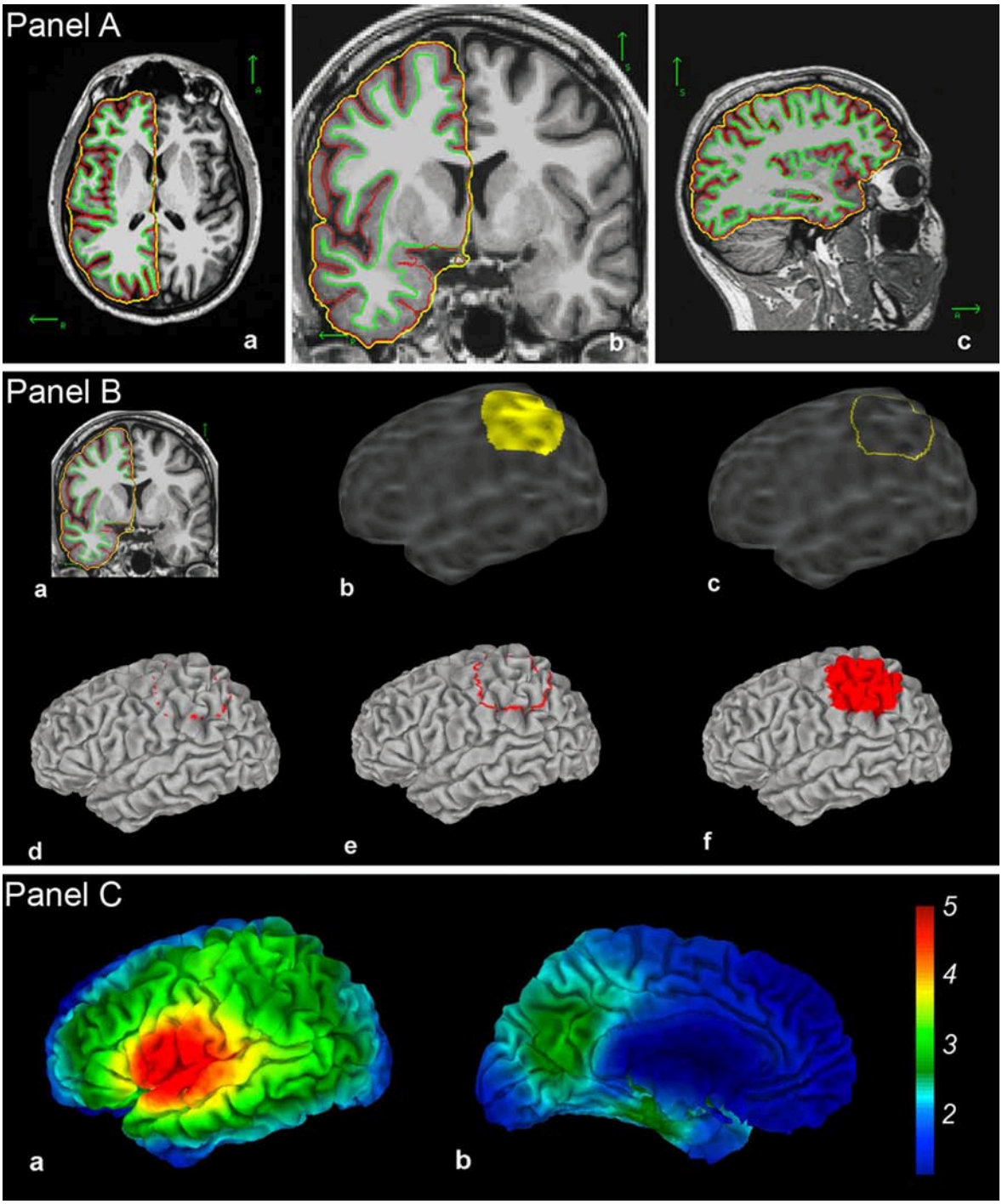

Figure 1: Local Gyrification Index (lGI) computation. *In Panel A, the white (in green) and pial (in red) cortical surfaces obtained using FreeSurfer are overlaid on axial (a), coronal (b) and sagittal (c) MRI images. The outer surface wrapping the brain is shown in yellow. Panel B shows mapping of a circular region of interest on the outer surface (ROI_O, in yellow) to a corresponding region of interest on the pial surface (ROI_P, in red). This correspondence is achieved through the transfer of a set of points from the ROI_O perimeter to the pial surface, which is then used to reconstruct the full geodesical cortical ROI_P. Panel C shows an example of an lGI-overlaid cortical map for a control participant (a: lateral, b: medial views).*

	Cluster area (mm^2)	Control	22q11DS	F
Average Right lGI		2.48 (0.12)	2.32 (0.09)	51.2
Right pre- and post-central gyri	7763.7	2.94 (0.17)	2.73 (0.12)	71.8
Right posterior cingulate gyrus	6217.8	2.31 (0.17)	1.99 (0.13)	134.0
Right orbitofrontal cortex	1972.8	1.64 (0.08)	1.54 (0.78)	39.3
Right superior temporal gyrus	1035.7	3.32 (0.27)	3.09 (0.23)	20.5
Right middle frontal gyrus	572.4	2.71 (0.20)	2.46 (0.18)	45.8
Average Left lGI		2.48 (0.13)	2.32 (0.11)	38.9
Left posterior cingulate gyrus	7921.3	2.46 (0.23)	2.15 (0.14)	68.4
Left pre- and post-central gyrus	6626.5	2.85 (0.22)	2.66 (0.15)	27.2
Left parieto-temporo-occipital junction	1229.7	2.83 (0.19)	2.64 (0.13)	29.8
Left medial frontal gyrus (rostral part)	1175.8	1.62 (0.08)	1.52 (0.99)	30.5
Left middle frontal gyrus	840.4	2.49 (0.20)	2.27 (0.16)	33.6
Left orbitofrontal cortex	594.9	2.11 (0.19)	1.96 (0.15)	15.5

Table 1: Average lGI values for significant clusters between control and 22q11.2DS groups. *Values taken from MANCOVA conducted on mean lGI per cluster, with age and gender as covariates. Significance of the overall MANCOVA was as follows:* $F_{11,83}$ *=15.3, p<0.001 (Wilks' Lambda). F values are shown for each individual cluster (all p<0.001).*

MRI acquisition & processing

Cerebral magnetic resonance images were acquired with a 3D volumetric pulse sequence using a Philips Intera 1.5T scanner. The following scan parameters were used: TR=35 msec, TE=6 msec, flip angle=45°, NEX=1, matrix size=256x192, field of view=24 cm^2, slice thickness=1.5 mm, 124 slices. Images were first imported into the software *FreeSurfer* (https://surfer.nmr.mgh.harvard.edu/) to produce precise three-dimensional representations of the cortical surfaces. A detailed description of image analysis is provided in the developers articles[14]. The white and pial surfaces were then carefully inspected, and topological defects contributing to surface inaccuracies were manually removed.

Based on the pial surface reconstruction produced in *FreeSurfer*, we developed an algorithm for measuring local 3D Gyrification Index at thousands of points across each hemisphere. This method, denoted as *l*GI, is now fully implemented in *FreeSurfer*, and thus freely available to the scientific community. Details of the *l*GI computation can be found in our validation paper[8] and in the corresponding *FreeSurfer* wiki page (https://surfer.nmr.mgh.harvard.edu/fswiki/LGI); only a brief description is presented below.

Local 3D Gyrification Index method is adapted from the classical Gyrification Index (2D-GI[15]), which is the ratio of the total pial cortical surface over the perimeter of the brain delineated on coronal sections. However, 2D-GI can present threats to accuracy, given that coronal slices do not take into account the inherent three-dimensional nature of the cortical surface. More specifically, perimeter measurements can easily become biased by slice orientation, or by the presence of buried sulci. Also, the use of two-dimensional slices does not allow for precise localization of gyral anomalies. Our method, *l*GI, addresses these issues by iteratively quantifying GI in circular three-dimensional regions of interest. After the creation of an outer envelope that tightly wraps the pial cortical surface, local measurement of circular Gyrification Index is computed for each vertex of the outer surface as the ratio of corresponding regions of interest (ROI) on the hull and pial meshes. Delineation of the regions of interest on both the outer surface (ROI_O) and pial surface (ROI_P) uses a matching algorithm based on geodesic constraints, so that the ROI_P takes into account the entire patch of cortical surface delineated by the ROI_O circular perimeter (see Figure 1). This means that at the end of the computational process, individual *l*GI cortical maps reflect the amount of cortex buried within the sulcal folds in the surrounding circular region (see Figure 1, Panel C).

Statistical Analyses

After the above-described steps, FreeSurfer was used to conduct vertex-based statistical analyses. A study-specific template was created by averaging the surfaces of the 97 participants. Individual cortical surfaces were then registered to the canonical surface, optimally aligning sulcal features across participants, and data were resampled to a common average spherical coordinate system. To increase the signal-to-noise ratio, resampled cortical maps of *l*GI values were

smoothed, using an iterative nearest-neighbor averaging procedure with the full width at a half maximum of 10 mm.

Statistical *l*GI difference maps were created by computing a general linear model (GLM) to assess the effect of diagnosis on the *l*GI value at each vertex. Gender was entered as a potential confounding factor in the GLM, and age effects were controlled by modeling the slope of *l*GI regressed on age in each sub-group ("Different Offset Different Slope design"). Corrections for multiple comparisons were done using a False Discovery Rate (FDR) of 0.01 to set the significance threshold[16]. To complement the vertex-wise maps of statistical differences, the GLM allowed for the extraction of mean *l*GI values for each cluster demonstrating significant differences; series of ANCOVA were then conducted on mean *l*GI per cluster, using age and gender as covariates. These confirmatory ANCOVA did not model a different effect of age on *l*GI in each subgroup (i.e. GLM with "same slope design").

A second GLM was then performed at each vertex to assess the effect of CHD on *l*GI distribution in the CHD vs no-CHD 22q11.2DS sub-groups, using age and gender as potential confounding factors. Similarly to the patients vs controls analysis, mean *l*GI values in clusters of significant differences between the CHD and no-CHD subgroups were extracted, and confirmed using series of ANCOVA.

Results

Patients vs controls

Average total cerebral volume was significantly smaller in patients (937.7 cm^3 [SD 112.7]) compared to controls (1062.3 cm^3 [SD 106.0]; F=31.4, p<0.001). Table 1 shows a significant reduction in average *l*GI in the patient compared to the control group. Within both the patient and control groups, *l*GI decreased significantly with age (all p<0.001, Control: R=-0.574 (left), R=-0.631 (right); 22q11.2DS: R=-0.517 (left), R=-0.510 (right)), and was significantly greater in males than females (Control: F=7.9, p=0.007 (left), F=9.8, p=0.003 (right); 22q11.2DS: F=8.3, p=0.006 (left), F=4.3, p=0.045 (right)). These between-group differences remained robustly significant when covarying for age and gender (p<0.001; $F_{3,93}$=49.0 (left), 72.2 (right)), and when covarying for age, gender and total brain volume (p<0.001; $F_{4,92}$=17.4 (left), 30.3 (right)).

Cortical maps illustrate clusters of significant reduction in the patient and control groups, after controlling for the effects of gender and age at each vertex (Left Panel in Figure 2). Mean *l*GI values in significant clusters, along with the F-tests details, are presented in Table 1.

Effect of CHD

Total cerebral volume was significantly smaller in patients with CHD (889.4 cm^3 [SD 124.0]) compared to no-CHD (979.6 cm^3 [SD 94.4] ; F=5.9, p=0.021). This reduction remained highly significant when covarying for age and gender ($F_{3,31}$=11.3, p=0.002). Subsequent analysis of the tissular compartments revealed that the reduction equally affected gray ($F_{3,31}$=9.3, p=0.005) and white matter ($F_{3,31}$=7.6, p=0.010).

Comparisons of average *l*GI values revealed a reduction in the right hemisphere of CHD patients vs. No-CHD patients (F=4.7, p=0.038) and a trend toward reduction in the left hemisphere (F=3.6, p=0.069), when covarying for age and gender. Vertex-wise analyses showed clusters of decreased *l*GI in the CHD group at the parieto-temporo-occipital (PTO) junction bilaterally, as well as smaller parietal clusters (Right Panel in Figure 2). Average *l*GI values for the corresponding clusters are presented in Table 2).

To identify whether gyral anomalies were associated with alterations to cortical thickness, we further explored differences in cortical thickness between CHD and no-CHD using two different methods. First, using vertex-by-vertex whole-brain statistical analyses, we did not observe regional differences in cortical thickness between the two sub-groups (p<0.05, uncorrected). Second, we did not observe changes in cortical thickness associated with CHD in the four regions corresponding to differences in *l*GI (see Table 2).

Finally, exploratory statistics comparing local gyrification between the 6 patients with tetralogy of Fallot and the 11 with acyanotic CHD did not reveal differences in gyral anomalies using an alpha level of p<0.05 (uncorrected). Larger samples may be needed to determine the effects of specific cardiac malformations on gyral anomalies.

Discussion

Using a method unrestricted by lobar boundaries, we observe several clusters of reduced local gyrification in 22q11.2DS. Given that the cortex grows through radial expansion[17], decreased surface area in circular regions of interest supports an early defect

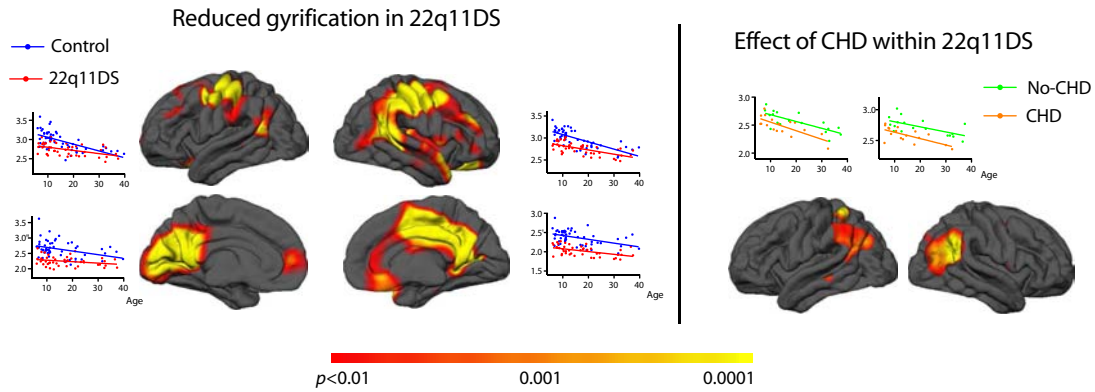

Figure 2: Statistical maps of the vertex-by-vertex lGI comparisons (colorbar: p values). *The left panel shows regions of decreased lGI in patients with 22q11.2DS compared to controls (FDR<0.01). No regions of increased lGI were observed in 22q11.2DS compared to controls. A detailed description of the clusters is provided in Table 1. The right panel illustrates reduced lGI in the CHD compared to no-CHD sub-groups (p<0.01). The cluster at the right parieto-temporo-occipital junction was more significant than the left one, and survived correction for multiple comparisons using FDR<0.05. No clusters of increased lGI value were observed in the sub-group with CHD compared to the sub-group without. Details of the mean lGI values per cluster are available in Table 2.*

of cortical expansion. This reduced surface area is likely to be additionally expressed in reduced gray matter quantity in the altered cortical regions. Indeed, bilateral *l*GI reduction in lateral (inferior parietal cortex, parieto-temporo-occipital junction, middle frontal gyrus) and medial (posterior cingulate gyrus) regions is consistent with previous volumetric studies in the syndrome[2-4].

Previous findings in 22q11.2DS

Consistent with our *l*GI findings, reduced cortical volumes in the inferior parietal lobe and supramarginal gyrus have been observed in previous studies of children and adolescents with 22q11.2DS[2-4]. In addition to structural anomalies, aberrant functional activation was also reported in these areas, such as increased activation during arithmetic reasoning in 22q11.2DS[18]. Cortical changes in the inferior parietal region are also thought to affect spatial reasoning[2], as well as complex cognitive manipulations relying on fronto-parietal connections, like working memory[19].

Our findings also point to gyrification changes in regions less frequently discussed in 22q11.2DS, such as the cingulate gyrus. The first study that analyzed cortical changes on the medial aspect of the brain using a method capable of detecting regional differences with (sub-lobar) precision, showed decreased gray matter density in the cingulate gyrus[2]. The authors suggested that reduced cingulate volume may contribute to frequently cited attentional deficits in 22q11.2DS[20], as well as impairments to patients sense of self, an awareness particularly relevant to psychotic manifestations frequently experienced by affected individuals[2]. More recently, we confirmed cingulate reduction using a region-of-interest method, and further observed a significant relationship between volumetric reduction and the occurrence of psychotic symptoms in 22q11.2DS[21]. The results presented here show reduced cortical surface area in the cingulate region, suggesting that early abnormalities in neuronal migration affecting gyrification may contribute to volumetric reductions. These cingulate reductions may, in turn, predispose individuals with 22q11.2DS to develop psychosis.

Pre- and post-central cortical areas have received less attention in 22q11.2DS, despite the fact that analogous alterations to white matter tracts have been reported[19]. We observed reduced gyrification in the primary motor and somatosensorial areas, regions largely implicated in hand and facial movements. Decreased *l*GI in those primary cortical areas supports impairments in fine motor skills (manual dexterity and grapho-motor control) frequently reported in the syndrome[22]. Likewise, oromotor control, related to the language difficulties typically associated with 22q11.2DS[5], may also be affected by the cortical anomalies.

		lGI			Thickness		
	Area (mm^2)	noCHD	CHD	Excluded	noCHD	CHD	Excluded
Left PTO	3448.2	2.72 (0.11)[a]	2.60 (0.15)[a]	2.66 (0.13)	2.674 (0.34)	2.80 (0.30)	2.70 (0.22)
Left parietal	364.6	2.59 (0.18)[b]	2.49 (0.17)[b]	2.50 (0.20)	2.32 (0.22)	2.22 (0.41)	2.09 (0.39)
Right PTO	3702.7	2.69 (0.14)[c]	2.57 (0.12)[c]	2.64 (0.12)	2.60 (0.36)	2.73 (0.33)	2.61 (0.24)
Right parietal	366.1	2.43 (0.16)[d]	2.36 (0.14)[d]	2.36 (0.16)	2.17 (0.28)	2.26 (0.23)	2.33 (0.30)

Table 2: Average lGI and cortical thickness values for clusters demonstrating significant lGI differences between the CHD and no-CHD sub-groups of 22q11.2DS patients. *Values for the sub-group of patients with unclear cardiac status are shown for information only, individualswere not included in the statistical analyses. MANCOVA for lGI values between the CHD and no-CHD was significant at $F_{4,28}=8.4$, $p<0.001$ (Wilks' Lambda). Follow-up ANCOVA per cluster were significant at $p<0.001$ with the values of [a]$F=16.2$; [b]$F=15.8$; [c]$F=27.9$; [d]$F=14.0$. To test whether differences in lGI were associated with change to cortical thickness, MANCOVA was conducted to compare mean cortical thickness values per cluster between CHD and no-CHD, while covarying for gender and age. MANCOVA comparing mean lGI values per cluster was highly significant, while MANCOVA comparing mean cortical thickness values for each cluster demonstrated no difference in thickness between sub-groups (Wilks' Lambda : $F_{4,28}=1.1$, $p=0.384$)*

Underlying etiopathogenesis

Defects in cortical expansion, as demonstrated by *l*GI reduction in 22q11.2DS, point toward early abnormalities in control over neuronal migration or proliferation. It would be tempting to think of medial changes in *l*GI as yet another midline anomaly resulting from genetically-induced disturbance to neural crest development[23]. However, abnormal control over neural crest development can only partially explain the pattern of *l*GI findings reported here. Cases of polymicrogyria, a severe cortical malformation frequently associated with 22q11.2DS[24], may shed light on alternative explanations for the observed cortical anomalies. Polymicrogyria is often traced back to ischemia[25], implicating cardio-vascular defects in gyrification changes. Given that polymicrogyria appears on MRI as extreme surface reduction due to sulcal shallowing, the degree of the reported *l*GI reductions in 22q11.2DS seems to qualify as subtle cortical deformation in the direction of polymicrogyria. Or more specifically, cortical malformations associated with 22q11.2DS may surface along a continuum, ranging from severe polymicrogyria, easily diagnosed by radiologists, to more subtle forms of gyral malformations, which require quantitative tools, such as *l*GI.

Effect of CHD

Similarities in neuroanatomical findings in patients with 22q11.2DS and non-syndromic patients with CHD (i.e. microcephaly, cortical malformations, agenesis of the corpus callosum, open operculum and white matter lesions[10,11]), suggest a strong association between cardiac and cerebral anomalies. In the present report, using stringent criteria, we observed reduced total brain volume in patients with 22q11.2DS with CHD compared to those without. We also report decreased *l*GI, in the absence of cortical thickness changes, in the parieto-temporo-occipital regions of individuals with 22q11.2DS and CHD. Although our sample sizes were small, the IQ scores of our CHD sub-groups suggest an effect of CHD on intellectual functioning in 22q11.2DS. Namely, the verbal-nonverbal IQ dissociation during childhood[13] and lower verbal IQ in adults[26] appear to differ between CHD sub-groups. If these effects can be replicated in larger samples of patients, these IQ differences would suggest that certain hallmark features of the 22q11.2DS cognitive phenotype might be related to the presence of cardiac malformations.

Two different interpretations can be considered to explain the observed association between brain anomalies and CHD in 22q11.2DS. A first explanation would be that common mechanisms disrupt the development of the cardiovascular and nervous systems, leading to the co-occurrence of both anomalies in one patient. For example, knock-out mice support a role for the TBX1 gene in cardiac defects[27]. If TBX1 is also expressed in the developing brain[27], the extent to which TBX1 may interact with cortical development remains unknown. Alternatively, cardiac malformations may pose a threat to cerebral hemodynamics, a phenomenon that could occur at different points in brain development. First, it has been postulated that CHD prevent brain sparing, an in utero protective mechanism that maintains a constant cerebral perfusion in case of reduced placental blood flow[28]. Second, decreased cerebral blood flow may occur after birth, due to inefficiency in the mal-

formed heart. Finally, surgery itself can be a potential cause of lesions on the developing brain. The fact that most cerebral alterations associated with CHD in non-syndromic patients are apparent at birth points to prenatal injury[10]. Our ability to identify the precise timing of the alterations, which will be critical for improving treatment, will rely on future studies using fetal or neonatal presurgical imaging. In the meantime, we can speculate that the mechanisms by which cardiac defects impair cortical development before and after birth may be similar. Indeed, almost all of the abovementioned putative mechanisms result in global hypoperfusion on the growing brain. In the only histopathological report published to date[29], the younger patients with a history of CHD showed evidence of focal tissue destruction that may have been caused by repeated hypotensive events. Studies of adults with carotid disease have taught us that the most distal fields of the main arterial territories are the regions at highest risk for low cerebral perfusion pressure, resulting in watershed infarcts[30]. The parieto-temporo-occipital junction corresponds topographically to the juncture of the most distal field of the three main cerebral arteries. The bilateral reduction in lGI observed in affected individuals with CHD could thus be similarly caused by a global hemodynamic failure largely affecting the developing cortex at its most susceptible location. The CHD analyses in the present study support a potential effect of hemodynamic factors on brain development in 22q11.2DS, and illustrate the potential for identifying factors that may contribute to heterogeneity of genetic expression throughout development.

Conclusion

The present study demonstrates how precise delineation of cortical anomalies can shed light on volumetric changes in 22q11.2DS, and how future work on cortical anomalies may help us to understand both disrupted neurodevelopment and the resulting behavioral and cognitive phenotype. Further, the current study supports cardiac malformations as a potential determinant of neurodevelopment and prognosis in the syndrome.

Acknowledgments

This research was supported by Swiss National Research Funds (grant 323500-111165 to M.S. and grants 3200-063135, 3232-063134, and PP00B-102864 to S.E.) and by NARSAD Institute, and by the Center for Biomedical Imaging of the Geneva - Lausanne Universities and the EPFL, as well as the foundations Leenaards and Louis-Jeantet (www.cibm.ch).

References

1. Tezenas Du Montcel S, Mendizabai H, Ayme S, Levy A, Philip N. Prevalence of 22q11 microdeletion. J Med Genet. 1996; 33(8): 719.
2. Simon TJ, Ding L, Bish JP, McDonald-McGinn DM, Zackai EH, Gee J. Volumetric, connective, and morphologic changes in the brains of children with chromosome 22q11.2 deletion syndrome: an integrative study. Neuroimage. 2005; 25(1): 169-80.
3. Eliez S, Schmitt JE, White CD, Reiss AL. Children and adolescents with velocardiofacial syndrome: a volumetric MRI study. Am J Psychiatry. 2000; 157(3): 409-15.
4. Kates WR, Burnette CP, Jabs EW, Rutberg J, Murphy AM, Grados M, et al. Regional cortical white matter reductions in velocardiofacial syndrome: a volumetric MRI analysis. Biol Psychiatry. 2001; 49(8): 677-84.
5. Gerdes M, Solot C, Wang PP, Moss E, LaRossa D, Randall P, et al. Cognitive and behavior profile of preschool children with chromosome 22q11.2 deletion. Am J Med Genet. 1999; 85(2): 127-33.
6. Bingham PM, Zimmerman RA, McDonald-McGinn D, Driscoll D, Emanuel BS, Zackai E. Enlarged Sylvian fissures in infants with interstitial deletion of chromosome 22q11. Am J Med Genet. 1997; 74(5): 538-43.
7. Schaer M, Schmitt JE, Glaser B, Lazeyras F, Delavelle J, Eliez S. Abnormal patterns of cortical gyrification in velo-cardio-facial syndrome (deletion 22q11.2): an MRI study. Psychiatry Res. 2006; 146(1): 1-11.
8. Schaer M, Cuadra MB, Tamarit L, Lazeyras F, Eliez S, Thiran JP. A surface-based approach to quantify local cortical gyrification. IEEE Trans Med Imaging. 2008; 27(2): 161-70.
9. McDonald-McGinn DM, Kirschner R, Goldmuntz E, Sullivan K, Eicher P, Gerdes M, et al. The Philadelphia story: the 22q11.2 deletion: report on 250 patients. Genet Couns. 1999; 10(1): 11-24.
10. Glauser TA, Rorke LB, Weinberg PM, Clancy RR. Congenital brain anomalies associated with the hypoplastic left heart syndrome. Pediatrics. 1990; 85(6): 984-90.
11. Miller SP, McQuillen PS. Neurology of congenital heart disease: insight from brain imaging. Arch Dis Child Fetal Neonatal Ed. 2007; 92(6): F435-7.
12. Bearden CE, van Erp TG, Dutton RA, Tran H, Zimmermann L, Sun D, et al. Mapping cortical thickness in children with 22q11.2 deletions. Cereb Cortex. 2007; 17(8): 1889-98.

13. Swillen A, Devriendt K, Legius E, Prinzie P, Vogels A, Ghesquiere P, et al. The behavioural phenotype in velo-cardio-facial syndrome (VCFS): from infancy to adolescence. Genet Couns. 1999; 10(1): 79-88.

14. Fischl B, Liu A, Dale AM. Automated manifold surgery: constructing geometrically accurate and topologically correct models of the human cerebral cortex. IEEE Trans Med Imaging. 2001; 20(1): 70-80.

15. Zilles K, Armstrong E, Schleicher A, Kretschmann HJ. The human pattern of gyrification in the cerebral cortex. Anat Embryol (Berl). 1988; 179(2): 173-9.

16. Genovese CR, Lazar NA, Nichols T. Thresholding of statistical maps in functional neuroimaging using the false discovery rate. Neuroimage. 2002; 15(4): 870-8.

17. Rakic P. Radial unit hypothesis of neocortical expansion. Novartis Found Symp. 2000; 228: 30-42; discussion -52.

18. Eliez S, Blasey CM, Menon V, White CD, Schmitt JE, Reiss AL. Functional brain imaging study of mathematical reasoning abilities in velocardiofacial syndrome (del22q11.2). Genet Med. 2001; 3(1): 49-55.

19. Barnea-Goraly N, Menon V, Krasnow B, Ko A, Reiss A, Eliez S. Investigation of white matter structure in velocardiofacial syndrome: a diffusion tensor imaging study. Am J Psychiatry. 2003; 160(10): 1863-9.

20. Gothelf D, Presburger G, Levy D, Nahmani A, Burg M, Berant M, et al. Genetic, developmental, and physical factors associated with attention deficit hyperactivity disorder in patients with velocardiofacial syndrome. Am J Med Genet B Neuropsychiatr Genet. 2004; 126(1): 116-21.

21. Dufour F, Schaer M, Debbane M, Farhoumand R, Glaser B, Eliez S. Cingulate gyral reductions are related to low executive functioning and psychotic symptoms in 22q11.2 deletion syndrome. Neuropsychologia. 2008.

22. Van Aken K, De Smedt B, Van Roie A, Gewillig M, Devriendt K, Fryns JP, et al. Motor development in school-aged children with 22q11 deletion (velocardiofacial/DiGeorge syndrome). Dev Med Child Neurol. 2007; 49(3): 210-3.

23. Scambler PJ. The 22q11 deletion syndromes. Hum Mol Genet. 2000; 9(16): 2421-6.

24. Robin NH, Taylor CJ, McDonald-McGinn DM, Zackai EH, Bingham P, Collins KJ, et al. Polymicrogyria and deletion 22q11.2 syndrome: window to the etiology of a common cortical malformation. Am J Med Genet A. 2006; 140(22): 2416-25.

25. Barkovich AJ, Rowley H, Bollen A. Correlation of prenatal events with the development of polymicrogyria. AJNR Am J Neuroradiol. 1995; 16(4 Suppl): 822-7.

26. Gothelf D, Penniman L, Gu E, Eliez S, Reiss AL. Developmental trajectories of brain structure in adolescents with 22q11.2 deletion syndrome: a longitudinal study. Schizophr Res. 2007; 96(1-3): 72-81.

27. Lindsay EA, Vitelli F, Su H, Morishima M, Huynh T, Pramparo T, et al. Tbx1 haploinsufficieny in the DiGeorge syndrome region causes aortic arch defects in mice. Nature. 2001; 410(6824): 97-101.

28. Donofrio MT, Bremer YA, Schieken RM, Gennings C, Morton LD, Eidem BW, et al. Autoregulation of cerebral blood flow in fetuses with congenital heart disease: the brain sparing effect. Pediatr Cardiol. 2003; 24(5): 436-43.

29. Kiehl TR, Chow EW, Mikulis DJ, George SR, Bassett AS. Neuropathologic Features in Adults with 22q11.2 Deletion Syndrome. Cereb Cortex. 2008.

30. Momjian-Mayor I, Baron JC. The pathophysiology of watershed infarction in internal carotid artery disease: review of cerebral perfusion studies. Stroke. 2005; 36(3): 567-77.

Regional cortical volumes and congenital heart disease: a MRI study in 22q11.2 deletion syndrome*

Marie Schaer†, Bronwyn Glaser, Marie-Christine Ottet, Maude Schneider, Meritxell Bach Cuadra, Martin Debbané, Jean-Philippe Thiran, Stephan Eliez

Abstract

Objective: *Children with congenital heart disease (CHD) who survive surgery often present impaired neurodevelopment and qualitative brain anomalies. However, no previous studies quantified the impact of CHD on total or regional brain volumes. The purpose of this study is to address this question in a sample of patients with 22q11.2 deletion syndrome (22q11DS), a neurogenetic condition frequently associated with CHD.*

Patients: *Sixty-one children, adolescents and young adults with confirmed 22q11.2 deletion were included, as well as eighty healthy participants matched for age and gender. Subsequent subdivision of the patients group according to CHD yielded a sub-group of 27 patients with 22q11DS and normal cardiac status, and a sub-group of 26 patients who underwent cardiac surgery during their first years of life (8 patients with unclear status were excluded).*

Methods: *An automated method for quantifying regional cortical volumes was applied to T1-weighted MRI. First, regional cortical volumes were compared between patients with 22q11DS and controls. Then, the association between regional cortical volumes and CHD was examined within a three-conditions fixed-factor. Robust protection against Type I error used Bonferroni correction.*

Results: *Smaller total cerebral volumes were observed in the sub-group of patients with CHD compared to both patients without CHD and control participants. The pattern of bilateral regional reductions associated with CHD encompassed the superior parietal region, the precuneus, the fusiform gyrus and the most anterior part of the cingulate cortex. When comparing patients with 22q11DS with CHD and patients without, the most significantly reduced regions were the right middle temporal and left superior frontal gyri, as well as the left parahippocampal region.*

Conclusions: *The present results of global and regional volumetric reductions contribute to further our understanding of the pathophysiology of brain alterations in patients with congenital heart disease, and may participate to the intellectual and behavioral problems observed in survivors of cardiac surgery.*

Introduction

Congenital heart diseases (CHD) are among the most frequent birth defects. Over the past few decades, progress in surgical techniques have allowed for the correction of most CHD, so that an increasing number of children and adults live with surgically corrected CHD[1]. Nevertheless, CHD and its correction still have neurological and developmental costs[2]. Survivors often present difficulties in expressive language, visuo-motor skills and fine motor function[3], as well as inattention and hyperactivity[4]. Non-specific structural brain anomalies associated with these impairements have been reported, which include microcephaly, abnormalities of the cortical mantle[5], and frequent periventricular leukomalacia[6]. The pathophysiology of brain anomalies associated with CHD has largely incriminated intra-operative support mechanisms, leading to continuous improvement of surgical procedures[7]. But more recently, it has also been evidenced that neurological abnormalities, such as microcephaly or leukomalacia, may be present before surgery[8-10]. As reduced cerebral blood flow has been shown in fetuses[11] and neonates with complex CHD[12], presurgical brain abnormalities may be the consequence of decreased perfusion pressure in the developing brain. Despite increasing evidence that reduced blood perfusion impairs brain growth in individuals with CHD, no single study quantified cerebral volumes in children or adults survivors. Further, the question as to how cerebral volume may be altered regionally in survivors remained similarly unadressed.

*This article is currently in revision

†**Corresponding author:** Marie Schaer, Service Médico-Pédagogique, 1 rue David Dufour, Case Postale 50, 1211 Geneva 8, Switzerland. E-mail: marie.schaer@unige.ch. Phone: +41 22 388 67 31 - Fax: +41 22 388 67 69.

Affiliations:

[1] Service Médico-Pédagogique, Geneva, Switzerland

[2] Swiss Federal Institute of Technology, Lausanne, Switzerland

[3] Department of Genetic Medicine and Development, Geneva, Switzerland

If we look at brain anomalies related to CHD from another point of view, we cannot ignore the numerous neurogenetic conditions frequently associated with CHD in which abnormalities of the brain structure are well documented, such as Williams syndrome, Down syndrome or 22q11.2 deletion syndrome (22q11DS)[13-17]. Among neurogenetic syndromes, the one with the strongest association with CHD is probably 22q11DS. Prospective studies of neonates with CHD have shown that deletion at 22q11.2 accounts for one third of patients with conotruncal heart defect (most often tetralogy of Fallot and truncus arteriosus) and one half of patients with interrupted aortic arch[18]. Moreover, 50 to 75% of patients with 22q11DS have CHD[19,20]. In addition to a strong bidirectional association between CHD and 22q11DS, striking similarities in the difficulties presented by children affected with 22q11DS and children with CHD have led to the suggestion that part of the cognitive or cerebral phenotype in 22q11DS may be caused by CHD[1]. Specifically, children with 22q11DS show visuospatial impairements, fine motor difficulties, executive dysfunction and frequent attention problems[21,22], all of which are commonly seen in non syndromic patients with CHD. Although patients with 22q11DS and CHD demonstrate more severe intellectual impairements than patients with CHD alone[23], comparing children with 22q11DS but with and without CHD offers an interesting framework to study the effect of CHD on brain structure and cognition. To date, no study has observed any differences in the cognitive outcome of children with 22q11DS with and without CHD[21,24-27]. In the present study, we address the question of regional volumetric reductions associated with CHD using a recent method that measure gyral volumes across the brain[28]. First, we will quantify volumetric reductions that are specific to the syndrome by comparing patients to controls. Then, we will identify the regions that are specifically altered in patients with CHD compared to patients without CHD.

Materials & Methods

Participants

Individuals with 22q11DS

Sixty-one individuals with 22q11.2 deletion syndrome participated in the current study. The sample consisted of children, adolescents and young adults, with an average age of 15.6±8.9 (36F/25M). Patients had an average IQ of 68.7±12.0. Participants were recruited through announcements to regional parent associations. All individuals were native French- or English-speaking individuals and were assessed in their native language. Only children with a confirmed 22q11.2 deletion were included in the study.

Cardiac malformations in 22q11DS

A history of cardiac surgery was documented using a questionnaire to the parents. In addition, medical reports, including ultrasound examinations and surgical reports, were examined. Twenty-seven patients with major cardiac defects were identified and constituted the CHD sub-group (17F/10M, mean age: 13.7±8.3). The type of CHD and the age at cardiac surgery are detailed for each patient in Table 1. Eight patients were excluded at analysis for unclear cardiac status (2 with retrooesophageal subclavian artery, 6 with documented interventricular communication with spontaneous closure at follow-up). Twenty-six patients with normal heart, or with benign heart murmurs at birth with normal ultrasound examination, were included in the noCHD sub-group (13F/13M, mean age: 17.6±9.8). Although the age difference between the CHD and noCHD sub-groups did not reach significance (p=0.121), age was covaried out in all statistical analyses.

IQ scores in the sub-group of patients with CHD (66.7±12.6) did not differ from IQ in the sub-group without (70.0±11.6, p=0.333), neither did PIQ (p=0.365) nor VIQ (p=0.364). In further exploratory statistics, we subdivided all patients who we included in the CHD analyses (n=53) into 2 sub-groups of equal size according to their IQ performances. The low performing sub-group (FSIQ≤67) was composed of 26 patients with an average IQ of 58.2±6.7 (mean age: 17.3±9.5), and the high performing sub-group (FSIQ≥68) was composed of 27 patients with an average IQ of 78.1±7.0 (mean age: 14.1±8.8). The proportion of low-performing patients in the CHD sub-group (17/27, 65.4%) was significantly higher than the proportion of low-performing patients in the no-CHD sub-group (9/26, 34.6%, p=0.039, ϕ= 0.283). This difference appeared mainly driven by the adolescents and adults with CHD, as the nine patients with CHD who were older than 14 years old were all low-performers.

Control group

The comparison group is comprised of 80 typically developing individuals (44 females, 36 males). The control group had an average age of 15.9±8.4, and an

Age	Sex[a]	CHD[b]	Age at cardiac surgery
6.1	F	ASD, VSD	3 months
6.1	M	PHT, VSD	3 months
6.3	F	PAH, VSD	Surgery planned
6.3	M	IAA, ASD, VSD	1 month & 3 months
6.4	M	ToF	5 months
7.0	F	IAA, VSD	1 month
7.3	F	TA, VSD	1 month
7.6	M	PA-VSD (ToF)	11 days
7.6	F	ASD, VSD	6 months
7.9	F	ToF	15 months
8.0	F	PA-VSD (ToF)	2 months & 3.5 years
8.6	F	ASD, VSD	5 months
10.9	F	ASD, VSD	8 months
11.2	F	IAA, VSD	8 days
11.9	M	IAA, VSD	9 days & 4 years
12.5	M	ToF	3 years
13.3	M	ToF	2.5 years
14.3	F	ToF	2 years
14.6	F	ToF	1 year
17.7	F	Unspecified	4 years & 14 years
18.1	M	IAA, VSD	At birth & 1 year
19.6	F	IAA, VSD	4 days & 3 months
21.6	M	ToF	17 months
23.3	M	Aortic dysplasia	During 1st year
30.0	F	ToF	3 years & 5 years
32.5	F	ASD	During 1st year
33.4	F	PAH, VSD	11 years

Table 1: Description of the sub-groups with 22q11DS according to a history of major congenital cardiac malformation and subsequent surgery.

[a] *F: Female, M: Male*

[b] *ToF=Tetralogy of Fallot; VSD=Ventricular Septal Defect; ASD=Atrial Septal Defect; IAA=Interrupted Aortic Arch; PAH=Pulmonary Artery Hypoplasia; PA-VSD=Pulmonary Atresia with Ventricular Septal Defect (often considered to be the most severe of the ToF defects); PHT=Pulmonary Hypertension, TA=Truncus Arteriosus*

average IQ of 111.7±12. Individuals were recruited through a newsletter distributed at public schools and in the Geneva community. A complete medical history, as well as parent-report (CBCL in children and adolescents)[29] and self-report (SCL-90R in adolescents and adults)[30] behavioral questionnaires were used to screen control participants. Subjects with a history of past or present neurological or psychiatric disorders were excluded. Written informed consent was received from all subjects, as well as the parents of subjects younger than 18 years of age, in accordance with protocols approved by the Institutional Review Board of Geneva University School of Medicine.

MRI acquisition & processing

Cerebral magnetic resonance images were acquired with a T1-weighted 3D volumetric pulse sequence using a Philips Intera 1.5 T scanner as a series of 124 contiguous coronal slices, with a voxel size of 0.9375 x 0.9375 x 1.5 mm (TR=35 msec, TE=6 ms, flip angle=45°, NEX=1).

Cortical reconstruction and volumetric segmentation were performed using published algorithms included in FreeSurfer software (Harvard University)[31,32]. Briefly, processing consisted of removal of non-brain tissue[33], automatic segmentation of the subcortical gray matter structures[34], and the extraction of cortical surfaces, which was performed according to previously published protocols[31,35]. Both intensity and continuity information from the entire three-dimensional MR volume are used in segmentation and deformation procedures, thus producing accurate representation of cortical thickness or volumes. These procedures have been validated against histological studies[36], manual measurements[37,38] and shown reliable across scanner manufacturers and field strengths[39].

Subsequent to cortical reconstruction, the cortex is subdivided into units based on gyral and sulcal structures[28]. This parcellation method based on major sulci has been shown to be both valid and reliable, with high intraclass correlation coefficient between the manual and automated procedures for both cortical volume estimates and parcel boundaries. The parcellation produces 34 gyral regions subdivided into 11 frontal regions, 9 temporal regions, 5 parietal regions, 4 occipital regions, 4 parts of the cingulate cortex, and finally the corpus callosum which is designed to improve the reliability of the placement of the other parcels (for details, please refer to the validation article[28]). In the present study, the frontal pole and the banks of the superior temporal sulcus regions, that exhibited relatively poor reliability in the validation article[28], were excluded from statistical analyses. Cortical volume was therefore estimated for 31 parcels in each hemisphere for each subject.

Statistical Analyses

Patients vs controls

ANOVA was used to compare total cerebral volume between groups. Subsequent MANCOVA compared the 31 ROIs in each hemisphere with diagnosis as the fixed factor, and both age and total cerebral volume as covariates. Results are reported both with a statistical threshold of $p<0.05$, and with a Bonferroni corrected threshold of $p<0.0016$.

		Control	22q11DS	F	p
	Total cerebral volume[a]	1072287 (101804)	939831 (114254)	52.7	<0.001
Cortical Regions Showing Relative Preservation in 22q11DS					
Left	Lateral Orbitofrontal	8227.3 (983.6)	8055.4 (1162.2)	20.4	<0.001
	Pars Opercularis	5176.7 (925.3)	5242.4 (984.8)	6.0	0.016
	Precentral	4684.5 (1575.4)	14188.6 (1841.1)	5.7	0.019
	Pars Orbitalis	2743.0 (456.8)	2628.7 (591.3)	5.7	0.019
	Superior Frontal	27430.5 (3653.1)	25494.9 (3990.5)	4.8	0.030
	Medial Orbitofrontal	5106.4 (880.8)	4955.8 (787.7)	4.3	0.041
Right	Precentral	14493.0 (1806.5)	14117.5 (2006.4)	15.0	<0.001
	Superior Frontal	25605.5 (3313.5)	24819.5 (3713.7)	13.5	<0.001
	Lateral Orbitofrontal	8273.2 (954.5)	7901.0 (1381.6)	12.2	<0.001
	Pars Orbitalis	3196.3 (630.0)	3097.5 (659.3)	5.3	0.023
Cortical Regions Showing Disproportionate Reductions in 22q11DS					
Left	Precuneus	11187.8 (1633.8)	9164.4 (1705.3)	23.3	<0.001
	Fusiform	10379.1 (1443.6)	8413.5 (1534.4)	16.8	<0.001
	Rostral Ant. Cingulate	2701.1 (600.7)	2025.7 (471.3)	12.7	<0.001
	Temporal Pole	2672.6 (500.4)	2278.3 (419.0)	11.4	<0.001
	Cuneus	3356.7 (686.1)	2636.8 (536.5)	9.4	0.003
	Superior Parietal	14728.9 (2562.2)	12750.4 (2058.1)	7.3	0.008
	Caudal Ant. Cingulate	2031.5 (583.1)	1567.9 (315.5)	6.8	0.010
	Pericalcarine	2258.7 (514.7)	1754.0 (426.1)	4.2	0.041
Right	Precuneus	11452.6 (1967.0)	9418.3 (1472.7)	19.6	<0.001
	Lingual	7545.5 (1292.4)	6122.9 (954.0)	13.5	<0.001
	Rostral Ant. Cingulate	2123.5 (430.2)	1658.0 (383.2)	13.4	<0.001
	Fusiform	9628.3 (1430.3)	7628.4 (1732.7)	11.8	<0.001
	Cuneus	3860.5 (791.1)	3118.3 (672.2)	5.8	0.017
	Rostral Middle Frontal	20440.6 (3307.4)	17679.1 (2576.0)	4.9	0.028
	Temporal Pole	2572.04 (574.1)	2178.6 (394.6)	4.8	0.030
	Caudal Ant. Cingulate	2450.1 (679.0)	1943.9 (434.3)	4.8	0.030
	Lateral Occipital	14206.3 (2243.5)	12217.8 (1992.1)	4.8	0.031
	Superior Parietal	14360.8 (2222.5)	12688.9 (1956.1)	4.5	0.036
	Pericalcarine	2593.0 (602.1)	2054.7 (417.9)	4.0	0.049

Table 2: Regional cortical volumetric changes in patients with 22q11DS compared to controls. *In both hemispheres, MANCOVA comparing regional brain volumes while covarying for age and total cerebral volume were significant at Wilks' Lambda of $p<0.001$ (left: $F_{33,105}=4.808$; right: $F_{33,105}=3.538$).*
[a] *= cortical gray matter + white matter (i.e. cerebellum and subcortical gray matter excluded)*

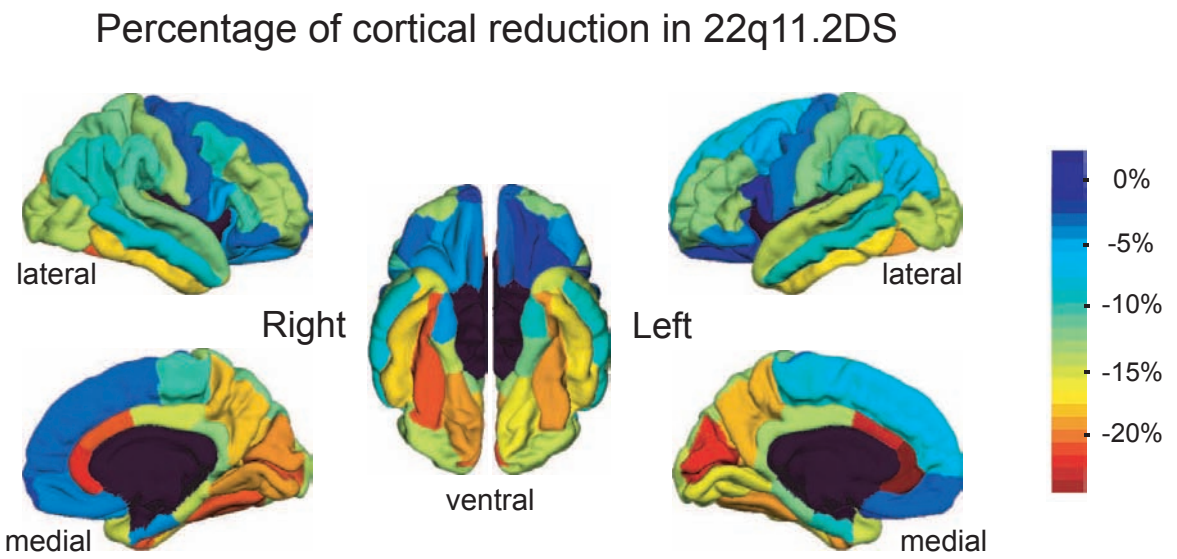

Figure 1: Distribution of cortical reduction associated with 22q11DS plotted on the average study-specific brain. *Percentage of volumetric reduction is illustrated using a scale centered at average cerebral reduction (-12%, green). Blue regions demonstrate relative preservation (i.e. less than 12% of reduction) and yellow to red regions indicate regions with the greatest percentage reduction.*

Patients with and without CHD

In order to test whether volumetric alterations were associated with CHD, we then conducted the same MANCOVA on the 31 parcels in each hemisphere, using age and total cerebral volume, but with three conditions as our fixed factor (control, patient with CHD, patient without CHD). Parcels that were significant at $p<0.05$ were further tested in pairs using a Scheffe post-hoc on cortical volumes residualized for age. Post-hoc results are also reported at $p<0.05$ and $p<0.0016$.

Results

Patients vs controls

A 12.4% reduction in cerebral volume was observed in patients with 22q11DS compared to controls (see Table 2), the regional distribution of which is further depicted in Figure 1. Specifically, Figure 1 demonstrated that cortical reductions seen in 22q11DS were largest in the posterior and medial parts of the brain.

Detailed statistical significance reported in Table 2 confirms the pattern of cortical alteration visible in Figure 1. Significantly preserved (i.e. relatively increased) cortical regions in the syndrome are exclusively located in the frontal lobes. Posterior regions with the greatest reduction in 22q11DS reach almost equal significance in both hemispheres, at the precuneus, fusiform gyrus and the most anterior part of the cingulate cortex. Widespread reductions are also observed in the parietal and occipital lobes, although these did not reach significance after correcting for the number of tests.

Patients with and without CHD

We observed prominent deleterious effect of congenital heart disease on total and regional cerebral volumes. While patients with 22q11DS and normal cardiac status showed a 6.9% reduction in total cerebral volume compared to controls, patients who underwent cardiac surgery had an average of 16.9% reduction. Statistical significance in Table 3 demonstrates two patterns of cortical changes in patients with 22q11DS and CHD, highlighted with different colors on Figure 2. First, in yellow regions on Figure 2, patients without CHD show an intermediate level of reduction between the typically developing subjects and the most affected patients with CHD. Second, 22q11DS patients with normal cardiac status showed completely normal volumes in three cortical regions that were exclusively reduced in CHD. These regions are highlighted in red on Figure 2 and consist of the right middle temporal, the left superior frontal and the left parahippocampal gyri.

		MANCOVA		Post-hoc (Scheffe test)		
		F	p	Ctl *vs* noCHD	Ctl *vs* CHD	noCHD *vs* CHD
	Cerebrum	31.5	<0.001	0.009	<0.001	0.001
Left	**Precuneus**	13.4	<0.001	**<0.001**	**<0.001**	0.031
	Lateral Orbitofrontal	10.8	<0.001	0.278	0.036	0.003
	Fusiform	7.6	0.001	**<0.001**	**<0.001**	0.120
	Rostral Ant. Cingulate	5.9	0.003	**<0.001**	**<0.001**	0.165
	Cuneus	4.8	0.010	**0.001**	**<0.001**	0.097
	Parahippocampal	4.7	0.010	0.399	**<0.001**	**0.001**
	Superior Parietal	3.9	0.022	0.010	**<0.001**	0.037
	Superior Frontal	3.4	0.035	0.978	**<0.001**	**0.001**
	Precentral	3.3	0.041	0.075	0.037	0.077
Right	**Precuneus**	10.3	<0.001	**<0.001**	**<0.001**	0.012
	Precentral	7.7	0.001	0.419	0.011	0.002
	Superior Frontal	6.5	0.002	0.720	0.008	0.006
	Rostral Ant. Cingulate	6.5	0.002	**0.001**	**<0.001**	0.033
	Lateral Orbitofrontal	6.4	0.002	0.994	0.013	0.046
	Fusiform	6.2	0.003	0.002	**<0.001**	**0.001**
	Lingual	5.5	0.005	**0.001**	**<0.001**	0.089
	Superior Parietal	3.1	0.049	0.030	**<0.001**	0.012
	Middle temporal	3.1	0.050	0.967	**<0.001**	0.002

Table 3: Statistical significance of regional cortical volume differences in the three groups comparison. *Cortical regions that showed significant difference in the 3-conditions fixed factor MANCOVA were further tested for differences two-by-two using a Scheffe test on the cortical volumes residualized for age. The whole MANCOVA was highly significant in both hemispheres (left: $F_{62,196}=2.803$; right: $F_{62,196}=2.268$). The most significant regions ($p<0.0016$) are highlighted in bold and further illustrated in Figure 2.*

Discussion

In the present study, we used an accurate method for measuring regional volumes over the cortex in 22q11DS with the specific aim of quantifying the effect of CHD on brain development in the syndrome. In the entire cohort of patients with 22q11DS, independent of their cardiac status, we were able to replicate previous volumetric results that used other methods[40-44]. In summary, the 12.4% reduction of the cerebrum observed here is in accordance with previous measurements[40,41]. Further, thanks to the increased precision allowed by maps of continuous volumetric changes over the cortex, we were able to confirm the rostro-caudal gradient in brain alterations that has been previously suggested using techniques with poorer spatial resolution. Indeed, as noted by Gothelf et al[16], a more important reduction of caudal structures was evidenced at the lobar level[40-42], as well as in specific regions-of-interests such as basal ganglia[43-45], the thalamus[46], the corpus callosum[47] and the fusiform gyrus[48]. Turning to potential implications of the rostro-caudal gradient of brain alterations, several authors have pointed out that frontal preservation may help to protect verbal performances in children with 22q11DS, while posterior reduction may alter arithmetic and visuo-spatial skills[40,42-44].

In addition to a rostro-caudal gradient, the precision brought by the continuous measurement over the three-dimensional cortical surface also demonstrates a previously unreported latero-medial gradient of brain alterations in 22q11DS. As a result of the rostro-caudal and latero-medial gradients, we observe that the regional distribution of cortical reductions on Figure 2 is proximal to the territory supplied by the posterior cerebral artery. The posterior cerebral artery supplies the brain stem, cerebellum, caudal part of the thalamus and striatum; and the uncus, fusiform gyrus, inferior temporal gyrus, pericalcarine region, cuneus, lingual gyrus, precuneus, and the occipital pole at the cortical level (see also Figure 3, reproduced from an article by van der Zwan & Hillen[49]). Given that various vascular anomalies are commonly associated with 22q11DS, Shprintzen have suggested that abnormal brain development in the syndrome may be caused by reduced perfusion related to cerebrovascular malformations[50]. However, we were missing empirical support for this hypothesis. Only one study reported cerebral angiography in the syndrome[51], observing up to 55% of minor vascular anomalies. Despite this angiographic study included a small num-

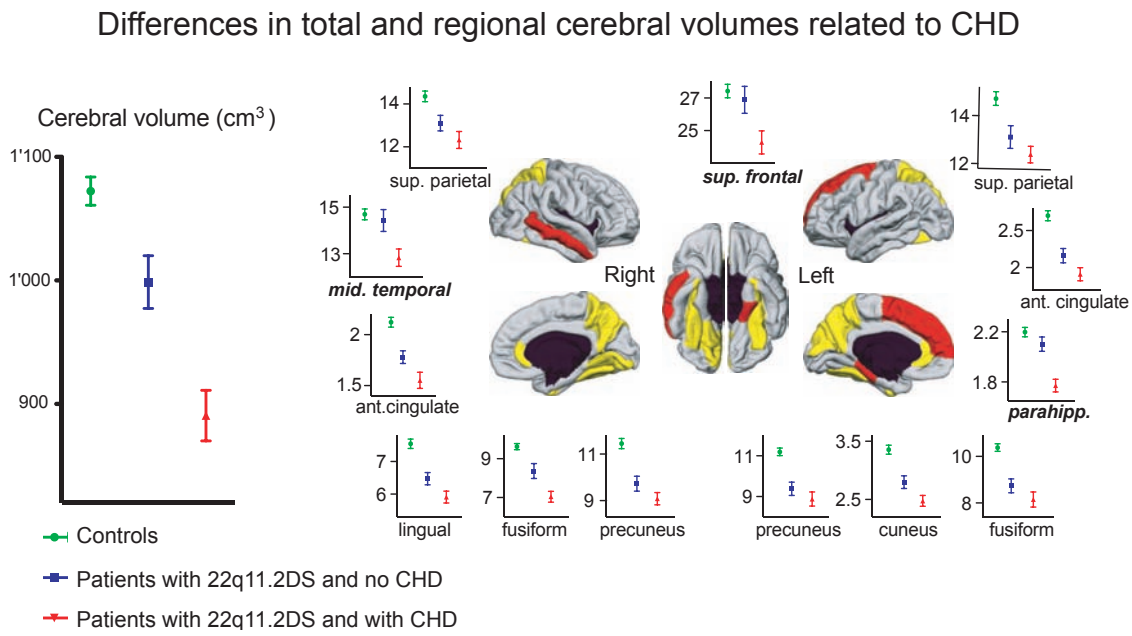

Figure 2: ***Total and regional volumetric differences related to CHD.*** *Patients with 22q11DS and CHD showed more drastic reductions in total brain volume than patients without CHD, compared to typically developing individuals. The regional distribution of the most significant parcels driving average cerebral reduction is also shown: yellow regions demonstrate areas where patients with normal cardiac status show intermediate reductions between normal controls and patients with CHD; red depicts regions where reduction is exclusively related to the presence of CHD.*

ber of subjects, Chow and colleagues reported an increased incidence of hypoplasia of the (right) posterior cerebral artery. Based on Shprintzen original hypothesis and on the angiographic observations by Chow et al, we speculate that the cortical reductions observed here point to reduced blood flow in the territory of the posterior cerebral artery, possibly altering cerebral growth in these regions. The observation that non-cortical regions supplied by this artery are also reduced corroborates this hypothesis (namely the brain stem[52], cerebellum[52,53], caudal part of the thalamus[46], and caudal part of the corpus callosum[47,54]). The potential implications of reduced blood supply over the territory of the posterior cerebral artery opens avenues for more detailed exploration of cerebrovascular anomalies in the syndrome.

A vascular hypothesis of cerebral alterations in the syndrome is even more likely given that CHD affects cortical volumes in 22q11DS. Among regions exclusively affected by the presence of congenital heart disease are the (left) superior frontal gyrus and the (right) middle temporal gyrus. Again, these differences may be analyzed in light of the arterial supply territories. As depicted in Figure 3, variability in arterial territories is relatively high. However, the superior frontal and the middle temporal gyri are the only two gyri for which their entire length is located at the junction between two arterial territories (namely, between the anterior and middle cerebral arteries). Decades of neurological observations have taught us that these regions, known as watershed areas, are the first to suffer with reduced perfusion pression in the brain[55,56]. We can thus speculate that hypoperfusion related to CHD has particularly impaired brain growth in the superior frontal and middle temporal gyri.

Finally, we also observed a specific reduction of the left parahippocampal region associated with CHD. While a direct association between this region and arterial territories is less straightforward, this finding becomes interesting in light of the known vulnerability of this region to a variety of stressful events. Indeed, the hippocampus (a non cortical region which was not measured in the present study, but which is known to be reduced in the syndrome[57-59]), is a structure known to be highly sensitive to anoxia[60,61] or to diverse kind of stress[62-64]. It is possible that the nearby parahippocampal region is similarly sensitive to stress related to CHD or to surgery on the post-natal developing brain.

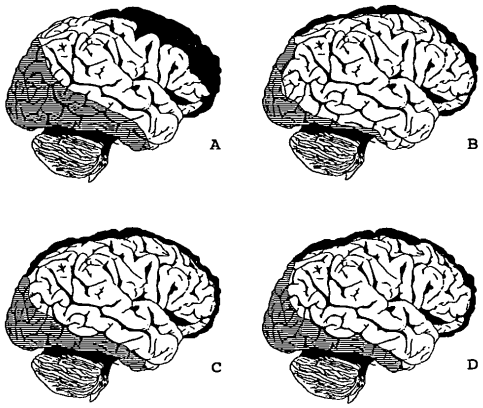

Figure 3: Variability in the arterial territories (reproduced from the article by van de Zwan & Hillen[49]). *Territories supplied by the anterior (white), middle (black) and posterior (gray) cerebral are schematically reproduced, illustrating possible variations (from A to D).*

Although the above-mentionned reasons support a role for haemodynamic factors in reduced cortical volumes in patients with CHD, alternative explanations also need to be considered. Indeed, the association between CHD and the observed cerebral anomalies may be a co-occurrence rather than a causative effect. Common embryologic origins of the malformed heart and brain could be incriminated. For instance, abnormal migration of cells of the neural crest is thought to be partially responsible for heart anomalies in 22q11DS[65], and may also be a good candidate for certain brain alterations.

The present study opens avenues for furthering our understanding of the pathophysiology of brain alterations in 22q11DS and related to CHD. However, the establishment of a clear relationship between hemodynamic status and the observed volumetric reductions remains impaired by some limitations. First, cardiac defects are largely incomparable in terms of hemodynamic disturbance, and unfortunately the present sample size does not allow explorations of the effect of specific cardiac malformations on brain structure. Second, information about cardiac status was obtained retrospectively from cardiologists, at the time of the patients evaluation in our reseach program. In the present sample, surgical procedures were performed in different hospitals in Switzerland or in France between 1971 and 1996. As a result, measures which would have been interesting to correlate with brain volumes, such as for instance oxymetry, were not available. Finally, due to the lack of angiographic data, we were not able to confirm a clear association between cerebrovascular malformations and cerebral reductions. Accordingly, recommandations for future studies in the syndrome include: (1) a precise data collection about cardiac history in all patients with 22q11DS, (2) if possible, the acquisition of angiographic exams (e.g. magnetic resonance angiography) jointly with other structural MRI acquisitions.

Whatever the cause of the additional volumetric alterations in patients with CHD, the findings of the current study point to potential cognitive repercussions. For instance, we observed that a significantly larger proportion of low performing patients were found in the CHD than in the noCHD subgroups. We also observed that none of the adults with 22q11DS who underwent cardiac surgery were included in the high-performing sub-group of patients. If we expected stronger cognitive differences, there may be several explanations for the absence of a clearer association between performances and CHD in the present study. First, heterogeneity of CHD and surgical procedures in the CHD subgroup may explain a lack of clear differences in cognitive performances in patients with and without CHD. Indeed, different CHD[8], different surgeries[66], or different ages at surgery[67] have all been identified as important determinants of cognitive outcome. Second, it is possible that the effect of CHD on cognitive outcome, as we are able to measure it, may remain subtle in this genetic syndrome which is already associated with a consequent mental delay (i.e. without CHD). Even if we identified specific volumetric alterations related to CHD, these alterations may not be directly translated into isolated cognitive deficits. Similarly, Bellinger[68] has discussed how pediatric cardiac surgery differs from adult surgery, pointing out that one occurs in a developmental and plastic setting, whereas the other is more likely to result in "static neuropsychological deficits". Finally, the lack of clear relationship between CHD and intelligence in the entire sample of patient contrasts the difference in cognitive performances observed between adults with and without CHD. As Bellinger suggested[68], some deficits may remain silent until the child learns more complex tasks. Or, more optimistically, the difference between children and adults' outcomes may rely on evolution in cardiac surgical procedures during the last decade.

Conclusion

In the present study, we show that the distribution of reduced cortical volumes support an impact of hemo-

dynamic alterations both in 22q11DS and in CHD, opening avenues for exploring cerebrovascular malformations and their relationship with cognitive outcome in the syndrome. This study is also the first to report changes to cortical volume related to CHD. Even if these changes occur within the wider context of the syndrome, we argue that they provide clues for furthering our understanding of the neurology of CHD and of the intellectual impairments often reported in survivors of surgery.

Acknowledgments

This research was supported by Swiss National Research Funds (grant 323500-111165 to M.S. and grants 3200-063135, 3232-063134, and PP00B-102864 to S.E.) and by NARSAD Institute, and by the Center for Biomedical Imaging of the Geneva - Lausanne Universities and the EPFL, as well as the foundations Leenaards and Louis-Jeantet (www.cibm.ch).

References

1. G. Wernovsky, A. J. Shillingford and J. W. Gaynor. Central nervous system outcomes in children with complex congenital heart disease. Current opinion in cardiology. 2005; 20(2): 94-9.
2. J. Wray. Intellectual development of infants, children and adolescents with congenital heart disease. Developmental science. 2006; 9(4): 368-78.
3. D. C. Bellinger, D. Wypij, K. C. Kuban, L. A. Rappaport, P. R. Hickey, G. Wernovsky, et al. Developmental and neurological status of children at 4 years of age after heart surgery with hypothermic circulatory arrest or low-flow cardiopulmonary bypass. Circulation. 1999; 100(5): 526-32.
4. A. J. Shillingford, M. M. Glanzman, R. F. Ittenbach, R. R. Clancy, J. W. Gaynor and G. Wernovsky. Inattention, hyperactivity, and school performance in a population of school-age children with complex congenital heart disease. Pediatrics. 2008; 121(4): e759-67.
5. T. A. Glauser, L. B. Rorke, P. M. Weinberg and R. R. Clancy. Congenital brain anomalies associated with the hypoplastic left heart syndrome. Pediatrics. 1990; 85(6): 984-90.
6. J. W. Gaynor. Periventricular leukomalacia following neonatal and infant cardiac surgery. Semin Thorac Cardiovasc Surg Pediatr Card Surg Annu. 2004; 7: 133-40.
7. D. P. Nelson, D. B. Andropoulos and C. D. Fraser, Jr. Perioperative neuroprotective strategies. Semin Thorac Cardiovasc Surg Pediatr Card Surg Annu. 2008: 49-56.
8. C. Limperopoulos, A. Majnemer, M. I. Shevell, B. Rosenblatt, C. Rohlicek and C. Tchervenkov. Neurologic status of newborns with congenital heart defects before open heart surgery. Pediatrics. 1999; 103(2): 402-8.
9. W. T. Mahle, F. Tavani, R. A. Zimmerman, S. C. Nicolson, K. K. Galli, J. W. Gaynor, et al. An MRI study of neurological injury before and after congenital heart surgery. Circulation. 2002; 106(12 Suppl 1): I109-14.
10. S. P. Miller, P. S. McQuillen, S. Hamrick, D. Xu, D. V. Glidden, N. Charlton, et al. Abnormal brain development in newborns with congenital heart disease. N Engl J Med. 2007; 357(19): 1928-38.
11. M. T. Donofrio, Y. A. Bremer, R. M. Schieken, C. Gennings, L. D. Morton, B. W. Eidem, et al. Autoregulation of cerebral blood flow in fetuses with congenital heart disease: the brain sparing effect. Pediatric cardiology. 2003; 24(5): 436-43.
12. D. J. Licht, J. Wang, D. W. Silvestre, S. C. Nicolson, L. M. Montenegro, G. Wernovsky, et al. Preoperative cerebral blood flow is diminished in neonates with severe congenital heart defects. J Thorac Cardiovasc Surg. 2004; 128(6): 841-9.
13. A. Meyer-Lindenberg, C. B. Mervis and K. F. Berman. Neural mechanisms in Williams syndrome: a unique window to genetic influences on cognition and behaviour. Nature reviews. 2006; 7(5): 380-93.
14. M. Schaer and S. Eliez. From genes to brain: understanding brain development in neurogenetic disorders using neuroimaging techniques. Child Adolesc Psychiatr Clin N Am. 2007; 16(3): 557-79.
15. S. J. Teipel and H. Hampel. Neuroanatomy of Down syndrome in vivo: a model of preclinical Alzheimer's disease. Behav Genet. 2006; 36(3): 405-15.
16. D. Gothelf, M. Schaer and S. Eliez. Genes, brain development and psychiatric phenotypes in velo-cardio-facial syndrome. Dev Disabil Res Rev. 2008; 14(1): 59-68.
17. M. A. Martens, S. J. Wilson and D. C. Reutens. Research Review: Williams syndrome: a critical review of the cognitive, behavioral, and neuroanatomical phenotype. J Child Psychol Psychiatry. 2008; 49(6): 576-608.
18. B. N. Hay. Deletion 22q11: spectrum of associated disorders. Semin Pediatr Neurol. 2007; 14(3): 136-9.
19. D. M. McDonald-McGinn, R. Kirschner, E. Goldmuntz, K. Sullivan, P. Eicher, M. Gerdes, et al. The Philadelphia story: the 22q11.2 deletion: report on 250 patients. Genet Couns. 1999; 10(1): 11-24.
20. A. K. Ryan, J. A. Goodship, D. I. Wilson, N. Philip, A. Levy, H. Seidel, et al. Spectrum of clinical features associated with interstitial chromosome 22q11 deletions: a European collaborative study. J Med Genet. 1997; 34(10): 798-804.

21. M. Gerdes, C. Solot, P. P. Wang, E. Moss, D. LaRossa, P. Randall, et al. Cognitive and behavior profile of preschool children with chromosome 22q11.2 deletion. Am J Med Genet. 1999; 85(2): 127-33.
22. A. Swillen, K. Devriendt, E. Legius, P. Prinzie, A. Vogels, P. Ghesquiere, et al. The behavioural phenotype in velo-cardio-facial syndrome (VCFS): from infancy to adolescence. Genet Couns. 1999; 10(1): 79-88.
23. J. Atallah, A. R. Joffe, C. M. Robertson, N. Leonard, P. M. Blakley, A. Nettel-Aguirre, et al. Two-year general and neurodevelopmental outcome after neonatal complex cardiac surgery in patients with deletion 22q11.2: a comparative study. J Thorac Cardiovasc Surg. 2007; 134(3): 772-9.
24. T. J. Simon, C. E. Bearden, E. Moss, D. McDonald-McGinn, E. Zackai and P. Wang. Cognitive development in VCFS. Progress in Pediatric Cardiology. 2002; 15(2): 109-17.
25. C. E. Bearden, M. F. Woodin, P. P. Wang, E. Moss, D. McDonald-McGinn, E. Zackai, et al. The neurocognitive phenotype of the 22q11.2 deletion syndrome: selective deficit in visual-spatial memory. J Clin Exp Neuropsychol. 2001; 23(4): 447-64.
26. A. Swillen, K. Devriendt, E. Legius, B. Eyskens, M. Dumoulin, M. Gewillig, et al. Intelligence and psychosocial adjustment in velocardiofacial syndrome: a study of 37 children and adolescents with VCFS. J Med Genet. 1997; 34(6): 453-8.
27. B. De Smedt, K. Devriendt, J. P. Fryns, A. Vogels, M. Gewillig and A. Swillen. Intellectual abilities in a large sample of children with Velo-Cardio-Facial Syndrome: an update. J Intellect Disabil Res. 2007; 51(Pt 9): 666-70.
28. R. S. Desikan, F. Segonne, B. Fischl, B. T. Quinn, B. C. Dickerson, D. Blacker, et al. An automated labeling system for subdividing the human cerebral cortex on MRI scans into gyral based regions of interest. Neuroimage. 2006; 31(3): 968-80.
29. T. M. Achenbach. Manual for the Child Behavior Checklist/4-18 and 1991 Profile. Burlington, VT: University of Vermont, Department of Psychiatry; 1991.
30. L. R. Derogatis. SCL-90-R Administration, Scoring and Procedures Manual II. Towson, MD: Clinical Psychometric Research; 1983.
31. A. M. Dale, B. Fischl and M. I. Sereno. Cortical surface-based analysis. I. Segmentation and surface reconstruction. Neuroimage. 1999; 9(2): 179-94.
32. B. Fischl, A. Liu and A. M. Dale. Automated manifold surgery: constructing geometrically accurate and topologically correct models of the human cerebral cortex. IEEE Trans Med Imaging. 2001; 20(1): 70-80.
33. F. Segonne, A. M. Dale, E. Busa, M. Glessner, D. Salat, H. K. Hahn, et al. A hybrid approach to the skull stripping problem in MRI. Neuroimage. 2004; 22(3): 1060-75.
34. B. Fischl, D. H. Salat, E. Busa, M. Albert, M. Dieterich, C. Haselgrove, et al. Whole brain segmentation: automated labeling of neuroanatomical structures in the human brain. Neuron. 2002; 33(3): 341-55.
35. B. Fischl and A. M. Dale. Measuring the thickness of the human cerebral cortex from magnetic resonance images. Proc Natl Acad Sci U S A. 2000; 97(20): 11050-5.
36. H. D. Rosas, A. K. Liu, S. Hersch, M. Glessner, R. J. Ferrante, D. H. Salat, et al. Regional and progressive thinning of the cortical ribbon in Huntington's disease. Neurology. 2002; 58(5): 695-701.
37. G. R. Kuperberg, M. R. Broome, P. K. McGuire, A. S. David, M. Eddy, F. Ozawa, et al. Regionally localized thinning of the cerebral cortex in schizophrenia. Arch Gen Psychiatry. 2003; 60(9): 878-88.
38. D. H. Salat, R. L. Buckner, A. Z. Snyder, D. N. Greve, R. S. Desikan, E. Busa, et al. Thinning of the cerebral cortex in aging. Cereb Cortex. 2004; 14(7): 721-30.
39. X. Han, J. Jovicich, D. Salat, A. van der Kouwe, B. Quinn, S. Czanner, et al. Reliability of MRI-derived measurements of human cerebral cortical thickness: the effects of field strength, scanner upgrade and manufacturer. Neuroimage. 2006; 32(1): 180-94.
40. S. Eliez, J. E. Schmitt, C. D. White and A. L. Reiss. Children and adolescents with velocardiofacial syndrome: a volumetric MRI study. Am J Psychiatry. 2000; 157(3): 409-15.
41. W. R. Kates, C. P. Burnette, E. W. Jabs, J. Rutberg, A. M. Murphy, M. Grados, et al. Regional cortical white matter reductions in velocardiofacial syndrome: a volumetric MRI analysis. Biol Psychiatry. 2001; 49(8): 677-84.
42. T. J. Simon, L. Ding, J. P. Bish, D. M. McDonald-McGinn, E. H. Zackai and J. Gee. Volumetric, connective, and morphologic changes in the brains of children with chromosome 22q11.2 deletion syndrome: an integrative study. Neuroimage. 2005; 25(1): 169-80.
43. W. R. Kates, C. P. Burnette, B. A. Bessette, B. S. Folley, L. Strunge, E. W. Jabs, et al. Frontal and caudate alterations in velocardiofacial syndrome (deletion at chromosome 22q11.2). J Child Neurol. 2004; 19(5): 337-42.
44. L. E. Campbell, E. Daly, F. Toal, A. Stevens, R. Azuma, M. Catani, et al. Brain and behaviour in children with 22q11.2 deletion syndrome: a volumetric and voxel-based morphometry MRI study. Brain. 2006; 129(Pt 5): 1218-28.
45. S. Eliez, N. Barnea-Goraly, J. E. Schmitt, Y. Liu and A. L. Reiss. Increased basal ganglia volumes in velocardio-facial syndrome (deletion 22q11.2). Biol Psychiatry. 2002; 52(1): 68-70.
46. J. P. Bish, V. Nguyen, L. Ding, S. Ferrante and T. J. Simon. Thalamic reductions in children with chromosome 22q11.2 deletion syndrome. Neuroreport. 2004; 15(9): 1413-5.

47. A. M. Machado, T. J. Simon, V. Nguyen, D. M. McDonald-McGinn, E. H. Zackai and J. C. Gee. Corpus callosum morphology and ventricular size in chromosome 22q11.2 deletion syndrome. Brain research. 2007; 1131(1): 197-210.
48. B. Glaser, M. Schaer, S. Berney, M. Debbane, P. Vuilleumier and S. Eliez. Structural changes to the fusiform gyrus: a cerebral marker for social impairments in 22q11.2 deletion syndrome? Schizophr Res. 2007; 96(1-3): 82-6.
49. A. van der Zwan and B. Hillen. Review of the variability of the territories of the major cerebral arteries. Stroke; a journal of cerebral circulation. 1991; 22(8): 1078-84.
50. R. J. Shprintzen. Velo-cardio-facial syndrome: a distinctive behavioral phenotype. Ment Retard Dev Disabil Res Rev. 2000; 6(2): 142-7.
51. E. W. Chow, D. J. Mikulis, R. B. Zipursky, L. E. Scutt, R. Weksberg and A. S. Bassett. Qualitative MRI findings in adults with 22q11 deletion syndrome and schizophrenia. Biol Psychiatry. 1999; 46(10): 1436-42.
52. S. Eliez, J. E. Schmitt, C. D. White, V. G. Wellis and A. L. Reiss. A quantitative MRI study of posterior fossa development in velocardiofacial syndrome. Biol Psychiatry. 2001; 49(6): 540-6.
53. J. P. Bish, A. Pendyal, L. Ding, H. Ferrante, V. Nguyen, D. McDonald-McGinn, et al. Specific cerebellar reductions in children with chromosome 22q11.2 deletion syndrome. Neurosci Lett. 2006; 399(3): 245-8.
54. K. M. Antshel, J. Conchelos, G. Lanzetta, W. Fremont and W. R. Kates. Behavior and corpus callosum morphology relationships in velocardiofacial syndrome (22q11.2 deletion syndrome). Psychiatry Res. 2005; 138(3): 235-45.
55. A. Y. Liu, R. A. Zimmerman, J. C. Haselgrove, L. T. Bilaniuk and J. V. Hunter. Diffusion-weighted imaging in the evaluation of watershed hypoxic-ischemic brain injury in pediatric patients. Neuroradiology. 2001; 43(11): 918-26.
56. C. P. Chao, C. G. Zaleski and A. C. Patton. Neonatal hypoxic-ischemic encephalopathy: multimodality imaging findings. Radiographics. 2006; 26 Suppl 1: S159-72.
57. M. Debbane, M. Schaer, R. Farhoumand, B. Glaser and S. Eliez. Hippocampal volume reduction in 22q11.2 deletion syndrome. Neuropsychologia. 2006; 44(12): 2360-5.
58. T. Deboer, Z. Wu, A. Lee and T. J. Simon. Hippocampal volume reduction in children with chromosome 22q11.2 deletion syndrome is associated with cognitive impairment. Behav Brain Funct. 2007; 3: 54.
59. W. R. Kates, A. M. Miller, N. Abdulsabur, K. M. Antshel, J. Conchelos, W. Fremont, et al. Temporal lobe anatomy and psychiatric symptoms in velocardiofacial syndrome (22q11.2 deletion syndrome). J Am Acad Child Adolesc Psychiatry. 2006; 45(5): 587-95.
60. M. Di Paola, C. Caltagirone, L. Fadda, U. Sabatini, L. Serra and G. A. Carlesimo. Hippocampal atrophy is the critical brain change in patients with hypoxic amnesia. Hippocampus. 2008; 18(7): 719-28.
61. P. Jourdain, I. Nikonenko, S. Alberi and D. Muller. Remodeling of hippocampal synaptic networks by a brief anoxia-hypoglycemia. J Neurosci. 2002; 22(8): 3108-16.
62. J. D. Bremner, P. Randall, T. M. Scott, R. A. Bronen, J. P. Seibyl, S. M. Southwick, et al. MRI-based measurement of hippocampal volume in patients with combat-related posttraumatic stress disorder. Am J Psychiatry. 1995; 152(7): 973-81.
63. B. S. McEwen. Stress and hippocampal plasticity. Annu Rev Neurosci. 1999; 22: 105-22.
64. R. M. Sapolsky. Glucocorticoids and hippocampal atrophy in neuropsychiatric disorders. Arch Gen Psychiatry. 2000; 57(10): 925-35.
65. P. J. Scambler. The 22q11 deletion syndromes. Hum Mol Genet. 2000; 9(16): 2421-6.
66. D. C. Bellinger, R. A. Jonas, L. A. Rappaport, D. Wypij, G. Wernovsky, K. C. Kuban, et al. Developmental and neurologic status of children after heart surgery with hypothermic circulatory arrest or low-flow cardiopulmonary bypass. N Engl J Med. 1995; 332(9): 549-55.
67. J. W. Newburger, A. R. Silbert, L. P. Buckley and D. C. Fyler. Cognitive function and age at repair of transposition of the great arteries in children. N Engl J Med. 1984; 310(23): 1495-9.
68. D. C. Bellinger. Cardiac surgery and the brain: differences between adult and paediatric studies. Heart (British Cardiac Society). 2003; 89(4): 365-6.

Deviant trajectories of cortical maturation in 22q11.2 deletion syndrome (22q11DS): a cross-sectional and longitudinal study*

Marie Schaer†, Martin Debbané, Meritxell Bach Cuadra, Marie-Christine Ottet, Bronwyn Glaser, Jean-Philippe Thiran, Stephan Eliez

Abstract

Context: *22q11.2 deletion syndrome is associated with an increasing susceptibility to develop schizophrenia. Despite a large body of literature documented abnormal brain structure in 22q11DS, the question as to how the brain matures throughout life in the syndrome remained scarcely addressed.*

Objective: *To map cortical maturation from childhood to adulthood in 22q11.2 deletion syndrome.*

Design: *Cross-sectional cortical thickness trajectories with age were approximated over age bins of three years; repeated-measures were conducted on longitudinal data confirm the cross-sectional trajectories.*

Setting: *A longitudinal study of 22q11DS at Geneva University.*

Participants: *Fifty-nine patients with 22q11DS, aged 6 to 40, and eighty typically developing controls. Longitudinal assessments included twenty-seven patients and twenty-six controls*

Main outcome measure: *Cortical thickness across the cerebrum. Exploratory measures of cortical thickness differences related to COMT polymorphism, intelligence, and schizophrenia were also conducted.*

Results: *Deviant trajectories of cortical thickness changes with age were observed in patients with 22q11DS. In affected preadolescents, larger prefrontal thickness was observed compared to age-matched controls. Afterward, convergence of cortical thickness values by the end of adolescence suggested greater cortical loss during adolescence in patients compared to controls. No compelling evidence for an effect of COMT polymorphism on cortical maturation was observed. Within 22q11DS, thickness measurements were related to cognitive level in children and adolescents, and to schizophrenia in adults.*

Conclusions: *Deviant trajectories of cortical thickness from childhood to adulthood support disrupted cortical maturation associated with 22q11.2 deletion syndrome, with greater cortical thickness loss during adolescence suggesting an aberrant pruning.*

Introduction

22q11.2 deletion syndrome (22q11DS) is a neurogenetic condition which draws particular interest as a model to understand the pathogenesis of schizophrenia[1]. Since more than one decade, a large body of literature aimed at delineating the cerebral phenotype in these individuals at risk for developing schizophrenia for genetic reasons. Series of structural neuroimaging studies have reported specific patterns of volumetric alterations in children and in adults with the syndrome[2,3]. However, aside from two recent longitudinal studies[4,5], between-groups comparisons in sample with restrained age ranges only provide snapshots over the dynamic unfolding of structural brain changes with age. As a result, the question of how the brain matures throughout life in individuals affected by 22q11DS remains scarcely documented. Providing a comprehensive picture of the dynamic of brain maturation from childhood to adulthood in the syndrome is all the more important, when theories argue that schizophrenia involves a disruption in the cortical maturational processes during adolescence[6,7].

To study structural brain maturation in vivo using MRI, cortical thickness emerges as the ideal technique among other methods. The typical curvilinear trajectories of cortical thickness changes with age share strikingly similar temporal and regional similarities with the progression of synaptic pruning as observed postmortem, confirming the potential of cor-

*This article is currently in revision

†**Corresponding author:** Marie Schaer, Service Médico-Pédagogique, 1 rue David Dufour, Case Postale 50, 1211 Geneva 8, Switzerland. E-mail: marie.schaer@unige.ch. Phone: +41 22 388 67 31 - Fax: +41 22 388 67 69.

Affiliations:

[1] Service Médico-Pédagogique, Geneva, Switzerland

[2] Swiss Federal Institute of Technology, Lausanne, Switzerland

[3] Department of Genetic Medicine and Development, Geneva, Switzerland

tical thickness to reliably identify the brains critical development periods[8-12]. Moreover, cortical thickness studies have an exquisite resolution, allowing for the identification of local alterations with high precision. Consequently, a growing amount of studies apply cortical thickness measurement as an index of development in patients with various conditions, such as attention deficit / hyperactivity disorder (ADHD)[13,14], autism[15-17], or schizophrenia[12,18,19]. In 22q11DS, previous studies by Bearden and colleagues in 21 affected children and adolescents compared to 13 controls reported a thinner cortex in the superior parietal and right parieto-occipital region[20] and in the ventro-medial occipito-temporal cortex[21]. However, these studies did not account for cortical thickness changes with age during that period, warranting further exploration of the dynamic of cortical thickness over a more encompassing age range.

In the present study, we exploited neuroimaging data from patients with 22q11DS who have been participating in our research project since 2001[22-24]. Cerebral MRI was available for 59 patients aged from 6 to 40 years old, along with 80 healthy participants matched for age and gender. Follow-up cerebral MRI was also available for 27 patients and 26 controls. We approximated the trajectories of thickness changes with age during childhood and adolescence by subdividing our sample of participants into age bins encompassing 3 years periods. Then, we conducted repeated-measures on the longitudinal data to confirm the dynamic of brain maturation observed in the cross-sectional analysis. Although the direction of cortical thickness changes was difficult to infer a priori at each age, we expected that patients will show a more intense thinning than controls in the prefrontal regions during adolescence, supporting previous longitudinal volumetric observations[4].

In subsequent analyses, we also explored the effect of specific parameters on cortical thickness within the syndrome. First, we explored the possibility that patients with 22q11DS will show different cortical thickness depending of their genetic polymorphism on the COMT[158] (Val *vs* Met allele). Previous studies have identified the low activity allele (Met) as a risk factor for poorer outcome in 22q11DS[4,25,26]. Second, we subdivided our sample of patients with 22q11DS into children and adolescents (below 18 years old), and adults. In the younger sub-group of patients, we investigated cortical thickness differences related to IQ. In accordance with previous observations of higher gray matter density or thicker cortex in high-functioning individuals compared to those with lower IQ[10,27-30], we expected that children and adolescents with poorer performances will show thinner cortices than those with higher IQ scores. In the adult 22q11DS sub-sample, we searched for cortical thickness differences between patients with schizophrenia and patients without. As observed in non-syndromic adults with schizophrenia[18,19], we expected that a thinner cortex in the frontal and temporal regions will characterize patients with schizophrenia compared to those without.

	Cross-sectional		Longitudinal	
	Control	22q11DS*	Control	22q11DS*
6 to 9	16	15 (0/0)	10	8 (0/0; 0/3)
9 to 12	22	11 (0/4)	9	9 (0/4; 0/5)
12 to 15	8	10 (0/2)	4	6 (0/0; 0/1)
15 to 18	7	4 (0/3)	3	4 (0/3; 1/3)
18+	27	19 (6/15)		
TOTAL	80	59 (6/26)	26	27 (1/12)

Table 1: Repartition of the participants in the different age bins. *The right part of the table details the sub-sample who participated in the follow-up examination.*
**In the patients' columns, psychiatric statuses are described in brackets as follow: "(number of schizophrenic patients / number of patients presenting either hallucinations or delusions or both)". For the longitudinal subgroups, psychiatric characteristics are presented similarly, but with "(status at Time 1 ; status at Time 2)".*

Materials & Methods

Participants

Patients with 22q11DS were recruited through announcement in regional parents associations. Fifty-nine patients, with confirmed 22q11.2 deletion, were included in the study, including 35 females and 24 males. The 59 patients had an average age of 15.9±8.9 (detailed distribution over the age range is provided in Table 1). Cognitive assessment used the Wechsler Full Scale IQ, all participants being tested in their native language (French or English). The group of patients had an average IQ of 69.0±12.0. Hemizygosity for either the COMT[158]Met or the COMT[158]Val allele was determined by polymerase chain reaction with the restriction enzyme NlaIII[31]. At the time of evaluation, 7 patients received antipsychotic treatment (age range: 19.6 - 36.6), 3 received methylphenidate for ADHD (age range: 6.4 - 12.6) and one received antiepileptic treatment (11.5 years old).

Eighty healthy participants were recruited through a newsletter distributed at public schools in Geneva and in the community (44F/36M). Subjects with a history

of past or present neurological or psychiatric disorders were excluded. The control group had a mean age of 15.9±8.4 and an average IQ of 111.7±12.8. Written informed consent was received from participants and their parents (for subjects younger than 18 years of age), under protocols approved by the Institutional Review Board of Geneva University School of Medicine.

Twenty-seven patients who were younger than 18 years old at the first evaluation participated at follow-up examination (time interval: 3.1±0.3 years). The longitudinal subgroup of patients had a mean age of 11.2±3.6 at time 1 (T1) and 14.2±3.6 at time 2 (T2) and was composed of 16 females and 11 males. The average IQ for this subgroup did not differ at T1 (71.6±11.5) and T2 (73.0±12.9). Twenty-six healthy participants matched for age and gender also participated in the follow-up examination (average time interval: 3.0±0.3 years). The longitudinal subgroup of controls had a mean age of 10.6±3.2 at T1 and 13.6±3.2 at T2, encompassing 15 females and 11 males. The 26 controls had an average IQ of 112.0±12.1 at T1 and 108.3±10.4 at T2.

Imaging

Coronal cerebral MRI was acquired using a Philips 1.5T Intera scanner with a 3D volumetric pulse sequence. The following scan parameters were used: TR=35 msec, TE=6 msec, flip angle=45°, NEX=1, matrix size=256x192, field of view=24 cm^2, slice thickness=1.5 mm, 124 slices.

Images were imported into the software *FreeSurfer* (http://surfer.nmr.mgh.harvard.edu, Athinoula Center for Biomedical Imaging, Massachusetts General Hospital) to reconstruct accurate cortical surface models and measure cortical thickness. The algorithms used for cortical thickness estimation were previously validated against manual delineation on MRI sections[19] and on postmortem brains[32]. Further, the cortical thickness measurements have been proven reliable, independently of scanner manufacturer, upgrade or field strength[33].

Fully automated image processing included resampling into cubic voxels, intensity normalization, and skull stripping. Subsequent accurate cortical surfaces reconstructions used deformation algorithms based on the local intensity value, geometrical and topological constraints[34,35]. The final three-dimensional cortical surfaces include the white (gray-white boundary) and the pial (gray-CSF interface) surfaces, reconstructed with a submillimeter accuracy. Cortical thickness was measured in the native space of the images, as the shortest distance between the white and the pial surfaces[36]. As a result, cortical thickness values were available at more than 150'000 points over each hemisphere.

Statistical Analyses

Cross-sectional 22q11DS vs control comparisons

Statistical analyses employed a general linear model (GLM) to estimate the effect of diagnosis, age and diagnosis by age at each cortical point. Cortical thickness changes with age were fitted using a linear model. Interactions for gender were not included in the final model because they did not contribute significantly to the explanatory power of the model across the cortical surface (after employing a FDR correction). A false discovery rate at FDR<0.05 was employed to correct for Type 2 errors related to multiple comparisons.

Cross-sectional analyses: subdivision into age bins

In order to refine the delineation of the trajectories of cortical changes with age, we further subdivided the sample of subjects into 5 age bins: participants from 6 to 9, 9 to 12, 12 to 15, 15 to 18, and more than 18 years old. The 3 years interval was chosen in order to keep a sufficient number of subjects within each age bin (see details in Table 1), while keeping an appropriate temporal resolution in the period where the most cortical changes are known to occur. Moreover, 3 years corresponded exactly to the interval between the two time-points for longitudinal analyses. Within each age bin, a GLM was employed to assess the effect of diagnosis at each vertex. Given the restricted age range in each bin, age was not introduced as an explanatory variable.

Longitudinal descriptive analyses in significant clusters

Mixed effect models, which would have been the gold standard technique to combine cross-sectional and longitudinal cortical thickness data, commonly encompass more than 500 scans[10,11,13,14,37] or 3-4 time points[9,18]. Given the limited size of our sample, we preferred the use of repeated-measures to identify longitudinal differences in cortical thickness changes in clusters previously identified by cross-sectional analyses. Average thickness change for each cluster was computed for each age bins, with the exception of the sub-groups that were between 12 and 15, and those that were between 15 and 18 at Time 1; the latter

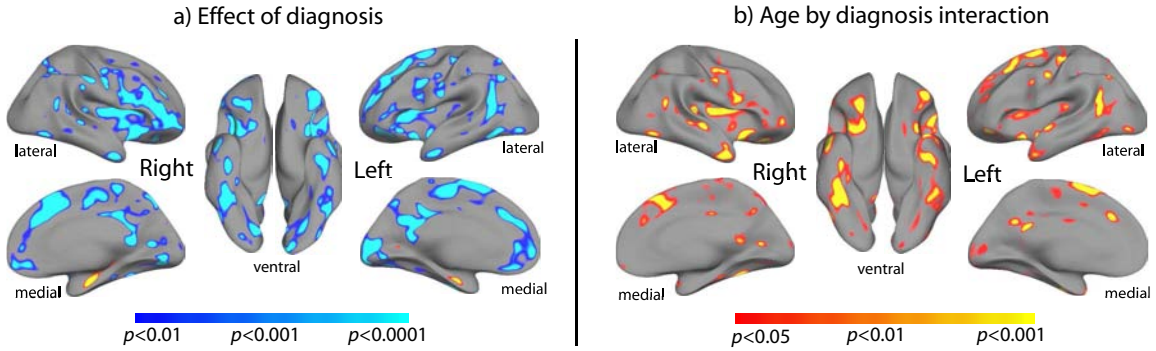

Figure 1: Vertex-wise comparisons of cortical thickness between groups (cross-sectional). *(a) When comparing the entire sample, we observe extensive areas of thicker cortex in patients with 22q11DS compared to controls (in blue). Small regions of thinner cortex in 22q11DS are shown around the bilateral entorhinal and parahippocampal regions. (b) Clusters in red / yellow show regions of significant age by diagnosis interaction, meaning that the regression line of cortical thickness changes with age showed a significantly steeper slope in patients with 22q11DS compared to controls.*

two sub-groups were merged in a single 12 to 18 subgroup, based on two considerations: (1) their small sample size if taken alone; (2) a priori cross-sectional analyses showing a comparable average thickness loss in these two bins.

Within group factors that may interact with cortical thickness

a) COMT polymorphism

Of the 59 patients, information about the COMT^{158}Val/Met status was not available for 2 of them. The remaining 57 showed the following COMT polymorphism: 29 patients had the Met allele (18F/11M; mean age: 16.8±8.8; average IQ: 68.7±10.7) and 28 had the Val allele (16F/12M; mean age: 15.4±9.3; average IQ: 68.3±13.1). The Val and Met subgroups did not differ neither in age distribution (p=0.541), nor in IQ (p=0.907). In order to determine the effect of COMT polymorphism on cortical thickness changes, a GLM was applied at each cortical vertex, modeling the effect of age, COMT polymorphism, and COMT polymorphism by age.

b) Cognitive abilities and psychiatric statuses

The extent to which cortical thickness changes in 22q11DS were associated to the level of cognitive performance and to schizophrenia were separately assessed in patients below and above 18 years old.

First, we defined a low performing subgroup with all children and adolescents who had an established mental delay, as defined by an IQ lower or equal to 65 (n=13, 7F/6M, FSIQ: 58.9±5.5, range: 44-64). Twenty-one children and adolescents scored above 75 (13F/8M, FSIQ: 81.1±4.6, range: 75-91) and constituted the high performing subgroup. The patients scoring in the intermediate interval between 66 and 74 were not considered in this analysis. The high and low performing group had similar average age (low: 11.2±4.5; high: 10.2±4.0, p=0.371). Cortical thickness differences between the high and low performing subgroups were assessed using a GLM at each vertex to assess the effect of group, age and age by group interaction on cortical thickness.

Second, cortical thickness changes associated with schizophrenia were examined in the 46 individuals who were older than 18 years old. The control group was composed of 27 adults (14F/13M, mean age: 26.0±5.9). Among the adults with 22q11DS, six were schizophrenic (SZ group, 3F/3M, mean age: 31.6 4.1). The remaining 13 adults with 22q11DS (no-SZ group, 8F/5M) had a mean age of 24.8±6.2. There was a trend for a significant difference in age distribution between the 3 subgroups (p=0.063 F=2.944). Post-hoc analyses demonstrated no age difference between the control and the no-SZ group (p=0.843) or between the control and the SZ group (p=0.113). However, a trend for a significant difference between the no-SZ and SZ groups (p=0.073). Because of this age difference, no age by group interaction could be assessed; rather the effect of age was covaried out at each vertex. A GLM assessed the effect of group and age on cortical thickness at each vertex.

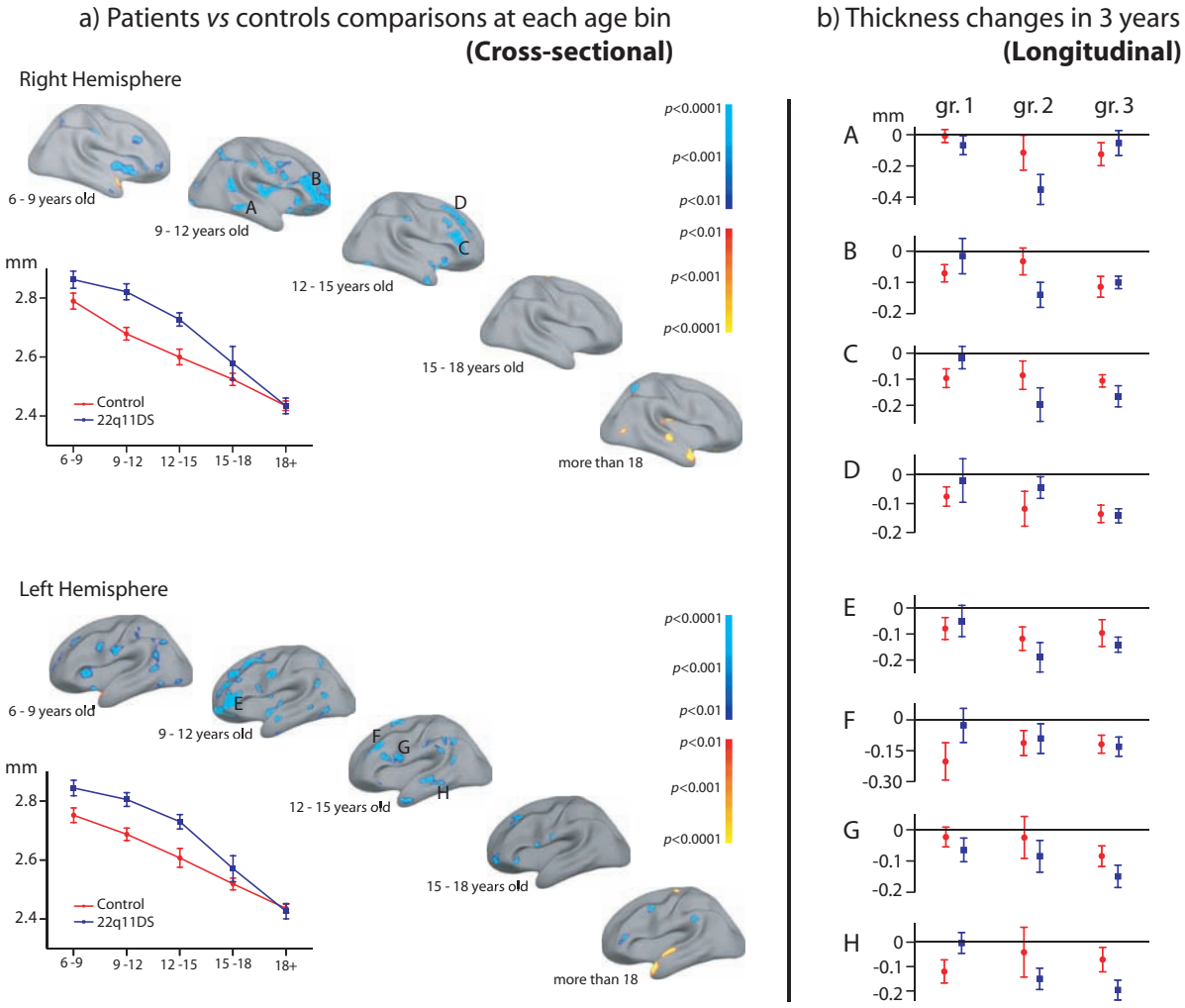

gr. 1: individuals that were between 6 and 9 at T1
gr. 2: individuals that were between 9 and 12 at T1
gr. 3: individuals that were between 12 and 18 at T1

Figure 2: Trajectories of cortical thickness change with age (cross-sectional and longitudinal; for detailed sample size please refer to Table 1) *a) Cortical thickness differences between patients and controls in multiple age bins shows that the larger clusters of thicker cortex are observed between 9 and 12 years old in the prefrontal regions (Clusters B & E). Between 12 and 15 years old, clusters of thicker cortex are mostly located in the dorsal prefrontal region (Clusters C, D, F & G). In adults, prominent clusters of thinner clusters are seen around the superior temporal gyrus, bilaterally. b) Longitudinal cortical thickness changes over a period of three years in clusters that showed the largest differences in cross-sectional analyses. In clusters B, C, D, E, F and H, the younger controls showed a greater thickness loss than patients. Most of the clusters that showed thicker cortex in the cross-sectional analyses also showed larger thickness loss between the three years interval in group 2 (namely clusters A, B, C, E, G and H), or in group 3 (namely clusters C, E, G and H). However, none of these differences reached significance (see text).*

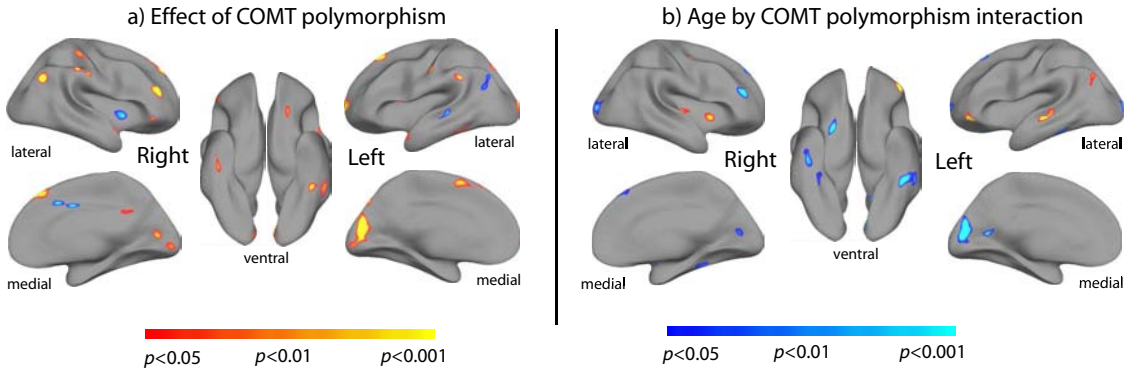

Figure 3: Effect of COMT polymorphism on cortical thickness within 22q11DS. *Apart from a cluster of thinner cortex at the left cuneus in patients with Met compared to Val allele (which was also associated with a steeper slope of cortical thickness changes with age in patients with Val compared to Met allele), only modest clusters of significant differences associated with COMT polymorphism are observed.*

Results

Cross-sectional analyses

ANOVA comparing mean thickness values over the whole sample revealed significantly higher thickness in patients (2.67±0.20 mm) than controls (2.60±0.16 mm; p=0.016, F=5.934). The effect of diagnosis on mean thickness became even more significant when covarying for age (p<0.001, $F_{2,136}$=17.785) or age and gender (p<0.001, $F_{3,135}$=17.701). Statistical cortical maps revealed that regions of thicker cortex were relatively widespread, touching extensively the frontal regions (Figure 1a). At the same time than increased thickness, a significant age by diagnosis interaction was observed, with a steeper slope of cortical thickness changes with age in patients than controls (Figure 1b). Thinner cortex in patients compared to controls was only observed on the medial aspect of the brain.

Cortical trajectories in the age bins

Figure 2a illustrates the profile of mean cortical thickness over the different age bins, while statistical maps depict the detailed distribution of cortical thickness differences between groups across hemispheres. In the youngest bin, patients show significantly higher thickness values than controls in the left hemisphere (p=0.016, F=6.541) and a trend for a thicker cortex in the right hemisphere (p=0.076, F=3.3387). At this age, detailed maps show that average thicker cortex in patients is driven by small widely distributed clusters. In the subsequent 9 to 12 age bin, highly significant average thicker cortex is observed in both hemispheres (right: p<0.001, F=15.490; left: p=0.002, F=12.076), which is driven by prominent cluster of thicker cortex mostly distributed in the frontal lobe. In the 12 to 15 age bin, higher average thickness values are still observed in both hemispheres (right: p=0.002, F=13.496; left: p=0.007, F=9.616), that appear to be mostly driven by thicker cortex in the dorsal frontal regions. In the 15 to 18 bin, we do not observe any differences in average thickness (right: p=0.302, F=1.186; left: p=0.232, F=1.618). Although the absence of significant difference may be driven by the smallest sample size, the absence of significant average thickness difference in the subsequent adult bin (right: p=0.825, F=0.050; left: p=0.571, F=0.326) further confirms the disappearance of the thicker cortex observed in younger patients with 22q11DS compared to controls.

Longitudinal analyses

The thicker cortex in preadolescents with the syndrome was quite surprising, and can result either from a delay in the normal process of maturational thickness loss with age, or from artifactual differences driven for instance by inter-subject variability. In that context, we used the longitudinal data to confirm that the clusters of thicker cortex were truly the result of deviant pattern of maturation. In such longitudinal design, the use of each subject as his / her own control dismisses the interference usually related to inter-subject variability. Repeated measures were conducted in each age bin (the 12 to 15 and 15 to 18 bins being merged, see *Statistical analyses* section) on cortical thickness at T1 and T2 in the clusters identified by cross-sectional analyses. Although the

direction of the cortical changes corroborated a less important cortical loss in patients than controls in the younger subgroup (see descriptive plots in Figure 2b), only cluster H at the left superior approached significance (greater loss in controls, p=0.093). Also, as inferred from the cross-sectional analyses, patients in the two older sub-groups showed greater thickness loss than controls. However, similarly to the younger sub-group, only two clusters approached significance: cluster B at the right prefrontal region showed larger thickness loss in intermediate age bin (p=0.086) and the cluster H at the left superior temporal sulcus in the older sub-group (greater loss in patients, p=0.07).

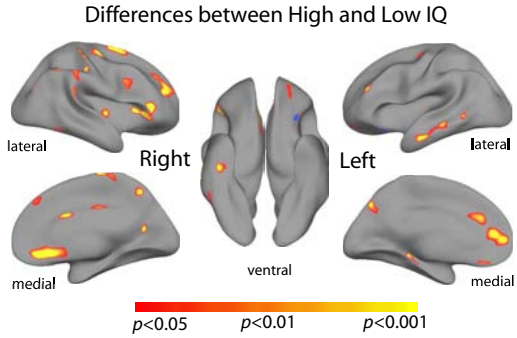

Figure 4: Differences in cortical thickness related to cognitive abilities within 22q11DS. *Clusters in red / yellow depict regions where children and adolescents with 22q11DS who score above 75 on the IQ tests show larger thickness values than those with IQ below 65. This association between thicker cortex and better performances seem to hold true at each age, as no significant clusters of group by age interaction were evidenced at p<0.05 (statistical maps not shown).*

Within group effects

a) COMT polymorphism

No significant effect on COMT polymorphism was observed on mean cortical thickness values (Met: 2.63±0.21 mm; Val: 2.70±0.20 mm, p=0.194, F=1.732). The statistical maps (Figure 3) did not reveal a compelling intensity and direction of changes associated with COMT polymorphism or to age by group interaction.

b) Cognitive abilities and psychiatric statuses

In the patients with 22q11DS below 18 years old, we did not observe significant difference in mean cortical thickness between the group of patients with poorer score on the IQ tests (2.75±0.16 mm) compared to those scoring above 75 (2.80±0.11 mm; p=0.236, F=1.461). Despite the absence of difference on mean thickness values, the statistical maps demonstrated numerous clusters of thinner cortex in low performing compared to high performing subgroup. Namely, thinner cortex in the medial frontal gyri bilaterally, the superior and inferior right frontal gyri, and the left superior temporal sulcus were seen in the low-performing sub-group (Figure 4). No group by age interaction was observed.

Statistical maps of cortical thickness difference in adult participants (Figure 5) demonstrate that (1) patients without schizophrenia show a combination of increased and decreased thickness compared to healthy participants; (2) schizophrenic patients show extended regions of cortical thinning, as compared to healthy controls and to non-schizophrenic patients with 22q11DS. Among the region in which thinnest cortex was associated with schizophrenia, arrow heads on Figure 5 at the right fusiform / lingual region and at the left superior frontal gyrus depict reduction in schizophrenic patients compared to both the controls and the non-schizophrenic patients. Thin arrows at the right middle frontal gyrus and the left superior temporal sulcus illustrate an intriguing pattern of thickness change, with normal thickness in patients with schizophrenia, whereas aberrantly high thickness in these regions was observed in patients without schizophrenia.

Discussion

The work presented here uses cortical thickness to quantify the course of cerebral maturation over a wide age range in 22q11.2 deletion syndrome. When comparing the entire sample of patients to age matched controls, we observe several clusters of thicker cortex (Figure 1a). In subsequent analyses, we demonstrate that these clusters of thicker cortex are mostly driven by larger cortical thickness values in preadolescents with the syndrome (Figure 2a). The observation of thicker cortex partially modifies the classical view that patients with 22q11DS consistently show differences in the reduced direction. Indeed, volumetric studies have always reported reduced cortical volume in the syndrome[38-42]. If cortical volume is undeniably the product of its surface and thickness, surface changes are more susceptible to result in volumetric changes than thickness alterations[43]. Thus, the drastic cortical surface reduction that we observed in previous studies[24,44] may better predict the decreased volume than subtle thickness changes, more subject to maturational alterations. The present observation of thicker cortex in preadolescents with 22q11DS

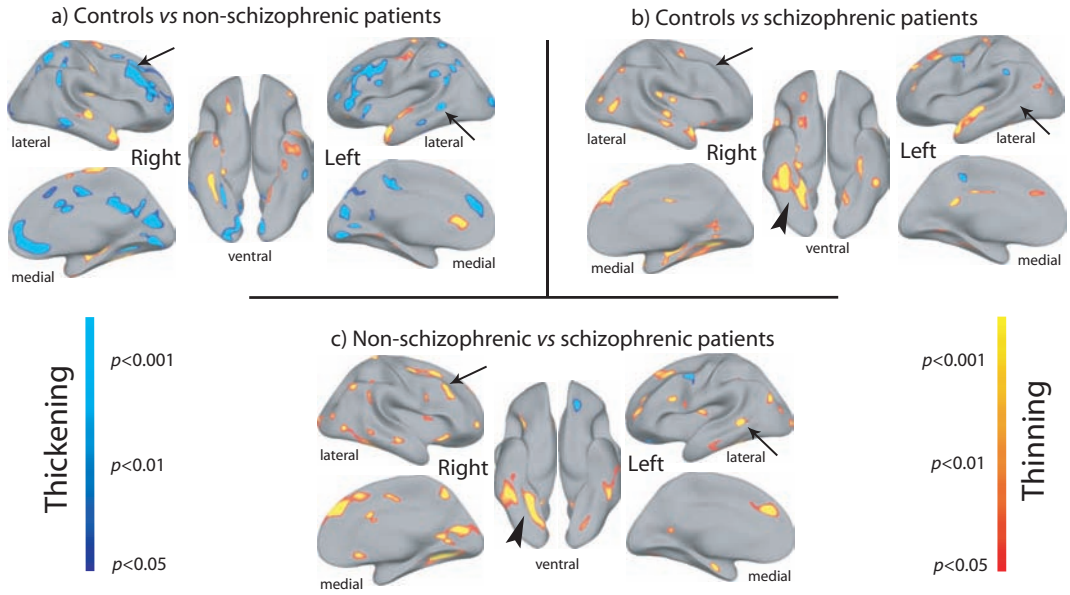

Figure 5: Cortical thickness differences related to schizophrenia in adults. *In the controls vs non-schizophrenic patients, clusters in blue demonstrate thicker cortex in patients than controls, whereas red / yellow clusters show thinner cortex in patients compared to controls. When controls are compared to schizophrenic patients, only clusters of thinner cortex (red / yellow) are found in patients. Finally, the comparison within 22q11DS reveals mostly areas of cortical thinning (red / yellow) in schizophrenic compared to non-schizophrenic patients (see also text).*

also contrast with observations of thinner cortex in children aged from 8 to 17 years old[20,21]. However, methodological differences between these studies and ours, such as scaling of the brain, divergences in cortical thickness measurements, and absence of correction for an effect of age in the statistical analyses, may account for a different direction of the results.

Thicker frontal cortex in preadolescents with 22q11DS corroborates the hypothesis that the dynamic rather than the absolute value of cortical thickness is more relevant during brain development[10,13]. Given that we observe an increasing divergence of cortical thickness differences from the youngest age bin to the 9 to 12 or the 12 to 15 age bins, we speculate that the thicker cortex in patients was driven by a delay in the normal process of cortical thinning with age. Although the longitudinal analyses did not reach significance, a less important cortical loss in patients that were between 6 and 9 and became 9 to 12 compared to controls at the same age supports delayed cortical maturation in the syndrome. Retarded onset of cortical thinning was also recently observed in attention deficit / hyperactivity disorder (ADHD)[13]. Contrarily to their observation of parallel trajectories of cortical thickness change in ADHD and controls (simple delay), the delay observed here in 22q11DS is associated with deviant trajectories of cortical changes. Indeed, while preadolescents with 22q11DS show highly significant thicker cortex, no more difference is observed from the age of 15 years old, suggesting that a larger cortical loss during adolescence is responsible for the disappearance of the difference. Although not reaching significance, further longitudinal analyses tend to confirm a higher rate of cortical thickness loss with age observed in 22q11DS after the age of 12. The later excessive rate of thinning may reflect a disturbance in the maturational processes occurring during adolescence, namely a defect in the programmed synaptic elimination.

Relevance of abnormal pruning in 22q11DS for the susceptibility to develop schizophrenia

More than two decades ago, Feinberg[45] proposed that a defect in programmed synaptic elimination may be associated with schizophrenia, a theory which is corroborated by the observation of decreased neuropil on neuropathological examinations[46]. As a result of excessive pruning, the hypothesis that hypoconnectivity or misconnectivity favors the onset of the psychiatric symptomatology has received a large interest. If aberrant connectivity remains difficult to prove in

vivo, e.g. using EEG[47], fMRI[48], or DTI[49], experimental neural network models provide an interesting framework to investigate the impact of changes to connectivity on the onset of symptoms. Using neural network model of language perception[50-52], Hoffman and McGlashan demonstrated that pruning could have distinct consequence depending of its intensity. They observed that moderate reduction of connections was first associated with an increased efficiency of the network (as it may be the case during normal maturation); whereas continued pruning resulted in several levels of deficits. First, they observed that prolongation of pruning was observed to drive decreased efficiency of the network, corroborating the initial hypothesis by Keshavan that abnormal maturation in the prefrontal cortex may impair the emergence of increased functional efficiency related to executive and social cognition[53]. Hoffman and McGlashan then observed that further reduction to connectivity triggered abnormal perceptions comparable to hallucinations. Ultimately, they observed that a regression of the hallucinatory symptomatology and an exacerbation of the negative symptoms were associated with additional pruning. Given the similarities with clinical observations of patients with first episode or chronic schizophrenia, their neural network model provides an attractive experimental setting for the identification of factors interacting with the outcome of the disease. Two factors were indeed defined as primary determinants of the outcome: (1) a faster rate of pruning appears as deleterious, precipitating the onset of schizophrenic symptoms; (2) a high baseline level of connections may be a protective factor, preserving from the hallucinatory symptomatology.

The current observations of cortical thickness changes in 22q11DS indeed nicely fit the conceptual framework of Hoffman and McGlashan. The faster thinning observed after 12 years old in the group of patients recall their first determinant, becoming meaningful for the increased risk of schizophrenia in 22q11DS. We also believe that our results are in agreement with the second hypothesis of the baseline level of connections as a factor of good prognosis. Figure 5 shows that patients without schizophrenia demonstrate preserved thickness as compared to age-matched controls. Contrarily, patients with schizophrenia show a thinner cortex, as compared to patients without, suggesting that adult patients with schizophrenia have undergone excessive pruning whereas adults without did not. A distinct neuroanatomical phenotype in patients with and without schizophrenia is in agreement with previous volumetric studies in the syndrome. In a cross-sectional study, van Amelsvoort reported smaller frontal and temporal gray matter in patients with as compared to patients without schizophrenia[54]. More recently, using a longitudinal design, Gothelf et al demonstrated that a more drastic the prefrontal reduction was associated with the emergence of psychotic symptoms[4]. If future studies following the course of cortical changes during adolescence confirm that exaggerated pruning is specifically seen in individuals developing symptoms, the search for factors interacting with synaptic pruning may serve as a guide for future targeted preventions.

Cortical thickness and cognitive abilities in 22q11DS

Finally, we also observed that children with 22q11DS with higher cognitive performances demonstrates thicker cortex (Figure 4). As discussed earlier, one interpretation could be that, the level of connections is tightly related to the network efficiency. As a result, within individuals similarly affected by a neurodevelopmental condition, a thinner cortex may reflect a lower level of connections and be associated with poorer performances. Many previous studies on cortical thickness support the view that more is better. Specifically, larger cortical thickness was associated with better cognitive functioning in elderly individuals[30]. Also, increased thickness was found to be a valuable predictor of long term memory in healthy adults[55]. However, a unidirectional relationship between thickness value and performance is less clear during normal brain maturation[10]. In the present study, the absence of age by group interaction on cortical thickness values in 22q11DS suggests that, at each age, patients with thicker cortex demonstrate preserved cognitive abilities. A similar observation that thicker cortex is associated with better outcome than thinner cortex was reported in children with ADHD [14]. Shaw et al speculated that a larger period of thicker cortex allowed for prolonged period of circuitry sculpting, a hypothesis that may also apply to explain the interaction between thickness and IQ within 22q11DS.

In summary, the present cross-sectional and longitudinal analyses provide compelling evidence for a disruption in the normal process of cortical maturation in 22q11DS, possibly characterized by (1) delayed cortical maturation, followed by (2) an excessive intensity of the rate of cortical thinning after 12 years old. We speculated that the deviant trajectories of cortical maturation observed in 22q11DS provide strong in vivo cues for a defect in the programmed synaptic elimination. Such a defect in neuronal pruning has been largely put forward in the pathogenesis of schizophrenia, and may thus explain the susceptibility of patients with 22q11DS to develop psychosis. We also observed that adult patients without schizophre-

nia demonstrate preserved frontal cortical thickness, further strengthening the possibility that accelerated cortical thinning is tightly related with the onset of psychotic symptoms. Such a prominent role of deregulated pruning in the emergence of psychiatric and cognitive symptomatology of schizophrenia opens avenues for further exploring the factors interacting with the maturational processes.

Acknowledgments

This research was supported by Swiss National Research Funds (grant 323500-111165 to M.S. and grants 3200-063135, 3232-063134, and PP00B-102864 to S.E.) and by NARSAD Institute, and by the Center for Biomedical Imaging of the Geneva - Lausanne Universities and the EPFL, as well as the foundations Leenaards and Louis-Jeantet (www.cibm.ch).

References

1. K. C. Murphy and M. J. Owen. Velo-cardio-facial syndrome: a model for understanding the genetics and pathogenesis of schizophrenia. Br J Psychiatry. 2001; 179: 397-402.
2. M. Schaer and S. Eliez. From genes to brain: understanding brain development in neurogenetic disorders using neuroimaging techniques. Child Adolesc Psychiatr Clin N Am. 2007; 16(3): 557-79.
3. D. Gothelf, M. Schaer and S. Eliez. Genes, brain development and psychiatric phenotypes in velo-cardio-facial syndrome. Dev Disabil Res Rev. 2008; 14(1): 59-68.
4. D. Gothelf, S. Eliez, T. Thompson, C. Hinard, L. Penniman, C. Feinstein, et al. COMT genotype predicts longitudinal cognitive decline and psychosis in 22q11.2 deletion syndrome. Nat Neurosci. 2005; 8(11): 1500-2.
5. D. Gothelf, L. Penniman, E. Gu, S. Eliez and A. L. Reiss. Developmental trajectories of brain structure in adolescents with 22q11.2 deletion syndrome: a longitudinal study. Schizophr Res. 2007; 96(1-3): 72-81.
6. R. E. Hoffman and S. K. Dobscha. Cortical pruning and the development of schizophrenia: a computer model. Schizophr Bull. 1989; 15(3): 477-90.
7. M. S. Keshavan, S. Anderson and J. W. Pettegrew. Is schizophrenia due to excessive synaptic pruning in the prefrontal cortex? The Feinberg hypothesis revisited. J Psychiatr Res. 1994; 28(3): 239-65.
8. E. R. Sowell, B. S. Peterson, P. M. Thompson, S. E. Welcome, A. L. Henkenius and A. W. Toga. Mapping cortical change across the human life span. Nat Neurosci. 2003; 6(3): 309-15.
9. N. Gogtay, J. N. Giedd, L. Lusk, K. M. Hayashi, D. Greenstein, A. C. Vaituzis, et al. Dynamic mapping of human cortical development during childhood through early adulthood. Proc Natl Acad Sci U S A. 2004; 101(21): 8174-9.
10. P. Shaw, D. Greenstein, J. Lerch, L. Clasen, R. Lenroot, N. Gogtay, et al. Intellectual ability and cortical development in children and adolescents. Nature. 2006; 440(7084): 676-9.
11. P. Shaw, N. J. Kabani, J. P. Lerch, K. Eckstrand, R. Lenroot, N. Gogtay, et al. Neurodevelopmental trajectories of the human cerebral cortex. J Neurosci. 2008; 28(14): 3586-94.
12. P. M. Thompson, K. M. Hayashi, E. R. Sowell, N. Gogtay, J. N. Giedd, J. L. Rapoport, et al. Mapping cortical change in Alzheimer's disease, brain development, and schizophrenia. Neuroimage. 2004; 23 Suppl 1: S2-18.
13. P. Shaw, K. Eckstrand, W. Sharp, J. Blumenthal, J. P. Lerch, D. Greenstein, et al. Attention-deficit/hyperactivity disorder is characterized by a delay in cortical maturation. Proc Natl Acad Sci U S A. 2007; 104(49): 19649-54.
14. P. Shaw, J. Lerch, D. Greenstein, W. Sharp, L. Clasen, A. Evans, et al. Longitudinal mapping of cortical thickness and clinical outcome in children and adolescents with attention-deficit/hyperactivity disorder. Arch Gen Psychiatry. 2006; 63(5): 540-9.
15. M. K. Chung, S. M. Robbins, K. M. Dalton, R. J. Davidson, A. L. Alexander and A. C. Evans. Cortical thickness analysis in autism with heat kernel smoothing. Neuroimage. 2005; 25(4): 1256-65.
16. N. Hadjikhani, R. M. Joseph, J. Snyder and H. Tager-Flusberg. Abnormal activation of the social brain during face perception in autism. Hum Brain Mapp. 2007; 28(5): 441-9.
17. A. Y. Hardan, S. Muddasani, M. Vemulapalli, M. S. Keshavan and N. J. Minshew. An MRI study of increased cortical thickness in autism. Am J Psychiatry. 2006; 163(7): 1290-2.
18. D. Greenstein, J. Lerch, P. Shaw, L. Clasen, J. Giedd, P. Gochman, et al. Childhood onset schizophrenia: cortical brain abnormalities as young adults. J Child Psychol Psychiatry. 2006; 47(10): 1003-12.
19. G. R. Kuperberg, M. R. Broome, P. K. McGuire, A. S. David, M. Eddy, F. Ozawa, et al. Regionally localized thinning of the cerebral cortex in schizophrenia. Arch Gen Psychiatry. 2003; 60(9): 878-88.
20. C. E. Bearden, T. G. van Erp, R. A. Dutton, H. Tran, L. Zimmermann, D. Sun, et al. Mapping cortical thickness in children with 22q11.2 deletions. Cereb Cortex. 2007; 17(8): 1889-98.
21. C. E. Bearden, T. G. van Erp, R. A. Dutton, A. D. Lee, T. J. Simon, T. D. Cannon, et al. Alterations in Midline Cortical Thickness and Gyrification Patterns Mapped in Children with 22q11.2 Deletions. Cereb Cortex. 2008.
22. M. Debbane, B. Glaser, M. K. David, C. Feinstein and S. Eliez. Psychotic symptoms in children and adolescents with 22q11.2 deletion syndrome: Neuropsychological and behavioral implications. Schizophr Res. 2006; 84(2-3): 187-93.

23. B. Glaser, M. Debbane, C. Hinard, M. A. Morris, S. P. Dahoun, S. E. Antonarakis, et al. No evidence for an effect of COMT Val158Met genotype on executive function in patients with 22q11 deletion syndrome. Am J Psychiatry. 2006; 163(3): 537-9.
24. M. Schaer, J. E. Schmitt, B. Glaser, F. Lazeyras, J. Delavelle and S. Eliez. Abnormal patterns of cortical gyrification in velo-cardio-facial syndrome (deletion 22q11.2): an MRI study. Psychiatry Res. 2006; 146(1): 1-11.
25. J. Zinkstok, N. Schmitz, T. van Amelsvoort, M. Moeton, F. Baas and D. Linszen. Genetic variation in COMT and PRODH is associated with brain anatomy in patients with schizophrenia. Genes Brain Behav. 2008; 7(1): 61-9.
26. T. van Amelsvoort, J. Zinkstok, M. Figee, E. Daly, R. Morris, M. J. Owen, et al. Effects of a functional COMT polymorphism on brain anatomy and cognitive function in adults with velo-cardio-facial syndrome. Psychol Med. 2008; 38(1): 89-100.
27. M. Wilke, J. H. Sohn, A. W. Byars and S. K. Holland. Bright spots: correlations of gray matter volume with IQ in a normal pediatric population. Neuroimage. 2003; 20(1): 202-15.
28. S. Frangou, X. Chitins and S. C. Williams. Mapping IQ and gray matter density in healthy young people. Neuroimage. 2004; 23(3): 800-5.
29. K. L. Narr, R. P. Woods, P. M. Thompson, P. Szeszko, D. Robinson, T. Dimtcheva, et al. Relationships between IQ and regional cortical gray matter thickness in healthy adults. Cereb Cortex. 2007; 17(9): 2163-71.
30. A. M. Fjell, K. B. Walhovd, I. Reinvang, A. Lundervold, D. Salat, B. T. Quinn, et al. Selective increase of cortical thickness in high-performing elderly–structural indices of optimal cognitive aging. Neuroimage. 2006; 29(3): 984-94.
31. H. M. Lachman, B. Morrow, R. Shprintzen, S. Veit, S. S. Parsia, G. Faedda, et al. Association of codon 108/158 catechol-O-methyltransferase gene polymorphism with the psychiatric manifestations of velo-cardio-facial syndrome. Am J Med Genet. 1996; 67(5): 468-72.
32. H. D. Rosas, A. K. Liu, S. Hersch, M. Glessner, R. J. Ferrante, D. H. Salat, et al. Regional and progressive thinning of the cortical ribbon in Huntington's disease. Neurology. 2002; 58(5): 695-701.
33. X. Han, J. Jovicich, D. Salat, A. van der Kouwe, B. Quinn, S. Czanner, et al. Reliability of MRI-derived measurements of human cerebral cortical thickness: the effects of field strength, scanner upgrade and manufacturer. Neuroimage. 2006; 32(1): 180-94.
34. A. M. Dale, B. Fischl and M. I. Sereno. Cortical surface-based analysis. I. Segmentation and surface reconstruction. Neuroimage. 1999; 9(2): 179-94.
35. B. Fischl, A. Liu and A. M. Dale. Automated manifold surgery: constructing geometrically accurate and topologically correct models of the human cerebral cortex. IEEE Trans Med Imaging. 2001; 20(1): 70-80.
36. B. Fischl and A. M. Dale. Measuring the thickness of the human cerebral cortex from magnetic resonance images. Proc Natl Acad Sci U S A. 2000; 97(20): 11050-5.
37. P. Shaw, J. P. Lerch, J. C. Pruessner, K. N. Taylor, A. B. Rose, D. Greenstein, et al. Cortical morphology in children and adolescents with different apolipoprotein E gene polymorphisms: an observational study. Lancet Neurol. 2007; 6(6): 494-500.
38. S. Eliez, J. E. Schmitt, C. D. White and A. L. Reiss. Children and adolescents with velocardiofacial syndrome: a volumetric MRI study. Am J Psychiatry. 2000; 157(3): 409-15.
39. W. R. Kates, C. P. Burnette, B. A. Bessette, B. S. Folley, L. Strunge, E. W. Jabs, et al. Frontal and caudate alterations in velocardiofacial syndrome (deletion at chromosome 22q11.2). J Child Neurol. 2004; 19(5): 337-42.
40. W. R. Kates, C. P. Burnette, E. W. Jabs, J. Rutberg, A. M. Murphy, M. Grados, et al. Regional cortical white matter reductions in velocardiofacial syndrome: a volumetric MRI analysis. Biol Psychiatry. 2001; 49(8): 677-84.
41. T. J. Simon, L. Ding, J. P. Bish, D. M. McDonald-McGinn, E. H. Zackai and J. Gee. Volumetric, connective, and morphologic changes in the brains of children with chromosome 22q11.2 deletion syndrome: an integrative study. Neuroimage. 2005; 25(1): 169-80.
42. T. van Amelsvoort, E. Daly, D. Robertson, J. Suckling, V. Ng, H. Critchley, et al. Structural brain abnormalities associated with deletion at chromosome 22q11: quantitative neuroimaging study of adults with velo-cardio-facial syndrome. Br J Psychiatry. 2001; 178: 412-9.
43. K. Im, J. M. Lee, O. Lyttelton, S. H. Kim, A. C. Evans and S. I. Kim. Brain Size and Cortical Structure in the Adult Human Brain. Cereb Cortex. 2008.
44. M. Schaer, M. B. Cuadra, L. Tamarit, F. Lazeyras, S. Eliez and J. P. Thiran. A surface-based approach to quantify local cortical gyrification. IEEE Trans Med Imaging. 2008; 27(2): 161-70.
45. I. Feinberg. Schizophrenia: caused by a fault in programmed synaptic elimination during adolescence? J Psychiatr Res. 1982; 17(4): 319-34.
46. S. E. Arnold. Neurodevelopmental abnormalities in schizophrenia: insights from neuropathology. Dev Psychopathol. 1999; 11(3): 439-56.
47. S. Micheloyannis, E. Pachou, C. J. Stam, M. Breakspear, P. Bitsios, M. Vourkas, et al. Small-world networks and disturbed functional connectivity in schizophrenia. Schizophr Res. 2006; 87(1-3): 60-6.
48. Y. Liu, M. Liang, Y. Zhou, Y. He, Y. Hao, M. Song, et al. Disrupted small-world networks in schizophrenia. Brain. 2008; 131(Pt 4): 945-61.

49. M. Kubicki, R. McCarley, C. F. Westin, H. J. Park, S. Maier, R. Kikinis, et al. A review of diffusion tensor imaging studies in schizophrenia. J Psychiatr Res. 2007; 41(1-2): 15-30.
50. R. E. Hoffman and T. H. McGlashan. Synaptic elimination, neurodevelopment, and the mechanism of hallucinated "voices" in schizophrenia. Am J Psychiatry. 1997; 154(12): 1683-9.
51. R. E. Hoffman and T. H. McGlashan. Using a speech perception neural network computer simulation to contrast neuroanatomic versus neuromodulatory models of auditory hallucinations. Pharmacopsychiatry. 2006; 39 Suppl 1: S54-64.
52. T. H. McGlashan and R. E. Hoffman. Schizophrenia as a disorder of developmentally reduced synaptic connectivity. Arch Gen Psychiatry. 2000; 57(7): 637-48.
53. M. S. Keshavan and G. E. Hogarty. Brain maturational processes and delayed onset in schizophrenia. Dev Psychopathol. 1999; 11(3): 525-43.
54. T. van Amelsvoort, E. Daly, J. Henry, D. Robertson, V. Ng, M. Owen, et al. Brain anatomy in adults with velocardiofacial syndrome with and without schizophrenia: preliminary results of a structural magnetic resonance imaging study. Arch Gen Psychiatry. 2004; 61(11): 1085-96.
55. K. B. Walhovd, A. M. Fjell, A. M. Dale, B. Fischl, B. T. Quinn, N. Makris, et al. Regional cortical thickness matters in recall after months more than minutes. Neuroimage. 2006; 31(3): 1343-51

Part III

Discussion & Perspectives

Main contributions

Taken together, the 8 articles presented in the *Results* section achieve the following original contributions:

- **Demonstration of specific reductions of the hippocampal body, posterior fusiform gyrus and anterior cingulate cortex in patients affected by 22q11DS,** which is relevant for their cognitive and psychiatric phenotype
- **Development of a new method for the quantification of local cortical folding,** which is now available freely for the scientific community through *FreeSurfer* software
- **Demonstration of cortical folding abnormalities in 22q11DS,** which suggest early abnormal brain development in the syndrome
- **Demonstration of a rostro-caudal and latero-medial gradient in volumetric alterations,** the distribution of which is highly suggestive of abnormal cerebral growth along the territory of the posterior cerebral artery
- **Demonstration of a deleterious effect of congenital heart disease on brain structure in 22q11DS,** which further our understanding of the pathogenesis of acquired brain injury related to CHD and its surgery
- **Demonstration of abnormal patterns of cortical thickness during pre-adolescence and adolescence,** which suggest abnormal brain maturation in patients with 22q11DS, in turn relevant for their susceptibility to develop schizophrenia

Given that each article include its own discussion, this last part of the thesis will elaborate series of links between these findings, and some perspectives for future research will be delineated. A first chapter brings together results on brain structure in 22q11DS. Then, some considerations related to cortical folding and the newly developed algorithm will be addressed.

1 An integrative view on brain alterations in 22q11DS

1.1 Relationship between brain alterations in 22q11DS

In the three first studies (*Studies 1a, 1b & 1c*), we identified reduced volume of specific structures, which we related to specific parts of the cognitive and psychiatric phenotype. *Study 1a* discussed the reduction of the hippocampal body in relation to mnesic impairments presented by affected individuals. *Study 1b* addressed the hypothesis that reduced posterior fusiform gyrus may be responsible for social difficulties in the syndrome. Finally, *Study 1c* provided strong evidence of a relationship between cingulate gyrus volume and executive dysfunction or psychosis in patients with 22q11DS. Together, these studies illustrate a scheme common to most ROI studies, in which the structure is *a priori* chosen, given its frequent implication in a specific cognitive process known to be altered in the population of interest. When identified, volumetric changes may be correlated with some cognitive performances, or with the intensity of certain psychiatric symptoms. At the end, these classical ROI studies most often address the potential functional repercussions of the observed volumetric changes.

Conversely, newer methods allow the measurement of structural brain alterations without regional *a priori*. For instance, gyral volumes, cortical thickness and local gyrification in *Studies 4, 5 & 6* were measured over the entire hemisphere, without being bound to arbitrary limits. We believe that such "new generation" studies may change the way researchers will conduct neuroimaging studies and interpret results in the future. Still, structure – function correlation can be conducted, but new possibilities also emerge to elaborate more conceptual links bringing together the different alterations. Indeed, the cortex is a planar structure, so that cortical volume can be approximated as the product of its thickness times its surface. Thanks to the newer three-dimensional methods, it thus becomes possible to identify the determinants of cortical volumetric differences previously observed with older methods.

The relevance of a precise identification of the nature of the alterations underlying volumetric changes relies on the fact that, as discussed in the *Introduction*, thickness and surface

(or folding) are distinctly regulated during brain development. Therefore, the identification of the nature of structural alterations help to build hypotheses on the etiopathogenesis of abnormal brain development in a given condition.

1.2 Identify the pathways leading to brain alterations in 22q11DS

Nature of the anomalies

In Study 4,
we demonstrated a highly significant reduction to cortical folding and surface area in patients with 22q11Ds and controls, which was largely affecting the medial view of the brain, but also the dorsal frontal and parietal regions bilaterally, along with the parieto-temporo-occipital junction in the right hemisphere. This pattern of surface reduction is reminiscent of the volumetric reduction observed by previous volumetric studies or VBM studies in the syndrome (Eliez et al., 2000; Kates et al., 2001; Simon et al., 2005), and to the pattern of regional reductions that we observed in a larger overlapping sample in *Study 5*. The lateral and medial reduction in cortical surface may indeed be the primary determinant of previously observed parietal reduction. The fact that these reductions are already observed in children with the syndrome, along with the fact that gyrification is mostly determined early, point to an early cause of the parietal abnormalities, rather than to a neurodegenerative process. For instance, abnormal control of asymmetric division of neuronal precursors, or disrupted neuronal migration may be responsible for the observed anomalies.

In Study 6,
we observed that preadolescents with 22q11DS show larger thickness values in the frontal regions, whereas the same clusters converged to similar or even lower thickness by the end of adolescence. Our preliminary longitudinal data confirmed the direction of a greater cortical thickness loss during adolescence, although the difference did not reach significance in this small sample. Observation of a greater thickness loss in the frontal region corroborates a previous volumetric longitudinal observation in the syndrome. Gothelf and colleagues (2005) observed a larger prefrontal reduction in 24 adolescents with 22q11DS compared to 23 with idiopathic developmental disabilities.

The above considerations illustrate how volumetric changes may be mediated by distinct pathological processes at different time of the individual's development. We strongly believe that a precise identification of the mechanisms responsible for the brain anomalies will be crucial for building future therapeutic strategies.

Localization of the anomalies

The regional distribution of the anomalies is another key factor that can help to unravel the etiology and / or the timing of disrupted brain development. Among the studies presented in the *Results* section, the following three examples illustrate how we grounded hypotheses based on the localization of lesions:

In *Study 1c,*
we showed reduced volume of the cingulate gyrus, which we confirmed more recently in *Study 5* using the Desikan's parcellation method (Desikan et al., 2006) over a larger sample

of subjects. Given its localization, cingulate reduction may be another midline alterations in the syndrome. Midline anomalies in the brain of patients with 22q11DS include the cavum septum pellucidum, vermis of the cerebellar vermis, and frequent cysts around the frontal horns of the ventricle (Mitnick et al., 1994; Chow et al., 1999; van Amelsvoort et al., 2001; Shashi et al., 2004). Non-cerebral midline malformations are also frequent in 22q11DS, encompassing cleft palate, cardiac malformations and thymic hypoplasia (Shprintzen et al., 1978). Such a high prevalence of anomalies along the midline in 22q11DS potentially points to a common etiology. The midline tissues that are frequently involved in the syndrome are derived from the rostral neural crest; genetically induced perturbation of early neural crest development may thus explain the higher incidence of the malformations associated with 22q11DS (Scambler, 2000). To confirm a common etiology of the cerebral midline anomalies, future research might correlate their intensity, with the idea that a correlation between them supports a shared origin. Alternatively, studies in mouse models of 22q11.2 deletion may also help to address this issue.

In *Study 5,*
we measured regional cortical volumes over the entire brain of 61 patients with 22q11DS compared to 80 healthy controls. Thanks to the increased precision of this method, we were able to confirm the rostro-caudal gradient in brain alterations previously suggested by lobar and regions-of-interest studies. Further, we revealed a previously unreported latero-medial gradient in cortical reductions. As a result, we observed that cortical reductions were strikingly distributed along the territory supplied by the posterior cerebral artery. In light of the high frequency of vascular malformations in the syndrome (Shprintzen, 2000) and of a previous angiographic observation (Chow et al., 1999), we speculated that reduced blood perfusion pressure along the territory of the cerebral posterior artery may be responsible for impaired cortical growth in these regions (see also Figure 1.1). We suggest that future studies in the syndrome collect angiographic data, to be able to explore the relationship between cerebrovascular anomalies and cortical volumes.

In *Study 4 & 5,*
we evidenced brain anomalies that were exclusively related to the presence of congenital heart disease (CHD) in 22q11DS. Namely, we observed that cortical reductions at the superior frontal and middle temporal gyri, along with parahipocampal reduction, were associated with CHD. We also reported decreased gyrification at the parieto-occipital (PTO) junction of patients with compared to without CHD. We suggested that the distribution of the cortical reductions and reduced gyrification at the PTO jonction both points to the location of the watershed territories of major cerebral arteries. If the superior frontal, middle temporal and PTO junction are three distributed at the intersection between territories supplied by three main arteries, we believe that methodological specificities may explain why the two methods did not reveal exactly the same distribution of the alterations. Indeed, the superior frontal and the middle temporal gyri are the only two parcels for which their entire length (as measured by the Desikan's method) is located at the junction between two arterial territories. Conversely, as discussed in the validation article *Study 3*, the local GI algorithm is not very sensitive to gyrification differences in regions where the hull has a high curvature, such as the superior sagittal vault, and maybe also near to the inferior temporal gyrus. As a result, *l*GI may not be able to catch any difference in these areas, whereas it may be more sensitive than the volumetric parcellation at the PTO junction, where volume differences may be diluted into several parcels.

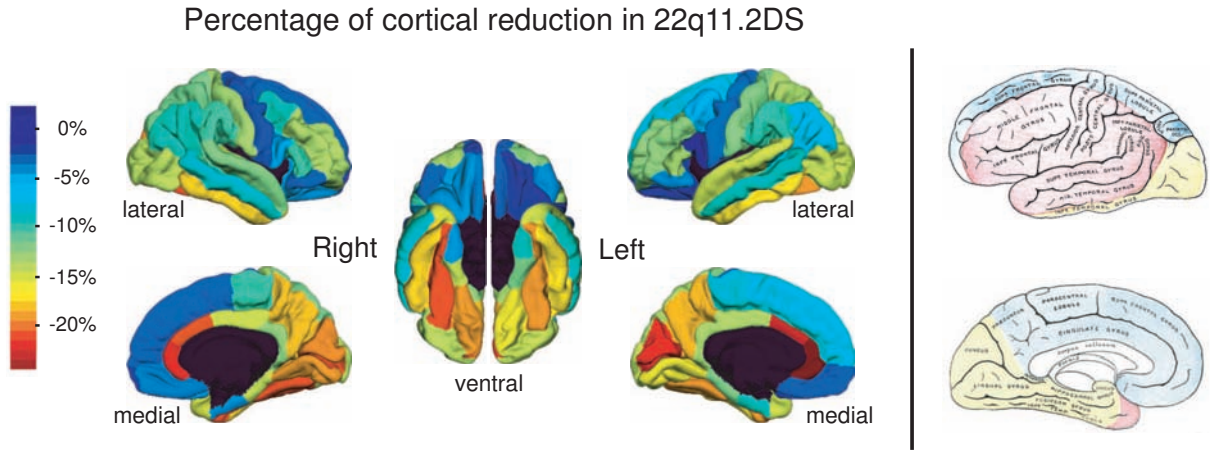

Figure 1.1: *Reduced cortical volumes, reproduced from Study 5. The major arterial territories are depicted on the right panel (reproduced from the book "Henry Gray's Anatomy of the Human Body"). Aside from the cingulate, all cortical regions that show disproportionate reduction (green to red) are distributed along the territory supplied by the posterior cerebral artery (in yellow on the right panel).*

Within group factors

Finally, within group factors are also one important factor that may further our understanding of the pathogenesis of brain alterations in 22q11DS or in other conditions.

In *Study 4 & 5,*
we provided compelling that congenital heart disease affects brain structure and is associated with poorer cognitive performances in adults (*Study 4 & 5*). In particular, the 6.9% cerebral reduction in patients with 22q11DS without CHD strikingly contrasts with the 16.9% reduction in those with CHD. As a result, we can speculate that CHD have largerly contributed to exacerbate the pattern of volumetric findings previously reported in the syndrome. We recommend that future research carefully collect informations about cardiac status in patients with 22q11DS, to distinguish the contribution of the deletion and the contribution of CHD on altered brain structures. Alternatively, it may also be interesting to quantify brain structure using similar methods in non-syndromic patients with CHD.

In *Study 6,*
we explored cortical thickness differences related to genetic polymorphism of the catecholamine-O-methyltransferase (COMT). Given the potential implication of dopamine in schizophrenia pathogenesis, genetic polymorphism of the COMT, involved in dopamine degradation, has received considerable interest in 22q11DS (Gothelf et al., 2005; Glaser et al., 2006; Kates et al., 2006; van Amelsvoort et al., 2008; Zinkstok et al., 2008) and in schizophrenia (Zinkstok et al., 2006; McIntosh et al., 2007). In the thickness article (*Study 6*), we did not observe major clusters of cortical thickness differences, nor divergent trajectories of cortical thickness changes with age related to COMT polymorphism. Of note, we also did not observe significant differences in lobar brain volumes, nor gyrification according to COMT polymorphism. The absence of a prominent effect of the Val or Met allele diverges from

observation by others (Gothelf et al., 2005; Kates et al., 2006; Zinkstok et al., 2008; van Amelsvoort et al., 2008), but is consistent with some negative reports (Glaser et al., 2006; Mata et al., 2008). Specifically, using a sub-sample of the group of patients examined in *Study 6*, we previously reported no difference in cognitive function according to COMT polymorphism (Glaser et al., 2006). The inconsistencies in COMT findings are puzzling, and one could wonder whether the genetic polymorphism could not be modulated by other factors. In this direction, Mata et al (2008) recently suggested that medication could be one interaction, as suggested by the exacerbation of cognitive difference associated with COMT polymorphism following 6 months of antipsychotic treatment (Woodward et al., 2007). The absence of a preponderant COMT difference that we observed in a mostly untreated group of patients corroborates the hypothesis that medication may be one factor potentiating the genetic polymorphism.

1.3 Identify risk factors associated with the development of psychosis

In *Study 6,*
we measured cortical thickness changes over the course of brain maturation from childhood to adulthood. Our cross-sectional results, and the direction of longitudinal changes, provided compelling evidence for abnormal cortical maturation in the syndrome. We observed a thicker cortex exclusively in pre-adolescents with 22q11DS, which completely disappeared thereafter. We suggested that the observed thickness differences reflected (1) a delayed cortical maturation (retarded onset of thinning) and (2) abnormal pruning of the cortical circuitry, which is relevant for the susceptibility to develop schizophrenia. Indeed, increased rate of pruning is consistent with neuropathological studies that observed reduced neuropil in the brain of patients with schizophrenia (Arnold, 1999). We also discussed how cortical thickness changes fit the conceptual framework that Hoffman & McGlashan (1997; 2006) built based on their neural network models. They suggested that the baseline level of connections may be a protective factor. Accordingly, we identified that children and adolescents who performed better on IQ scores had thicker cortices than those with lower performances. A second determinant of prognosis suggested by Hofman & McGlashan is the faster rate of pruning, which seems associated with the onset of hallucinatory symptomatology in their neural network models. We similarly observed that patients with 22q11DS tend to show faster cortical thinning than controls during adolescence, corroborating a previous volumetric observation by Gothelf and colleagues (2005). We also showed that adults patients with 22q11DS and without schizophrenia showed preserved thickness compared to those with schizophrenia. Thus, abnormal pruning potentially represent a central factor in the pathogenesis of schizophrenia. Future longitudinal studies following the course of cortical changes during large periods are required to confirm the association between exaggerated pruning and the onset of schizophrenia. In the meantime, the search for factors interacting with synaptic pruning may serve as a guide for future targeted preventions.

Possible causes for an abnormal pruning in 22q11DS
If a faster pruning seems relevant for the psychiatric symptomatology in 22q11DS, what are the possible underlying mechanisms triggering it? Two models have been largely discussed

in the pathogenesis of schizophrenia. Feinberg (1982) extensively discussed how abnormal cortical maturation may participate to the pathogenesis of schizophrenia, as a "late neurodevelopmental model". By contrast, Weinberger (1987) proposed that most of the brain anomalies that predispose to later onset of schizophrenia are caused by a defect in early brain development (the "neurodevelopmental hypothesis"). A few years later, Keshavan et al. (1994; 1999) conciliated these two models in a single unified framework, proposing that abnormal pruning in schizophrenia is caused by the interaction of an early, pre- or perinatal, lesion with the critical period of pruning in adolescence.

In 22q11DS, an early, genetically-driven, insult is clearly pertinent, given the association of the syndrome with physical anomalies such as cardiac and vascular malformations, electrolytic disorder, or immune deficiency. Aside from our observations of abnormal gyrification, other neuroanatomical findings associated with 22q11DS puts forward an early abnormal neurodevelopment, e.g. polymicrogyria (Robin et al., 2006), enlarged sylvian fissure (Bingham et al., 1997), or cavum pellucidum (Chow et al., 1999). Various mechanisms have been proposed to answer the question as to how, in 22q11DS or schizophrenia, an early adversity interacts with the normal course of brain maturation, and causes abnormal, excessive, pruning. Given that brain development follows highly complex series of sequential and parallel events, Keshavan et al. (1999) suggested that a disruption in one step will impair the correct evolution of all subsequent steps. If the specific factors involved in such a deleterious cascade culminating in accelerated pruning and emergence of symptoms remain to be elucidated, the authors proposed that dysfunction of the glutamatergic or dopaminergic systems both represents pertinent candidates.

Gyrification & psychosis

In the studies presented in the *Results* section, we did not address the question as to how gyrification may differ according to psychosis in our sample of participants. Here, we present these additional statistical analyses. From the cohort of 44 patients presented in the *l*GI comparisons *Study 4*, we selected all patients who presented psychosis, as defined by the presence of both delusions and hallucinations. Twenty-two psychotic patients were identified, aged from 10 to 37 years old. These 22 psychotic subjects were the individually matched for age and gender with 22 healthy participants from the pool of controls, and *l*GI was compared on a vertex-wise basis exactly as reported in *Study 4*. As shown on Figure 1.2, patients with psychosis presented a highly significant[1] *l*GI reduction. On the medial aspect of the brain, the reduction observed in psychotic patients was relatively comparable to the one observed when comparing the entire sample of patients with 22q11DS and controls (i.e. extensively affecting the medial posterior region). However, we observed a different pattern of reduction on the lateral view of both hemispheres, with frontal regions being more largely reduced than what we observed in the whole sample. No cluster of increased gyrification in the psychotic compared to control group was observed. The pattern of reduced gyrification over the medial aspect of the brain further supports an implication of the cingulate gyrus in the psychotic symptomatology, as discussed in *Study 4*. Further, specific frontal *l*GI decrease observed in psychotic patients with 22q11DS corroborates previously published studies in non-syndromic patients with schizophrenia compared to controls (Kulynych et al, 1997; Sallet et al., 2003; Jou et al., 2005).

[1] corrected for multiple comparisons using a False Discovery Rate of FDR<0.01

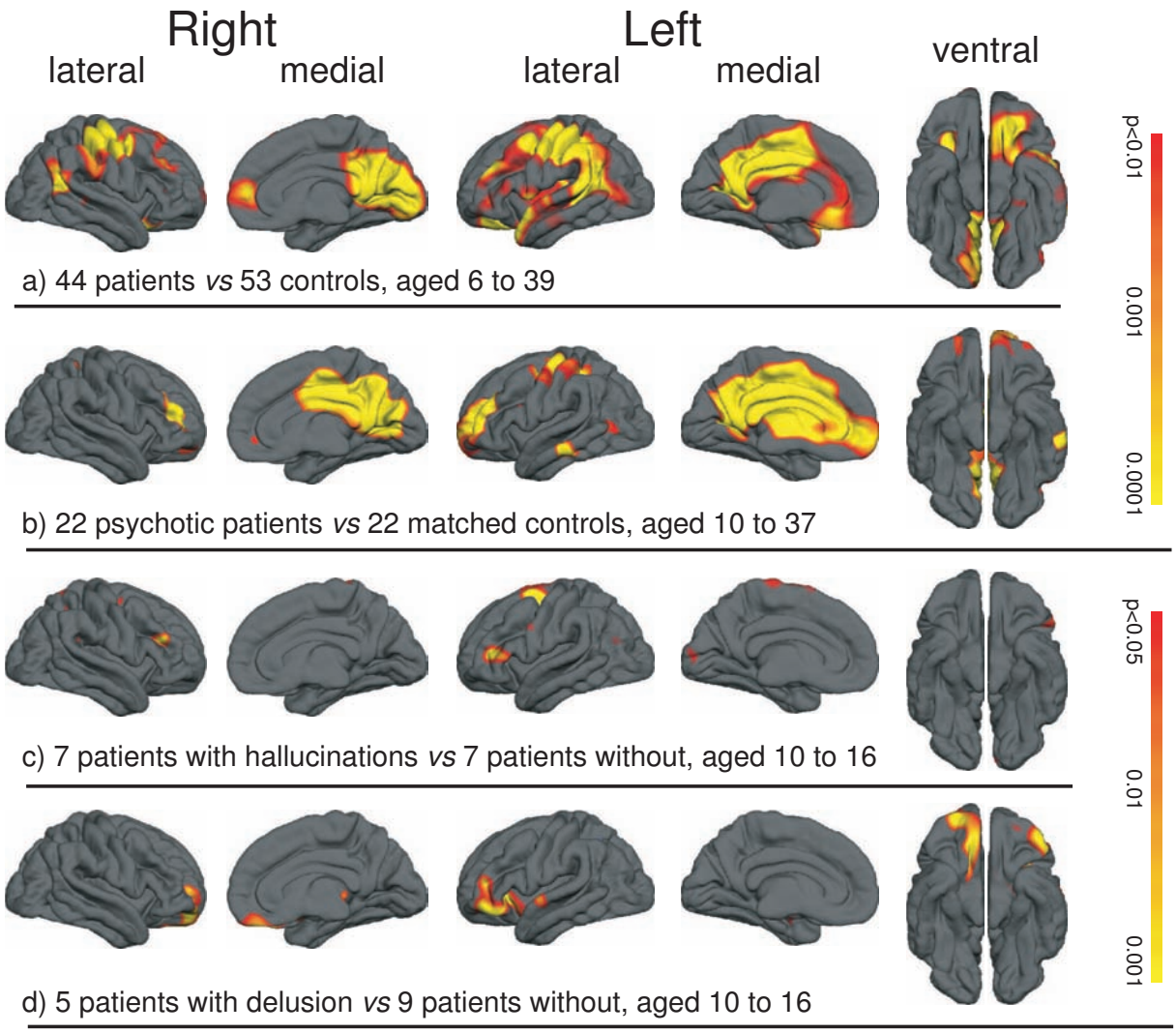

Figure 1.2: *lGI comparisons according to psychosis in 22q11DS. The first row depicts comparisons between the entire sample of patients and controls. The second shows only patients with psychotic symptoms compared to controls. These two comparisons were corrected for multiple comparisons using a False Discovery threshold of FDR<0.01. The last two rows depict gyrification changes associated with psychotic symptoms within the syndrome, during the prodromal period of 10 to 16 years old.*

In subsequent exploratory analysis, we aimed at comparing patients with 22q11DS with and without psychotic symptoms. For this within group analysis, we chose to keep only patients between 10 and 16 years old, i.e. over the prodromal period during which patients usually show the first symptoms[2]. In our sample of patients between 10 and 16 years old, the first analysis compared those who present hallucinations (n=7) compared to those who do not (n=7). A second analysis compared those who showed delusions (n=5) to those without (n=9). In both cases, these exploratory comparisons on small sample could not be

[2]In addition to allow for a focus on structural changes associated with the very first symptoms, this restricted age range also permitted the obtention of age-matched sub-groups within the syndrome

corrected for multiple comparisons, but nevertheless yielded interesting results (see Figure 1.2). Patients with hallucinations showed reduced gyrification at the right middle frontal and left frontal superior gyri, whereas a large cluster of reduced right prefrontal gyrification was observed in patients with hallucinations compared to those without. But the most interesting finding was probably reduced gyrification at the left inferior frontal gyrus in both comparisons, close to the Broca's area. Reduced gyrification around the Broca's area corroborates recent results by Cachia et al. (2008) in schizophrenic patients with resistant auditory hallucinations. Further, the implication of language areas reminds a large body of literature pointing to disrupted semantic integration in schizophrenia (reviewed by (Kuperberg, 2008)).

Turning to mechanisms underlying reduced gyrification in patients with psychosis, a lot of questions remain open. In particular, it remains difficult to distinguish whether the reduced gyrification observed here constitutes a vulnerability which is determined early in development. Alternatively, the restricted size of the clusters also makes it possible that the observed changes correspond to remodeling of the cortical surface occurring during adolescence (i.e. at the time of the observation). We are currently analyzing longitudinal data to address this issue. In particular, we are interested in knowing whether the *l*GI algorithm is able to reflect and quantify cortical surface changes associated with maturation (i.e. a sort of "tangential atrophy" by contrast to the classically measured "perpendicular" or "radial" cortical thinning). In addition to require longitudinal studies to be verified, the present question also raises the necessity of applying *l*GI to larger samples of typically developing subjects or individuals with various neurodevelopmental or neurodegenerative conditions, to understand more deeply its behavior.

2 local Gyrification Index (*l*GI), a new method

To better understand what *l*GI can bring to further our understanding of gyrification, the algorithm should be applied to large cohorts of individuals. To achieve a large applications, we employed two strategies. First, thanks to *FreeSurfer*'s developers, the *l*GI method is now freely available for the scientific community. Second, we are currently quantifying *l*GI in our own cohorts, as well as on data provided by diverse collaborations.

FreeSurfer software, distributed by the Athinoula Center for Biomedical Imaging from the Massachusetts Harvard Hospital (MGH) and Massachusetts Institute of Technology (MIT), is among the most popular neuroimaging software. Having met *FreeSurfer*'s developers at the *Human Brain Mapping* conference in Chicago last year, I was proposed the opportunity to include the local Gyrification Index code in their software. After two weeks in Boston in last october and some e-mails exchange, we were able to full integrate the method within the *FreeSurfer*'s pipeline. Even if my code was originally written in Matlab, thanks to a partial rewritting, the *l*GI method is now a combination of Matlab and C code routines. The access to the source code allowed a drastic reduction in the time processing of the highly iterative *l*GI computation[1], which was reduced from about 2 days of processing to 3 hours per hemisphere! This reduction was mostly permitted by the use of the surfaces' topological information embedded in the hidden *FreeSurfer*'s file format, that previously had to be entirely recalculated in Matlab with highly time-consuming loops. Local GI algorithm was included as a beta version in *FreeSurfer*'s release on March 31, 2008; the bug-free version was released on May 6, 2008. Information for users is available on the wiki page, a screenshot of which is depicted on Figure 2.1. As shown by numerous questions on the mailing list, *l*GI already received a large interest. We hope that the wide distribution ensured by the software will permit its application in various pathological conditions, thereby increasing the knowledge of the algorithm's behavior. Further, the integration of the *l*GI method within this highly dynamic platform will also ensure continuity of technical developments.

[1] obtaining the entire *l*GI map over one hemisphere requires about 800 to 1'200 computations

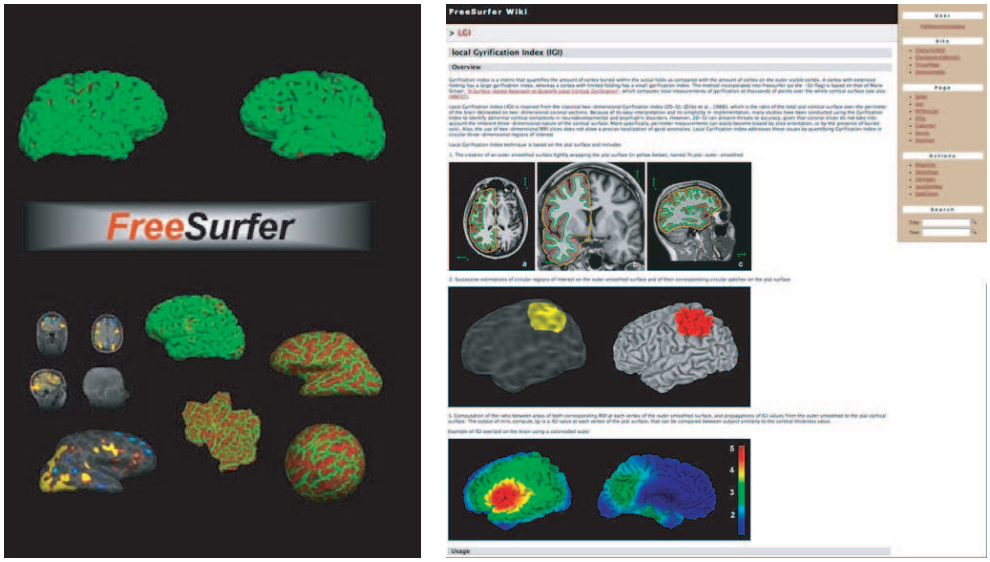

Figure 2.1: *Screenshot from the FreeSurfer's lGI wiki page, which can be found at* ***https://surfer.nmr.mgh.harvard.edu/fswiki/LGI***

In addition to provide the *l*GI algorithm to other groups through *FreeSurfer*, we are also currently applying it to our own data, and to MRI data in collaboration with other groups. Before quantifying *l*GI in diverse pathological conditions, we will determine the factors that influence *l*GI in typically developing children, adolescents and adults.

2.1 Determinants of *l*GI in healthy participants

As a first step toward the delineation of the factors correlated with average *l*GI value, we measured *l*GI in the sample of healthy participants from our 22q11DS Geneva cohort. This sample of control participants is the one used in *Studies 5 & 6*, encompassing 44 females and 36 males, with a mean age of 15.9 ±8.4 (range: 6 – 39) and an average IQ of 111.7 ±12.8.

To quantify the contribution of various parameters on *l*GI value, we conducted a stepwise multiple regression model. Average *l*GI was used as the dependent variable, and total brain volume, age, gender, average hemispheric thickness and IQ were the independent variables. Among the 5 independent variables included in the regression analysis, we observed that only age, brain volume and average thickness contributed significantly to the variance in average *l*GI. These three variables combined accounted for 60.9% and 57.6% of the variance in average *l*GI values of the left and right hemispheres, respectively. In both hemispheres, the independent factors affecting *l*GI were entered in the following order (see Table 2.1): first, a negative correlation with age, as the main determinant of average local Gyrification Index, followed by a positive correlation with cerebral volume, and a negative correlation with mean hemispheric cortical thickness. Gender and IQ did not significantly contribute to the final model. Some elements of discussion related to the three determinants of *l*GI follows.

	Right hemisphere			Left hemisphere		
	Adj. R^2	β	p	Adj. R^2	β	p
1. Age	0.452	-0.853	<0.001	0.412	-0.819	<0.001
2. Brain Volume	0.575	0.356	<0.001	0.543	0.375	<0.001
3. Mean Thickness	0.609	-0.307	0.007	0.576	-0.306	0.010

Table 2.1: Hierarchical contributions to the variance in average lGI
Adjusted R^2 measure the proportion of the variance accounted for by the inclusion of each additional independent variables on lGI values. β denotes standardized correlation coefficients.

First determinant: Age

The regression model presented in Table 2.1 confirm the dynamic change in gyrification with age previously observed in *Study 4*. The intensity of the observed association, as the primary determinant of *l*GI, strikingly contrasts with previous large-scale 2D studies that consistently report a stable GI throughout brain development and maturation (Armstrong et al., 1995; Zilles et al., 1988). During the first years of life, the relative stability of the degree of folding has been explained by "compensation" between sulci (i.e. sulcal depth is counterbalanced by neighboring sulci during brain growth) (Armstrong et al., 1995). However, no GI studies have focused on gyrification during late childhood and adolescence, when major maturation processes take place. Here, we observe that *l*GI significantly decreases with age, suggesting that the cortical surface undergoes major continuous remodeling as it matures. However, as mentioned in the first chapter of the *Discussion*, the nature of the processes underlying this linear decrease remains difficult to explain and may reflect a sort of "tangential" cortical maturation. Other authors have observed sulcal shape modifications after the age of 20 years (Kochunov et al., 2005; Magnotta et al., 1999). Further, the simultaneous cortical thinning and brain growth driven by myelination observed during brain maturation (Sowell et al., 2003) may exert mechanical constraint on the sulcal shape. It could be postulated that the pressure exerted by the expansion of the underlying axonal mass may deform the thinning cortex outwardly, thereby decreasing sulcal depth. To explore these hypotheses, we are currently conducting intra-individual analyses to determine whether *l*GI changes occur at the same time and in the same regions where cortical thickness loss is observed.

Second determinant: Brain Volume

Our results also provide evidence that Gyrification Index in humans is affected by brain volume. As the divisor in the Gyrification Index quotient is the global brain perimeter, one could expect that the resulting ratio would already account for inter-individual differences in brain volume. However, the positive correlation between GI and cerebral volume means that bigger brains demonstrate a larger percentage of cortical area hidden within the sulci. Studies of comparative neuroanatomy and fractal geometry provide ways for understanding the relationship between gyrification and cerebral volume.

As mentionned in the *Introduction* part, comparative studies of mammalian brains observed

that bigger brains, such as those of dolphins or elephants, were often highly convoluted (Jerison et al., 1961; Haug, 1987). Following these observations, quantitative assessments of the relationship between gyrification and volume across species have proposed the use of fractal geometry to characterize brain architecture (Hofman, 1991). According to geometric principles, the relationship of any object's area with its volume is described by the law:

$$\mathbf{Area} = \mathbf{Volume}^{\mathbf{D/3}} \tag{2.1}$$

where D is the surface dimension.

Simple objects, like a sphere or a cube, follow the rule of geometric similarity; their surface scales to the two thirds power of their volume (D=2). Convoluted, or fractal, objects, are defined as objects for which surface area scale with their volume proportionally larger than the geometric similarity rule would predict (D>2). Fractal surfaces are thus "near-space filling surface" (Mandelbrot, 1982). As remarked by Mandelbrot in its famous treaty "the fractal geometry of nature", quantitative studies of the relationship between cortical surface and brain volume across species beautifully fit in fractal geometry[2]. Solving the above equation, Hofman (1991) indeed estimated D across species at 2.7. In order to further define if the positive correlation between GI and volume may be related to a similar fractal scaling rule, we estimated the surface dimension D in our sample of healthy human brains[3].

Using the same method as Hofman in our sample of 80 healthy subjects, we obtained surface dimension estimates of D=2.61 (adj. R^2=0.89, p<0.01) and D=2.69 (adj. R^2=0.86, p<0.01), respectively for the left and right hemispheres. The surface dimensions observed here in humans is relatively similar to the one estimated by Hofman across species (Hofman, 1991). This makes it tempting to argue that this further confirms that the human brain architecture is, along with other mammalian brains (Hofman, 1991; Zhang & Sejnowski, 2000), governed by a universal scaling rule. However, the surface dimension method requires large variations in area or volume to accurately predict the D value. Box-counting methods for each individual, which may be more appropriate when inter-individuals variations do not encompass large order of magnitude, usually report FD around 2.5 in humans (Im et al., 2006). Nevertheless, the surface dimension equation provide a framework to explain why, by necessity, Gyrification Index would be positively correlated with brain volume. GI is indeed computed as the ratio between the total cortical area (having a surface dimension which we estimated around 2.6) divided by its outer envelope (by definition a simple object, thus more likely to have a surface dimension close from 2). Formally:

$$\mathbf{GI} = \frac{Pial_{area}}{Hull_{area}} = \frac{k_1 V^{\approx 2.6/3}}{k_2 V^{\approx 2/3}} = kV^{\approx 0.6/3} \tag{2.2}$$

[2]And he ironically adds "Knowing that the extent of folding is of purely geometric origin relieves Man from feeling threatened by Dolphins or Whales : they are bigger than us but need not to be more highly evolved."

[3]The method used here for estimating Fractal Dimension, based on the relationship between area and volume, differs from the classical box-counting method that is traditionnally used in clinical studies. To avoid confusion, we have denoted it "surface dimension" (D). More specifically, the box-counting method measures FD for each individual brain, thus resulting in values that can be compared between groups. The measurement of surface dimension presented here and used in comparative neuroanatomy is derived from the area - volume relationship, as described in Mandelbrot (1982) and illustrated in Hofman (1991), and results in a single value for the whole group.

The above equation demonstrates why, with accurate three-dimensional reconstruction, we observe a significant relationship between Gyrification Index and brain volume.

Third determinant: Mean Thickness

As observed in the multiple regression model, another structural determinants of *l*GI is average thickness. We observe a negative correlation between gyrification and mean cortical thickness[4] which recalls the simultaneous observation of a thicker cortex and reduced folding in 22q11DS *(Studies 3 & 6)*. The negative correlation between cortical complexity and thickness is also consistent with observations using Fractal Dimension in healthy individuals (Im et al., 2006). Moreover, similar to the relationship between volume and gyrification, comparative neuroanatomists have also observed, in extreme cases, an inverse relationship between cortical thickness and the degree of folding. For example, dolphins and manatees are cetaceans of similar size, but the thin cortex of dolphins shows a high degree of folding, whereas the very thick cortex of the manatee is almost lissencephalic (Haug, 1987). It is possible that such extreme cases illustrate that thicker cortices are, for purely mechanical reasons, less prone to be highly folded.

Together, both interactions between *l*GI and volume or thickness in healthy brains support the hypothesis that gyrification closely depends upon complex structural constraints, which are not yet fully understood.

Gender & *l*GI

Finally, although gender was not a significant parameter in our regression model, we also observed higher *l*GI values in males than females (detailed values are reported in *Study 4*). Gender differences in gyrification have already been reported using other three-dimensional measurements of cortical complexity. Higher Fractal Dimension (Luders et al., 2004) and increased curvature (Luders et al., 2006) were observed in females compared to males. As females have smaller brain volumes than males (Giedd et al., 1997), increased spatial frequency of fissuration of the brain surface in females has been suggested as a compensatory mechanism to increase cortical area in their smaller brains (Luders et al., 2004). Conversely, our results of smaller GI in females to males show that the higher fissuration and curvature previously reported in the cortex of females does not allow for increased area. On the contrary, females do not only have smaller absolute cortical surfaces, but also proportionally smaller cortical area than males. Despite this absolute gender difference, it is interesting that gender does not appear as a significant determinant of Gyrification Index in our hierarchical regression model. It may be that gender differences in gyrification are primarily driven by differences in brain volume and cortical thickness, rather than correspond to a specific sexual dimorphism of the brain.

[4]having age as another parameter in the same model allows to account for the effect of age on cortical thickness, and thus the remaining association between *l*GI and thickness remains significant after removing the effect of age on both variables

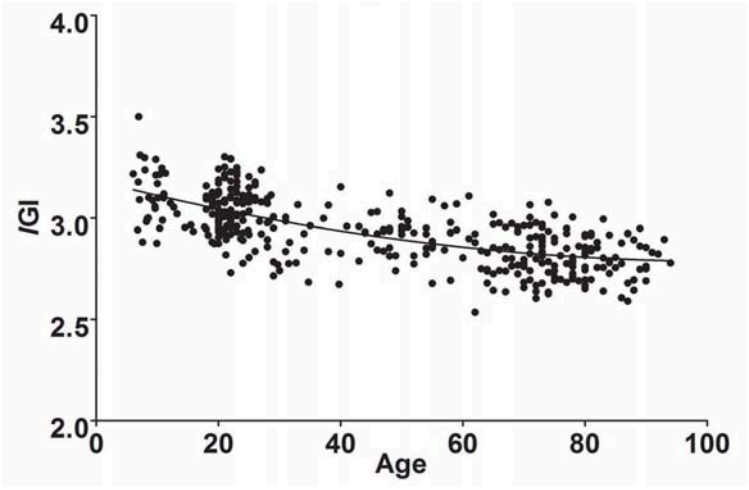

Figure 2.2: *Average lGI in the left hemisphere as a function of age. Measurements are shown for 380 healthy participants aged from 6 to 100 years old (combination of our own data and the OASIS cohort)*

In an attempt to confirm the above considerations in a larger sample of subjects, we are currently analyzing data from a normative cohort including more than 300 normative subjects, aged 18 to 96. The Open Acess Series of Imaging Studies (OASIS, www.oasis-brains.org) is a project of free normative MRI dataset initiated by Dr. Randy Buckner at the Howard Hughes Medical Institute (HHMI) at Harvard University, the Neuroinformatics Research Group (NRG) at Washington University School of Medicine, and the Biomedical Informatics Research Network (BIRN). Thanks to the collaboration with the MGH who provided the entire dataset processed in *FreeSurfer* pipeline, we measured *l*GI in these individuals. Preliminary results confirm the linear *l*GI decrease with age (see Figure 2.2); further explorations are under way.

In addition to identify normal influences on gyrification by "looking back" from grown-up brains and infer what happened during early cerebral development, we are also addressing the question from the other way around. Thanks to a collaboration with Professor Guibaud in Debrousse hospital (Lyon, France), we have access to fetal MR images and explore the technical challenge of obtaining 3D representations of the fetal brain. As mentioned in the *Introduction*, issues related to *in utero* MRI encompass fetal motion and the low resolution of the images. During his master thesis, Damien Ferrario worked on the combination of a set of low resolution images, to obtain a high resolution image of the fetal brain that are more suitable for accurate subsequent reconstruction. The preliminary 3D cortical mesh models that he could obtain are promising (see Figure 2.3, from the conference paper accepted at EUSIPCO 2008). We currently pursue efforts to optimize these cortical reconstructions, with the goal to obtain sufficiently accurate models allowing for the quantification of the relationship between brain volume, degree of folding and thickness during very early brain development. In addition to provide an *in vivo* framework for testing a variety of hypotheses on how the cortex folds, such information would open nice avenues for the establishment of quantitative milestones useful in clinical settings.

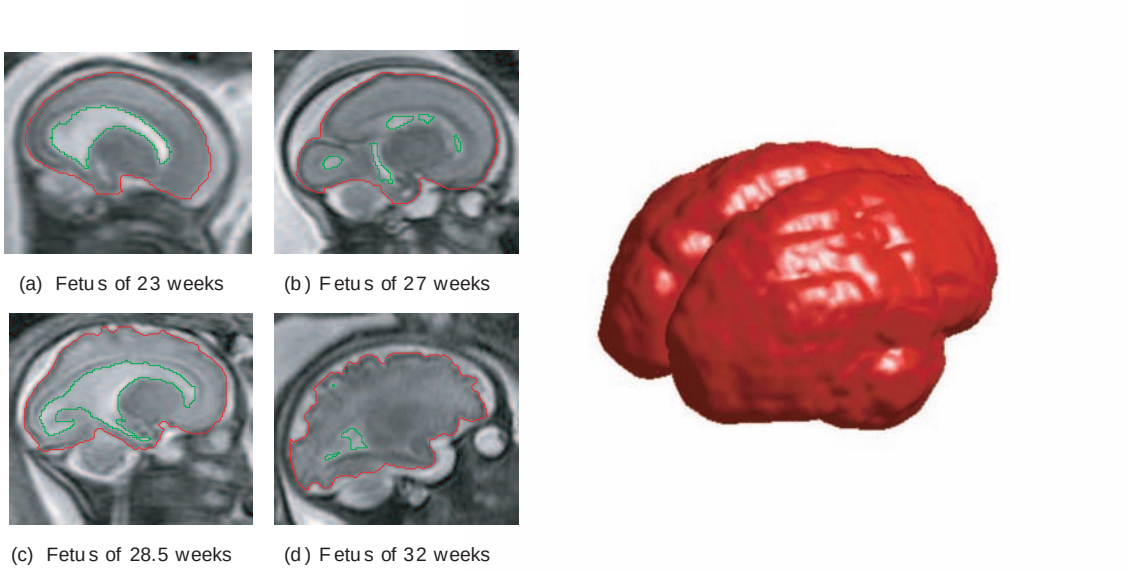

Figure 2.3: *Sagittal MRI sections of the fetal brain, with the outer cortical surface overlaid in red. On the right, a preliminary 3D cortical reconstruction is shown (Figures from D. Ferrario's work accepted at EUSIPCO conference in Lausanne, www.eusipco2008.org)*

2.2 Applications of *l*GI in pathological conditions

Finally, we also aim at delineating the determinants of *l*GI in a variety of conditions associated with abnormal brain structure.

- Evidently, we are interested in measuring *l*GI in **patients with schizophrenia** who not affected by 22q11.2 deletion syndrome. In collaboration with Dr Merlo in Geneva, we have access to MRI data of patients at their first psychotic episode. Other opportunities for measuring *l*GI in large cohorts of patients, or in relation to diffusion data and tractographic reconstructions, are currently under discussion.

- **Among the neurodevelopmental conditions**, we measured *l*GI in the brain of 14 high-functioning adult with **autism** (Hadjikhani et al., 2006), but were not able to identify differences in gyrification compared to 14 matched controls. Given a previous report of higher 2D-GI in the frontal lobe of autistic children (Hardan et al., 2004), it remains unclear if the absence of difference is related some to neurodegenerative process occuring in these adults' brains, or to methodological differences.

  Another neurodevelopmental condition in which we applied *l*GI is **microcephalia vera**. In collaboration with A. Verloes in Robert Debré hospital in Paris, we measured a major gyrification decrease in a small sample of patients affected by this very rare genetic condition. The observation of increased thickness in these patients with microcephalia further support a negative association between thickness and folding, along with a position association between folding and volume.

- Finally, we are also measuring *l*GI in **neurodegenerative conditions**. In collabora-

tion with SH. Woodward at Stanford University, we identified clusters of reduced gyrification in 50 combat veterans affected by **posttraumatic stress disorder** (PTSD) to 47 veterans without PTSD (Woodward et al., 2006). The clusters of reduced *l*GI in the brain of PTSD+ subjects were located at the left insula, right superior temporal sulcus and bilaterally in the occipital lobes, suggesting that *l*GI is also able to capture differences in brain shape related to a neurodegenerative process.

At last, we will also measure *l*GI in the brain of the patients included in the OASIS cohort who present mild symptoms of **Alzheimer disease**, and explore whether *l*GI is sensitive to the first atrophic changes associated with this devastating disease.

"Le mot de la fin"

For the reader who finally reached the end of this *longer-than-expected* dissertation, I would like to conclude on a very brief and less rigorous note.

Throughout this dissertation, different aspects of brain maturation and neuroimaging were discussed, and I hope that I was able to transmit that I enjoyed a lot these three years of research. I particularly liked the possibility to elaborate links between different disciplines. Of course, as a MD-PhD student co-directed by both the Faculty of Medicine and the Swiss Federal Institute of Technology, I was interested in bringing technical aspects and medically-oriented questions at the same place. But I also enjoyed bridging psychiatric aspects with neuroscience and neuroimaging, and with more somatic medical disciplines, as for instance exploring the impact of congenital heart disease on brain structure, or discussing with obstetricians in a fetal medicine congress.

As shown by the diverse studies published or under revision, this thesis represents a few contributions to the field of 22q11DS, and also hopefully, to the domain of cortical folding with the newly developed method. However, as raised in the *Discussion* part, an even greater number of studies are left for the future, which I am looking forward to address.

References

Andersson, F., B. Glaser, et al. (2007). "Impaired Activation of Face Processing Networks Revealed by Functional Magnetic Resonance Imaging in 22q11.2 Deletion Syndrome." Biol Psychiatry.

Antshel, K. M., A. Aneja, et al. (2007). "Autistic spectrum disorders in velo-cardio facial syndrome (22q11.2 deletion)." J Autism Dev Disord 37(9): 1776-86.

Antshel, K. M., J. Conchelos, et al. (2005). "Behavior and corpus callosum morphology relationships in velocardiofacial syndrome (22q11.2 deletion syndrome)." Psychiatry Res 138(3): 235-45.

Arinami, T., T. Ohtsuki, et al. (2001). "Screening for 22q11 deletions in a schizophrenia population." Schizophr Res 52(3): 167-70.

Armstrong, E., A. Schleicher, et al. (1995). "The ontogeny of human gyrification." Cereb Cortex 5(1): 56-63.

Arnold SE. (1999) "Neurodevelopmental abnormalities in schizophrenia: insights from neuropathology." Dev Psychopathol 11(3): 439-56.

Arnold, P. D., J. Siegel-Bartelt, et al. (2001). "Velo-cardio-facial syndrome: Implications of microdeletion 22q11 for schizophrenia and mood disorders." Am J Med Genet 105(4): 354-62.

Arnsten, A. F. and R. M. Shansky (2004). "Adolescence: vulnerable period for stress-induced prefrontal cortical function? Introduction to part IV." Ann N Y Acad Sci 1021: 143-7.

Ashburner, J. and K. J. Friston (2000). "Voxel-based morphometry–the methods." Neuroimage 11(6 Pt 1): 805-21.

Baillarger, M. (1853). "De l'étendue de la surface du cerveau et de ses rapports avec le développement de l'intelligence." Annales Médico-Psychologiques(5).

Baker, K. D. and D. H. Skuse (2005). "Adolescents and young adults with 22q11 deletion syndrome: psychopathology in an at-risk group." Br J Psychiatry 186: 115-20.

Barnea-Goraly, N., S. Eliez, et al. (2003). "White matter tract alterations in fragile X syndrome: preliminary evidence from diffusion tensor imaging." Am J Med Genet B Neuropsychiatr Genet 118(1): 81-8.

Barnea-Goraly, N., S. Eliez, et al. (2005). "Arithmetic ability and parietal alterations: a diffusion tensor imaging study in velocardiofacial syndrome." Brain Res Cogn Brain Res 25(3): 735-40.

Barnea-Goraly, N., V. Menon, et al. (2003). "Investigation of white matter structure in velocardiofacial syndrome: a diffusion tensor imaging study." Am J Psychiatry 160(10): 1863-9.

Bassett, A. S., E. W. Chow, et al. (2003). "The schizophrenia phenotype in 22q11 deletion syndrome." Am J Psychiatry 160(9): 1580-6.

Bassett, A. S., E. W. Chow, et al. (2005). "Clinical features of 78 adults with 22q11 Deletion Syndrome." Am J Med Genet A 138(4): 307-13.

Bassett, A. S., K. Hodgkinson, et al. (1998). "22q11 deletion syndrome in adults with schizophrenia." Am J Med Genet 81(4): 328-37.

Bastain, T. M., C. M. Lewczyk, et al. (2002). "Cytogenetic abnormalities in attention-deficit/hyperactivity disorder." J Am Acad Child Adolesc Psychiatry 41(7): 806-10.

Baumgardner, T. L., K. E. Green, et al. (1994). "A behavioral neurogenetics approach to developmental disabilities: gene-brain-behavior associations." Curr Opin Neurol 7(2): 172-8.

Bearden, C. E., A. F. Jawad, et al. (2005). "Effects of COMT genotype on behavioral symptomatology in the 22q11.2 Deletion Syndrome." Child Neuropsychol 11(1): 109-17.

Bearden, C. E., A. F. Jawad, et al. (2004). "Effects of a functional COMT polymorphism on prefrontal cognitive function in patients with 22q11.2 deletion syndrome." Am J Psychiatry 161(9): 1700-2.

Bearden, C. E., T. G. van Erp, et al. (2007). "Mapping cortical thickness in children with 22q11.2 deletions." Cereb Cortex 17(8): 1889-98.

Bearden, C. E., M. F. Woodin, et al. (2001). "The neurocognitive phenotype of the 22q11.2 deletion syndrome: selective deficit in visual-spatial memory." J Clin Exp Neuropsychol 23(4): 447-64.

Becker, D. B., T. Pilgram, et al. (2004). "Accuracy in identification of patients with 22q11.2 deletion by likely care providers using facial photographs." Plast Reconstr Surg 114(6): 1367-72.

Berman, J. I., P. Mukherjee, et al. (2005). "Quantitative diffusion tensor MRI fiber tractography of sensorimotor white matter development in premature infants." Neuroimage 27(4): 862-71.

Bingham, P. M., R. A. Zimmerman, et al. (1997). "Enlarged Sylvian fissures in infants with interstitial deletion of chromosome 22q11." Am J Med Genet 74(5): 538-43.

Bird, L. M. and P. Scambler (2000). "Cortical dysgenesis in 2 patients with chromosome 22q11 deletion." Clin Genet 58(1): 64-8.

Bish, J. P., V. Nguyen, et al. (2004). "Thalamic reductions in children with chromosome 22q11.2 deletion syndrome." Neuroreport 15(9): 1413-5.

Bish, J. P., A. Pendyal, et al. (2006). "Specific cerebellar reductions in children with chromosome 22q11.2 deletion syndrome." Neurosci Lett 399(3): 245-8.

Blanton, R. E., J. G. Levitt, et al. (2001). "Mapping cortical asymmetry and complexity patterns in normal children." Psychiatry Res 107(1): 29-43.

Blouin, J. L., B. A. Dombroski, et al. (1998). "Schizophrenia susceptibility loci on chromosomes 13q32 and 8p21." Nat Genet 20(1): 70-3.

Bolland, E., A. Y. Manzur, et al. (2000). "Velocardiofacial syndrome associated with atrophy of the shoulder girdle muscles and cervicomedullary narrowing." Eur J Paediatr Neurol 4(2): 73-6.

Botto, L. D., K. May, et al. (2003). "A population-based study of the 22q11.2 deletion: phenotype, incidence, and contribution to major birth defects in the population." Pediatrics 112(1 Pt 1): 101-7.

Burn, J., A. Takao, et al. (1993). "Conotruncal anomaly face syndrome is associated with a deletion within chromosome 22q11." J Med Genet 30(10): 822-4.

Cachia, A., J. F. Mangin, et al. (2003). "A generic framework for the parcellation of the cortical surface into gyri using geodesic Voronoi diagrams." Med Image Anal 7(4): 403-16.

Cachia, A., M. L. Paillere-Martinot, et al. (2008). "Cortical folding abnormalities in schizophrenia patients with resistant auditory hallucinations." Neuroimage 39(3): 927-35.

Campbell, L. E., E. Daly, et al. (2006). "Brain and behaviour in children with 22q11.2 deletion syndrome: a volumetric and voxel-based morphometry MRI study." Brain 129(Pt 5): 1218-28.

Carlson, C., H. Sirotkin, et al. (1997). "Molecular definition of 22q11 deletions in 151 velo-cardio-facial syndrome patients." Am J Hum Genet 61(3): 620-9.

Carter, C. S., M. M. Botvinick, et al. (1999). "The contribution of the anterior cingulate cortex to executive processes in cognition." Rev Neurosci 10(1): 49-57.

Casanova, M. F., J. Araque, et al. (2004). "Reduced brain size and gyrification in the brains of dyslexic patients." J Child Neurol 19(4): 275-81.

Cayler, G. G. (1969). "Cardiofacial syndrome. Congenital heart disease and facial weakness, a hitherto unrecognized association." Arch Dis Child 44(233): 69-75.

Changeux, J. P. and A. Danchin (1976). "Selective stabilisation of developing synapses as a mechanism for the specification of neuronal networks." Nature 264(5588): 705-12.

Chen, J., B. K. Lipska, et al. (2004). "Functional analysis of genetic variation in catechol-O-methyltransferase (COMT): effects on mRNA, protein, and enzyme activity in post-mortem human brain." Am J Hum Genet 75(5): 807-21.

Chenn, A. and C. A. Walsh (2002). "Regulation of cerebral cortical size by control of cell cycle exit in neural precursors." Science 297(5580): 365-9.

Chi, J. G., E. C. Dooling, et al. (1977). "Gyral development of the human brain." Ann Neurol 1(1): 86-93.

Chow, E. W., D. J. Mikulis, et al. (1999). "Qualitative MRI findings in adults with 22q11 deletion syndrome and schizophrenia." Biol Psychiatry 46(10): 1436-42.

Chow, E. W., R. B. Zipursky, et al. (2002). "Structural brain abnormalities in patients with schizophrenia and 22q11 deletion syndrome." Biol Psychiatry 51(3): 208-15.

Chugani, H. T., M. E. Phelps, et al. (1987). "Positron emission tomography study of human brain functional development." Ann Neurol 22(4): 487-97.

Chung, M. K., S. M. Robbins, et al. (2005). "Cortical thickness analysis in autism with heat kernel smoothing." Neuroimage 25(4): 1256-65.

Cohen, I. L., G. S. Fisch, et al. (1988). "Social gaze, social avoidance, and repetitive behavior in fragile X males: a controlled study." Am J Ment Retard 92(5): 436-46.

Courchesne, E. and K. Pierce (2005). "Why the frontal cortex in autism might be talking only to itself: local over-connectivity but long-distance disconnection." Curr Opin Neurobiol 15(2): 225-30.

Courchesne, E., O. Saitoh, et al. (1994). "Abnormality of cerebellar vermian lobules VI and VII in patients with infantile autism: identification of hypoplastic and hyperplastic subgroups with MR imaging." AJR Am J Roentgenol 162(1): 123-30.

Cowan, W. M., J. W. Fawcett, et al. (1984). "Regressive events in neurogenesis." Science 225(4668): 1258-65.

Crews, F., J. He, et al. (2007). "Adolescent cortical development: a critical period of vulnerability for addiction." Pharmacol Biochem Behav 86(2): 189-99.

Dale, A. M., B. Fischl, et al. (1999). "Cortical surface-based analysis. I. Segmentation and surface reconstruction." Neuroimage 9(2): 179-94.

Debbane, M., B. Glaser, et al. (2006). "Psychotic symptoms in children and adolescents with 22q11.2 deletion syndrome: Neuropsychological and behavioral implications." Schizophr Res 84(2-3): 187-93.

Debbane, M., B. Glaser, et al. (2005). "Temporal perception in velo-cardio-facial syndrome." Neuropsychologia 43(12): 1754-62.

Debbane, M., M. Schaer, et al. (2006). "Hippocampal volume reduction in 22q11.2 deletion syndrome." Neuropsychologia 44(12): 2360-5.

Deboer, T., Z. Wu, et al. (2007). "Hippocampal volume reduction in children with chromosome 22q11.2 deletion syndrome is associated with cognitive impairment." Behav Brain Funct 3(1): 54.

Dehay, C., P. Giroud, et al. (1996). "Contribution of thalamic input to the specification of cytoarchitectonic cortical fields in the primate: effects of bilateral enucleation in the fetal monkey on the boundaries, dimensions, and gyrification of striate and extrastriate cortex." J Comp Neurol 367(1): 70-89.

Dekaban, A. S. (1977). "Tables of cranial and orbital measurements, cranial volume, and derived indexes in males and females from 7 days to 20 years of age." Ann Neurol 2(6): 485-91.

Desikan, R. S., F. Segonne, et al. (2006). "An automated labeling system for subdividing the human cerebral cortex on MRI scans into gyral based regions of interest." Neuroimage 31(3): 968-80.

Devriendt, K., J. P. Fryns, et al. (1998). "The annual incidence of DiGeorge/velocardiofacial syndrome." J Med Genet 35(9): 789-90.

DiGeorge, A. M. (1965). "Discussion on: "A new concept of the cellular basis of immunity" by Cooper M.D, Peterson R.D. and Good, R.A." The Journal of Pediatrics 67(5): 907-908.

Driscoll, D. A. (2001). "Prenatal diagnosis of the 22q11.2 deletion syndrome." Genet Med 3(1): 14-8.

Driscoll, D. A., N. B. Spinner, et al. (1992). "Deletions and microdeletions of 22q11.2 in velo-cardio-facial syndrome." Am J Med Genet 44(2): 261-8.

DSM-IV (2000). Diagnostic and Statistical Manual of Mental Disorders DSM-IV-TR Fourth Edition (Text Revision), American Psychiatric Association.

Dubois, J., M. Benders, et al. (2008). "Mapping the early cortical folding process in the preterm newborn brain." Cereb Cortex 18(6): 1444-54.

Dufour, F., M. Schaer, et al. (2008). "Cingulate gyral reductions are related to low executive functioning and psychotic symptoms in 22q11.2 deletion syndrome." Neuropsychologia 46(12): 2986-92.

Dykens, E. M. (1995). "Measuring behavioral phenotypes: provocations from the "new genetics"." Am J Ment Retard 99(5): 522-32.

Eckert, M. A., A. Tenforde, et al. (2006). "To modulate or not to modulate: differing results in uniquely shaped Williams syndrome brains." Neuroimage 32(3): 1001-7.

Egan, M. F., T. E. Goldberg, et al. (2001). "Effect of COMT Val108/158 Met genotype on frontal lobe function and risk for schizophrenia." Proc Natl Acad Sci USA 98(12): 6917-22.

Eliez, S., S. E. Antonarakis, et al. (2001). "Parental origin of the deletion 22q11.2 and brain development in velocardiofacial syndrome: a preliminary study." Arch Gen Psychiatry 58(1): 64-8.

Eliez, S., N. Barnea-Goraly, et al. (2002). "Increased basal ganglia volumes in velo-cardio-facial syndrome (deletion 22q11.2)." Biol Psychiatry 52(1): 68-70.

Eliez, S., C. M. Blasey, et al. (2001). "Functional brain imaging study of mathematical reasoning abilities in velocardiofacial syndrome (del22q11.2)." Genet Med 3(1): 49-55.

Eliez, S., C. M. Blasey, et al. (2001). "Velocardiofacial syndrome: are structural changes in the temporal and mesial temporal regions related to schizophrenia?" Am J Psychiatry 158(3): 447-53.

Eliez, S., J. E. Schmitt, et al. (2000). "Children and adolescents with velocardiofacial syndrome: a volumetric MRI study." Am J Psychiatry 157(3): 409-15.

Eliez, S., J. E. Schmitt, et al. (2001). "A quantitative MRI study of posterior fossa development in velocardiofacial syndrome." Biol Psychiatry 49(6): 540-6.

Feinberg I. (1982) "Schizophrenia: caused by a fault in programmed synaptic elimination during adolescence?" J Psychiatr Res 17(4): 319-34.

Feinstein, C., S. Eliez, et al. (2002). "Psychiatric disorders and behavioral problems in children with velocardiofacial syndrome: usefulness as phenotypic indicators of schizophrenia risk." Biol Psychiatry 51(4): 312-8.

Fernandez, L., P. Lapunzina, et al. (2005). "Comparative study of three diagnostic approaches (FISH, STRs and MLPA) in 30 patients with 22q11.2 deletion syndrome." Clin Genet 68(4): 373-8.

Ferrario D., M. Bach Cuadra, et al. (2008). "Brain surface segmentation of magnetic resonance images of the fetus." EUSIPCO Conference, Lausanne.

Fine, S. E., A. Weissman, et al. (2005). "Autism Spectrum Disorders and Symptoms in Children with Molecularly Confirmed 22q11.2 Deletion Syndrome." J Autism Dev Disord 35(4): 461-470.

Fischl, B. and A. M. Dale (2000). "Measuring the thickness of the human cerebral cortex from magnetic resonance images." Proc Natl Acad Sci USA 97(20): 11050-5.

Fischl, B., M. I. Sereno, et al. (1999). "Cortical surface-based analysis. II: Inflation, flattening, and a surface-based coordinate system." Neuroimage 9(2): 195-207.

Fischl, B., M. I. Sereno, et al. (1999). "High-resolution intersubject averaging and a coordinate system for the cortical surface." Hum Brain Mapp 8(4): 272-84.

Flint, J. (1998). "Behavioral phenotypes: conceptual and methodological issues." Am J Med Genet 81(3): 235-40.

Fokstuen, S., K. Vrticka, et al. (2001). "Velofacial hypoplasia (Sedlackova syndrome): a variant of velocardiofacial (Shprintzen) syndrome and part of the phenotypical spectrum of del 22q11.2." Eur J Pediatr 160(1): 54-7.

Fombonne, E., C. Du Mazaubrun, et al. (1997). "Autism and associated medical disorders in a French epidemiological survey." J Am Acad Child Adolesc Psychiatry 36(11): 1561-9.

Fryer, A. (1996). "Monozygotic twins with 22q11 deletion and discordant phenotypes." J Med Genet 33(2): 173.

Fujiwara, H., K. Hirao, et al. (2007). "Anterior cingulate pathology and social cognition in schizophrenia: a study of gray matter, white matter and sulcal morphometry." Neuroimage 36(4): 1236-45.

Ganser, K. A., H. Dickhaus, et al. (2004). "A deformable digital brain atlas system according to Talairach and Tournoux." Med Image Anal 8(1): 3-22.

Gaser, C., E. Luders, et al. (2006). "Increased local gyrification mapped in Williams syndrome." Neuroimage 33(1): 46-54.

Gauthier, I. and C. A. Nelson (2001). "The development of face expertise." Curr Opin Neurobiol 11(2): 219-24.

Gerdes, M., C. Solot, et al. (1999). "Cognitive and behavior profile of preschool children with chromosome 22q11.2 deletion." Am J Med Genet 85(2): 127-33.

Giannotti, A., M. C. Digilio, et al. (1994). "Cayler cardiofacial syndrome and del 22q11: part of the CATCH22 phenotype." Am J Med Genet 53(3): 303-4.

Giedd, J. N., J. Blumenthal, et al. (1999). "Brain development during childhood and adolescence: a longitudinal MRI study." Nat Neurosci 2(10): 861-3.

Giedd, J. N., F. X. Castellanos, et al. (1997). "Sexual dimorphism of the developing human brain." Prog Neuropsychopharmacol Biol Psychiatry 21(8): 1185-201.

Gill, M., H. Vallada, et al. (1996). "A combined analysis of D22S278 marker alleles in affected sib-pairs: support for a susceptibility locus for schizophrenia at chromosome 22q12. Schizophrenia Collaborative Linkage Group (Chromosome 22)." Am J Med Genet 67(1): 40-5.

Gimenez, M., C. Junque, et al. (2006). "Abnormal orbitofrontal development due to prematurity." Neurology 67(10): 1818-22.

Glaser, B., M. Debbane, et al. (2006). "No evidence for an effect of COMT Val158Met genotype on executive function in patients with 22q11 deletion syndrome." Am J Psychiatry 163(3): 537-9.

Glaser, B., V. Moskvina, et al. (2006). "Analysis of ProDH, COMT and ZDHHC8 risk variants does not support individual or interactive effects on schizophrenia susceptibility." Schizophr Res 87(1-3): 21-7.

Glaser, B., M. Schaer, et al. (2007). "Structural changes to the fusiform gyrus: a cerebral marker for social impairments in 22q11.2 deletion syndrome?" Schizophr Res 96(1-3): 82-86.

Glaser, B., D. L. Mumme, et al. (2002). "Language skills in children with velocardiofacial syndrome (deletion 22q11.2)." J Pediatr 140(6): 753-8.

Glauser, T. A., L. B. Rorke, et al. (1990). "Congenital brain anomalies associated with the hypoplastic left heart syndrome." Pediatrics 85(6): 984-90.

Gogos, J. A., M. Santha, et al. (1999). "The gene encoding proline dehydrogenase modulates sensorimotor gating in mice." Nat Genet 21(4): 434-9.

Gogtay, N., J. N. Giedd, et al. (2004). "Dynamic mapping of human cortical development during childhood through early adulthood." Proc Natl Acad Sci USA 101(21): 8174-9.

Golding-Kushner, K. J., G. Weller, et al. (1985). "Velo-cardio-facial syndrome: language and psychological profiles." J Craniofac Genet Dev Biol 5(3): 259-66.

Goldman-Rakic, P. S. (1980). "Morphological consequences of prenatal injury to the primate brain." Prog Brain Res 53: 1-19.

Goldman-Rakic, P. S., E. C. Muly, 3rd, et al. (2000). "D(1) receptors in prefrontal cells and circuits." Brain Res Brain Res Rev 31(2-3): 295-301.

Good, C. D., I. S. Johnsrude, et al. (2001). "A voxel-based morphometric study of ageing in 465 normal adult human brains." Neuroimage 14(1 Pt 1): 21-36.

Gothelf, D., S. Eliez, et al. (2005). "COMT genotype predicts longitudinal cognitive decline and psychosis in 22q11.2 deletion syndrome." Nat Neurosci 8(11): 1500-2.

Gothelf, D., C. Feinstein, et al. (2007). "Risk factors for the emergence of psychotic disorders in adolescents with 22q11.2 deletion syndrome." Am J Psychiatry 164(4): 663-9.

Gothelf, D., A. Frisch, et al. (1997). "Velocardiofacial manifestations and microdeletions in schizophrenic inpatients." Am J Med Genet 72(4): 455-61.

Gothelf, D., L. Penniman, et al. (2007). "Developmental trajectories of brain structure in adolescents with 22q11.2 deletion syndrome: a longitudinal study." Schizophr Res 96(1-3): 72-81.

Gothelf, D., G. Presburger, et al. (2004). "Genetic, developmental, and physical factors associated with attention deficit hyperactivity disorder in patients with velocardiofacial syndrome." Am J Med Genet B Neuropsychiatr Genet 126(1): 116-21.

Gothelf, D., M. Schaer, et al. (2008). "Genes, Brain Development and Psychiatric Phenotypes in Velo-Cardio-Facial Syndrome." Ment Retard Dev Disabil Res Rev in press.

Gray, H., W. H. Lewis (1918). "Anatomy of the Human Body." Philadelphia, Lea & Febiger.

Greenstein, D., J. Lerch, et al. (2006). "Childhood onset schizophrenia: cortical brain abnormalities as young adults." J Child Psychol Psychiatry 47(10): 1003-12.

Gripp, K. W., D. M. McDonald-McGinn, et al. (1997). "Nasal dimple as part of the 22q11.2 deletion syndrome." Am J Med Genet 69(3): 290-2.

Ha, T. H., U. Yoon, et al. (2005). "Fractal dimension of cerebral cortical surface in schizophrenia and obsessive-compulsive disorder." Neurosci Lett 384(1-2): 172-6.

Hadjikhani, N., R. M. Joseph, et al. (2006). "Anatomical differences in the mirror neuron system and social cognition network in autism." Cereb Cortex 16(9): 1276-82.

Hagerman, R. J., M. Y. Ono, et al. (2005). "Recent advances in fragile X: a model for autism and neurodegeneration." Curr Opin Psychiatry 18(5): 490-6.

Hagmann, P., M. Kurant, et al. (2007). "Mapping human whole-brain structural networks with diffusion MRI." PLoS ONE 2(7): e597.

Hagmann, P., J. P. Thiran, et al. (2003). "DTI mapping of human brain connectivity: statistical fibre tracking and virtual dissection." Neuroimage 19(3): 545-54.

Han, Y. and H. Park (2004). "Automatic registration of brain magnetic resonance images based on Talairach reference system." J Magn Reson Imaging 20(4): 572-80.

Hardan, A. Y., R. J. Jou, et al. (2004). "Increased frontal cortical folding in autism: a preliminary MRI study." Psychiatry Res 131(3): 263-8.

Hardan, A. Y., S. Muddasani, et al. (2006). "An MRI study of increased cortical thickness in autism." Am J Psychiatry 163(7): 1290-2.

Harris, J. M., H. Whalley, et al. (2004). "Abnormal cortical folding in high-risk individuals: a predictor of the development of schizophrenia?" Biol Psychiatry 56(3): 182-9.

Harris, J. M., S. Yates, et al. (2004). "Gyrification in first-episode schizophrenia: a morphometric study." Biol Psychiatry 55(2): 141-7.

Haug, H. (1987). "Brain sizes, surfaces, and neuronal sizes of the cortex cerebri: a stereological investigation of man and his variability and a comparison with some mammals (primates, whales, marsupials, insectivores, and one elephant)." Am J Anat 180(2): 126-42.

Hay, B. N. (2007). "Deletion 22q11: spectrum of associated disorders." Semin Pediatr Neurol 14(3): 136-9.

Henry, J. C., T. van Amelsvoort, et al. (2002). "An investigation of the neuropsychological profile in adults with velo-cardio-facial syndrome (VCFS)." Neuropsychologia 40(5): 471-8.

Hensch, T. K. (2005). "Critical period plasticity in local cortical circuits." Nat Rev Neurosci 6(11): 877-88.

Hoffman, R. E. and S. K. Dobscha (1989). "Cortical pruning and the development of schizophrenia: a computer model." Schizophr Bull 15(3): 477-90.

Hoffman R. E. and T. H. McGlashan. (1997) "Synaptic elimination, neurodevelopment, and the mechanism of hallucinated voices in schizophrenia." Am J Psychiatry 154(12): 1683-9.

Hoffman R. E. and T. H. McGlashan. (2006) "Using a speech perception neural network computer simulation to contrast neuroanatomic versus neuromodulatory models of auditory hallucinations." Pharmacopsychiatry 39 Suppl 1: S54-64.

Hofman, M. A. (1985). "Size and shape of the cerebral cortex in mammals. I. The cortical surface." Brain Behav Evol 27(1): 28-40.

Hofman M. A. (1991) "The fractal geometry of convoluted brains." J Hirnforsch 32(1): 103-11.

Huang, C. C. (1991). "Sonographic cerebral sulcal development in premature newborns." Brain Dev 13(1): 27-31.

Hubel, D. H. and T. N. Wiesel (1964). "Effects of Monocular Deprivation in Kittens." Naunyn Schmiedebergs Arch Exp Pathol Pharmakol 248: 492-7.

Huttenlocher, P. R. (1979). "Synaptic density in human frontal cortex - developmental changes and effects of aging." Brain Res 163(2): 195-205.

Huttenlocher, P. R. (1999). "Dendritic and Synaptic Development in Human Cerebral Cortex: Time Course and Critical Periods." Developmental Neuropsychology 16(3): 347-349.

Im K., J. M. Lee, et al. (2006) "Gender difference analysis of cortical thickness in healthy young adults with surface-based methods." Neuroimage 31(1):31-8.

Imamizu, H., S. Miyauchi, et al. (2000). "Human cerebellar activity reflecting an acquired internal model of a new tool." Nature 403(6766): 192-5.

Jerison, H. J. (1961). "Quantitative analysis of evolution of the brain in mammals." Science 133: 1012-4.

Jerome, L. A. and V. E. Papaioannou (2001). "DiGeorge syndrome phenotype in mice mutant for the T-box gene, TBX1." Nat Genet 27(3): 286-91.

Jou, R. J., A. Y. Hardan, et al. (2005). "Reduced cortical folding in individuals at high risk for schizophrenia: a pilot study." Schizophr Res 75(2-3): 309-13.

Kanal, E., J. Gillen, et al. (1993). "Survey of reproductive health among female MR workers." Radiology 187(2): 395-9.

Kandel, E. R. (1998). "A new intellectual framework for psychiatry." Am J Psychiatry 155(4): 457-69.

Karayiorgou, M., M. A. Morris, et al. (1995). "Schizophrenia susceptibility associated with interstitial deletions of chromosome 22q11." Proc Natl Acad Sci USA 92(17): 7612-6.

Kates, W. R., M. T. Abrams, et al. (1997). "Reliability and validity of MRI measurement of the amygdala and hippocampus in children with fragile X syndrome." Psychiatry Res 75(1): 31-48.

Kates, W. R., K. M. Antshel. (2006). "A gender-moderated effect of functional polymorphism on prefrontal brain morphology and function in velo-cardio-facial syndrome (22q11.2 deletion syndrome)." Am J Genet B Neuropsychiatr Genet 5;141: 274-80.

Kates, W. R., C. P. Burnette, et al. (2004). "Frontal and caudate alterations in velocardiofacial syndrome (deletion at chromosome 22q11.2)." J Child Neurol 19(5): 337-42.

Kates, W. R., C. P. Burnette, et al. (2001). "Regional cortical white matter reductions in velocardiofacial syndrome: a volumetric MRI analysis." Biol Psychiatry 49(8): 677-84.

Kates, W. R., B. R. Krauss, et al. (2007). "The neural correlates of non-spatial working memory in velocardiofacial syndrome (22q11.2 deletion syndrome)." Neuropsychologia.

Kates, W. R., A. M. Miller, et al. (2006). "Temporal lobe anatomy and psychiatric symptoms in velocardiofacial syndrome (22q11.2 deletion syndrome)." J Am Acad Child Adolesc Psychiatry 45(5): 587-95.

Kates, W. R., I. S. Warsofsky, et al. (1999). "Automated Talairach atlas-based parcellation and measurement of cerebral lobes in children." Psychiatry Res 91(1): 11-30.

Keshavan, M. S., S. Anderson, et al. (1994). "Is schizophrenia due to excessive synaptic pruning in the prefrontal cortex? The Feinberg hypothesis revisited." J Psychiatr Res 28(3): 239-65.

Keshavan M. S. (1999) "Development, disease and degeneration in schizophrenia: a unitary pathophysiological model." J Psychiatr Res 33(6): 513-21.

Kesler, S. R., B. Vohr, et al. (2006). "Increased temporal lobe gyrification in preterm children." Neuropsychologia 44(3): 445-53.

Kippenhan, J. S., R. K. Olsen, et al. (2005). "Genetic contributions to human gyrification: sulcal morphometry in Williams syndrome." J Neurosci 25(34): 7840-6.

Kochunov, P., J. F. Mangin, et al. (2005). "Age-related morphology trends of cortical sulci." Hum Brain Mapp 26(3): 210-20.

Koolen, D. A., J. A. Veltman, et al. (2004). "Chromosome 22q11 deletion and pachygyria characterized by array-based comparative genomic hybridization." Am J Med Genet A 131(3): 322-4.

Kraynack, N. C., R. W. Hostoffer, et al. (1999). "Agenesis of the corpus callosum associated with DiGeorge-velocardiofacial syndrome: a case report and review of the literature." J Child Neurol 14(11): 754-6.

Kubicki, M., R. McCarley, et al. (2007). "A review of diffusion tensor imaging studies in schizophrenia." J Psychiatr Res 41(1-2): 15-30.

Kulynych, J. J., L. F. Luevano, et al. (1997). "Cortical abnormality in schizophrenia: an in vivo application of the gyrification index." Biol Psychiatry 41(10): 995-9.

Kuperberg, G. R., M. R. Broome, et al. (2003). "Regionally localized thinning of the cerebral cortex in schizophrenia." Arch Gen Psychiatry 60(9): 878-88.

Kuperberg G. R. (2008) "Building meaning in schizophrenia." Clin EEG Neurosci 39(2): 99-102.

Lee, J. M., U. Yoon, et al. (2004). "Analysis of the hemispheric asymmetry using fractal dimension of a skeletonized cerebral surface." IEEE Trans Biomed Eng 51(8): 1494-8.

Lerch, J. P. and A. C. Evans (2005). "Cortical thickness analysis examined through power analysis and a population simulation." Neuroimage 24(1): 163-73.

Leyfer, O. T., J. Woodruff-Borden, et al. (2006). "Prevalence of psychiatric disorders in 4 to 16-year-olds with Williams syndrome." Am J Med Genet B Neuropsychiatr Genet 141(6): 615-22.

Lindsay, E. A. (2001). "Chromosomal microdeletions: dissecting del22q11 syndrome." Nat Rev Genet 2(11): 858-68.

Lindsay, E. A., R. Goldberg, et al. (1995). "Velo-cardio-facial syndrome: frequency and extent of 22q11 deletions." Am J Med Genet 57(3): 514-22.

Lindsay, E. A., F. Vitelli, et al. (2001). "TBX1 haploinsufficieny in the DiGeorge syndrome region causes aortic arch defects in mice." Nature 410(6824): 97-101.

Luders, E., K. L. Narr, et al. (2007). "Mapping the Relationship between Cortical Convolution and Intelligence: Effects of Gender." Cereb Cortex.

Luders, E., K. L. Narr, et al. (2004). "Gender differences in cortical complexity." Nat Neurosci 7(8): 799-800.

Luders, E., P. M. Thompson, et al. (2006). "A curvature-based approach to estimate local gyrification on the cortical surface." Neuroimage 29(4): 1224-30.

Machado, A. M., T. J. Simon, et al. (2007). "Corpus callosum morphology and ventricular size in chromosome 22q11.2 deletion syndrome." Brain Res 1131(1): 197-210.

Magnotta, V. A., N. C. Andreasen, et al. (1999). "Quantitative in vivo measurement of gyrification in the human brain: changes associated with aging." Cereb Cortex 9(2): 151-60.

Mandelbrot, B. B. (1982). "Fractal geometry of nature." New York, W. H. Freeman & Company.

Mangin, J. F., D. Riviere, et al. (2004). "A framework to study the cortical folding patterns." Neuroimage 23 Suppl 1: S129-38.

Mann, D. M. (1988). "The pathological association between Down syndrome and Alzheimer disease." Mech Ageing Dev 43(2): 99-136.

Mata I., R. Perez-Iglesias, et al. (2008). "Lack of influence of COMT Val158Met genotype on cognition in first-episode non-affective psychosis." Schizophr Res 102(1-3): 206-9.

Martin, J. B. (2002). "The integration of neurology, psychiatry, and neuroscience in the 21st century." Am J Psychiatry 159(5): 695-704.

Matsuoka, R., A. Takao, et al. (1994). "Confirmation that the conotruncal anomaly face syndrome is associated with a deletion within 22q11.2." Am J Med Genet 53(3): 285-9.

Mattay, V. S., T. E. Goldberg, et al. (2003). "Catechol O-methyltransferase val158-met genotype and individual variation in the brain response to amphetamine." Proc Natl Acad Sci USA 100(10): 6186-91.

Maynard, T. M., G. T. Haskell, et al. (2002). "22q11 DS: genomic mechanisms and gene function in DiGeorge/velocardiofacial syndrome." Int J Dev Neurosci 20(3-5): 407-19.

Mazzocco, M. M., W. R. Kates, et al. (1997). "Autistic behaviors among girls with fragile X syndrome." J Autism Dev Disord 27(4): 415-35.

McDermid, H. E. and B. E. Morrow (2002). "Genomic disorders on 22q11." Am J Hum Genet 70(5): 1077-88.

McDonald-McGinn, D. M., D. A. Driscoll, et al. (1995). "Autosomal dominant "Opitz" GBBB syndrome due to a 22q11.2 deletion." Am J Med Genet 59(1): 103-13.

McDonald-McGinn, D. M., R. Kirschner, et al. (1999). "The Philadelphia story: the 22q11.2 deletion: report on 250 patients." Genet Couns 10(1): 11-24.

McDonald-McGinn, D. M., N. Minugh-Purvis, et al. (2005). "The 22q11.2 deletion in African-American patients: an underdiagnosed population?" Am J Med Genet A 134(3): 242-6.

McGuffin, P., M. J. Owen, et al. (1995). "Genetic basis of schizophrenia." Lancet 346(8976): 678-82.

McIntosh A. M., B. J. Baig, et al. (2007). "Relationship of catechol-O-methyltransferase variants to brain structure and function in a population at high risk of psychosis." Biol Psychiatry 61(10): 1127-34.

Menon, V., S. M. Rivera, et al. (2000). "Functional optimization of arithmetic processing in perfect performers." Cognitive Brain Research 9: 343-345.

Menon, V., K. Mackenzie, et al. (2002). "Prefrontal cortex involvement in processing incorrect arithmetic equations: evidence from event-related fMRI." Hum Brain Mapp 16(2): 119-30.

Merscher, S., B. Funke, et al. (2001). "TBX1 is responsible for cardiovascular defects in velo-cardio-facial/DiGeorge syndrome." Cell 104(4): 619-29.

Meyer-Lindenberg, A., P. D. Kohn, et al. (2005). "Midbrain dopamine and prefrontal function in humans: interaction and modulation by COMT genotype." Nat Neurosci 8(5): 594-6.

Miller, S. P., P. S. McQuillen, et al. (2007). "Abnormal brain development in newborns with congenital heart disease." N Engl J Med 357(19): 1928-38.

Mitnick, R. J., J. A. Bello, et al. (1994). "Brain anomalies in velo-cardio-facial syndrome." Am J Med Genet 54(2): 100-6.

Molko, N., A. Cachia, et al. (2004). "Brain anatomy in Turner syndrome: evidence for impaired social and spatial-numerical networks." Cereb Cortex 14(8): 840-50.

Moorhead, T. W., J. M. Harris, et al. (2006). "Automated computation of the Gyrification Index in prefrontal lobes: methods and comparison with manual implementation." Neuroimage 31(4): 1560-6.

Mori, S., W. E. Kaufmann, et al. (2002). "Imaging cortical association tracts in the human brain using diffusion-tensor-based axonal tracking." Magn Reson Med 47(2): 215-23.

Moss, E. M., M. L. Batshaw, et al. (1999). "Psychoeducational profile of the 22q11.2 microdeletion: A complex pattern." J Pediatr 134(2): 193-8.

Mukherjee, P., J. H. Miller, et al. (2002). "Diffusion-tensor MR imaging of gray and white matter development during normal human brain maturation." AJNR Am J Neuroradiol 23(9): 1445-56.

Murphy, K. C., L. A. Jones, et al. (1999). "High rates of schizophrenia in adults with velo-cardio-facial syndrome." Arch Gen Psychiatry 56(10): 940-5.

Murphy, K. C. and M. J. Owen (2001). "Velo-cardio-facial syndrome: a model for understanding the genetics and pathogenesis of schizophrenia." Br J Psychiatry 179: 397-402.

Narr, K. L., R. M. Bilder, et al. (2004). "Abnormal gyral complexity in first-episode schizophrenia." Biol Psychiatry 55(8): 859-67.

Nordahl, C. W., D. Dierker, et al. (2007). "Cortical folding abnormalities in autism revealed by surface-based morphometry." J Neurosci 27(43): 11725-35.

Ono, M., S. Kubic, et al. (1990). "Atlas of the cerebral sulci." New York, Thieme.

Oskarsdottir, S., M. Belfrage, et al. (2005). "Disabilities and cognition in children and adolescents with 22q11 deletion syndrome." Dev Med Child Neurol 47(3): 177-84.

Ou, Z., J. S. Berg, et al. (2008). "Microduplications of 22q11.2 are frequently inherited and are associated with variable phenotypes." Genet Med 10(4): 267-77.

Paterlini, M., S. S. Zakharenko, et al. (2005). "Transcriptional and behavioral interaction between 22q11.2 orthologs modulates schizophrenia-related phenotypes in mice." Nat Neurosci 8(11): 1586-94.

Paylor, R., B. Glaser, et al. (2006). "TBX1 haploinsufficiency is linked to behavioral disorders in mice and humans: implications for 22q11 deletion syndrome." Proc Natl Acad Sci USA 103(20): 7729-34.

Paylor, R. and E. Lindsay (2006). "Mouse models of 22q11 deletion syndrome." Biol Psychiatry 59(12): 1172-9.

Pierpaoli, C., P. Jezzard, et al. (1996). "Diffusion tensor MR imaging of the human brain." Radiology 201(3): 637-48.

Prothero, J. W. and J. W. Sundsten (1984). "Folding of the cerebral cortex in mammals. A scaling model." Brain Behav Evol 24(2-3): 152-67.

Pulver, A. E., M. Karayiorgou, et al. (1994). "Follow-up of a report of a potential linkage for schizophrenia on chromosome 22q12-q13.1: Part 2." Am J Med Genet 54(1): 44-50.

Pulver, A. E., G. Nestadt, et al. (1994). "Psychotic illness in patients diagnosed with velo-cardio-facial syndrome and their relatives." J Nerv Ment Dis 182(8): 476-8.

Rakic, P. (1988). "Specification of cerebral cortical areas." Science 241(4862): 170-6.

Regis, J., J. F. Mangin, et al. (2005). ""Sulcal root" generic model: a hypothesis to overcome the variability of the human cortex folding patterns." Neurol Med Chir (Tokyo) 45(1): 1-17.

Reiss, A. L., S. Eliez, et al. (2000). "Brain imaging in neurogenetic conditions: realizing the potential of behavioral neurogenetics research." Ment Retard Dev Disabil Res Rev 6(3): 186-97.

Reiss, A. L., S. Eliez, et al. (2000). "IV. Neuroanatomy of Williams syndrome: a high-resolution MRI study." J Cogn Neurosci 12 Suppl 1: 65-73.

Reiss, A. L., F. Faruque, et al. (1993). "Neuroanatomy of Rett syndrome: a volumetric imaging study." Ann Neurol 34(2): 227-34.

Reiss, A. L., L. Freund, et al. (1991). "Neuroanatomy in fragile X females: the posterior fossa." Am J Hum Genet 49(2): 279-88.

Richman, D. P., R. M. Stewart, et al. (1975). "Mechanical model of brain convolutional development." Science 189(4196): 18-21.

Riviere, D., J. F. Mangin, et al. (2002). "Automatic recognition of cortical sulci of the human brain using a congregation of neural networks." Med Image Anal 6(2): 77-92.

Robin, N. H., C. J. Taylor, et al. (2006). "Polymicrogyria and deletion 22q11.2 syndrome: window to the etiology of a common cortical malformation." Am J Med Genet A 140(22): 2416-25.

Rodriguez-Carranza, C., P. Mukherjee, et al. (2006). "A system for measuring regional surface folding of the neonatal brain from MRI." Med Image Comput Comput Assist Interv Int Conf Med Image Comput Comput Assist Interv 9(Pt 2): 201-8.

Rousseau, F., O. A. Glenn, et al. (2006). "Registration-based approach for reconstruction of high-resolution in utero fetal MR brain images." Acad Radiol 13(9): 1072-81.

Russell, H. F., D. Wallis, et al. (2006). "Increased prevalence of ADHD in Turner syndrome with no evidence of imprinting effects." J Pediatr Psychol 31(9): 945-55.

Ryan, A. K., J. A. Goodship, et al. (1997). "Spectrum of clinical features associated with interstitial chromosome 22q11 deletions: a European collaborative study." J Med Genet 34(10): 798-804.

Saitta, S. C., S. E. Harris, et al. (2004). "Aberrant interchromosomal exchanges are the predominant cause of the 22q11.2 deletion." Hum Mol Genet 13(4): 417-28.

Sallet, P. C., H. Elkis, et al. (2003). "Reduced cortical folding in schizophrenia: an MRI morphometric study." Am J Psychiatry 160(9): 1606-13.

Scambler, P. J., D. Kelly, et al. (1992). "Velo-cardio-facial syndrome associated with chromosome 22 deletions encompassing the DiGeorge locus." Lancet 339(8802): 1138-9.

Schaer, M. and S. Eliez (2007). "From genes to brain: understanding brain development in neurogenetic disorders using neuroimaging techniques." Child Adolesc Psychiatr Clin N Am 16(3): 557-79.

Schaer, M., J. E. Schmitt, et al. (2006). "Abnormal patterns of cortical gyrification in velo-cardio-facial syndrome (deletion 22q11.2): an MRI study." Psychiatry Res 146(1): 1-11.

Schaer, M., M. Bach Cuadra, et al. (2008). "A surface-based approach to quantify local cortical gyrification." IEEE Transactions on Medical Imaging 27(2): 161-170.

Schaer, M., B. Glaser, et al. (2008). "Congenital heart disease affects local cortical gyrification in 22q11.2 deletion syndrome (22q11.2DS)." Dev Med Child Neurol *in press*.

Scherer, N. J., L. L. D'Antonio, et al. (1999). "Early speech and language development in children with velocardiofacial syndrome." Am J Med Genet 88(6): 714-23.

Schmitt, J. E., S. Eliez, et al. (2001). "Enlarged cerebellar vermis in Williams syndrome." J Psychiatr Res 35(4): 225-9.

Schmitt, J. E., K. Watts, et al. (2002). "Increased gyrification in Williams syndrome: evidence using 3D MRI methods." Dev Med Child Neurol 44(5): 292-5.

Sedlackova, E. (1955). "Insufficiency of palatolaryngeal passage as a developmental disorder." Cas Lek Cesk 94(47-48): 1304-7.

Sengpiel, F. (2007). "The critical period." Curr Biol 17(17): R742-3.

Shallice, T., P. Fletcher, et al. (1994). "Brain regions associated with acquisition and retrieval of verbal episodic memory." Nature 368(6472): 633-5.

Shashi, V., S. Muddasani, et al. (2004). "Abnormalities of the corpus callosum in nonpsychotic children with chromosome 22q11 deletion syndrome." Neuroimage 21(4): 1399-406.

Shaw, P., K. Eckstrand, et al. (2007). "Attention-deficit/hyperactivity disorder is characterized by a delay in cortical maturation." Proc Natl Acad Sci USA 104(49): 19649-54.

Shaw, P., D. Greenstein, et al. (2006). "Intellectual ability and cortical development in children and adolescents." Nature 440(7084): 676-9.

Shaw, P., N. J. Kabani, et al. (2008). "Neurodevelopmental trajectories of the human cerebral cortex." J Neurosci 28(14): 3586-94.

Shaw, P., J. Lerch, et al. (2006). "Longitudinal mapping of cortical thickness and clinical outcome in children and adolescents with attention-deficit/hyperactivity disorder." Arch Gen Psychiatry 63(5): 540-9.

Shaw, S. H., M. Kelly, et al. (1998). "A genome-wide search for schizophrenia susceptibility genes." Am J Med Genet 81(5): 364-76.

Shenton, M. E., C. C. Dickey, et al. (2001). "A review of MRI findings in schizophrenia." Schizophr Res 49(1-2): 1-52.

Shprintzen, R. J. (2000). "Velo-cardio-facial syndrome: a distinctive behavioral phenotype." Ment Retard Dev Disabil Res Rev 6(2): 142-7.

Shprintzen, R. J., R. B. Goldberg, et al. (1978). "A new syndrome involving cleft palate, cardiac anomalies, typical facies, and learning disabilities: velo-cardio-facial syndrome." Cleft Palate J 15(1): 56-62.

Simon, T. J., L. Ding, et al. (2005). "Volumetric, connective, and morphologic changes in the brains of children with chromosome 22q11.2 deletion syndrome: an integrative study." Neuroimage 25(1): 169-80.

Smith, F. W., A. H. Adam, et al. (1983). "NMR imaging in pregnancy." Lancet 1(8314-5): 61-2. Smith, S. M., M. Jenkinson, et al. (2006). "Tract-based spatial statistics: voxelwise analysis of multi-subject diffusion data." Neuroimage 31(4): 1487-505.

Sobin, C., K. Kiley-Brabeck, et al. (2004). "Networks of attention in children with the 22q11 deletion syndrome." Dev Neuropsychol 26(2): 611-26.

Sobin, C., K. Kiley-Brabeck, et al. (2005). "Neuropsychological characteristics of children with the 22q11 Deletion Syndrome: a descriptive analysis." Child Neuropsychol 11(1): 39-53.

Sobin, C., S. H. Monk, et al. (2006). "Neuromotor deficits in children with the 22q11 deletion syndrome." Mov Disord 21(12): 2082-9.

Solot, C. B., M. Gerdes, et al. (2001). "Communication issues in 22q11.2 deletion syndrome: children at risk." Genet Med 3(1): 67-71.

Sowell, E. R., B. S. Peterson, et al. (2003). "Mapping cortical change across the human life span." Nat Neurosci 6(3): 309-15.

Sowell, E. R., P. M. Thompson, et al. (2004). "Longitudinal mapping of cortical thickness and brain growth in normal children." J Neurosci 24(38): 8223-31.

Sporn, A., A. Addington, et al. (2004). "22q11 deletion syndrome in childhood onset schizophrenia: an update." Mol Psychiatry 9(3): 225-6.

Strong, W. B. (1968). "Familial syndrome of right-sided aortic arch, mental deficiency, and facial dysmorphism." J Pediatr 73(6): 882-8.

Sullivan, K., D. Hatton, et al. (2006). "ADHD symptoms in children with FXS." Am J Med Genet A 140(21): 2275-88.

Sun, H., P. A. Yushkevich, et al. (2007). "Shape-Based Normalization of the Corpus Callosum for DTI Connectivity Analysis." IEEE Transactions on Medical Imaging *in press*.

Swillen, A. (2006). "Cognitive development in children and adolescents with del22q11.2." Annual Meeting of the Society for the Study of Behavioral Phenotypes. Dublin.

Swillen, A., K. Devriendt, et al. (1997). "Intelligence and psychosocial adjustment in velocardiofacial syndrome: a study of 37 children and adolescents with VCFS." J Med Genet 34(6): 453-8.

Swillen, A., K. Devriendt, et al. (1999). "The behavioural phenotype in velo-cardio-facial syndrome (VCFS): from infancy to adolescence." Genet Couns 10(1): 79-88.

Swillen, A., K. Devriendt, et al. (1998). "Familial deletions of chromosome 22q11: the Leuven experience." Am J Med Genet 80(5): 531-2.

Swillen, A., L. Vandeputte, et al. (1999). "Neuropsychological, learning and psychosocial profile of primary school aged children with the velo-cardio-facial syndrome (22q11 deletion): evidence for a nonverbal learning disability?" Child Neuropsychol 5(4): 230-41.

Tae, W. S., S. S. Kim, et al. (2008). "Validation of hippocampal volumes measured using a manual method and two automated methods (FreeSurfer and IBASPM) in chronic major depressive disorder." Neuroradiology.

Talairach, J. and P. Tournoux (1988). "Co-Planar Stereotaxic Atlas of the Human Brain." Stuttgart, New York, Georg Thieme Verlag.

Tamm, L., V. Menon, et al. (2002). "Maturation of brain function associated with response inhibition." J Am Acad Child Adolesc Psychiatry 41(10): 1231-8.

Taylor, W. D., E. Hsu, et al. (2004). "Diffusion tensor imaging: background, potential, and utility in psychiatric research." Biol Psychiatry 55(3): 201-7.

Tezenas Du Montcel, S., H. Mendizabai, et al. (1996). "Prevalence of 22q11 microdeletion." J Med Genet 33(8): 719.

Thompson, P. M., K. M. Hayashi, et al. (2003). "Dynamics of gray matter loss in Alzheimer's disease." J Neurosci 23(3): 994-1005.

Thompson, P. M., K. M. Hayashi, et al. (2004). "Mapping cortical change in Alzheimer's disease, brain development, and schizophrenia." Neuroimage 23 Suppl 1: S2-18.

Thompson, P. M., C. Schwartz, et al. (1996). "Three-dimensional statistical analysis of sulcal variability in the human brain." J Neurosci 16(13): 4261-74.

Van Aken, K., B. De Smedt, et al. (2007). "Motor development in school-aged children with 22q11 deletion (velocardiofacial/DiGeorge syndrome)." Dev Med Child Neurol 49(3): 210-3.

van Amelsvoort, T., E. Daly, et al. (2001). "Structural brain abnormalities associated with deletion at chromosome 22q11: quantitative neuroimaging study of adults with velo-cardio-facial syndrome." Br J Psychiatry 178: 412-9.

van Amelsvoort, T., E. Daly, et al. (2004). "Brain anatomy in adults with velocardiofacial syndrome with and without schizophrenia: preliminary results of a structural magnetic resonance imaging study." Arch Gen Psychiatry 61(11): 1085-96.

van Amelsvoort, T., J. Zinkstok, et al. (2008). "Effects of a functional COMT polymorphism on brain anatomy and cognitive function in adults with velo-cardio-facial syndrome." Psychol Med 38:89-100.

Van Essen, D. C. (1997). "A tension-based theory of morphogenesis and compact wiring in the central nervous system." Nature 385(6614): 313-8.

Van Essen, D. C. (2005). "A Population-Average, Landmark- and Surface-based (PALS) atlas of human cerebral cortex." Neuroimage 28(3): 635-62.

Van Essen, D. C., D. Dierker, et al. (2006). "Symmetry of cortical folding abnormalities in Williams syndrome revealed by surface-based analyses." J Neurosci 26(20): 5470-83.

Vantrappen, G., N. Rommel, et al. (1998). "The velo-cardio-facial syndrome: the otorhinolaryngeal manifestations and implications." Int J Pediatr Otorhinolaryngol 45(2): 133-41.

Vogeley, K., T. Schneider-Axmann, et al. (2000). "Disturbed gyrification of the prefrontal region in male schizophrenic patients: A morphometric postmortem study." Am J Psychiatry 157(1): 34-9.

Vogeley, K., R. Tepest, et al. (2001). "Right frontal hypergyria differentiation in affected and unaffected siblings from families multiply affected with schizophrenia: a morphometric mri study." Am J Psychiatry 158(3): 494-6.

Vorstman, J. A., M. E. Morcus, et al. (2006). "The 22q11.2 deletion in children: high rate of autistic disorders and early onset of psychotic symptoms." J Am Acad Child Adolesc Psychiatry 45(9): 1104-13.

Vrticka, K. (2007). "Present-day importance of the velocardiofacial syndrome. To commemorate the late prof. Eva Sedlackova, MD, on the 50th anniversary of her original publication." Folia Phoniatr Logop 59(3): 141-6.

Wang, P. P., M. F. Woodin, et al. (2000). "Research on behavioral phenotypes: velocardiofacial syndrome (deletion 22q11.2)." Dev Med Child Neurol 42(6): 422-7.

Weinberger D. R. (1987) "Implications of normal brain development for the pathogenesis of schizophrenia." Arch Gen Psychiatry 44(7): 660-9.

Welker, W. (1990). "Why does cerebral cortex fissure and fold? A review of determinants of gyri and sulci." In: Cerebral Cortex, Jones EG, Peters A. New York, Plenum.

Wigren, M. and S. Hansen (2005). "ADHD symptoms and insistence on sameness in Prader-Willi syndrome." J Intellect Disabil Res 49(Pt 6): 449-56.

Williams, H. J., N. Williams, et al. (2003). "Association between PRODH and schizophrenia is not confirmed." Mol Psychiatry 8(7): 644-5.

Wilson, D. I., J. Burn, et al. (1993). "DiGeorge syndrome: part of CATCH 22." J Med Genet 30(10): 852-6. Wilson, H. R. (1988). "Development of spatiotemporal mechanisms in infant vision." Vision Res 28(5): 611-28.

Woodward N. D., K. Jayathilake, et al. (2007) "COMT val108/158met genotype, cognitive function, and cognitive improvement with clozapine in schizophrenia." Schizophr Res 90(1-3): 86-96.

Woodward S. H., D. G. Kaloupek, et al. (2006) "Decreased anterior cingulate volume in combat-related PTSD." Biol Psychiatry 59(7): 582-7.

Worthen, N. J., V. Gilbertson, et al. (1986). "Cortical sulcal development seen on sonography: relationship to gestational parameters." J Ultrasound Med 5(3): 153-6.

Yagi, H., Y. Furutani, et al. (2003). "Role of TBX1 in human del22q11.2 syndrome." Lancet 362(9393): 1366-73.

Yakovlev, P. I. and A. Lecours (1967). "The myelogenetic cycles of regional maturation in the brain." In: regional development of the brain in early life, Minkowski A. England.

Yip, Y. P., C. Capriotti, et al. (1994). "Effects of MR exposure at 1.5 T on early embryonic development of the chick." J Magn Reson Imaging 4(5): 742-8.

Zafeiriou, D. I., A. Ververi, et al. (2007). "Childhood autism and associated comorbidities." Brain Dev 29(5): 257-72.

Zhang, K. and T. J. Sejnowski (2000). "A universal scaling law between gray matter and white matter of cerebral cortex." Proc Natl Acad Sci USA 97(10): 5621-6.

Zilles, K., E. Armstrong, et al. (1989). "Gyrification in the cerebral cortex of primates." Brain Behav Evol 34(3): 143-50.

Zilles, K., E. Armstrong, et al. (1988). "The human pattern of gyrification in the cerebral cortex." Anat Embryol (Berl) 179(2): 173-9.

Zinkstok, J., N. Schmitz, et al. (2006). "The COMT val158met polymorphism and brain morphometry in healthy young adults." Neurosci Lett 405: 34-39.

Zinkstok, J., N. Schmitz, et al. (2008). "Genetic variation in COMT and PRODH is associated with brain anatomy in patients with schizophrenia." Genes Brain Behav 7(1): 61-9.

Zweier, C., H. Sticht, et al. (2007). "Human TBX1 missense mutations cause gain of function resulting in the same phenotype as 22q11.2 deletions." Am J Hum Genet 80(3): 510-7.

Annexes

Annex 1 – Psychotic symptoms in our cohort of patients with 22q11DS

The three graphics presented below detail the distribution of psychotic symptoms across age in 65 patients with 22q11DS from our Geneva study cohort.

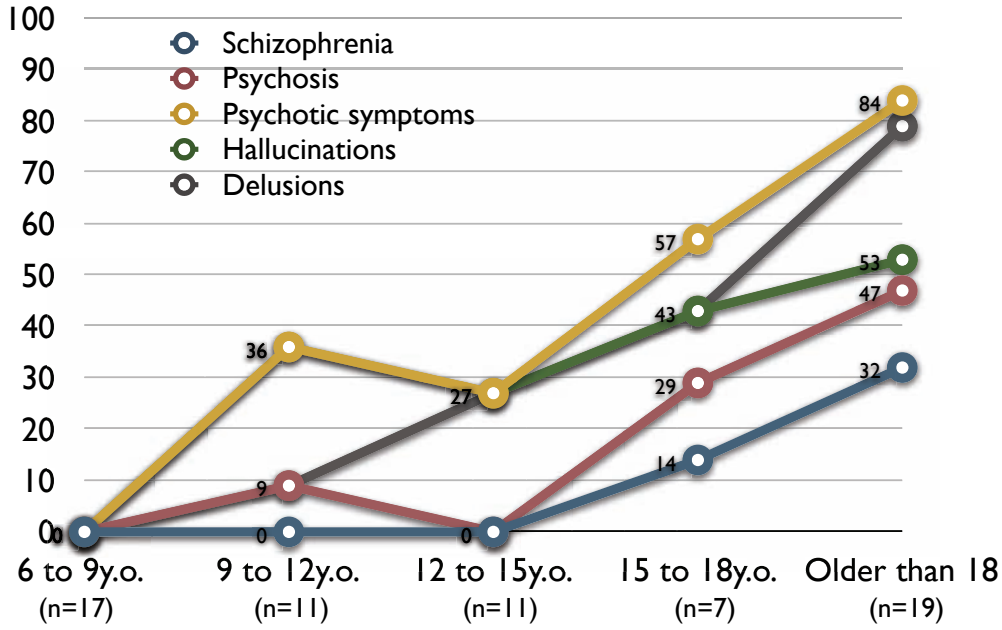

Distribution of psychotic symptomatology:
- blue – schizophrenia
- red – psychosis (i.e. hallucinations AND delusions)
- yellow – psychotic symptoms (i.e. hallucinations OR delusions)

Units are given in percentage for each age bin.

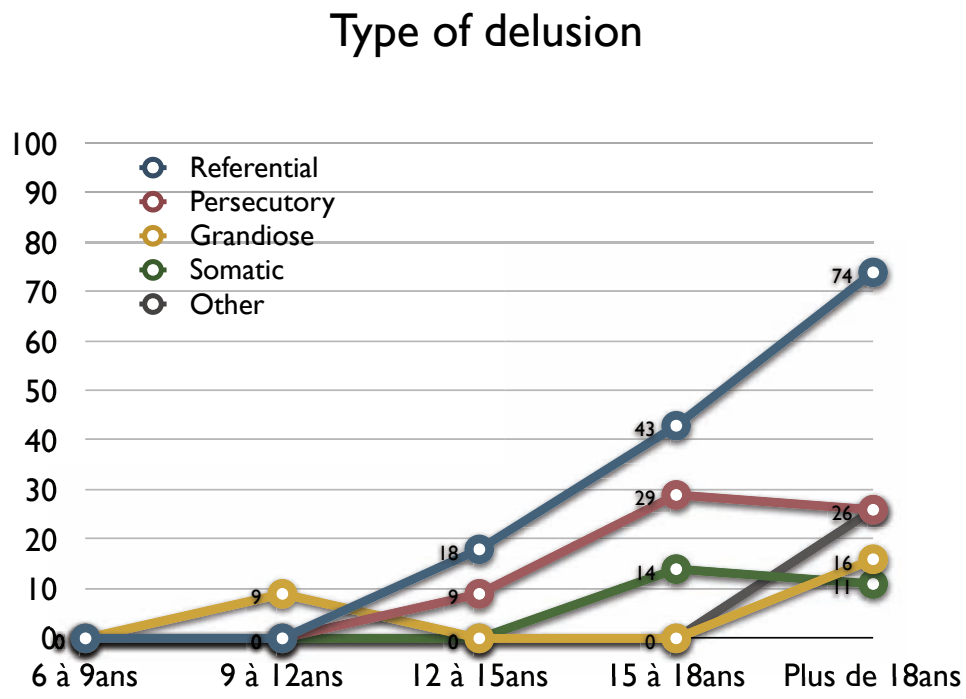
Type of delusion
100
90
80
70
60
50
40
30
20
10
0
Referential
Persecutory
Grandiose
Somatic
Other
74
43
29
26
18
9
9
16
14
11
0
0
0
0
0
6 à 9ans
9 à 12ans
12 à 15ans
15 à 18ans
Plus de 18ans

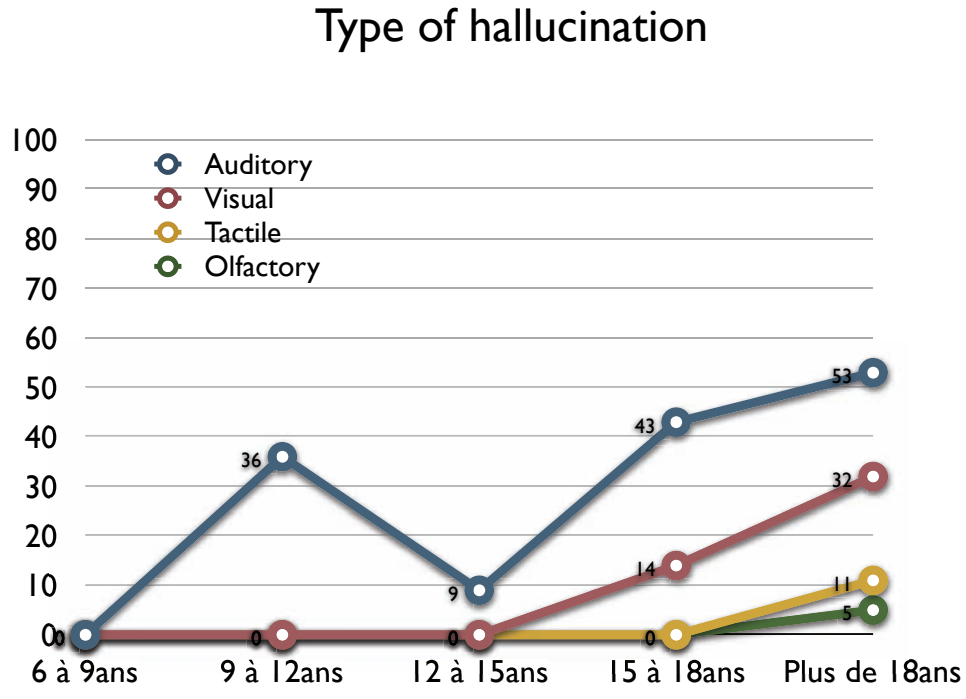
Type of hallucination
100
90
80
70
60
50
40
30
20
10
0
Auditory
Visual
Tactile
Olfactory
53
43
36
32
14
11
9
5
0
0
0
0
0
6 à 9ans
9 à 12ans
12 à 15ans
15 à 18ans
Plus de 18ans

Annex 2 – References for the Table 4.1

1. Schmidt-Sidor B, Wisniewski KE, Shepard TH, Sersen EA. Brain growth in Down syndrome subjects 15 to 22 weeks of gestational age and birth to 60 months. Clin Neuropathol. Jul-Aug 1990; 9(4): 181-190.
2. Pinter JD, Eliez S, Schmitt JE, Capone GT, Reiss AL. Neuroanatomy of Down's syndrome: a high-resolution MRI study. Am J Psychiatry. Oct 2001; 158(10): 1659-1665.
3. Jernigan TL, Bellugi U. Anomalous brain morphology on magnetic resonance images in Williams syndrome and Down syndrome. Arch Neurol. May 1990; 47(5): 529-533.
4. Kesslak JP, Nagata SF, Lott I, Nalcioglu O. Magnetic resonance imaging analysis of age-related changes in the brains of individuals with Down's syndrome. Neurology. Jun 1994; 44(6): 1039-1045.
5. Raz N, Torres IJ, Briggs SD, et al. Selective neuroanatomic abnormalities in Down's syndrome and their cognitive correlates: evidence from MRI morphometry. Neurology. Feb 1995; 45(2): 356-366.
6. Jernigan TL, Bellugi U, Sowell E, Doherty S, Hesselink JR. Cerebral morphologic distinctions between Williams and Down syndromes. Arch Neurol. Feb 1993; 50(2): 186-191.
7. Reiss AL, Abrams MT, Greenlaw R, Freund L, Denckla MB. Neurodevelopmental effects of the FMR-1 full mutation in humans. Nat Med. Feb 1995; 1(2): 159-167.
8. Mostofsky SH, Mazzocco MM, Aakalu G, Warsofsky IS, Denckla MB, Reiss AL. Decreased cerebellar posterior vermis size in fragile X syndrome: correlation with neurocognitive performance. Neurology. Jan 1998; 50(1): 121-130.
9. Eliez S, Schmitt JE, White CD, Reiss AL. Children and adolescents with velocardiofacial syndrome: a volumetric MRI study. Am J Psychiatry. Mar 2000; 157(3): 409-415.
10. Eliez S, Antonarakis SE, Morris MA, Dahoun SP, Reiss AL. Parental origin of the deletion 22q11.2 and brain development in velocardiofacial syndrome: a preliminary study. Arch Gen Psychiatry. Jan 2001; 58(1): 64-68.
11. Kates WR, Burnette CP, Jabs EW, et al. Regional cortical white matter reductions in velocardiofacial syndrome: a volumetric MRI analysis. Biol Psychiatry. Apr 15 2001; 49(8): 677-684.
12. White NS, Alkire MT, Haier RJ. A voxel-based morphometric study of nondemented adults with Down Syndrome. Neuroimage. Sep 2003; 20(1): 393-403.
13. Aylward EH, Habbak R, Warren AC, et al. Cerebellar volume in adults with Down syndrome. Arch Neurol. Feb 1997; 54(2): 209-212.
14. Weis S, Weber G, Neuhold A, Rett A. Down syndrome: MR quantification of brain structures and comparison with normal control subjects. AJNR Am J Neuroradiol. Nov-Dec 1991; 12(6): 1207-1211.
15. Ieshima A, Kisa T, Yoshino K, Takashima S, Takeshita K. A morphometric CT study of Down's syndrome showing small posterior fossa and calcification of basal ganglia. Neuroradiology. 1984; 26(6): 493-498.
16. Kaufmann WE, Cooper KL, Mostofsky SH, et al. Specificity of cerebellar vermian abnormalities in autism: a quantitative magnetic resonance imaging study. J Child Neurol. Jul 2003; 18(7): 463-470.
17. Bellugi U, Bihrle A, Jernigan T, Trauner D, Doherty S. Neuropsychological, neurological and neuroanatomical profile of Williams syndrome. Am J Med Genet Suppl. 1990; 6: 115-125.
18. Schmitt JE, Eliez S, Warsofsky IS, Bellugi U, Reiss AL. Enlarged cerebellar vermis in Williams syndrome. J Psychiatr Res. Jul-Aug 2001; 35(4): 225-229.
19. Reiss AL, Eliez S, Schmitt JE, et al. Neuroanatomy of Williams syndrome: a high-resolution MRI study. J Cogn Neurosci. 2000; 12 Suppl 1: 65-73.
20. Jones W, Hesselink J, Courchesne E, Duncan T, Matsuda K, Bellugi U. Cerebellar abnormalities in infants and toddlers with Williams syndrome. Dev Med Child Neurol. Oct 2002; 44(10): 688-694.

21. Reiss AL, Patel S, Kumar AJ, Freund L. Preliminary communication: neuroanatomical variations of the posterior fossa in men with the fragile X (Martin-Bell) syndrome. Am J Med Genet. Oct 1988; 31(2): 407-414.

22. Reiss AL, Aylward E, Freund LS, Joshi PK, Bryan RN. Neuroanatomy of fragile X syndrome: the posterior fossa. Ann Neurol. Jan 1991; 29(1): 26-32.

23. Reiss AL, Freund L, Tseng JE, Joshi PK. Neuroanatomy in fragile X females: the posterior fossa. Am J Hum Genet. Aug 1991; 49(2): 279-288.

24. Guerreiro MM, Camargo EE, Kato M, et al. Fragile X syndrome. Clinical, electroencephalographic and neuroimaging characteristics. Arq Neuropsiquiatr. Mar 1998; 56(1): 18-23.

25. Mazzocco MM, Kates WR, Baumgardner TL, Freund LS, Reiss AL. Autistic behaviors among girls with fragile X syndrome. J Autism Dev Disord. Aug 1997; 27(4): 415-435.

26. Eliez S, Schmitt JE, White CD, Wellis VG, Reiss AL. A quantitative MRI study of posterior fossa development in velocardiofacial syndrome. Biol Psychiatry. Mar 15 2001; 49(6): 540-546.

27. Bish JP, Pendyal A, Ding L, et al. Specific cerebellar reductions in children with chromosome 22q11.2 deletion syndrome. Neurosci Lett. May 22 2006; 399(3): 245-248.

28. Reiss AL, Eckert MA, Rose FE, et al. An experiment of nature: brain anatomy parallels cognition and behavior in Williams syndrome. J Neurosci. May 26 2004; 24(21): 5009-5015.

29. Eckert MA, Tenforde A, Galaburda AM, et al. To modulate or not to modulate: differing results in uniquely shaped Williams syndrome brains. Neuroimage. Sep 2006; 32(3): 1001-1007.

30. Kates WR, Folley BS, Lanham DC, Capone GT, Kaufmann WE. Cerebral growth in Fragile X syndrome: review and comparison with Down syndrome. Microsc Res Tech. May 1 2002; 57(3): 159-167.

31. Kates WR, Burnette CP, Bessette BA, et al. Frontal and caudate alterations in velocardiofacial syndrome (deletion at chromosome 22q11.2). J Child Neurol. May 2004; 19(5): 337-342.

32. Simon TJ, Ding L, Bish JP, McDonald-McGinn DM, Zackai EH, Gee J. Volumetric, connective, and morphologic changes in the brains of children with chromosome 22q11.2 deletion syndrome: an integrative study. Neuroimage. Mar 2005; 25(1): 169-180.

33. Chow EW, Zipursky RB, Mikulis DJ, Bassett AS. Structural brain abnormalities in patients with schizophrenia and 22q11 deletion syndrome. Biol Psychiatry. Feb 1 2002; 51(3): 208-215.

34. van Amelsvoort T, Daly E, Robertson D, et al. Structural brain abnormalities associated with deletion at chromosome 22q11: quantitative neuroimaging study of adults with velo-cardio-facial syndrome. Br J Psychiatry. May 2001; 178: 412-419.

35. Boddaert N, Mochel F, Meresse I, et al. Parieto-occipital grey matter abnormalities in children with Williams syndrome. Neuroimage. Apr 15 2006; 30(3): 721-725.

36. Meyer-Lindenberg A, Kohn P, Mervis CB, et al. Neural basis of genetically determined visuospatial construction deficit in Williams syndrome. Neuron. Sep 2 2004; 43(5): 623-631.

37. Eckert MA, Hu D, Eliez S, et al. Evidence for superior parietal impairment in Williams syndrome. Neurology. Jan 11 2005; 64(1): 152-153.

38. Thompson PM, Lee AD, Dutton RA, et al. Abnormal cortical complexity and thickness profiles mapped in Williams syndrome. J Neurosci. Apr 20 2005; 25(16): 4146-4158.

39. Reiss AL, Lee J, Freund L. Neuroanatomy of fragile X syndrome: the temporal lobe. Neurology. Jul 1994; 44(7): 1317-1324.

40. Eliez S, Blasey CM, Schmitt EJ, White CD, Hu D, Reiss AL. Velocardiofacial syndrome: are structural changes in the temporal and mesial temporal regions related to schizophrenia? Am J Psychiatry. Mar 2001; 158 (3): 447-453.

41. Reiss AL, Eliez S, Schmitt JE, Patwardhan A, Haberecht M. Brain imaging in neurogenetic conditions: realizing the potential of behavioral neurogenetics research.

Ment Retard Dev Disabil Res Rev. 2000; 6(3): 186-197.

42. Frangou S, Aylward E, Warren A, Sharma T, Barta P, Pearlson G. Small planum temporale volume in Down's syndrome: a volumetric MRI study. Am J Psychiatry. Oct 1997; 154(10): 1424-1429.
43. Eckert MA, Galaburda AM, Karchemskiy A, et al. Anomalous sylvian fissure morphology in Williams syndrome. Neuroimage. Oct 15 2006; 33(1): 39-45.
44. Pinter JD, Brown WE, Eliez S, Schmitt JE, Capone GT, Reiss AL. Amygdala and hippocampal volumes in children with Down syndrome: a high-resolution MRI study. Neurology. Apr 10 2001; 56(7): 972-974.
45. Teipel SJ, Schapiro MB, Alexander GE, et al. Relation of corpus callosum and hippocampal size to age in nondemented adults with Down's syndrome. Am J Psychiatry. Oct 2003; 160(10): 1870-1878.
46. Kates WR, Abrams MT, Kaufmann WE, Breiter SN, Reiss AL. Reliability and validity of MRI measurement of the amygdala and hippocampus in children with fragile X syndrome. Psychiatry Res. Aug 8 1997; 75(1): 31-48.
47. Jakala P, Hanninen T, Ryynanen M, et al. Fragile-X: neuropsychological test performance, CGG triplet repeat lengths, and hippocampal volumes. J Clin Invest. Jul 15 1997; 100(2): 331-338.
48. Kates WR, Miller AM, Abdulsabur N, et al. Temporal lobe anatomy and psychiatric symptoms in velocardiofacial syndrome (22q11.2 deletion syndrome). J Am Acad Child Adolesc Psychiatry. May 2006; 45(5): 587-595.
49. Debbane M, Schaer M, Farhoumand R, Glaser B, Eliez S. Hippocampal volume reduction in 22q11.2 deletion syndrome. Neuropsychologia. 2006; 44(12): 2360-2365.
50. van Amelsvoort T, Daly E, Henry J, et al. Brain anatomy in adults with velocardiofacial syndrome with and without schizophrenia: preliminary results of a structural magnetic resonance imaging study. Arch Gen Psychiatry. Nov 2004; 61(11): 1085-1096.
51. Aylward EH, Li Q, Habbak QR, et al. Basal ganglia volume in adults with Down syndrome. Psychiatry Res. May 16 1997; 74(2): 73-82.
52. Eliez S, Blasey CM, Freund LS, Hastie T, Reiss AL. Brain anatomy, gender and IQ in children and adolescents with fragile X syndrome. Brain. Aug 2001; 124(Pt 8): 1610-1618.
53. Eliez S, Barnea-Goraly N, Schmitt JE, Liu Y, Reiss AL. Increased basal ganglia volumes in velo-cardio-facial syndrome (deletion 22q11.2). Biol Psychiatry. Jul 1 2002; 52(1): 68-70.
54. Campbell LE, Daly E, Toal F, et al. Brain and behaviour in children with 22q11.2 deletion syndrome: a volumetric and voxel-based morphometry MRI study. Brain. May 2006; 129(Pt 5): 1218-1228.
55. Bish JP, Nguyen V, Ding L, Ferrante S, Simon TJ. Thalamic reductions in children with chromosome 22q11.2 deletion syndrome. Neuroreport. Jun 28 2004; 15(9): 1413-1415.
56. Wang PP, Doherty S, Hesselink JR, Bellugi U. Callosal morphology concurs with neurobehavioral and neuropathological findings in two neurodevelopmental disorders. Arch Neurol. Apr 1992; 49(4): 407-411.
57. Tomaiuolo F, Di Paola M, Caravale B, Vicari S, Petrides M, Caltagirone C. Morphology and morphometry of the corpus callosum in Williams syndrome: a T1-weighted MRI study. Neuroreport. Dec 3 2002; 13 (17): 2281-2284.
58. Schmitt JE, Eliez S, Warsofsky IS, Bellugi U, Reiss AL. Corpus callosum morphology of Williams syndrome: relation to genetics and behavior. Dev Med Child Neurol. Mar 2001; 43(3): 155-159.
59. Antshel KM, Conchelos J, Lanzetta G, Fremont W, Kates WR. Behavior and corpus callosum morphology relationships in velocardiofacial syndrome (22q11.2 deletion syndrome). Psychiatry Res. Apr 30 2005; 138(3): 235-245.
60. Shashi V, Muddasani S, Santos CC, et al. Abnormalities of the corpus callosum in non-psychotic children with chromosome 22q11 deletion syndrome. Neuroimage. Apr 2004; 21(4): 1399-1406.
61. Usiskin SI, Nicolson R, Krasnewich DM, et al. Velocardiofacial syndrome in childhood-onset schizophrenia. J Am Acad Child Adolesc Psychiatry. Dec 1999; 38(12): 1536-1543.

62. Barnea-Goraly N, Eliez S, Hedeus M, et al. White matter tract alterations in fragile X syndrome: preliminary evidence from diffusion tensor imaging. Am J Med Genet B Neuropsychiatr Genet. Apr 1 2003; 118(1): 81-88.

63. Barnea-Goraly N, Eliez S, Menon V, Bammer R, Reiss AL. Arithmetic ability and parietal alterations: a diffusion tensor imaging study in velocardiofacial syndrome. Brain Res Cogn Brain Res. Dec 2005; 25(3): 735-740.

64. Logdberg B, Brun A. Prefrontal neocortical disturbances in mental retardation. J Intellect Disabil Res. Oct 1993; 37 (5): 459-468.

65. Jackowski AP, Schultz RT. Foreshortened dorsal extension of the central sulcus in Williams syndrome. Cortex. Jun 2005; 41(3): 282-290.

66. Schmitt JE, Watts K, Eliez S, Bellugi U, Galaburda AM, Reiss AL. Increased gyrification in Williams syndrome: evidence using 3D MRI methods. Dev Med Child Neurol. May 2002; 44(5): 292-295.

67. Gaser C, Luders E, Thompson PM, et al. Increased local gyrification mapped in Williams syndrome. Neuroimage. Oct 15 2006; 33(1): 46-54.

68. Van Essen DC, Dierker D, Snyder AZ, Raichle ME, Reiss AL, Korenberg J. Symmetry of cortical folding abnormalities in Williams syndrome revealed by surface-based analyses. J Neurosci. May 17 2006; 26(20): 5470-5483.

69. Kippenhan JS, Olsen RK, Mervis CB, et al. Genetic contributions to human gyrification: sulcal morphometry in Williams syndrome. J Neurosci. Aug 24 2005; 25(34): 7840-7846.

70. Schaer M, Schmitt JE, Glaser B, Lazeyras F, Delavelle J, Eliez S. Abnormal patterns of cortical gyrification in velo-cardio-facial syndrome (deletion 22q11.2): an MRI study. Psychiatry Res. Jan 30 2006; 146(1): 1-11.

71. Wisniewski KE, French JH, Rosen JF, Kozlowski PB, Tenner M, Wisniewski HM. Basal ganglia calcification (BGC) in Down's syndrome (DS)–another manifestation of premature aging. Ann N Y Acad Sci. 1982; 396: 179-189.

72. Takashima S, Becker LE. Basal ganglia calcification in Down's syndrome. J Neurol Neurosurg Psychiatry. Jan 1985; 48(1): 61-64.

73. Mann DM, Esiri MM. The pattern of acquisition of plaques and tangles in the brains of patients under 50 years of age with Down's syndrome. J Neurol Sci. Feb 1989; 89(2-3): 169-179.

74. Irwin SA, Galvez R, Greenough WT. Dendritic spine structural anomalies in fragile-X mental retardation syndrome. Cereb Cortex. Oct 2000; 10(10): 1038-1044.

75. Hinton VJ, Brown WT, Wisniewski K, Rudelli RD. Analysis of neocortex in three males with the fragile X syndrome. Am J Med Genet. Dec 1 1991; 41(3): 289-294.

76. Rudelli RD, Brown WT, Wisniewski K, et al. Adult fragile X syndrome. Clinico-neuropathologic findings. Acta Neuropathol (Berl). 1985; 67(3-4): 289-295.

77. Wisniewski KE, Segan SM, Miezejeski CM, Sersen EA, Rudelli RD. The Fra(X) syndrome: neurological, electrophysiological, and neuropathological abnormalities. Am J Med Genet. Feb-Mar 1991; 38(2-3): 476-480.

Curriculum Vitæ

Contact

Marie SCHAER
84b, rue Ancienne – 1227 Carouge – Phone: +41 78 657 97 91
E-mail: marie.schaer@unige.ch ; marie.schaer@epfl.ch

Personal

Date of birth	May 6th, 1981
Place of birth	Geneva, Switzerland
Citizenship	Swiss and French

Languages

French	mother tongue
English	fluent
German	high school level

Actual Position

02/2005 – 09/2008 – Lemanic Neuroscience doctoral school, MD-PhD program

Ongoing projects & collaborations

- Image processing and brain morphometry for:
  - squirrel monkeys brain, with AF. Schatzberg and DM. Lyons, Stanford University, California, USA
  - patients with combat-related PTSD, with SH. Woodward, Stanford University, California, USA
  - in utero fetal brains, with L. Guibaud, CHU Lyon, France
- Integration of algorithms quantifying local cortical gyrification within the *FreeSurfer* software, with B. Fischl, Harvard University and Massachusetts Institute of Technology, Boston, USA (http://surfer.nmr.mgh.harvard.edu/fswiki/LGI)

Education

January 2005 – Federal Medical Diploma
10/1998 – 09/2004 – Faculty of Medicine, Geneva University, "APP" (Problem-based learning) & "AMC" (learning in clinical community) courses
06/1998 – Federal Certificate of Scientific Maturity, mention très bien, Collège de Candolle, Geneva

Clinical Activities

08/2004 – 09/2004 –Elective in Pediatric, Riviera Hospital, Vevey
05/2004 – 07/2004 – Elective in Internal Medicine, Geriatric Hospital, Geneva
02/2004 - 03/2004 – Elective in Community Medicine, Dharan, Nepal
10/2003 – 12/2003 – Elective in Child Psychiatry, Child Psychiatry Department, Geneva
01/2003 – Elective training as an assistant in an orphanage, India
10/2001 – 4/2003 – Assistant, Clair-Bois home for patients with cerebral palsy, Geneva
10/2001 – 9/2002 –Night assistant for EEG monitoring, sleep laboratory, Geneva
06/2001 – Community medicines work: Management of autistic children in Geneva
07/1999 – 08/1999 – Horse assisted Therapy with psychotic children, Belgium & France

Honors & Awards

09/2005 – 08/2008– MD-PhD Grant, awarded by the Swiss National Fund and Swiss Academy of Medical Sciences (323500-111165)
June 2007 – Travel Award for the Human Brain Mapping Conference in Chicago
May 2007 – Selected to attend the 57th Meeting of Nobel Laureates in Physiology or Medicine, July 2007 (www.lindau-nobel.de)
September 2006 – Jean-Falk Vairant Best Poster Prize, 3rd Annual Meeting of the Lemanic Neuroscience Program
April 2006 – Department of Genetic Medicine and Development Best Poster Prize, GenDev Retreat, Chamonix
July 2006 – Travel Award for the 5th International 22q11.2 deletion syndrome Conference in Marseille
March 1999 – Gillet Travel Award, awarded by the Geneva College and the Geneva Academic Society, for two months of training in Horse assisted Therapy

Publications

International Peer-Reviewed Journal Articles

M. Schaer, S. Eliez (2008) "Contribution of structural brain imaging to our understanding of cortical development process", *in press* European Psychiatric Reviews

M. Schaer, B. Glaser, M. Bach Cuadra, M. Debbané, J.-P. Thiran, S. Eliez (2008) "Congenital heart disease affects local gyrification in 22q11.2 deletion syndrome (22q11.2DS)", *in press* Developmental Medicine & Child Neurology

SH. Woodward, M. Schaer, DG Kaloupek, L. Cediel, S. Eliez (2008) "Cerebral cortical volume is globally and regionally smaller in combat-related posttraumatic stress disorder", *in press* Archives of General Psychiatry

F. Dufour, M. Schaer, M. Debbané, R. Fahroumand, B. Glaser, S. Eliez (2008) "Cingulate gyral reductions are related to low executive functioning and psychotic symptoms in 22q11.2 deletion syndrome", Neuropsychologia 46(12):2986-92

D. Gothelf, M. Schaer, S. Eliez (2008) "Genes, brain development and psychiatric phenotype in velocardiofacial syndrome", Mental Retardation & Developmental Disabilities Research Reviews, 14(1):59-68

M. Schaer, M. Bach Cuadra, L. Tamarit, F. Lazeyras, S. Eliez, J.-P. Thiran (2008) "A surface-based approach to quantify local cortical gyrification", IEEE Transactions on Medical Imaging, 27(2):161-170

SH. Woodward, DG Kaloupek, M. Schaer, C. Martinez, S. Eliez (2008) "Right anterior cingulate cortical volume covaries with respiratory sinus arrythmia magnitude in combat survivors", Journal of Rehabilitation Research and Development, 45(3):451-64

B. Glaser, M. Schaer, S. Berney, M. Debbané, S. Eliez (2007) "Structural changes to the fusiform gyrus : a cerebral marker for social impairments in 22q11.2 deletion syndrome ?", Schizophrenia Research, 96: 82-86

M. Schaer, S. Eliez (2007) "From genes to brain: understanding brain development in neurogenetic disorders using neuroimaging techniques", Child and Adolescent Psychiatric Clinics of North America 16(3): 557-79

M. Debbané, M. Schaer, R. Farhoumand, B. Glaser, S. Eliez (2006) "Hippocampal volume reduction in 22q11 deletion syndrome", Neuropsychologia, 44: 2360-5

M. Schaer, J. E. Schmitt, B. Glaser, F. Lazeyras, J. Delavelle, S. Eliez (2006) "Abnormal pattern of cortical gyrification in velo-cardio-facial/DiGeorge syndrome (deletion 22q11.2): an MRI study", Psychiatry Research, 146: 1-11

SH. Woodward, DG Kaloupek, CC Streeter, C. Martinez, M. Schaer, S. Eliez (2006) "Decreased anterior cingulate volume in combat-related PTSD", Biological Psychiatry, 59(7): 582-7

Manuscripts under review

M. Schaer, M. Debbané, M. Bach Cuadra, B. Glaser, S. Eliez. "Trajectories of cortical thickness changes in 22q11 deletion syndrome (22q11DS): a cross-sectional and longitudinal study", *Submitted*

M. Katz, C. Liu, M. Schaer, K. J. Parker, A. Epps, M.-C. Ottet, C. L. Buckmaster, R. Bammer, M. E. Moseley, A. F. Schatzberg, S. Eliez, D. M. Lyons. "Stress inoculation-induced adaptations in primate prefrontal development", Developmental Neuroscience *Under review*

M. Schaer, B. Glaser, M.-C. Ottet, M. Schneider, M. Bach Cuadra, M. Debbané, J.-P. Thiran, S. Eliez. "Regional cortical volumes & congenital heart disease: a MRI study in 22q11.2 deletion syndrome", *Submitted*

Book Chapter

S. Eliez, M. Schaer (2007) "La maturation du cerveau humain de la naissance à l' âge adulte", Traité de Neuropsychologie de l'Enfant. Marseille: Editions Solal (M. Poncelet, S. Majerus, & M. Van der Linden, Eds.), *In press*

Conferences

Conference papers

D. Ferrario, M. Bach Cuadra, M. Schaer, N. Houhou, D. Zosso, S. Eliez, L. Guibaud, J.-P. Thiran (2008) "Brain surface segmentation of the magnetic resonance images of the fetus", EUSIPCO 2008 Conference, Lausanne, Switzerland, 27/08/2008

Oral communications

Dynamic of cortical changes in 22q11 deletion syndrome: a cross-sectional and longitudinal MRI study, 6th International 22q11.2 Conference, Utrecht, Holland, 21/6/2008

Measuring local gyrification using MRI, CIBM Research day, Geneva, Switzerland, 1/04/2008

Disturbed cortical gyrification in 22q11 deletion syndrome: potential cues to the etiology of brain malformations in the syndrome, 14th Winter Workshop on Schizophrenia and Bipolar Disorders, Montreux, Switzerland, 6/02/2008

Measuring cortical folding : potential cues on the etiology of brain malformations in 22q11 deletion syndrome, 4th Annual Meeting of the Lemanic Neuroscience Program, Les Diablerets, Switzerland, 15/9/2007

Anomalies de la gyration et du développement cérébral chez les patients atteints de microdélétion 22q11, 12^{e} journées de Médecine Fœtale, Morzine, France, 30/3/2007

Abnormal cortical folding in the brain of patients affected by velo-cardio-facial syndrome, 12th Annual VCFSEF International Scientific Meeting, Strasbourg, France, 08/07/2006

Neuroimaging methods applied to the study of aneuploidy: 22q11.2 deletion syndrome as an illustration, GenDev Retreat, Chamonix, France, 10/04/2006

A new method for measuring cortical folding in a 3D space from MR images, Alpine Brain Imaging Meeting, Champéry, Switzerland, 26/01/2006

Posters

M. Schaer, M. Debbané, M. Bach Cuadra, B. Glaser, S. Eliez. Cortical thickness in 22q11 deletion syndrome: alterations in affected children and evolution into adulthood, 14th Winter Workshop on Schizophrenia and Bipolar Disorders, Montreux, Switzerland, 5/02/2008

M. Schaer, M. Debbané, M. Bach Cuadra, L. Tamarit, B. Glaser, J.-P. Thiran, S. Eliez. A surface-based approach to quantify local cortical gyrification in 22q11 deletion syndrome, Alpine Brain Imaging Meeting, Champéry, 14-18/01/2007

M. Schaer, M. Bach Cuadra, Lucas Tamarit, J.-P. Thiran, S. Eliez. Determinants of cortical gray matter volume: hypothesis based on developmental cohorts with normal and abnormal cortical morphology & Futures Directions, 3rd Annual Meeting of the Lemanic Neuroscience Program, Les Diablerets, 8/09/2006. *Awarded Jean-Falk Vairant "Best Poster"*

M. Schaer, M. Bach Cuadra, D. Gabriel Mounir, J. Glauser, M. Debbané, B. Glaser, S. Eliez. Cortical thickness in 22q11 deletion syndrome: a MRI study, 5th International 22q11.2 deletion syndrome Conference, Marseille, France, 10/07/2006.

M. Schaer, M. Bach Cuadra, J.-P- Thiran, S. Eliez. Determinants of cortical gray matter volume: hypothesis based on developmental cohorts with normal and abnormal cortical morphology, Human Brain Mapping, Florence, Italy, 12/06/2006

M. Schaer, J. E. Schmitt, B. Glaser, F. Lazeyras, J. Delavelle, S. Eliez. Quantifying cortical folding in a 3D space from MR images, 4th scientific meeting of the MD-PhD program, 20/3/2006; also presented and *awarded "Best Poster" in GenDev Retreat*, Chamonix, France, 10/04/2006

Services

Reviewer for the Journals:
Biological Psychiatry
Archives of General Psychiatry
Brain
Cerebral Cortex
Psychiatry Research

Teaching Experience

Lectures

Normal Cerebral Development, Bachelor in Psychology, Lausanne University, March 2007
Structural Morphometry of the cerebral cortex: voxel-based and other approaches, Lemanic Neuroscience Doctoral School, March 2007 & October 2007

Student co-supervision

Master's work in Electricity, Swiss Federal Institute of Technology (Lausanne):
Damien Ferrario, "Brain segmentation of MRI images of fetus", February 2008

Diploma's work in Experimental Psychology, Geneva University:
Sandra Berney, "Fusiform gyrus and face recognition in children and young adults affected with velo-cardio-facial syndrome", October 2006

Elective training for Bachelor and Master in Psychology, Geneva University:
Maude Schneider, "Regional cortical volumes in patients affected by VCFS", May 2008
Léa Zahnd, "Longitudinal brain alterations in velo-cardio-facial syndrome", September 2007
Jérôme Glauser, "Cortical thickness and velo-cardio-facial syndrome", June 2006
Daniela Gabriel Mounir, "Exploratory study of the relationship between perception temporal reproduction and caudate nucleus volume in patients affected by VCFS", February 2006

MD thesis, Geneva University:
Astrid Flahault, "Hippocampal volume in velo-cardio-facial syndrome: a longitudinal study", ongoing
Federico Dufour, "Cingulate morphology and psychosis in 22q11 deletion syndrome", ongoing

Skills

Broad knowledge of FreeSurfer and BrainImage software, as well as Linux/UNIX administration

Good knowledge of Matlab programming and SPM software
Basic knowledge of BrainVISA, FSL and AFNI and SUMA software

Courses

FreeSurfer & FSL Course, 18-24/6/2006, Siena, Italy
AFNI Course, 18-20/1/2006, EPFL
Linux, Administration and Network, 15-18/3/2005, EPFL